UNIVERSIDAD DE JAÉN

FACULTAD DE CIENCIAS DE LA SALUD

DEPARTAMENTO DE CIENCIAS DE LA SALUD

TESIS DOCTORAL

PAPEL DE LAS CÉLULAS MADRE TUMORALES EN LA RESPUESTA A NUEVOS FÁRMACOS SELECTIVOS FRENTE A CÁNCER DE COLON Y MAMA

PRESENTADA POR:

ALBERTO RAMÍREZ RIVERA

DIRIGIDA POR:

DR. D. JUAN ANTONIO MARCHAL CORRALES

DRA. DÑA. MACARENA PERÁN QUESADA

DRA. DÑA. HOURIA BOULAIZ TASSI

JAÉN, 21 DE FEBRERO DE 2014

ISBN 978-84-8439-846-2

El doctorando D. ALBERTO RAMÍREZ RIVERA ha disfrutado de una beca de investigación F.P.D.I. *Formación de Personal Docente e Investigador predoctoral en áreas de conocimiento consideradas deficitarias por necesidades docentes* (convocatoria de 10 de febrero de 2009 –BOJA nº 47 de 10 de marzo).

Para optar a la mención de "Doctor Internacional", el doctorando realizó durante el periodo de formación una estancia de tres meses en:

- Institute for Cancer Research and Treatment, en Turin (Italia). Trabajo realizado en el grupo perteneciente a Dña. Maria Flavia Di Renzo (M.D.), (Cancer Genetics) y directora del Departamento de Ciencias Oncologicas de la Universidad de Turin.

Los resultados de esta Tesis Doctoral han sido aceptados en las siguientes publicaciones que cumplen con los criterios de calidad exigidos (ver anexo):

-Morales-Marín *Fátima, Ramirez *Alberto, Conejo-García Ana, Morata Cynthia, Marchal Juan A., Campos Joaquín M. Anti-proliferative Activity of 2,6-Dichloro-9- or 7-(Ethoxycarbonylmethyl)-9H-or 7H-Purines against Several Human Solid Tumour Cell Lines. Eur J Med Chem., 2014.

*These authors contributed equally to this work. ACEPTADO CON CAMBIOS MENORES.

-Lopez-Cara LC, Conejo-Garcia A, Marchal JA, Macchione G, Cruz-Lopez O, Boulaiz H, Garcia MA, Rodriguez-Serrano F, Ramirez A, Cativiela C, Jimenez AI, Garcia-Ruiz JM, Choquesillo-Lazarte D, Aranega A, Campos JM.. New (RS)-benzoxazepin-purines with antitumour activity: The chiral switch from (RS)-2,6-dichloro-9-[1-(p-nitrobenzenesulfonyl)-1,2,3,5-tetrahydro-4,1-benzoxazep in-3-yl]-9H-purine. Eur J Med Chem 46:249-258, 2011.

- Ramírez A, Boulaiz H, Morata C, Perán M, Jiménez G, Agil A, Cruz-Lopez O, Conejo A, Campos J, Sánchez A, García MA, Marchal J A. Bozepinib is a novel small compound that targets Her2-signaling pathway, proliferative kinases and cancer stem cells. Cancer Research. Enviado, 2014.

-Marchal JA, Carrasco E, Ramirez A, Jimenez G, Olmedo C, Peran M, Agil A, Conejo-Garcia A, Cruz-Lopez O, Campos JM, Garcia MA. Bozepinib, a novel small antitumor agent, induces PKR-mediated apoptosis and synergizes with IFNalpha triggering apoptosis, autophagy and senescence. Drug Des Devel Ther 7:1301-1313, 2013.

-Patente con número de solicitud: P201430048. Título: Sulfonamidas derivadas de aminas secundarias con grupos 1,3-dioxolanilalquílicos y fenilmetilpurínicos, y su utilización como agentes anticancerígenos.

El doctorando D. **ALBERTO RAMÍREZ RIVERA** y los directores de la tesis doctoral titulada ***"PAPEL DE LAS CÉLULAS MADRE TUMORALES EN LA RESPUESTA A NUEVOS FÁRMACOS SELECTIVOS FRENTE A CÁNCER DE COLON Y MAMA."*** garantizamos al firmar estas tesis doctoral, que el trabajo ha sido relizado por el doctorando bajo la dirección de los directores de la tesis y hasta donde nuestro conocimiento alcanza, en la realización del trabajo, se han respetado los derechos de otros autores a ser citados, cuando se han utilizado sus resultados o publicaciones.

Jaén, 24 de Enero de 2014

Doctorando

Fdo. D. Alberto Ramírez Rivera.

Directores de la Tesis

Fdo. D. Juan Antonio Marchal Corrales.

Fdo. Dña. Macarena Perán Quesada.

Fdo. Dña. Houria Boulaiz Tassi.

Quisiera expresar mi más sincero agradecimiento:

A mis directores de Tesis:

D. Juan Antonio Marchal Corrales, Dña. Macarena Perán Quesada y Dña. Houria Boulaiz Tassi, por su guía y apoyo, tanto a nivel científico como personal, fundamentales para el desarrollo de este trabajo. Todo un ejemplo a seguir.

Me gustaría agradecer de manera especial la ayuda y el consejo prestado por la Dra. Maria Ángel García Chaves, a quien considero parte fundamental de este proyecto.

Al grupo de Química Farmacéutica y Orgánica de la Universidad de Granada, cuya colaboración ha sido fundamental para la realización de este trabajo. Agradecer de forma especial a los profesores Joaquín Mª Campos Rosa y Ana Conejo García, así como a María Eugenia García Rubiño y Fátima Morales Marín.

A los doctores Jaime Lazuén Alcon y Gustavo Ortiz Ferrón, por la paciencia y dedicación mostrada en el desarrollo de este trabajo.

A mis compañeras de laboratorio Cynthia, Gema y Elena con los que tantas vivencias he compartido, tanto dentro como fuera de él. De igual manera me gustaría agradecer el apoyo y la amistad de otros "compañeros de fatigas", a los que conocí durante la realización de esta Tesis: Blanca, Esther, Ana, Jesús, Milán y Manuel con quienes comparto una gran amistad, a pesar de no seguir trabajando juntos. De igual manera quisiera agradecer los buenos momentos compartidos en el "cafelillo" de la mañana con algunos otros compañeros de laboratorio como Macarena, Ester, Juan, Salva o Gloria. Y con la idea de no extenderme mucho, agradecer a todas aquellas personas que durante el desarrollo de esta Tesis han pasado por mi vida, enriqueciéndola tanto a nivel profesional como personal.

Agradecer a toda mi familia el interés y el apoyo que me han demostrado durante el desarrollo de la Tesis, y en estos momentos quisiera recordar de manera especial a los que ya no están con nosotros, porque estoy convencido de que el recuerdo es la mejor manera de hacerlos partícipes de este momento.

Finalmente me gustaría dedicar esta Tesis a mis padres y mi hermana, por su apoyo día a día, por la comprensión demostrada y por su confianza. Sin duda alguna, esta Tesis no hubiera sido posible sin ellos. Gracias.

NOTA

A lo largo del texto se han utilizado las abreviaturas de varios términos en inglés. Esto es debido al uso extendido de la lengua inglesa en publicaciones científicas y al uso de abreviaturas en inglés de forma cotidiana en el lenguaje científico. En el glosario, al final de este trabajo, se detalla la descripción en inglés y en castellano de cada una de las abreviaturas. Así mismo, en este glosario se recogen las abreviaturas de los términos usados en castellano.

ÍNDICE

I. INTRODUCCIÓN

ABSTRACT

Recent studies have estimated that incidence of cancer for 2030 will reach 20.3 million cases in comparison with 12.7 million estimated cases for 2008. It has been shown that cancer stem cells (CSCs) play a critical role on tumorigenesis and resistance against conventional therapies, resulting on appearance of recurrence and metastasis. This CSCs subpopulation, that exist inside tumors, has unlimited proliferation potential, ability to self-renew, and capacity to generate a differentiated population from the major tumor cells. For this reason, many efforts are made to isolate and characterize this subpopulation, so as to develop new targeted therapies able to selectively target CSCs instead of reduce overall size tumor. This could allow a decrease in cancer recurrence and increase disease-free survival of patients.

The aim of this work is to determine the anticancer activity, the molecular targets, and signaling pathways, regulated by new purine and 5-fluorouracil derivatives in differentiated cells and CSCs of breast and colon cancer. To reach this objective, we study the antitumor activity of several newly synthesized purine and 5-fluorouracil derivatives in established tumoral cell lines, to select those with a higher selective antitumor activity by determining its therapeutic index (TI), inhibitory concentration 50 (IC_{50}) and its ability to induce apoptosis. Moreover, we analyze the effect of this new synthesized drug in pathways involved in cancer cell proliferation by kinome and proteomic assays, and test them *in vivo* to evaluate its antitumor activity. To study the effect on CSCs, we isolate this subpopulation from breast and colon cancer cell lines to evaluate the cytotoxic effect and the effectiveness to inhibit signaling pathways involved on *stem* properties.

Our results demonstrate that all the compounds have an intense antitumor effect in set of established tumor cell lines. The most effective one, named Bozepinib, possesses high antitumor capacity (determined by their low IC_{50}), a selective efficacy against normal cells (determined by their IT) and was able to selectively act against CSCs. Furthermore, our studies have revealed that Bozepinib inhibit the signaling pathway of HER-2 involved in uncontrolled cell proliferation of cancer cells and various related kinases tumorigenic process. Moreover, we have shown that the Bozepinib acts on proteins involved in metabolic pathways related to stem properties (such as Notch, Wnt, Hedgehog pathways) of the CSCs, highlighting his anti-CSCs activity characteristics. In our in vivo study, high doses of Bozepinib do not induce chronic or acute toxicity and exhibits potent antitumor activity. These results indicate

the effectiveness of Bozepinib as pharmacological agent against CSCs that may improve the response of patients with this pathology.

I. INTRODUCCIÓN

El cáncer es un proceso que consta de varias etapas causado por una acumulación de alteraciones de carácter tanto genético como epigenético que afecta a oncogenes, genes supresores de tumores y otros genes implicados en la regulación del crecimiento y proliferación celular (Heeg et al., 2006). Según los últimos datos aportados por la Organización Mundial de la Salud (OMS), esta enfermedad provoca la muerte de unas 7.6 millones de personas cada año y se estima que para el 2030 la cifra aumente a o 13.1 millones. En Europa, los porcentajes de muerte por cáncer en el año 2000 variaron según sexo, perteneciendo la mayor ratio en hombres a Hungría, con un 258,5 por cada 100.000 hombres y la menor a Suecia, con 122 muertes por cada 100.000 hombres. En mujeres el patrón geográfico fue diferente, correspondiendo la mayor ratio, un 136,7 por cada 100.000 mujeres a Dinamarca, mientras que en España se registraba la mínima ratio con un 76,4 por cada 100.000 mujeres. La Sociedad Española de Oncología Médica augura para el año 2015 una incidencia global de cáncer para la población española de 222.069 personas (136.961 hombres y 85.108 mujeres), siendo el tipo más frecuente el cáncer colorectal, por delante, en términos globales, del cáncer de pulmón y el de mama. La tasa de mortalidad española por cáncer en general es una de las más bajas de la UE con 153 defunciones por 100.000 habitantes (INE 7/2012).

1. MODELOS SOBRE EL ORÍGEN DEL CÁNCER

La formación y mantenimiento de los diferentes tejidos en el organismo siguen un esquema común organizado de manera jerárquica, donde las células madre forman el ápice de esta pirámide. A partir de estas células madre se forman células que proliferan rápidamente y se diferencian para posibilitar la función del órgano (Radtke and Clevers, 2005). Este modelo puede ser encontrado también en los tumores, donde las células exhiben diferentes características funcionales en base a su proliferación y diferenciación, denominándose a esta característica como *heterogenicidad tumoral* (Dick, 2008). Un ejemplo es el cáncer de pulmón, caracterizado por poseer con alta frecuencia una alta heterogeneidad tumoral, donde se ha observado la presencia de más de un subtipo histológico. Esto da lugar a la presunción de que el cáncer de pulmón deriva de una célula multipotente con características "*stem"* que es capaz de generar esta variedad de componentes histológicos (Gottschling et al., 2012).

La heterogenicidad celular dentro de los tumores fue puesta de manifiesto a principios del siglo XIX por el patólogo Rudolf Virchow, gracias a la utilización del microscopio. A partir de aquí, los numerosos avances realizados en la metodología experimental (histopatología, citogenética, etc.) permitieron el desarrollo de teorías que trataban de explicar el desarrollo de los tumores y su transformación en un proceso maligno. Estos hechos, junto con la aceptación de la teoría que trataba de explicar la aparición del cáncer a través de la acumulación de sucesivas mutaciones genéticas (Nordling, 1953; Knudson, 1971) llevaron al desarrollo de la teoría de la Evolución Clonal por Peter Nowell, quien describía el proceso de formación del tumor tomando como referencia la Teoría de la Evolución de Darwin, creando un paralelismo entre las células tumorales individuales y el desarrollo de las especies bajo un proceso de selección y diversificación (Nowell, 1976).

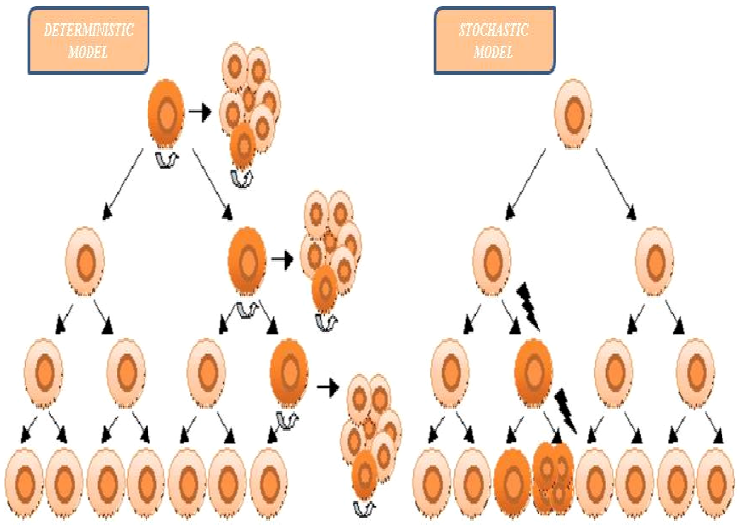

Figura 1. Modelos sobre la formación del cáncer. A.) Modelo jerárquico. El tumor se inicia a partir de una célula madre cancerígena (CMC) (marrón oscura), la cual genera a su vez células tumorales así como CMC mediante división asimétrica. B.) Modelo estocástico. El tumor se inicia al adquirir las células tumorales sucesivas alteraciones genéticas y estas, mediante evolución clonal, generan clones dominantes con propiedades de CMC mediante división simétrica. Adaptado de (Gottschling et al., 2012).

Se han descrito múltiples oncogenes y genes supresores tumorales que participan en la iniciación y progresión tumoral (Weinberg, 1995; Vogelstein and Kinzler, 2004). Gracias a los conocimientos aportados por estos estudios se han llegado a desarrollar dos posibles teorías para explicar los patrones de proliferación celular dentro del tumor (Figura 1).

1. 1. Modelo estocástico

En el modelo estocástico es la célula somática la que presenta una mutación y de ella, a través de un proceso de división no controlada se van acumulando nuevas alteraciones genéticas que otorgan a esta célula una ventaja proliferativa, hasta alcanzar el estado de célula tumoral. Cada célula del tumor comparte inicialmente las mismas características y puede formar nuevos tumores primarios, produciéndose la acumulación de eventos tanto a nivel genético como epigenético que dan lugar a la progresiva selección de subclones cada vez más agresivos, siendo estos subclones los responsables de la heterogenicidad presente en el tumor (Wicha et al., 2006; Campbell and Polyak, 2007).

Durante muchos años se ha buscado cual es el mecanismo molecular de la transformación cancerosa. Estudios recientes han identificado tres grupos de genes que resultan frecuentemente mutados, y que en condiciones normales desempeñan un papel fundamental en el control de la proliferación celular, la apoptosis y la organogénesis; son los protooncogenes, oncogenes y genes supresores de tumores (Weinberg, 1989).

Protooncogenes y Oncogenes: Un protooncogén es un gen normal implicado principalmente en procesos de proliferación celular, cuya alteración es capaz de inducir una o más características de la transformación tumoral (Plumb et al., 2003). La versión mutada del protooncogén se llama oncogén. La sobreexpresión y la amplificación de los oncogenes suele ser la principal causa de la aparición del tumor. Entre estos, nos podemos encontrar factores de transcripción, factores de crecimiento y sus respectivos receptores, moléculas implicadas en la transducción de señales o reguladores de apoptosis (Croce, 2008).

Un ejemplo de oncogén es el gen HER-2 (también conocido como HER-2/neu o erbB2), cuya sobreexpresión aparece en aproximadamente el 15% de los casos de cáncer de mama, dando lugar a la activación constitutiva de la ruta de señalización que

promueve la proliferación celular, así como la invasión y supervivencia de las células tumorales (Citri and Yarden, 2006). Otro miembro de la familia erbB, el oncogén EGFR (o erbB1), tras la unión a su ligando (EGF), homo- o hetero-dimeriza con otros receptores de su misma familia, dando lugar a la fosforilación del dominio intracelular, y a la transducción de señales de forma descendente desde el receptor, que median rutas implicadas en la supervivencia celular, la proliferación y la invasión de las células tumorales (Laurent-Puig et al., 2009).

Los genes pertenecientes a la familia Ras (H-Ras, K-Ras y N-Ras) juegan un papel fundamental en la regulación del crecimiento celular, así como en la diferenciación y supervivencia de la célula (D'Incalci et al., 2003). Se ha observado que la vía de señalización del oncogén Ras está alterada en aproximadamente un 30% de los tumores primarios, y casi en un 90% de los tumores metastásicos (Aytes et al., 2013). Dentro de esta vía de señalización, Ras ejerce su actividad sobre rutas de señalización implicadas en la reparación del daño tisular vía EGFR, regulación del ciclo celular a través de la ciclina D1, señales antiapoptóticas, mediante su influencia sobre PI3-K y AKT o la estimulación de la angiogénesis (Friday and Adjei, 2005).

Genes supresores de tumores: Son los encargados de controlar la proliferación y división celular, así como de estimular la muerte celular para el mantenimiento del equilibrio de las células del organismo. También están involucrados en la reparación del ADN, previniendo la acumulación de mutaciones. Es por esto que cuando se ven afectados por una mutación las células adquieren una capacidad proliferativa anormal, dando lugar a la aparición del tumor (Weinberg, 1996a). Entre los genes supresores de tumores más estudiados se encuentran:

a.) Gen p53: Este gen fue descrito por primera vez en 1979 e inicialmente se creó que era un oncogén, aunque más tarde se identificó como el primer gen supresor de tumores conocido. Entre las funciones de p53 podemos destacar la eliminación e inhibición de células anormales, previniendo el desarrollo del cáncer (Figura 2) (Gasco et al., 2002). La inactivación de este gen supresor de tumores, presente en el 50% de todos los tipos de cáncer (Sigal and Rotter, 2000), es un evento frecuente en el proceso de tumorigénesis, dando lugar a una proteína mutante estable que pierde su actividad supresora de tumores y además, puede conferir a las células una mayor capacidad proliferativa y de supervivencia (Rivlin et al., 2011).

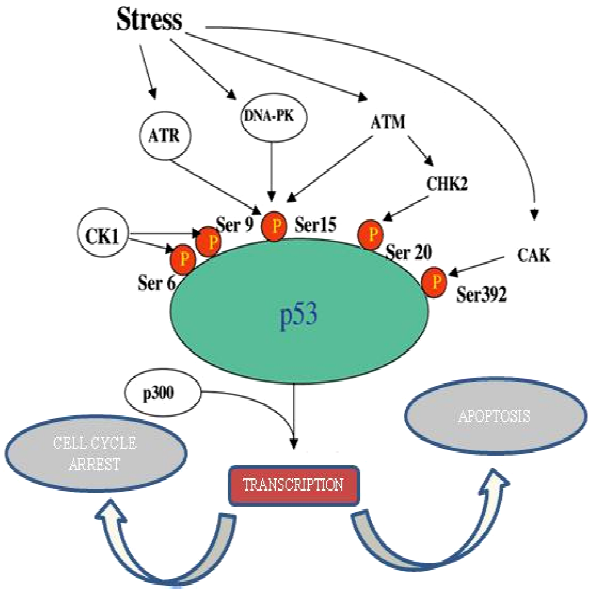

Figura 2. Modelo simplificado de los componentes implicados en la señalización mediada por p53. Adaptado de (Gasco et al., 2002).

b.) Gen Rb: El producto del gen supresor de tumores Rb, ejerce su efecto durante la primera parte de la fase G1 del ciclo celular, donde mediante el secuestro del factor de transcripción E2F evita el comienzo de la fase S del ciclo. La mutación de este gen da lugar a una proliferación celular incontrolada (Du and Pogoriler, 2006; Bosco and Knudsen, 2007). La principal característica del producto del gen Rb es la de controlar el ciclo mediante su unión al factor de transcripción E2F, bloqueando su capacidad para inducir la transcripción de genes necesarios para el avance del ciclo celular. La entrada de la célula en el ciclo celular da lugar a la fosforilación de la proteína Rb por los complejos ciclina/Cdk, liberando de esta manera a E2FS y los reguladores de la cromatina en la transición a la fase G1-S (Dick, 2007).

c.) BRCA: Las proteínas producto del gen supresor de tumores BRCA están involucradas en la reparación del daño del ADN por entrecruzamiento mediante recombinación homóloga (Yuan et al., 1999). La inactivación heterocigoto de BRCA1 y BRCA2 está asociada a un aumento del riesgo de desarrollar cáncer de mama y ovario.

Estos tumores suelen mostrar la pérdida de heterocigosidad del alelo salvaje y la mutación del gen p53 (Bouwman et al., 2010).

1.2. Modelo jerárquico

En el modelo jerárquico o modelo de la célula madre cancerígena (CMC), sólo una pequeña subpoblación del tumor, formado por CMCs, es la encargada de iniciar el tumor. Esta característica es exclusiva de CMCs que además son capaces de producir células hijas que, al diferenciarse, otorgan la heterogeneidad presente en el tumor. Esta idea se ve corroborada por la capacidad que tienen las CMCs de originar tumores cuando son inoculadas en bajo número en animales de experimentación (Dalerba et al., 2007; O'Brien et al., 2007; Prince et al., 2007).

Este modelo se basa en dos hechos, el primero sería la capacidad de las células madre (CM) para acumular alteraciones genéticas debido a su prolongada vida ya que se ha estimado que es necesario que se den entre tres y 6 eventos oncogénicos para que una célula normal adquiera un fenotipo maligno (Hahn and Weinberg, 2002). La segunda razón sería que tanto CMC como CM poseen capacidad de autorenovación.

2. ETIOLOGÍA Y PATOGENIA DEL CÁNCER

El cáncer es una enfermedad cuyo desarrollo se produce de forma progresiva, con una etiología multifactorial. En su patogenia intervienen diferentes factores entre los que podemos destacar:

- Factores genéticos: Las mutaciones de genes involucrados en la carcinogénesis que presentan una alta penetrancia y que confieren un alto riesgo a padecer cáncer, representan una pequeña proporción de la susceptibilidad individual a desarrollar esta patología. La susceptibilidad conferida por genes que presentan una menor penetrancia viene determinada por variantes comunes en los mismos genes que predisponen al cáncer (polimorfismos de un solo nucleótido, o SNPs), que poseen un efecto disruptivo menor en la función de la proteína que las mutaciones con alta penetrancia, o por mutaciones en genes que median en el metabolismo de carcinógenos. Se ha observado que genes implicados en enfermedades poco frecuentes relacionadas con el cáncer muestran polimorfismos comunes cuyos efectos en la función de la proteína son leves (por ejemplo, una enzima de reparación del ADN). Sin embargo, estos efectos, de carácter leve en la reparación del ADN, predisponen a padecer cáncer. Otra categoría

estaría representada por los polimorfismos presentes en genes metabólicos, como CYP1A1, GSTM1, GSTT1, NAT2, y otros. Estas serían condiciones comunes, que presentan una baja penetrancia en las cuales, la función de la proteína (una enzima involucrada en el metabolismo de agentes químicos tóxicos o carcinógenos) está dañada, confiriendo una mayor susceptibilidad a los efectos de tóxicos ambientales (Cobrinik et al., 1996; Jacks and Weinberg, 1996; Krauss et al., 1996; Wang et al., 1996).

- Radiaciones ionizantes y no ionizantes: Los modelos actuales de carcinogénesis están basados en la relación entre la inducción de un daño celular a nivel de ADN y la aparición de mutaciones en los genes/cromosomas a través de errores en la reparación de dicho daño. Existe una teoría biofísica, según la cual, cada radiación ionizante aumenta la probabilidad de provocar daños y incrementar de manera dosis-dependiente las mutaciones a nivel del ADN y por lo tanto, el riesgo a padecer cáncer (Weinberg, 1996b).

Según la Asociación Americana del Cáncer (2013), la radiación no ionizante es un tipo de radiación de baja frecuencia que posee la energía suficiente para dañar el ADN. Entre este tipo de radiaciones podemos encontrar algunos rayos ultravioletas (UV), la luz visible, rayos infrarrojos, microondas o los campos electromagnéticos. Sin embargo, las evidencias epidemiológicas sugieren que las radiaciones ultravioletas (UV) procedentes de los rayos del Sol son el principal factor de riesgo para padecer cáncer de piel. Este tipo de radiación incluye aproximadamente un 95% de UVA y un 5% de UVB, que pueden causar daños en el ADN, y están considerados como uno de los factores etiológicos que predisponen a padecer cáncer. Entre las vías de señalización celular que pueden ser afectadas por las radiaciones ultravioletas encontramos aquellas en las que están implicadas entre otras, las quinasa ERK, JNK, AKT o p38, involucradas en procesos tales como proliferación, diferenciación o supervivencia celular (Bezemer et al., 2005).

- Factores ambientales: Los factores carcinógenos ambientales incluyen en un sentido estricto los contaminantes tanto provenientes del aire libre como de recintos cerrados, así como los presentes en la tierra y en el agua potable (Li et al., 2004b). Según la OMS (2013), entre estos contaminantes podemos destacar los asbestos,

benzopirenos, bencenos, algunos metales, el humo del tabaco presentes en el aire libre y arsénico inorgánico o compuestos clorados en el agua potable (Li et al., 2004b).

- Factores asociados a los hábitos de vida:

a.) Sobrepeso/obesidad: En los EEUU, se piensa que el sobrepeso contribuye entre un 14-20% a las muertes relacionadas con el cáncer. El sobrepeso o la obesidad están relacionados con un incremento en el riesgo de padecer ciertos tipos de cáncer (como son el de mama, colorectal, esófago, riñón o páncreas) a través de una variedad de mecanismos, que incluyen efectos sobre la función inmune y la inflamación, los niveles y el metabolismo de numerosas hormonas (insulina o estradiol) o factores que regulan la proliferación celular y el crecimiento (IGF-1) (Kushi et al., 2012).

b.) Tabaco: En el año 2000 se estimó en 4,9 millones el número de muertes relacionadas con el tabaco, y se piensa que para el año 2020, el número de muertes alcanzará los 10 millones al año, el 70% de ellas en los países desarrollados. El tabaco es el mayor factor de riesgo para desarrollar cáncer oral y faríngeo, así como otros tipos de cáncer que afectan al tracto aerodigestivo superior (Warnakulasuriya et al., 2005) .

Se conoce que alrededor de 80 componentes del humo del tabaco pueden ser considerados como carcinógenos humanos. Entre ellos, los compuestos nitrogenados que están implicados en la mayor parte del daño por alquilación en humanos. El primer compuesto nitroso identificado en el tabaco fue la dimetilnitrosamina (DMN), a niveles prácticamente inapreciables en cada cigarrillo. Entre estos compuestos, los más carcinogénico son la N´-nitrosonornicotina (NNN), 4-(metilnitrosamino)-1-(3-piridil)-1-butanona (NNK) y su metabolito, el 4-(metilnitrosamino)-1-(3-piridil)-1-butanol (NNAL) (Christmann and Kaina, 2012).

c.) Dieta: Estudios experimentales y epidemiológicos han estimado que los factores dietéticos influyen un 30-40% sobre la incidencia del cáncer (Rohan et al., 2007). El papel de la dieta se pone de relevancia en diversos tipos de cáncer, tales como los del tracto gastrointestinal, mama, próstata y endometrio, aunque es difícil atribuir el efecto de la dieta a la hora de la aparición del tumor debido a la influencia de otros factores como los genéticos, ambientales u otros hábitos de vida (Gonzalez and Riboli, 2010).

Según estudios de la EPIC (*European Prospective Investigation into Cancer and Nutrition*), el riesgo de padecer cáncer de estómago es inversamente proporcional a la presencia, en los niveles circulantes en plasma, de la vitamina C, algunos carotenoides (β-criptoxantina y zeaxantina), α-tocoferol y retinol. Por otra parte, unos niveles altos de ingesta de fibra están asociados con una disminución en el riesgo de padecer este tipo de cáncer. Por el contrario, la alta ingesta de carnes rojas y procesadas está asociada a un incremento en el riesgo de padecer esta patología. Estos datos ponen de relevancia y avalan la importancia de la dieta mediterránea como estrategia de prevención del cáncer gracias al papel preventivo de frutas y verduras (Gonzalez and Riboli, 2010).

3. PROCESO DE FORMACIÓN DEL TUMOR

Actualmente, está ampliamente aceptado que la tumorigénesis es un proceso que consta de varias etapas, donde se encuentran implicadas una serie de alteraciones, tanto genéticas, como epigenéticas, tales como la inactivación de genes supresores de tumores, así como la activación de oncogenes (Figura 3). Estas mutaciones se acumulan en la célula provocando el paso de un crecimiento normal a un crecimiento descontrolado, que puede dar lugar a la invasión de los tejidos adyacentes y/o metástasis (Wu and Pandolfi, 2001).

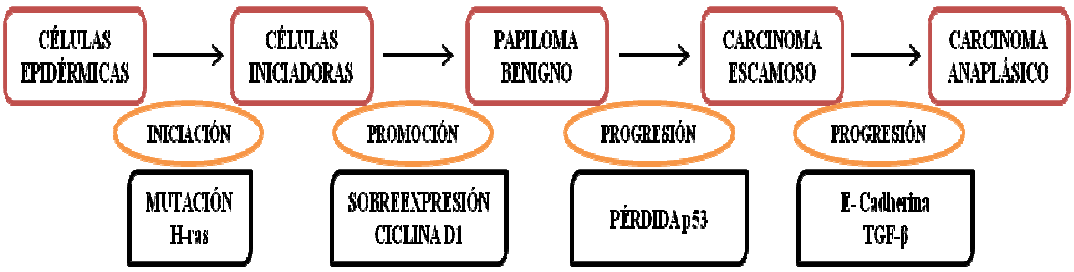

Figura 3 Ejemplo de tumorigénesis inducida por agentes químicos en un modelo de ratón. Adaptado de (Wu and Pandolfi, 2001).

Para que el cáncer llegue a desarrollarse es necesario que se den una serie de mutaciones en determinados genes que confieran a las células ciertas características, tales como la autonomía con respecto a señales de crecimiento, insensibilidad frente a señales de inhibición del crecimiento, evasión de la muerte celular programada

(apoptosis), adquisición de un potencial replicativo ilimitado, ser capaces de mantener un proceso de angiogénesis prolongado, así como la capacidad de invadir órganos y tejidos (metástasis) (Hanahan and Weinberg, 2000). En la célula, existen diversas vías de señalización implicadas en uno o más procesos de los anteriormente mencionados, entre las cuales podemos destacar:

3.1. Vía de señalización del EGFR (Epidermal Growth Factor Receptor)

La sobreexpresión o la anormal activación de alguno de los miembros de esta familia está implicada en el desarrollo y progresión de un gran número de tumores. La cascada de señalización mediada por este receptor promueve la proliferación celular, confiere resistencia a la apoptosis, induce angiogénesis y potencia los procesos de invasión y metástasis (Wu et al., 2013).

La familia del receptor EGFR comprende cuatro tipos diferentes de receptores: EGFR/ErbB-1, HER2/ErbB-2, HER3/ErbB-3 y HER4/ErbB-4. Están formados por una región extracelular, mediante la cual se unen a su ligando, una región transmembrana y una región citoplasmática con actividad enzimática. Estos receptores se activan mediante su homo/heterodimerización, induciendo una señal tirosina quinasa cuyo resultado final es la expresión de genes relacionados con diversas respuestas como la proliferación (Yarden, 2001), mediante la activación de cascadas de señalización como RAS/MAPK, PI3K/Akt, PLCγ/PKC y Jak/STAT (Dowlati et al., 2004; Brand et al., 2011; Glaysher et al., 2013; Neumann et al., 2013).

Actualmente, existen abundantes estudios que demuestran la sobreexpresión del receptor EGFR en una gran variedad de tumores epiteliales, lo que pone de relevancia su importante papel en la etiología de gran número de cánceres, como los de colon, páncreas o mama (Xu et al., 2011; Nourazarian et al., 2012; Hwangbo et al., 2013; Maron et al., 2013; Najar et al., 2013; Walsh et al., 2013).

3.2. Vía de señalización PI3K–Akt–mTOR

Esta vía de señalización tiene un papel crucial en la regulación de la proliferación celular, motilidad y supervivencia, estando implicado en la aparición de diversos tipos de cáncer (Vivanco and Sawyers, 2002). Akt es un mediador de la ruta de señalización descendente de la PI3K, y es activado mediante la estimulación de los

factores del crecimiento y la subsecuente activación de los receptores tirosina quinasa de la membrana celular. La activación de Akt puede dar lugar a la fosforilación de mTOR, el cual regula la proliferación celular mediante la transición a la fase G_1/S del ciclo celular (Markman et al., 2010; McAuliffe et al., 2010).

3.3. Vía de señalización Wnt/β-catenina

La vía de señalización canónica Wnt/β-catenina regula la proliferación celular, migración y diferenciación, siendo un potente regulador en el desarrollo del embrión y la tumorigénesis (MacDonald et al., 2009; Buikema et al., 2013).

La secreción de los ligandos Wnt actúan como factores de crecimientos de naturaleza pleiotrópica, afectando al menos a tres vías de señalización diferentes: la cascada de señalización canónica Wnt/β-catenina, la ruta Wnt/Ca^{2+} y la vía de señalización Wnt/polaridad planar celular. La mejor caracterizada de estas tres vías es la vía de señalización Wnt/β-catenina, implicada en gran variedad de cánceres y otras enfermedades (Veeck and Dahl, 2012).

La proteína β-catenina se identificó en primera instancia en las uniones tipo "*adherens"*, uniendo las cadherinas con el citoesqueleto, mediando en la adhesión celular y es la responsable de la transducción de señales de la vía Wnt canónica y el núcleo. La pérdida de la regulación de esta vía da lugar a la aparición de diversas enfermedades entre las cuales se incluye el cáncer (MacDonald et al., 2009), siendo la acumulación de esta proteína en el citoplasma y en el núcleo un potente indicador de la activación anormal de la vía Wnt (Korinek et al., 1997).

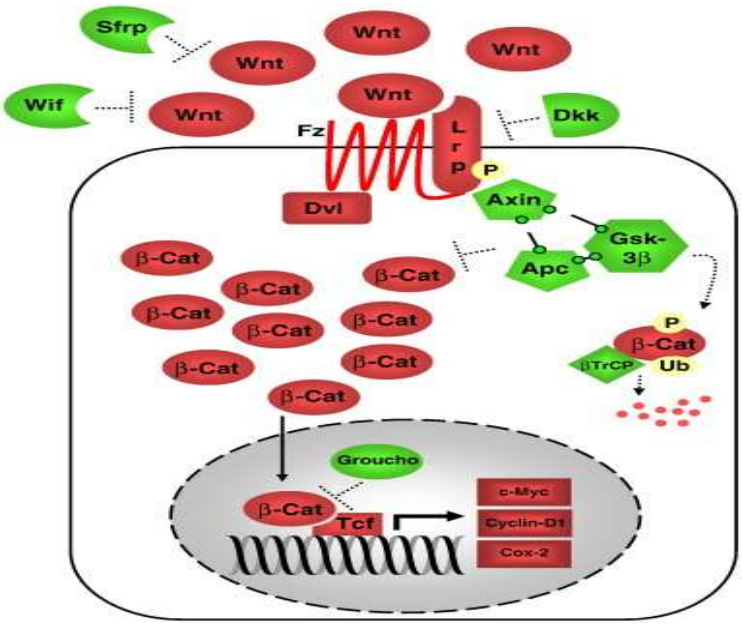

Figura 4. Cascada de señalización de WNT/β-catenina. Fuente: (Veeck and Dahl, 2012).

Como muestra la figura 4, la unión del ligando Wnt al receptor formado por el complejo Fz y Lrp estimulan la unión de Dvl a Fz a través del dominio citoplasmático del receptor. Tras la fosforilación de Lrp, la axina es liberada del complejo de destrucción de la β-catenina (el cual comprende a Axina, Apc y Gsk-3β), disminuyendo su capacidad de degradación. Tras esto, la β-catenina se acumula en el citoplasma y es translocada al núcleo, donde reemplaza al represor transcripcional Groucho en su unión a Tcf, actuando como un activador transcripcional e iniciando la expresión de genes como c-Myc, Ciclina-D1 y Cox-2 (Veeck and Dahl, 2012).

3.4. Vía de señalización de p53

La proteína p53 es quizás uno de los supresores de tumores más estudiados, estando involucrada en la respuesta celular frente a un amplio rango de tipos de stress celular (Hori et al., 2013) y daño en el genoma (Drygin et al., 2013). Se ha observado que esta proteína esta mutada en un 50% de los casos de cáncer, estando implicada en la regulación de genes relacionados con el ciclo celular o la apoptosis (Tabla 1) (Levine, 1997).

Gen	Efecto
p21, WAF-1, Cip1	Inhiben numerosas quinasas dependientes de ciclinas. Dan lugar a la parada del ciclo celular
MDM2	Producto de un oncogén; inactiva la transcripción mediada por p53 (autorregulación)
GADD45	Inducido por daño en el ADN. Se une a PCNA y puede inducir parada en ciclo celular
Bax	Perteneciente a la familia de BCL2, promueve apoptosis. No inducido en todas las células por p53
IGF-BP3	Bloquea la cascada de señalización de un factor de crecimiento mitogénico

Tabla1. Productos de genes transcripcionalmente activados por p53. Adaptado de Levine 1997.

3.5. Vía de señalización Notch

El oncogén Notch fue descubierto por primera vez en la leucemia linfoblástica aguda de células T, donde se encontró que una translocación cromosómica fusionaba la región N-terminal del receptor TCRβ al carbono terminal de Notch1 (Ellisen et al., 1991). Posteriormente se descubrió que la mitad de las leucemias linfoblásticas agudas presentaban mutaciones que activaban Notch (Weng et al., 2004).

La alteración de la expresión de los elementos que participan en la vía de señalización de Notch han sido descritos en una gran cantidad de tumores sólidos; cáncer de páncreas, pulmón, mama o colorectal (Bolos et al., 2013; Licciulli et al., 2013; Ma et al., 2013; Miyamoto et al., 2013).

Las alteraciones en la vía de señalización de Notch pueden contribuir al proceso de tumorigénesis mediante inhibición de la diferenciación, apoptosis o promoviendo la proliferación celular (Yang et al., 2004b; Curry et al., 2005; Groth and Fortini, 2012; Yabuuchi et al., 2013).

3.6. Vía de señalización del Transforming growth factor-β (TGF-β)

El TGF-β es una citoquina que juega un papel esencial en procesos fisiológicos tales como la proliferación celular, diferenciación, migración, angiogénesis o supervivencia celular (Elliott and Blobe, 2005).

Se ha observado que el TGF-β posee un doble papel en el desarrollo de la tumorigénesis (Figura 5). Inicialmente, posee las características de un supresor de tumores, debido a su capacidad para inhibir la inducción de apoptosis y la proliferación

celular. En fases más tardías del proceso, se transforma en un promotor de la tumorigénesis, mediante el aumento de la capacidad invasiva mientras que al mismo tiempo afecta a la diferenciación celular. Igualmente, cabe destacar la capacidad para evadir la respuesta inmune y estimular la angiogénesis (Pasche, 2001; Perrot et al., 2013).

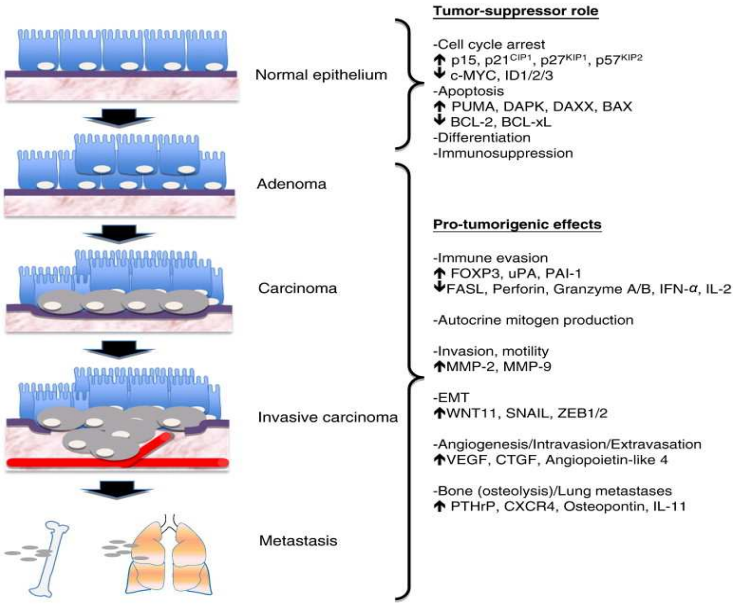

Figura 5. Efecto del TGF-β durante la progresión del cáncer. En el epitelio normal y durante las etapas tempranas del tumor actúa como un supresor de tumores (efecto citostático y anti-proliferativo). La pérdida de regulación en esta vía (mutación de los receptores TGF-β y SMADs, sobreexpresión de los ligandos TGF-β), provoca que las células escapen del programa citostático inicialmente mediado por TGF-β. Tras esto, TGF-β se comporta como un promotor del tumor, induciendo el inicio de la transición epitelio-mesénquima y volviéndose invasivas. TGF-β también permite al tumor evadir la respuesta inmunosupresora, promueve la angiogénesis y contribuye a la aparición de metástasis en sitios secundarios como el pulmón o huesos. Fuente: (Perrot et al., 2013).

3.7. Vía de señalización Hedgehog

La vía de señalización Hedgehog (Hh) juega un papel esencial en las vías de señalización implicadas en el desarrollo, cuyas mutaciones dan lugar a malformaciones de tipo congénito (Jiang and Hui, 2008).

Esta vía de señalización consta en mamíferos de tres componentes, Sonic HH (SHH), Indian HH (IHH) y Desert HH (DHH). DHH se encuentra involucrado en el desarrollo de las células germinales, IHH es un importante regulador en el crecimiento

de huesos y cartílago, mientras que SHH es el encargado de ejecutar una amplia gama de acciones biológicas, como el establecimiento de la asimetría del cuerpo o el desarrollo del sistema nervioso central y el ojo (Kar et al., 2012).

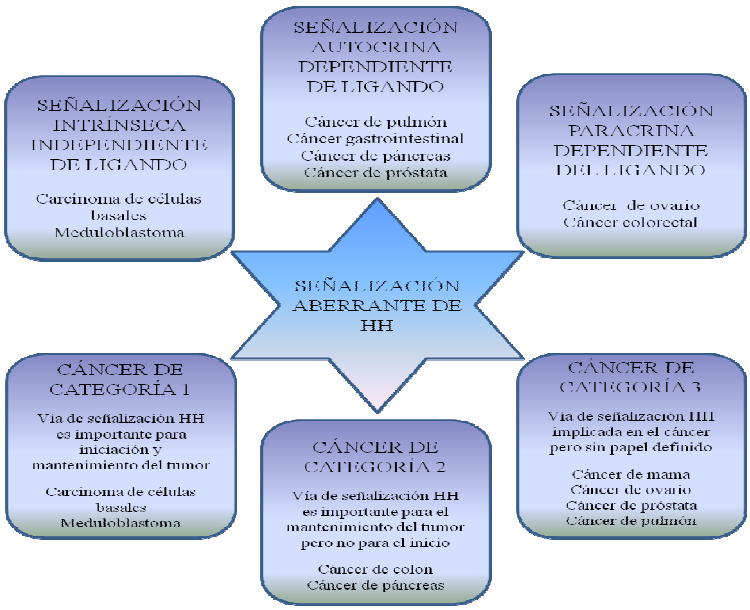

Figura 6. Representación esquemática de los diferentes modos de señalización aberrante de HH y clasificación de los diferentes tipos de cáncer en base a la etapa de la vía HH que influye en la progresión neoplásica. Adaptado de (Kar et al., 2012).

La activación de esta vía de señalización se produce mediante la unión del ligando Hh a su receptor patched (Ptch). Como resultado de esta unión, se produce la liberación de un segundo receptor, denominado Smoothened (Smo), el cual se desplaza a la membrana y da lugar a la activación de una serie de reacciones que resultan en la traslocación de activadores de la transcripción codificados por genes asociados a glioma (Gli1, Gli2 y Gli3) al núcleo, dando lugar a la transcripción de diferentes genes mediante su activación (Gli1 o Gli2) o inhibición (Gli2 o Gli3) (Merchant and Matsui, 2010).

La desregulación de esta vía de señalización está implicada en varios tipos de cáncer (Figura 6), tales como el carcinoma de células basales de piel, rabdomiosarcoma, cáncer de mama, colon o próstata (Kubo et al., 2004; Qualtrough et al., 2004; Sanchez et al., 2004; Tostar et al., 2006; Jorgensen et al., 2012)

4. DIAGNÓSTICO Y TRATAMIENTO

En la mayoría de los casos, la supervivencia de los pacientes que presentan cáncer viene determinada por la implantación de métodos de detección temprana así como la aplicación de un tratamiento adecuado. En la mayoría de los casos, estos métodos dependen de variables socio-demográficas así como de la posibilidad de ofrecer a la población una educación sobre los síntomas del cáncer y la preparación del personal sanitario para reconocer los mismos. Es por ello que se están implantando sistemas de "screening" dirigidos a la detección precoz del cáncer en la población asintomática con la idea de disminuir la mortalidad (Ott et al., 2009).

Localización tumoral	Síntomas comunes
Mama	Bulto en pecho, asimetría, retracción de la piel, cambios eczematosos en la areola, reciente retracción del pezón
Cuello de útero	Sangrado postcoital, excesiva descarga vaginal
Colon y recto	Cambio en los hábitos intestinales, pérdida de peso inexplicable, anemia, sangre en heces (recto)
Cavidad bucal	Lesiones blancas (leucoplaquia) o rojas (eritroplaquía), ulceraciones en la boca
Nasofaríngeo	Hemorragia nasal, obstrucción permanente de la nariz, sordera, nodos en la región superior del cuello
Laringe	Ronquera persistente.
Estómago	Dolor abdominal superior, aparición reciente de indigestión, pérdida de peso
Melanoma de piel	Lesión marrón que crece con bordes irregulares o zonas de coloración irregular que pueden picar o sangrar
Próstata	Dificultad (mucho tiempo) para orinar, micción nocturna frecuente
Retinoblastoma	Punto blanco en la pupila, estrabismo convergente (en niños)

Tabla 2. Adaptado de World Health Organization. Cancer control. Knowledge into action. WHO Guide for effective programmes: early detection. World Health Organization, Geneva (2007).

La tabla 2 recoge los signos y síntomas adecuados que, según la Organización Mundial de la Salud (OMS), permiten la temprana detección de algunos de los tipos de cáncer más comunes.

Actualmente no existe una única prueba que pueda ser utilizada para el diagnóstico del cáncer, por lo que se utilizan diferentes aproximaciones clínicas para detectarlo. Entre ellas podemos destacar:

a.) Examen físico: Un examen físico del paciente puede poner de manifiesto la aparición de signos que pueden hacer sospechar del desarrollo de una lesión tumoral. Un examen convencional de la cavidad oral puede dar lugar a la detección de lesiones, ulceraciones, etc., que potenciado con la utilización de factores adyuvantes como el azul de toluidina, la luz blanca difusa, la quimioluminiscencia o la pérdida de la autofluorescencia en los tejidos pueden ser utilizados para una detección temprana del cáncer (McCullough et al., 2010).

El examen físico es utilizado satisfactoriamente en el caso de cáncer de mama para detectar recurrencias loco-regionales en algunos pacientes asintomáticos (Lu et al., 2011) y en el caso del cáncer de próstata, donde una exploración digital rectal puede ser suficiente para sospechar del desarrollo del mismo (Issa et al., 2006; Heidenreich et al., 2011). Además, el examen total del cuerpo es uno de los métodos recomendados para facilitar la detección temprana del melanoma (Federman et al., 2002).

b.) Biopsia: La biopsia consiste en la extracción de una pequeña porción de tejido de un órgano o tejido del cuerpo para su posterior examen.

En el caso del cáncer de mama, la aspiración mediante aguja fina fue utilizada en principio debido a su alta sensibilidad (Ciatto et al., 1997), aunque a causa de sus otras limitaciones como la aparición de falsos negativos (Shannon et al., 2001) o la dependencia de la precisión del operador (Giard and Hermans, 1992) dio lugar a que esta técnica fuera reemplazada por la biopsia por punción con aguja gruesa. A partir de la década de los 80, esta técnica, ha sido implantada en la mayor parte de los diagnósticos mediante biopsia, gracias a su gran sensibilidad (Crystal et al., 2005; Schueller et al., 2008). Actualmente, el tipo de biopsia recomendado en los casos de melanoma por la Academia Americana de Dermatología es la biopsia por excisión, donde se extrae toda la masa de tejido sospechosa (Riker et al., 2005). Para el cáncer de próstata, una de las técnicas más utilizadas es la biopsia por punción con aguja hueca, aunque el número de muestras óptimo que se debe tomar está aún por determinar (Leibovici et al., 2011).

c.) Marcadores tumorales: Los marcadores tumorales incluyen a una variedad de sustancias entre las cuales podemos encontrar antígenos de superficie, proteínas

citoplasmáticas, enzimas, hormonas, receptores, así como oncogenes y sus productos (Sharma, 2009). La tabla 3 resume sus principales características.

Características	Observaciones
Altamente específico	Detectables solo en un tipo de tumor
Alta sensibilidad	No detectable en enfermedades de tipo benigno fisiológicas
Elevado tiempo de paso	Tiempo suficiente para la alteración del transcurso natural de la enfermedad
Niveles se correlacionan con el tamaño tumor	Valores prognósticos y predictivos
Corta vida media	Capaz de ser monitoreado de forma frecuente
Método simple y barato	Aplicable como un ensayo de rastreo
Fácil obtención de especímenes	Aceptación por la población objeto de estudio

Tabla 3. Principales características de los marcadores tumorales. Fuente: Adaptado de (Sharma, 2009).

Según la aplicación a la que está enfocado el marcador, podemos dividir estos en: a.) Marcadores de detección temprana: Con este tipo de marcadores se pretende detectar el cáncer en estadios tempranos; b.) Marcadores diagnósticos: Utilizados para la detección de la enfermedad; c.) Marcadores prognósticos: Tratan de calcular la probabilidad de supervivencia de los pacientes o bien determinar la agresividad del cáncer y cómo se comportará la enfermedad; d.) Marcadores predictivos: Tratan de predecir la efectividad de un fármaco o terapia, o bien monitorizar los resultados de un tratamiento; e.) Marcadores diana: Cuando la expresión de estos marcadores se ve afectada por una terapia sirven para identificar las dianas moleculares a las que afectan (Manne et al., 2005)

d.) Técnicas de imagen: Actualmente existe una gran variedad de técnicas basadas en la imagen para el diagnóstico y seguimiento del cáncer, convirtiéndose en una parte esencial en los protocolos clínicos. La mayor parte de los sistemas de imagen utilizados en la clínica están basados en la interacción de las radiaciones electromagnéticas con los tejidos y fluidos del cuerpo. Una excepción a esto son los ultrasonidos, los cuales están basados en la reflexión, dispersión y cambios en la frecuencia de las ondas de sonido.

Entre las modalidades clínicas basadas en la imagen, podemos destacar los rayos-x, ultrasonidos (US), tomografía computerizada, resonancia magnética nuclear (RMN), tomografía computarizada de emisión monofotónica (SPECT), tomografía

mediante emisión de positrones (PET). De entre estas técnicas podemos destacar la posibilidad de ofrecer imágenes en 3D de cuatro de ellas (CT, MRI, SPECT y PET) (Frangioni, 2008).

5. TIPOS DE CÁNCER

Según la Organización Mundial de la Salud (International Classification of Diseases for Oncology, 2000), el cáncer se puede clasificar según el tipo de tejido que lo origina (clasificación histológica) o por el lugar donde se origina.

- Tipos de cáncer según el tipo histológico:

1.) Carcinomas: Derivan de las células que se encuentran recubriendo la superficie interna o externa de los órganos. En él se incluyen los adenocarcinomas (derivan de células de origen glandular) y los carcinomas epidermoides (provenientes de células de origen no glandular).

2.) Sarcomas: Derivados del tejido conectivo, afectan a hueso, cartílago, grasa o músculo.

3.) Linfomas: Se originan en los ganglios linfáticos.

4.) Leucemias: Afectan a las células de la médula ósea que producen las células sanguíneas.

5.) Mieloma: Se origina en las células plasmáticas de la médula ósea.

- Tipos de cáncer según el lugar de origen:

Según afecte a determinados órganos o tejidos, podemos encontrar diversos tipos de cáncer; cáncer de mama, colon, pulmón, etc.

- Nomenclatura según la clasificación TNM:

La "*American Joint Committee on Cancer*" (AJCC) y la "*International Union for Cancer Control*" (UICC) utilizan la clasificación TNM como herramienta para los doctores a la hora de identificar el estadío de los diferentes tipos de cáncer. En el sistema TNM, a cada cáncer se le asigna una letra o un número para describir el tumor, el nodo y la metástasis. La T se utiliza para designar el tumor y se basa en el tamaño del tumor original (primario, medido en centímetros) y si ha crecido hacia los tejidos

cercanos. La letra N se usa para indicar el nodo, en el caso en el que el cáncer se haya diseminado a los nódulos linfáticos adyacentes. La M indica la presencia de metástasis, en el caso de que el tumor haya alcanzado partes alejadas del cuerpo (Sellers, 1971) .

5.1. Cáncer de mama

El cáncer de mama es el tipo de cáncer más frecuente en mujeres, aunque gracias a la implantación de medidas de detección precoz, así como los tratamientos desarrollados, se ha convertido en una enfermedad curable para la mayoría de pacientes detectados precozmente. Biológicamente hablando, el cáncer de mama se considera una enfermedad que presenta una alta heterogeneidad, pudiendo ser subdividido en diferentes subclases, cada una con su correspondiente relevancia clínica (Harbeck et al., 2010).

5.1.1. Subtipos de cáncer de mama

En la última década, los estudios genómicos han establecido cuatro subtipos intrínsecos de cáncer de mama (Luminal A, Luminal B, HER-2 enriquecido y de tipo basal), además de un subtipo conocido como cáncer de tipo normal, revelando importantes diferencias en cuanto a incidencia, supervivencia y respuesta al tratamiento se refiere (Prat and Perou, 2011).

En cuanto a los receptores de estrógenos (ER), alrededor del 70% de los pacientes que padecen cáncer de mama tienen tumores que expresan la proteína α del receptor de estrógenos, la cual es un marcador pronóstico favorable (ER+), mientras que los pacientes con tumores ER- tienen un pronóstico menos favorable (Bergamaschi et al., 2009). Dentro del subtipo ER- encontramos los subtipos de tipo basal y el HER2+/ER- y al menos dos tipos de tumores ER+ (Luminal A y Luminal B). Los tumores de tipo basal normalmente expresan HER2 y ER en bajo grado y una alta expresión de genes característicos de las capas epiteliales de tipo basal, como son la citoqueratina 5, 6 y 17. Los tumores HER2+ pueden presentar al menos dos grupos de expresión: aquellos que son ER- y que se agrupan cercanos a los tumores de tipo basal (subtipoHER2+/ER-) y los tumores que son ER+ (y que pueden ser positivos para el receptor de progesterona) y que se agrupan con los tumores de células de origen luminal como parte del subtipo Luminal B. Tanto el subtipo Luminal A como el B expresan ER, GATA3 y genes regulados por estos dos genes. En comparación, los tumores de tipo

Luminal A expresan mayores niveles de ER y GATA3 y muestran un pronóstico más favorable, mientras que los tumores de tipo Luminal B expresan en mayor medida HER1, HER2 y/o ciclina E1 (Carey et al., 2006).

5.1.2. Incidencia

En 2008, alrededor de 1,4 millones de mujeres fueron diagnosticadas con cáncer de mama en el mundo, con aproximadamente unas 459.000 muertes registradas (Figura 7).

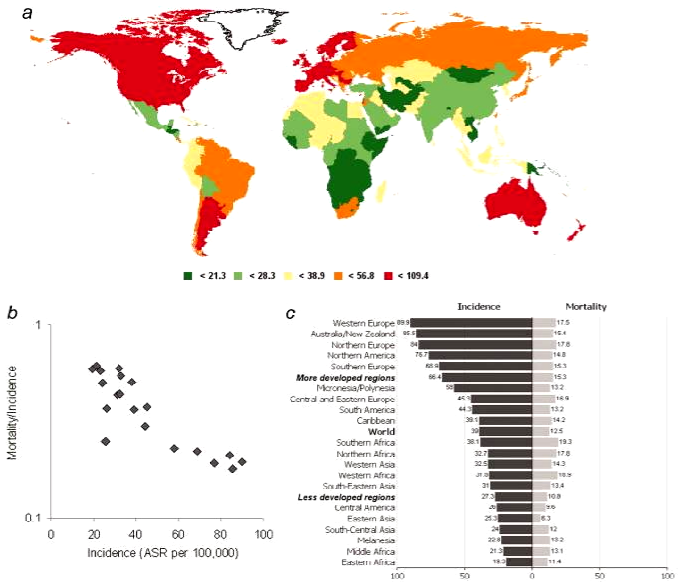

Figura 7. Incidencia de cáncer de mama por países, estandarizada según edades. Fuente: (Ferlay et al., 2010).

La tasa de incidencia fue mucho mayor en países desarrollados que en países menos desarrollados (71,7/100.000 respecto a 29,3/100.000 mujeres en 2000). Sin embargo, la supervivencia media a 5 años fue de un 12% en ciertas regiones de África, hasta de un 90% en EEUU, Australia y Canadá, basándose estas diferencias en la combinación de una detección precoz, el acceso a los tratamientos y las barreras culturales. Los avances en la supervivencia en los países más desarrollados en las últimas décadas se deben a la utilización de la mamografía para la detección precoz, así como la utilización sistémica de terapias adyuvantes (Youlden et al., 2012). En España se estima que en el año 2012 se diagnosticaron más de 25000 casos y morirán más de 6000 mujeres por cáncer de mama (Sanchez et al., 2010), siendo el cáncer de mama invasivo (IBC) el tumor más frecuente entre las mujeres. En el periodo 2000-2004, este

tipo de cáncer tuvo una incidencia de 83,8/100.000 mujeres (Puig-Vives et al., 2012). En cuanto a la distribución, las mujeres españolas mostraron una mayor incidencia del subtipo ER+ y/o PR+/HER2-, seguido del subtipo ER+ y/o PR+ y HER2+, triple negativo y HER2 sobreexpresado (Puig-Vives et al., 2013).

5.1.3. Etiología

En el inicio y desarrollo del cáncer de mama podemos encontrar dos grandes factores de riesgo, los genéticos y los no genéticos (Mavaddat et al., 2010).

- Factores no genéticos:

a.) Estrógenos: Se ha observado que la exposición a estrógenos está epidemiológicamente ligada a un aumento en el riesgo de padecer cáncer de mama en mujeres pre y postmenopaúsicas (Kaaks et al., 2005). Como muestra la figura 8, los metabolitos procedentes del metabolismo oxidativo de los estrógenos pueden reaccionar con el ADN y comportarse como carcinógenos químicos endógenos, capaces de generar las mutaciones que pueden dar lugar al inicio del cáncer (Cavalieri et al., 2006; Cavalieri and Rogan, 2011).

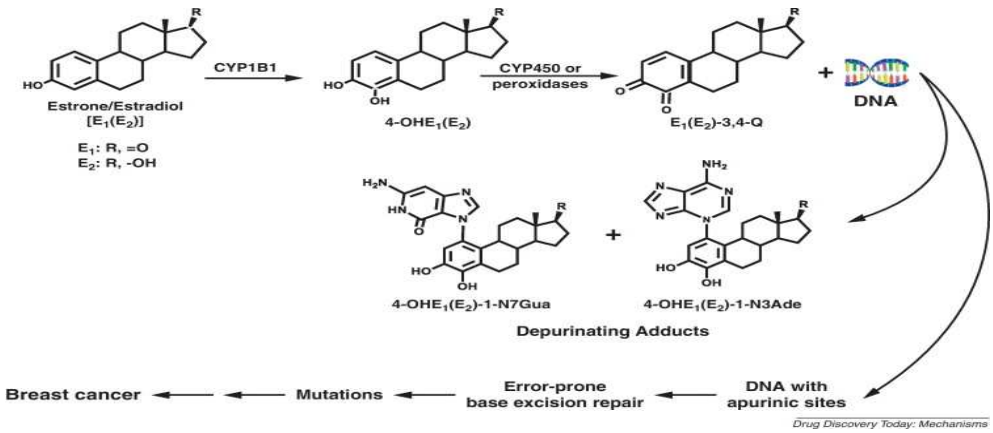

Figura 8. Mecanismo mediante el cual los metabolitos procedentes del metabolismo oxidativo de los estrógenos pueden dar lugar a mutaciones que provoquen el inicio del cáncer. Fuente: (Cavalieri and Rogan, 2004).

b.) Obesidad y sobrepeso: La obesidad y el sobrepeso se asocian a la aparición de cáncer de mama al involucrar diversos factores metabólicos, como la aparición de un cierto grado de proceso inflamatorio. Este último provoca la acumulación de macrófagos en el tejido adiposo causando la liberación de moléculas proinflamatorias implicadas en el cáncer. Un estudio proteómico detallado de muestras de tejido adiposo

fresco procedentes de tumores de pacientes con alto riesgo de padecer cáncer de mama reveló la presencia de un gran número de proteínas, tales como moléculas de señalización, hormonas, citoquinas o factores de crecimiento, implicados en vías de señalización relacionadas con el cáncer (transducción de señales, proliferación celular, respuesta inmune o apoptosis) (Celis et al., 2005)

c.) Dieta/Factores nutricionales: El daño procedente del metabolismo oxidativo, uno de los factores que provoca mutaciones en el ADN, y por lo tanto, contribuye a la aparición del cáncer, podría ser prevenido o limitado por los antioxidantes presentes en la dieta, sobre todo en frutas y hortalizas. Un ejemplo sería el de los productos derivados de la soja. Uno de los mecanismos por los que podría disminuir el riesgo de padecer cáncer de mama sería a través de la inhibición de la enzima aromatasa, así como mediante la reducción de la proporción de estrógenos libres circulantes en plasma, mediante la estimulación de los niveles de de la hormona sexual de unión a la globulina (SHBG) (Murkies et al., 1998; Magee and Rowland, 2004). Además, se ha visto que la ingesta de grasas podría modificar el riesgo de cáncer de mama. Se ha observado, en estudios *in vivo* que los ácidos grasos n-3 reducen el riesgo de padecer cáncer de mama, del mismo modo que los ácidos grasos n-6 lo aumentarían (Su et al., 2010).

- Factores genéticos:

Se ha descrito que la aparición de mutaciones en determinados genes aumenta la susceptibilidad de algunos individuos a sufrir cáncer de mama. Entre estos genes podemos encontrar:

a.) Genes *BRCA1* y *BRCA2*: *BRCA1* está implicado en la activación de la respuesta frente al daño en el ADN, la interacción con genes implicados en su reparación así como, la activación de puntos de control del ciclo celular. *BRCA2* está relacionado con la reparación de daños provocados en el ADN durante la replicación.

b.) Gen *MDR1*: Este gen, que codifica para la glicoproteína P (Pgp) está implicado en la resistencia a drogas naturales citotóxicas así como a xenobióticos potencialmente tóxicos, gracias a su acción transportadora de membrana (Bodor et al., 2005). Dentro de este gen, se ha observado que el polimorfismo C3435T conlleva la disminución de la actividad Pgp, estando este hecho relacionado con la susceptibilidad a padecer cáncer de mama (Wang et al., 2013).

c.) Tp53: Las mutaciones de Tp53 son una de las alteraciones más comunes en los carcinomas de mama, llegando a presentarse en un 30% de ellos (Dumay et al., 2013).

5.2. Cáncer colorectal

La mayor parte (75-80%) de los casos de cáncer de colon aparecen como casos esporádicos, con una pequeña proporción representada por las formas hereditarias de la enfermedad (pacientes con síndrome de Lynch, o poliposis adenomatosa familiar por citar algunos casos). Las mutaciones y otras alteraciones genéticas aparecen como responsables en un 15-20% de los casos (Hollande et al., 2010). El cáncer colorectal se divide en tres categorías cada una con diferentes características, así puede hablarse de cáncer de colon proximal, cáncer de colon distal y cáncer de recto (Li and Lai, 2009).

5.2.1. Subtipos de cáncer colorectal

Según la "*American Cancer Society*", podemos encontrar diferentes tipos de cáncer que afectan tanto al colon como al recto. Entre ellos podemos destacar:

a.) Adenocarcinomas: Representan más del 95% de los cánceres de tipo colorectal.

b.) Adenocarcinomas mucinosos: Subtipo histológico de cáncer colorectal, en el cual las células tumorales producen mucina extracelular en abundancia (puede representar hasta un 50% del volumen del tumor). Normalmente relacionados con fases avanzadas de la enfermedad. Se diferencian de los adenocarcinomas a nivel clínico, morfológico y molecular (Mekenkamp et al., 2012).

c.) Tumores gastrointestinales carcinoides: Los tumores de este tipo que afectan al recto suelen ser asintomáticos en un 50% de los casos y tener una baja probabilidad de causar metástasis, presentando una buena prognosis. Los tumores carcinoides que afectan al colon presentan una peor prognosis así como una mayor probabilidad de causar metástasis (Lauffer et al., 1999).

d.) Tumores gastrointestinales estromales: Representan las neoplasias de tipo mesenquimal más comunes presentes en el tracto gastrointestinal. Su desarrollo está relacionado con la aparición de procesos oncogénicos en los genes *KIT* y *PDGFRA*

(platelet-derived growth factor receptor alpha), ambos pertenecientes a la familia de los receptores tirosina quinasa, proteínas implicadas en la transducción de señales, así como la regulación del crecimiento celular, diferenciación y angiogénesis (Rutkowski et al., 2011).

e.) Linfomas: Los linfomas que suelen afectar al tracto gastrointestinal son los linfomas No-Hodking, tumores sólidos compuestos por linfocitos (Gou et al., 2012).

f.) Sarcomas: Este tipo de tumores suponen menos del 1% de los tumores malignos colorectales, originándose en las células del músculo liso de la pared intestinal (Alvite Canosa et al., 2009).

5.2.2. Incidencia

El cáncer de colon es el tercer tipo de cáncer más frecuente entre la población masculina, y el segundo en cuanto a importancia entre las mujeres. Además, la incidencia está aumentando en ciertas regiones debido en parte, al aumento en el consumo de grasas y a la elevada prevalencia de obesidad y consumo de tabaco. Se estima que en 2008 aparecieron 1,2 millones de nuevos casos de cáncer de colon en el mundo (Jemal et al., 2011). La incidencia del cáncer de colon en los países desarrollados tiende a estabilizarse, sin embargo, en España esta tendencia se ha visto aumentada desde la década de los años 70, debido en gran parte al aumento de ciertos factores de riesgo como la obesidad (Center et al., 2009). En España, el cáncer colorectal es el tipo de cáncer más frecuente tanto en hombres como en mujeres, aunque se ha observado una disminución en la morbilidad y en la mortalidad, estando esta disminución relacionada con el uso de la prueba de la sangre oculta en heces en los programas de cribado (Portillo et al., 2013). Los datos obtenidos en el año 2002 cifró el número de muertes en España por cáncer colorectal en unas 12000, cifra un 3,25% superior que en el año 2000 (Parkin et al., 2005).

5.2.3. Etiología

Algunos de los factores implicados en la aparición del cáncer de colon son:

- Factores no genéticos:

a.) Dieta: Este factor tiene una importante relación con la geografía y las características socioculturales. Se ha demostrado que la ingesta de fibra está asociada a un efecto protector frente al cáncer colorectal, disminuyendo el riesgo de padecer este tipo de cáncer en un 40% (Bingham et al., 2003).

Los estudios epidemiológicos sugieren una asociación entre el consumo de carne y el cáncer colorectal (siendo mayor el riesgo en el caso de la carne procesada con respecto a la carne fresca). En el caso de las carnes procesadas se han desarrollado varias hipótesis para explicar este hecho: a) El proceso carcinogénico es promovido por la grasa presente en la carne al incrementar la producción de bilis. b) El procesamiento de la carne a altas temperaturas da lugar a la formación de carcinógenos como las aminas heterocíclicas. c) El aumento de compuestos de naturaleza nitrosa favorece el proceso carcinogénico. d) El hierro procedente del grupo hemo promueve la carcinogénesis mediante el incremento de la proliferación en la mucosa a través de la oxidación de los lípidos (Pierre et al., 2013); (Andersen et al., 2013).

b.) Alcohol: El excesivo consumo de alcohol está relacionado con la aparición de cambios histopatológicos en la mucosa del recto (Moskal et al., 2007a). Estos cambios suelen presentar una relación dosis-dependiente, poniendo de manifiesto la relación entre el consumo de alcohol y la aparición del cáncer colorectal (Mizoue et al., 2008) (Moskal et al., 2007b). Se ha encontrado que la aparición de polimorfismos en las enzimas alcohol deshidrogenasa (ADH) y aldehído deshidrogenasa (ALDH) podría contribuir a la susceptibilidad del cáncer colorectal (Homann et al., 2009).

c.) Diabetes: Existen evidencias de la asociación entre diabetes y el desarrollo del cáncer colorectal (Seshasai et al., 2011). Esto se puede deber a las propiedades mitogénicas asociadas a la insulina, al promover la transición de las células a través de la fase G_1 del ciclo celular y evitar la apoptosis en tejido normal y tumoral de colon (Ahmed et al., 2006). Además, la insulina en alta concentración, aumenta la disponibilidad del factor de crecimiento relacionado con la insulina (IGF) que está asociado con un aumento del crecimiento y la proliferación celular (Yu and Rohan, 2000; Giovannucci et al., 2010).

- Factores genéticos:

Aproximadamente el 20% de los casos de cáncer colorectal tienen agregación familiar con más de dos miembros de la familia de primer grado afectados, mientras que el 5-10% se producen en el contexto de un síndrome hereditario (Lynch and de la Chapelle, 2003). La localización de la mutación depende del tipo de carcinoma de colon. Así pues, en el caso de la poliposis adenomatosa familiar (PAF) se conoce la herencia dominante de la mutación de la línea germinal en el gen oncosupresor APC en el cromosoma 5 (Kinzler et al., 1991). En el caso del cáncer de colon hereditario sin poliposis (HNPCC), también llamado síndrome de Lynch, se han encontrado mutaciones germinativas en los genes MSH2 y MLH1, que comprenden más del 60% de los casos de HNCPP. Las mutaciones en los genes MSH6 y PMS2 son menos frecuentes (Peltomaki and Vasen, 2004; Diggs et al., 2011; Manzano and Perez-Segura, 2012).

6. CÉLULAS MADRE TUMORALES

6.1. Definición y características

Uno de los principales problemas a los que se enfrenta la lucha contra el cáncer es la capacidad de los tumores de provocar recaídas y metástasis, originando de esta manera la aparición de nuevos tumores. Las hipótesis de células madre tumorales (CSCs) está cobrando cada vez más fuerza para explicar este proceso. Estas células se caracterizan por poseer una mayor resistencia a los agentes quimioterapéuticos actuales (Zhang and Rosen, 2006), así como por ser capaces de formar colonias esféricas al ser cultivadas en suspensión (Dontu et al., 2003). Otra de sus características es el alto potencial metastásico de estas células, Al-Hajj y colaboradores lograron demostrar que inyectar 200 células tumorales con marcadores de célula madre fue más eficaz a la hora de generar tumores en ratones inmunodeprimidos que la inyección de 50.000 células tumorales con marcadores de células diferenciadas de la misma estirpe histológica (Al-Hajj et al., 2003).

Actualmente, el concepto de las CSCs ha adquirido un gran interés y atractivo, en gran parte gracias a los avances conseguidos en los estudios orientados a comprender

la biología de las células madre, lo cual ha dado lugar a la consecución de logros tales como su identificación y aislamiento en un gran número de tumores humanos, incluyendo los de pulmón, mama, próstata o colon (Hermann et al., 2007; Patrawala et al., 2007; Chen et al., 2008; Li et al., 2008b; Botchkina et al., 2009; McDermott and Wicha, 2010).

Características	Observaciones	
Potencial replicativo	Gran potencial proliferativo y enorme capacidad regenerativa	Gran potencial proliferativo y enorme capacidad regenerativa
Habilidad de diferenciación	Todas las estirpes celulares de un tejido específico	Estirpes celulares heterogéneas existentes dentro del tumor
Actividad metabólica	Baja	Desconocida
Vía de señalización	Hedghog, Wnt, Notch y BMP	Regulación aberrante de Hedghog, Wnt, Notch , BMP y otras
Regulación del ciclo celular	Ciclo celular lento	Ciclo celular potencialmente lento
Adhesión	Gran adherencia	Baja adherencia
Potencial de migración	No, migración lenta	Capacidad transición epitelio-mesénquima

Tabla 4. Comparación de las características entre células madre adultas y células madre cancerígenas. Adaptado de (Moore and Lyle, 2011).

Las CSCs poseen las características propias de las células madre (Tabla 4), tales como la capacidad ilimitada de autorenovación, proliferación y diferenciación a diferente estirpes celulares (Moore and Lyle, 2011). Entre las características más destacables de las CSCs que las hacen fundamentales en el desarrollo de los tumores podemos encontrar:

1.) Mecanismos de resistencia a la apoptosis

La apoptosis es un mecanismo de muerte celular en el que se produce la destrucción controlada de la célula, minimizando los efectos nocivos que podrían afectar a los tejidos adyacentes (Kerr et al., 1972). Este proceso conlleva una serie de alteraciones morfológicas características, tales como la condensación del material nuclear así como la condensación y acumulación de la cromatina a lo largo de la envoltura nuclear. Tras esto, el proceso de apoptosis sigue con la fragmentación del núcleo y la aparición de plegamientos en la membrana nuclear. A nivel de la membrana celular, las fases tempranas de apoptosis presentan un redondeamiento de la morfología celular, pérdida de microvellosidades y la aparición de protuberancias en forma de

burbujas en la superficie celular. Conforme progresa la apoptosis, el citoplasma se condensa y se produce una compactación de los orgánulos celulares. En las fases más tardías de la apoptosis, las células aparecen fragmentadas, formando los denominados *cuerpos apoptóticos,* formados por fragmentos de membrana celular que contienen en su interior material nuclear, orgánulos citoplasmáticos intactos y citoplasma condensado. Por último, los *cuerpos apoptóticos* son fagocitados por los macrófagos (Compton, 1992; Wong, 2011).

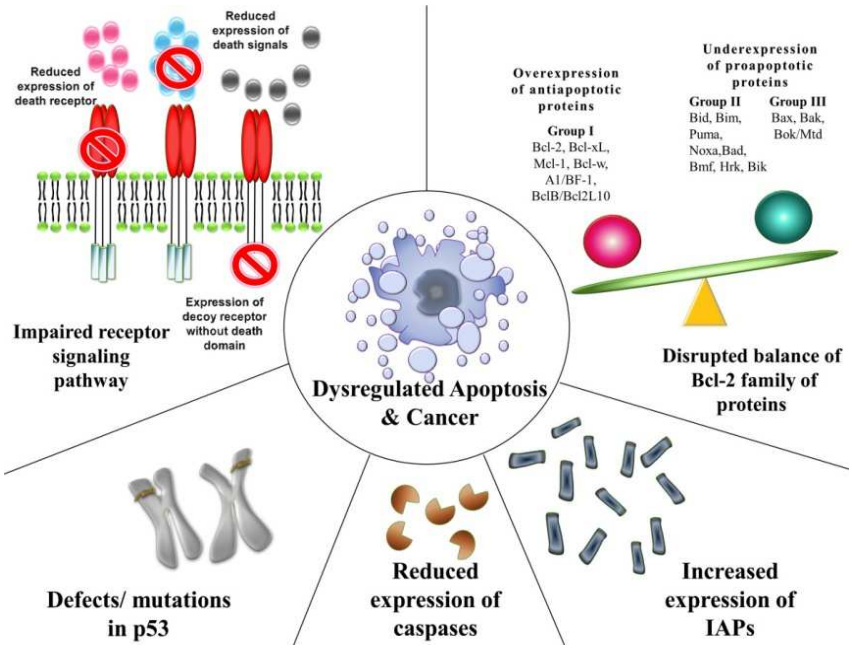

Figura 9. Mecanismos que contribuyen a la evasión de la apoptosis en el proceso carcinogénico. Fuente: (Wong, 2011).

Entre los mecanismos que contribuyen a la evasión del proceso de apoptosis en el cáncer (Figura 9) podemos destacar i) desequilibrio en el balance de proteínas pro-apoptóticas y anti-apoptóticas; ii) disminución en las funciones de las caspasas; y iii) señalización errónea de los receptores de muerte celular (Wong, 2011). La evasión de la apoptosis es una estrategia que favorece la supervivencia, tanto en células tumorales como en CSCs. Un ejemplo de ello es la presencia en glioblastomas de niveles altos de un gran número de ARN_m antiapotótico, incluyendo BCL-2, BCL-XL, IAPs y FLIP (Liu et al., 2006). También en células CD133+ de glioblastoma se ha observado que la resistencia a TRAIL, comparada con las células CD133- estaba relacionada con la supresión de la expresión de la caspasa-8 mediante la metilación del gen *CASP8* (Capper et al., 2009). Se ha observado que la secreción de diversos factores por parte de

las CSCs está relacionada con los mecanismos de resistencia a la apoptosis. En CSCs de colon, la producción autocrina de IL-4 por las células CD133+ parece que contribuye a la protección frente a la apoptosis inducida por quimioterapéuticos y TRAIL (Todaro et al., 2007).

2.) Quiescencia

La propiedad que tienen las CSCs para mantenerse en un estado de quiescencia (estado en el que la célula no se divide, permaneciendo permanente en la fase G_0 del ciclo celular (Arai et al., 2004)) les permite sobrevivir a la mayoría de los tratamientos anticancerígenos. Esta característica hace posible la reaparición del cáncer, incluso décadas después del tratamiento inicial, como es el caso del cáncer de colon o mama (Reya et al., 2001; Dick, 2008).

Las CSCs quiescentes han sido aisladas a partir de melanoma, cáncer de ovario, mama o páncreas (Dembinski and Krauss, 2009; Gao et al., 2010; Pece et al., 2010; Roesch et al., 2010), siendo utilizado en la mayoría de los estudios el método de la "retención del marcaje" (Figura 10). Para ello, se utilizó una proteína marcadora o un análogo de nucleótido. Tras esto, las células proseguirán su actividad proliferativa, perdiéndose con el tiempo el marcaje, mientras que las células en estado quiescente lo mantendrán, pudiendo ser posteriormente aisladas para su estudio (Pece et al., 2010; Buczacki et al., 2011).

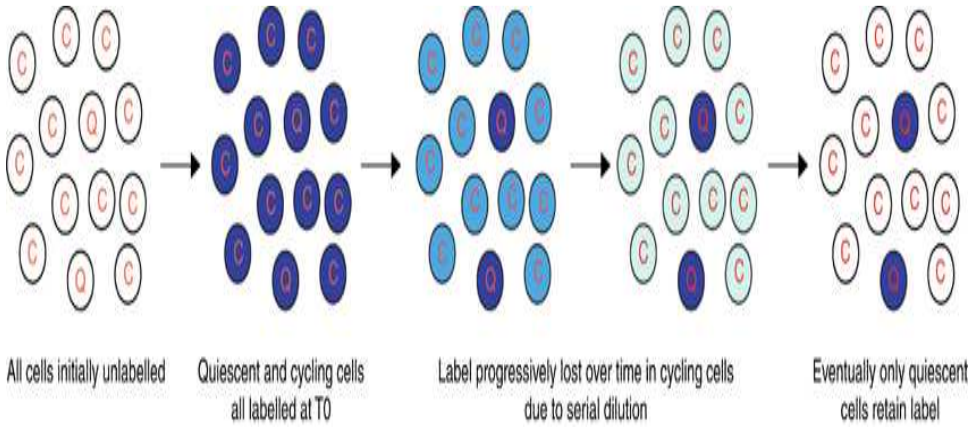

Figura 10. Estudio de retención de marcaje celular. C=célula en división; Q=célula quiescente. Todas las células se marcan con un análogo de nucleótido o una proteína fluorescente a tiempo 0. Las células en división van a diluir su marcador, mientras que las células quiescentes lo van a mantener, permitiendo su aislamiento de la población general mediante FACS. Fuente: (Buczacki et al., 2011).

3.) Resistencia a multidrogas

Uno de los grandes problemas a los que se enfrenta la terapia frente al cáncer es la aparición de resistencia a las terapias antitumorales convencionales. En última instancia, este tipo de terapias ejercen una presión selectiva frente a la masa tumoral, no llegando a erradicar la totalidad del tumor y dejando una población de células tumorales resistentes y responsables de la reaparición del tumor. Como consecuencia de la proliferación de esta subpoblación celular (CSCs), se produce la sobreexpresión de los transportadores ABC que utilizan la energía obtenida de la hidrólisis del ATP para expulsar los fármacos de las células (Leonard et al., 2003). Entre la familia de proteínas ABC, una de las más importantes es la glicoproteína P (P-gp), codificada por el gen ABCB1 (MDR1). La expresión de esta proteína es fundamental a la hora de expulsar hasta 20 tipos diferentes de fármacos citostáticos (Ozben, 2006). Existen evidencias que demuestran la generación de células que aumentan la eficiencia a la hora de formar esferas o la expresión de marcadores de CSCs al ser tratadas con cisplatino y paclitaxel *in vitro*, como es el caso de las células de cáncer de ovario OVCA 433 y HEY (Abubaker et al., 2013).

4.) Incremento de la capacidad de reparación del ADN

La capacidad de las CSCs para reparar el daño en el ADN es esencial para mantener la integridad y estabilidad del genoma. En la mayoría de los casos la respuesta generada es específica con respecto al tipo de daño generado (Hanahan and Weinberg, 2000; Feinberg et al., 2006). En las vías de la reparación del ADN se han encontrado multitud de proteínas implicadas, entre las cuales podemos destacar ATM, BRCA1, p53 o proteínas pertenecientes a la familia RAD (Wyman and Kanaar, 2006; Helleday et al., 2007). En las CSCs se ha observado que existe un aumento en la expresión de estos genes, favoreciendo la estabilidad genómica de estas células y por tanto, aumentando su habilidad para sobrevivir y actuar como promotoras del proceso tumoral e incrementando la eficiencia en la reparación del daño causado por los tratamientos anticancerígenos (Sarasin and Kauffmann, 2008).

6.2. Aislamiento y caracterización

Dada la relevancia que el estudio de las CSCs está tomando en la actualidad se están realizando grandes esfuerzos para desarrollar métodos que nos permitan su caracterización y aislamiento entre los cuales podemos destacar:

- Formación de colonias en esferas: Este método se basa en la propiedad que tienen las CSCs (al igual que las células madre) para formar esferas al ser cultivadas en baja densidad y en ausencia de suero bovino fetal, así como en presencia de determinados factores de crecimiento tales como EGF (epidermal growth factor) y FGF (fibroblast growth factor) (Qiu et al., 2012). En algunos estudios se ha demostrado que las células presentes en estas colonias de esferas mostraban una mayor tasa de autorenovación, mayor capacidad de invasividad y resistencia a drogas, al compararlas con células normales adherentes. Del mismo modo, se observó una mayor expresión de genes y proteínas relacionados con las células madre embrionarias (CME) (Cao et al., 2011; Liu et al., 2012).

- Ensayo de *side population*: Este método es utilizado para cuantificar la sobreexpresión de las proteínas transportadoras de la familia ABC en las CSCs, cuya actividad, dependiente de ATP permite a la célula expulsar ciertos colorantes, tales como el Hoescht o la rodamina, lo cual es detectado mediante citometría de flujo (Zhou et al., 2001; Patrawala et al., 2005). Este tipo de análisis ha sido utilizado en diferentes líneas tumorales, incluyendo cáncer de mama o colon, así como en glioma o leucemia (Chikazawa et al., 2010; Gross et al., 2010; Hu and Liu, 2010; Hiraga et al., 2011).

Al realizar la citometría de flujo mediante *side population*, se observa que sólo una pequeña proporción de la población celular perteneciente al tumor presenta una baja o nula fluorescencia al utilizarse colorantes vitales como el Hoescht 33342, SYTO-13 o rodamina123, los cuales son expulsados mediante las proteínas ABC (Bertoncello and Williams, 2004; Goodell, 2005).

- Ensayo de la actividad ALDH: Gracias a la alta actividad de la enzima aldehído deshidrogenasa (ALDH) presente en las CSCs estas muestran una alta resistencia a quimioterapéuticos (Hilton, 1984). Este hecho ha convertido el ensayo de citometría basado en el aldefluor en un método ampliamente utilizado para identificar y aislar CSCs en diferentes tipos de cáncer como el de mama o pulmón (Ginestier et al.,

2007; Jiang et al., 2009). Mediante esta técnica se utiliza como sustrato el boron-dipirrometano (BODIPY)- aminocetaldehido, el cual es convertido mediante la ALDH presente en alta proporción en las CSCs al producto fluorescente BODIPY-aminoacetato. El producto de esta reacción provoca que la subpoblación de CSCs fluorezca con alta intensidad y posibilita su detección y aislamiento mediante citometría de flujo (Storms et al., 1999).

A la hora de caracterizar las poblaciones de CSCs presentes en los tumores se puede utilizar el análisis mediante marcadores celulares de superficie. Las subpoblaciones de CSCs también pueden ser identificadas mediante la expresión de marcadores específicos de superficie. La expresión de marcadores como CD133, CD44, EpCAM o CD24 han sido relacionados con la presencia de CSCs en mama, próstata, cerebro o hígado (Singh et al., 2004; Ma et al., 2007; Hurt et al., 2008; Wright et al., 2008).

Mediante la inoculación de CSCs en ratones se demuestra la capacidad tumorigénica de las CSCs. Para tal fin, las células tumorales humanas son xenotransplantadas en ratones inmunodeprimidos, para luego analizar de forma histológica el desarrollo del tumor, utilizando para ello métodos *in vitro* (ensayo de formación de esferas) (Purton and Scadden, 2007; Pastrana et al., 2011). En algunos ensayos se ha observado que tras identificar y aislar la subpoblación de CSCs en tumores de mama, tan sólo hacía falta una pequeña cantidad de estas células (unas cien células) para originar un tumor al ser transplantadas en ratones inmunodeprimidos. Sin embargo, decenas de miles de células que no fueron sometidas al proceso de aislamiento de CSCs fracasaron a la hora de formar un nuevo tumor (Al-Hajj et al., 2003).

6.3. Estratégias terapéuticas frente a CSCs

Debido a las dificultades con que se enfrenta la terapia antitumoral convencional, puesta de manifiesto en la aparición de resistencia a los agentes quimioterapéuticos convencionales y desarrollo de metástasis tras la aplicación de dichos tratamientos, es necesario desarrollar fármacos antitumorales dirigidos frente a las células madre tumorales. Por esto que cabe destacar la importancia de la búsqueda de nuevos agentes quimioterapéuticos que no sólo eliminen las células tumorales, sino también las células madre tumorales (Rich and Bao, 2007). Estudios con células CD

133^+ procedentes de cultivos en esferas de cáncer de pulmón han demostrado la resistencia de estas células frente a quimioterapéuticos tales como el paclitaxel, etoposido o cisplatino, mostrando una pérdida de la capacidad de disminuir la viabilidad de estas células (Eramo et al., 2008). De igual manera, estudios llevados a cabo en cáncer de páncreas han demostrado que células CD 133^+ mostraban una mayor resistencia a la gemcitabina que las células CD 133^- aisladas del mismo tumor, además de favorecer la supervivencia de las CSCs presentes en el cultivo (Hermann et al., 2007). En CSCs aisladas de tumores de colon mediante este mismo marcador se observó que la población CD 133^- se mostraba altamente sensible al tratamiento con oxaliplatino y/o 5-fluorouracilo, mientras que las células aisladas CD 133^+ mostraron una gran resistencia frente a altas dosis de estos quimioterapéuticos usados en clínica (Todaro et al., 2007).

Una de las aproximaciones terapéuticas que se estudian actualmente para combatir las CSCs está relacionada con las vías de señalización implicadas en los procesos de su autorenovación, proliferación y diferenciación. Esto se debe a que la pérdida de la regulación de vías como Hedgehog (Hh), Notch y Wnt/β-catenina, da lugar a los procesos claves implicados en la formación de las CSCs. Actualmente, la terapia dirigida frente a estas rutas representa uno de los mecanismos de actuación más prometedores frente a las CSCs (Maugeri-Sacca et al., 2011; Takebe et al., 2011).

a.) Terapias dirigidas frente a la vía Hedgehog

Estudios recientes han demostrado que compuestos naturales, como la genisteína son capataces, como muestra la figura 11, de inhibir *in vivo* la tumorogénesis de CSCs procedentes de cáncer de próstata mediante la modulación de la vía Hedgehog–Gli (Zhang et al., 2012a).

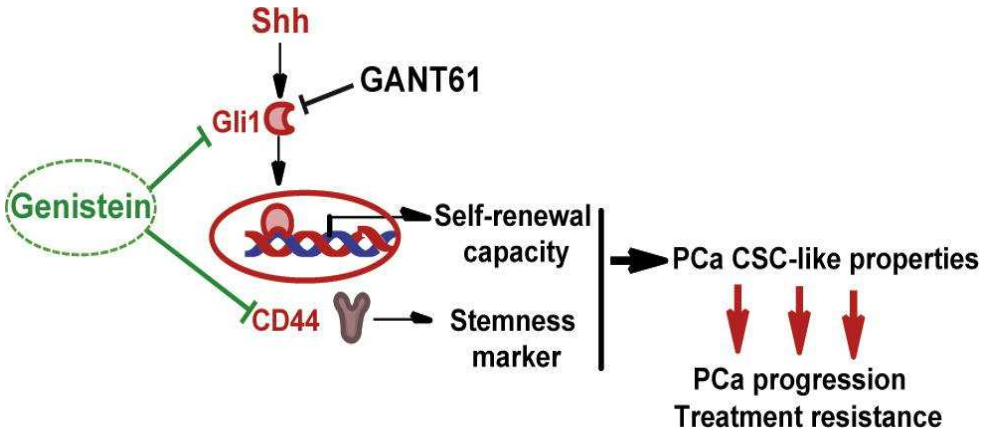

Figura 11. Efectos de la genísteina sobre CSCs de cáncer de páncreas. Fuente: (Zhang et al., 2012a).

Entre los inhibidores de la vía Hh (Figura 12) mediante Smo encontramos la ciclopamina y la jervina, dos compuestos con capacidades teratogénicas (Cooper et al., 1998); (Chen et al., 2002a).

Otras aproximaciones terapéuticas son los inhibidores sintéticos, entre los cuales podemos encontrar SANT1, Cur-61414 o AZD8542 (Chen et al., 2002b; Williams et al., 2003; Hwang et al., 2012). Otros inhibidores actúan a nivel de la unión de Hh-PITCH1, como es el caso de robotnikinin, del que se ha descrito *in vitro* la inhibición de la vía de señalización Shh de manera dosis-dependiente (Stanton et al., 2009).

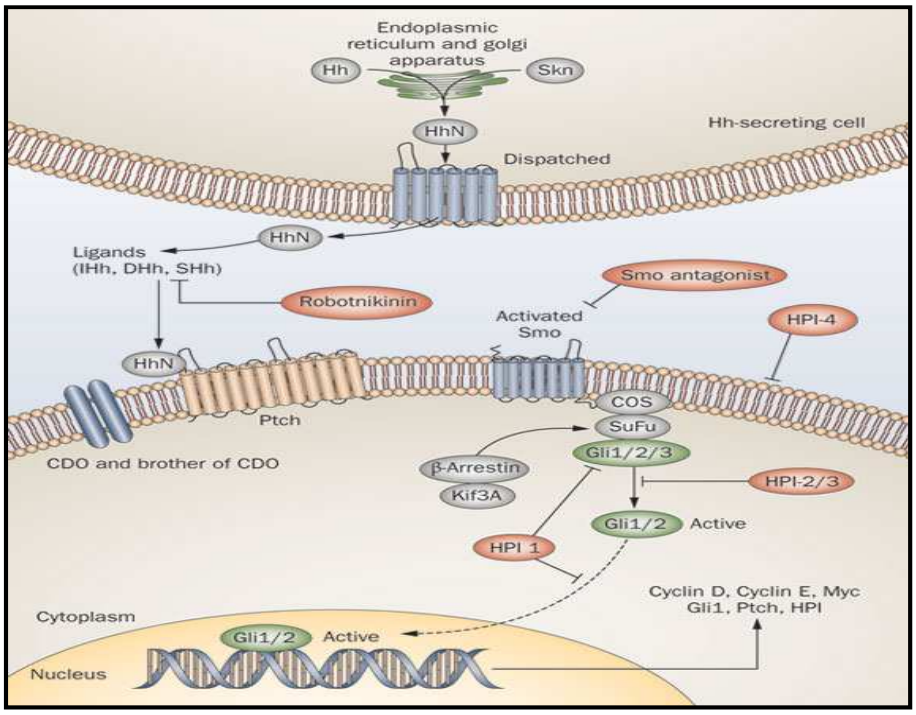

Figura 12. Inhibición de la vía de señalización Hedgeogh. Fuente: (Takebe et al., 2011).

b.) Terapias dirigidas frente a la vía Notch

En la vía de señalización de Notch el complejo γ-secretasa juega un papel fundamental, por lo que se ha convertido en un objetivo para el desarrollo de compuestos terapéuticos frente a Notch (Figura 13). Es el caso de los inhibidores de la actividad γ-secretasa, que previenen la activación del receptor Notch (Purow, 2012). Estos inhibidores han sido propuestos como estrategias terapéuticas frente a diferentes tipos de cáncer (Li et al., 2007; Meng et al., 2009; Watters et al., 2009; Purow, 2012; Hassan et al., 2013). PF-03084014 es una pequeña molécula desarrollada por Pfizer que inhibe la γ-secretasa, actualmente en ensayos clínicos (Fase I/II) la cual bloquea la activación proteolítica de los receptores Notch, inhibiendo la ruta de señalización e induciendo apoptosis en células tumorales (Lanz et al., 2010; Wei et al., 2010).

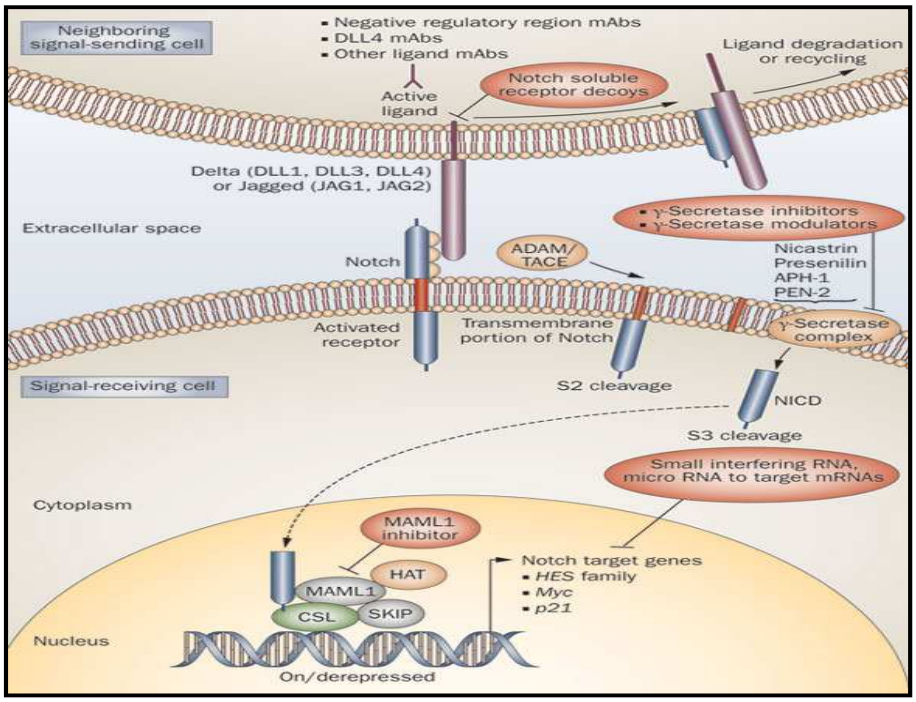

Figura 13. Inhibición de la vía de señalización Notch. Fuente: (Takebe et al., 2011).

El compuesto natural epigalocatequin-3-galate, el polifenol más abundante en el té verde es capaz de disminuir los niveles de Notch a nivel transcripcional, dando lugar a la inhibición de la vía de señalización Notch. Se ha demostrado que es capaz de inhibir en carcinoma escamoso de cabeza y cuello la capacidad de autorenovación de las CSCs mediante la supresión de la capacidad de formación de esferas y atenuando la expresión de marcadores de células tumorales, como Oct4, Sox2 o Nanog (Lee et al., 2013).

c.) Terapias dirigidas frente a la vía Wnt/β-catenina

Se ha observado que mutaciones en la proteína β-catenina provocan su acumulación en el núcleo dando lugar a la activación de genes tales como *c-Myc* o *ciclina D1*, que originan la proliferación descontrolada de las células tumorales, como es el caso del cáncer colorectal (Morin et al., 1997).

Uno de los compuestos naturales que se ha estudiado por tener actividad sobre esta vía de señalización es el resveratrol, flavonoide vegetal capaz de inhibir la actividad transcripcional mediada por β-catenina al intervenir en la interacción con T cell transcription factor 4 (TCF4) e inhibir la proliferación en células de cáncer colorectal (Chen et al., 2012). Otro compuesto natural, la curcumina, un polifenol de origen

vegetal obtenido de la planta *Curcuma longa* (Lin et al., 2009). Se ha observado que este compuesto es capaz de inhibir la expresión de diferentes componentes de la vía Wnt, tales como β-catenina, ciclina D1 o slug y alterar proteínas integrales como GSK3β y E-cadherina en líneas tumorales de cáncer de mama (Prasad et al., 2009).

Otra estrategia antitumoral, además de las vías anteriormente mencionadas, consiste en la inducción de apoptosis de manera selectiva en la subpoblación de CSCs.

La salinomicina (Figura 14) se extrajo por primera vez a comienzos de los años setenta, a partir del organismo *Streptomyces albus* (Miyazaki et al., 1974).

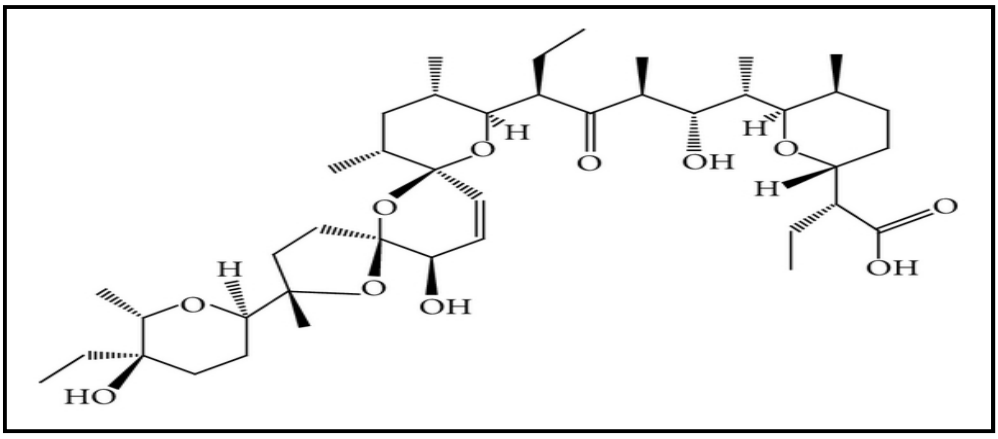

Figura 14. Fórmula estructural de la salinomicina. Fuente: (Naujokat and Steinhart, 2012).

Este compuesto, ionóforo de potasio, posee actividad antibiótica, utilizada durante años para el control de la coccidiosis en pollos y vacas (Danforth et al., 1977). El mecanismo de actuación de la salinomicina se ha estudiado en células de páncreas, donde induce apoptosis mediante el aumento intracelular de las especies reactivas del oxígeno (ROS), el cual va acompañado de una disminución del potencial de membrana mitocondrial, la traslocación de la proteína Bax a la mitocondria, liberación del citocromo c al citoplasma, activación de la caspasa-3, ruptura de PARP-1, así como una disminución en los niveles de expresión de la proteína implicada en la supervivencia celular Bcl-2 (Kim et al., 2011). Además, los efectos apoptóticos de la salinomicina han sido estudiados en subpoblaciones de CSCs de otros tipos de cáncer, como leucemia, cáncer de mama o cáncer colorectal (Fuchs et al., 2010; Gong et al., 2010; Zhou et al., 2013a).

Otro compuesto que ha sido estudiado debido a su capacidad para inducir apoptosis en CSCs es la rottlerina, un inhibidor de la ruta de señalización de la proteína quinasa C-delta (PKC-δ) (Gschwendt et al., 1994), el cual ha demostrado inducir apoptosis mediante la inhibición de la vía PI3K/Akt/mTOR en la subpoblación de CSCs de cáncer de páncreas, así como la activación de la ruta de las caspasas (Singh et al., 2012).

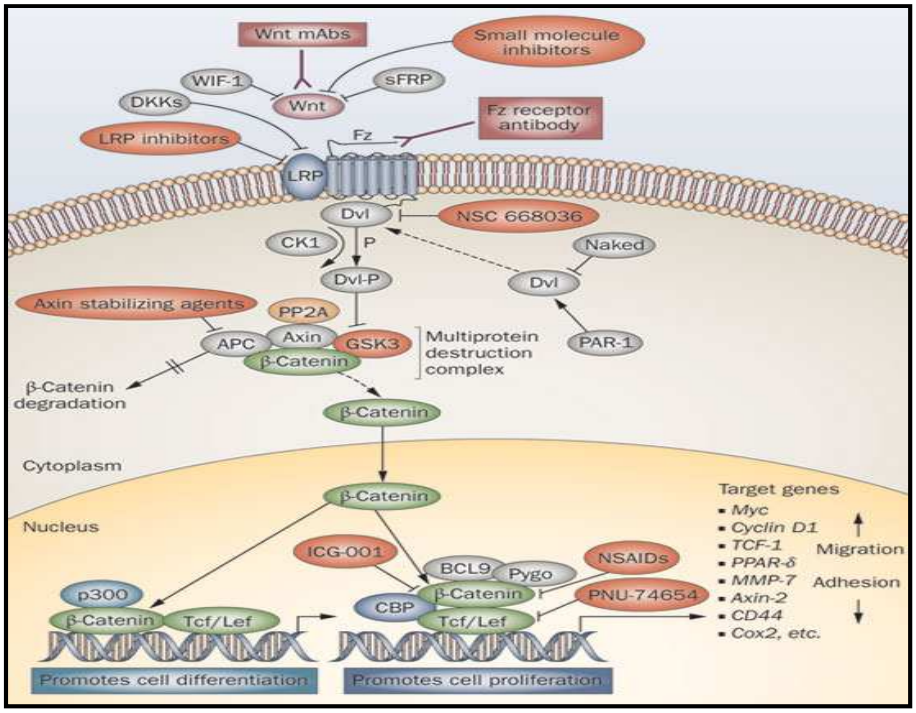

Figura 15. Inhibición de la vía de señalización Wnt/β-catenina. Fuente: (Takebe et al., 2011).

7. TRATAMIENTO DEL CÁNCER

Los tratamientos más utilizados frente al cáncer son:

a.) Quimioterapia: Este tipo de terapia se caracteriza por sus efectos sobre el ciclo celular. Las células cancerígenas muestran una proliferación incontrolada, debido a la adquisición de mutaciones a nivel de proto-oncogenes o genes supresores de tumores. Debido a esto, estas células se vuelven insensibles ante las señales de inhibición del crecimiento y son capaces de evadir la muerte celular programada o apoptosis. Los compuestos quimioterapéuticos provocan la muerte celular por apoptosis mediante la interferencia con el ADN o bien mediante la acción sobre proteínas clave

para la división celular. Sin embargo, este tipo de compuestos presentan el inconveniente de ser citotóxicos para las células normales en división (Mitchison, 2012). En líneas generales, la quimioterapia es utilizada con tres objetivos principales: disminuir la masa tumoral, antes de la cirugía, con el fin de realizar una operación lo más conservativa posible. A este tipo de quimioterapia se le conoce como neo-adyuvante. En segundo lugar, puede ser administrada de forma conjunta con radioterapia, es la quimioterapia concomitante. La quimioterapia también puede ser administrada tras la cirugía, con el objetivo de prevenir la aparición de metástasis, es la terapia adyuvante (Ottevanger and De Mulder, 2005).

b.) Radioterapia: La radioterapia es uno de los elementos básicos utilizados en clínica para combatir el cáncer. Se puede estimar que la proporción de pacientes que debería recibir radioterapia está alrededor de un 50-60% de los tumores detectados (Delaney et al., 2005; Palacios Eito et al., 2013). La utilización de radiaciones de tipo ionizante para el tratamiento del cáncer se basa en la capacidad de este tipo de radiaciones de inducir daños irreparables en el ADN mediante su ruptura (Pajonk et al., 2010).

c.) Cirugía: En el cáncer, la cirugía es utilizada ampliamente, dependiendo de la localización y extensión del tumor. Dentro de estos parámetros, podríamos diferenciar entre la cirugía paliativa y curativa. En la cirugía curativa es eliminada la totalidad del tumor, no quedando tumores microscópicos en la región operada, mientras que la cirugía paliativa trata de extirpar la mayor parte del tumor, aunque no puede evitar la aparición de márgenes microscópicos positivos para el tumor. Entre los avances que han aparecido en los tratamientos de cirugía para los enfermos de cáncer podemos destacar la terapia fotodinámica, la terapia de ablación por radiofrecuencia, criocirugía, ablación mediante la utilización de microondas o la utilización de ultrasonidos de alta intensidad concentrados (Noguchi, 2007).

7.1. Tratamiento del cáncer de mama

Según la sociedad Española de Oncología Médica, el tratamiento del cáncer de mama se podría establecer según el estadío en el que se encuentre el mismo. Dentro de los diferentes estadíos, podemos encontrar diferentes tipos de tratamientos:

- Cirugía conservadora o mastectomía más extirpación de los ganglios axilares o mediante la técnica del ganglio centinela. La cirugía conservadora consiste en la aplicación de cirugía para eliminar el tumor conservando la estructura de la mama, seguida por un tratamiento mediante radioterapia, siendo este tratamiento efectivo en estadios tempranos de cáncer de mama y presentando una supervivencia equivalente a la mastectomía (van Dongen et al., 1992; Jacobson et al., 1995; Fisher et al., 2002; Santiago et al., 2004). En la técnica del ganglio centinela, el cirujano extirpa los nódulos centinelas y estos son examinados en busca de metástasis. En caso de la aparición de metástasis, se procede a la disección del nódulo linfático axilar (Damgaard et al., 2013).

- Utilización de quimioterapia neoadyuvante si los factores de riesgo lo aconsejan. Este tipo de terapia es utilizado para disminuir el tamaño inicial del tumor para facilitar la terapia que permita la conservación de la mama (Kaufmann et al., 2012). Normalmente se administra de forma intravenosa en ciclos, con una duración de entre 4-6 meses, según el tratamiento elegido. Los tratamientos más utilizados son antraciclinas (doxorrubicina o epirrubicina) o taxanos (paclitaxel o docetaxel) (De Laurentiis et al., 2008; Vriens et al., 2013). Los taxanos fueron introducidos por primera vez en clínica a principios de los años 90. Tanto paclitaxel como docetaxel mostraron mayor eficacia que los tratamientos utilizados con anterioridad (ciclofosfamida, metotrexato, 5-fluorouracilo y prednisona) en cáncer de mama metastásico y de estadio temprano (Bishop et al., 1999; Evans et al., 2005). Actualmente, los taxanos se han convertido en una opción viable para el tratamiento del cáncer de mama de estadio temprano y cáncer de mama metastásico (King et al., 2009; Palmieri et al., 2010).

- Uso de radioterapia adyuvante si se realizó la cirugía conservadora o las características del tumor lo aconsejan. Gracias a los datos aportados por algunos ensayos clínicos se ha observado que la administración de radioterapia tras la cirugía conservadora de mama no solo disminuye el riesgo de recurrencia sino que también disminuye de forma moderada el riesgo de muerte por este tipo de cáncer. Esto se debe a que la utilización conjunta de cirugía y radioterapia elimina los focos microscópicos del tumor reduciendo la posibilidad de la aparición de recurrencia y metástasis distales (Fisher et al., 2002; Winzer et al., 2004; Darby et al., 2011). Actualmente, la radioterapia se ha convertido en el tratamiento estándar del cáncer de mama de estadio temprano, donde se utiliza una dosis de 60/66Gy/30-33 fracciones/61/2 semanas. Entre

las estrategias más modernas de radioterapia podemos encontrar la irradiación total de mama fraccionada (Whole breast irradiation, WBI) y la irradiación acelerada parcial de mama (Accelerated Partial Breast Irradiation, APBI) (Bourgier et al., 2013).

- Hormonoterapia adyuvante, en el caso de que el tumor sea hormonodependiente. La elección del tratamiento puede variar según sea la paciente premenopaúsica (prescripción de tamoxifeno) o postmenopaúsica (prescripción de inhibidores de aromatasa) (Charehbili et al., 2013; Zeng et al., 2013).

Tamoxifeno es considerado como un modulador selectivo del receptor de estrógenos, bloqueando la acción de los estrógenos mediante su unión a una de las dos regiones de activación del receptor de estrógenos (ER)-AF-2. Su mecanismo de acción se basa en la inhibición tanto de la traslocación como de la unión al núcleo del receptor de estrógenos (Clemons et al., 2002).

Los inhibidores de aromatasa son unos potentes inhibidores de la síntesis de estrógenos, pudiendo ser divididos actualmente (tercera generación) en inhibidores esteroideos (exemestano) y no esteroideos (anastrozole, letrozole), los cuales interaccionan con la enzima aromatasa de diferente forma. Los primeros se unen de manera no covalente y reversible a la enzima, mientras que los inhibidores de naturaleza no esteroidea se unen de manera covalente e irreversible (Miller et al., 2008; Sainsbury, 2013).

La utilización de hormonoterapia se está convirtiendo en una terapia de elección en el caso de pacientes que presentan cáncer de mama positivos para receptores de hormonas y va dirigida a la disminución del tamaño del tumor previo a la cirugía, observándose una mayor efectividad en este tipo de cáncer que la quimioterapia convencional (Petit et al., 2010).

Para el tratamiento de tumores HER-2 positivos, trastuzumab y lapatinib son algunos de los tratamientos adyuvantes más utilizados. El mecanismo de acción de trastuzumab implica la unión al dominio extracelular del receptor HER2, reduciendo de esta manera la cascada de señalización a través de las vías PI3K/Akt y Ras/Raf/MEK/MAPK. Esto da lugar a una sobreregulación de p27 a través de la activación de la síntesis de proteínas y su estabilización (Le et al., 2005). Además, este mecanismo de actuación implica la inhibición de la kinasa de la ciclina D induciendo

una parada del ciclo celular en la fase G_1 (Le et al., 2005), así como una inhibición de la reparación del ADN tras el daño por quimioterapia (Pietras et al., 1999) y radioterapia (Pietras et al., 1999). Por otra parte, el tratamiento con trastuzumab incluye otra serie de efectos con beneficios en el tratamiento antitumoral, tales como el efecto antiangiogénico que provoca una disminución en la secreción de factores angiogénicos como el VEGF y el TGF-α (Izumi et al., 2002). Otro de los tratamientos más utilizados dirigido frente a tumores que sobreexpresan HER2 es lapatinib. Esta pequeña molécula actúa como inhibidor de la unión del ATP al dominio intracelular tirosina-quinasa del receptor. Se ha observado que lapatinib actúa a este nivel, inhibiendo los receptores HER2 y EGFR (Rusnak et al., 2001). Al igual que trastuzumab, este fármaco inhibe las vías PI3K/Akt y Ras/Raf/MEK/MAPK, promoviendo la parada del ciclo celular, así como el proceso de apoptosis (Konecny et al., 2006).

En el caso en el que el tumor se encuentre en estadio IV, y se ha extendido mediante metástasis al resto del organismo, la posibilidad de curación es prácticamente nula, por lo que el tratamiento está dirigido a la cronificación y paliación de la enfermedad. Entre los tratamientos utilizados están la cirugía, aunque los estudios realizados no dejan claro el efecto sobre la enfermedad (Babiera et al., 2006; Bafford et al., 2009).

7.2. Tratamiento del cáncer colorectal

Uno de los tratamientos adyuvantes más utilizados en el cáncer colorectal es el 5-fluorouracilo (5-FU), cuya eficacia se ha demostrado en células en fase S del ciclo celular, inhibiendo la enzima timidilato- sintasa, la cual está involucrada en la síntesis de ADN. El 5-FU, es un agente quimioterapéutico utilizado desde año 1957 en el tratamiento del cáncer de colon (Grem, 2000). Como muestra la Figura 16, Este compuesto orgánico es un heterociclo con una estructura similar a la que presentan las moléculas pirimidínicas del ADN y ARN, es un análogo del uracilo con un átomo de fluor en el C-5 en lugar del hidrógeno (Rutman et al., 1954).

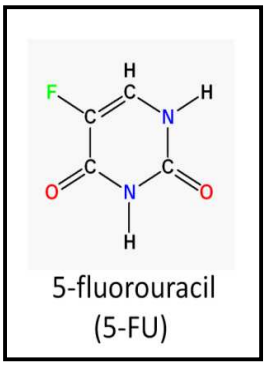

Figura 16. Estructura del 5-fluorouracilo. Fuente: (Alvarez et al., 2012).

Su mecanismo de acción implica la inhibición de la enzima timidilato sintasa por el 5´-fluoro-2´-desoxiuridina-5´-monofosfato (FdUMP), incorporación de 5-fluorouridina-5´-trifosfato (FUTP) al ARN y la incorporación de 5-fluoro-2´-desoxiuridina-5´-trifosfato (FdUTP) al ADN. De entre estos efectos, la inhibición de la expresión de la timidilato sintasa es el que mayormente se ha asociado al efecto antitumoral del 5-FU (Aschele et al., 2002; Li et al., 2004a; Noordhuis et al., 2004; Noda et al., 2006). En la práctica clínica se ha observado que la vida media del 5-FU en plasma es relativamente corta (sólo unos 11 min), por lo que al inyectarlo en forma de "bolus" se observó que sólo una pequeña proporción de células tumorales serían susceptibles al tratamiento (Fraile et al., 1980). Por esta razón, actualmente se ha recurrido a la administración del 5-FU mediante infusión continua (siendo liberado durante periodos de 24-48 horas) en lugar del tratamiento anteriormente mencionado, demostrándose una eficacia similar, pero con una toxicidad reducida (Chau et al., 2005; Poplin et al., 2005).

Para potenciar los tratamientos basados en el 5-FU, se ha sintetizado un gran número de compuestos basados en su estructura, tales como la capacitabina, tegafur o gemcitabina (Komatsu et al., 2000; Schellens, 2007; Hodge et al., 2011). Además, se ha recurrido a su utilización conjunta con otros compuestos quimioterapéuticos. Un ejemplo es la utilización conjunta de oxaliplatino/5FU/leucovorina (FOLFOX), donde se aprovecha la eficacia del oxaliplatino frente a la resistencia al cisplatino que presentan determinadas líneas celulares de carcinoma de colon, así como su actividad sinérgica. Además, la utilización en el mismo tratamiento de leucovorina aumenta la supervivencia libre de enfermedad (de Gramont et al., 2000). En el caso de cáncer de colon metastásico, los tratamientos basados en la utilización conjunta de capecitabina

mas irinotecan (XELIRI) y 5-FU junto a irinotecan (FOLFIRI) presentaron una eficacia similar, con unos efectos secundarios parecidos (Skof et al., 2009).

7.3. Nuevas moléculas selectivas frente al cáncer

Uno de los objetivos más perseguidos por los tratamientos actuales contra el cáncer, es el de encontrar una terapia selectiva, donde sólo las células cancerígenas y no las normales se vieran afectadas por el tratamiento. El termino *bala mágica* (magic bullet) hacía referencia al primer tratamiento eficaz de la sífilis y plasmaba el principio fundamental de la quimioterapia: la toxicidad selectiva (Winau et al., 2004). La idea de la terapia selectiva se basa en actuar de forma selectiva sobre aquellas rutas que se encuentran alteradas en las células cancerígenas. Actualmente se aplican un gran número de terapias selectivas, que han permitido aumentar la supervivencia media de los pacientes en un gran número de cánceres. Sin embargo, la aparición de resistencia a estos tratamientos, explicada en gran medida por la presencia de las CSCs hace que aumenten los esfuerzos por perfeccionar este tipo de terapias y aboga por buscar una terapia selectiva frente a las CSCs.

A continuación se exponen algunas de las terapias selectivas utilizadas en la actualidad en el tratamiento del cáncer y la búsqueda de tratamientos que de forma selectiva actúen frente a las CSCs.

a.) Terapias dirigidas frente a Her-2

La sobreexpresión del receptor de crecimiento epidérmico-2 (HER-2) y de su proteína se encuentran presentes en aproximadamente el 20% de los casos de cáncer de mama (Reese and Slamon, 1997; Gianni et al., 2011).

Trastuzumab (Herceptin) es un anticuerpo humanizado dirigido frente al dominio extracelular del receptor HER-2, ofreciendo beneficios clínicos en mujeres con cáncer de mama HER-2 positivo (Smith et al., 2007; Perez et al., 2011). Sin embargo, pacientes tratados con Trastuzumab solo o en combinación con quimioterapia llegan a presentar entre un 20%-50% de resistencia al tratamiento (Vogel et al., 2002; Yin et al., 2011). Algunos de los mecanismos de resistencia implicados son la inhibición de la unión de Trastuzumab al receptor mediante la ruptura del dominio extracelular, interacciones con otros miembros de la familia ErbB, expresión constitutiva de la vía de señalización PI3KIN/Akt o pérdida de la actividad de PTEN (Nagata et al., 2004;

Scaltriti et al., 2007; Kataoka et al., 2010; McDonagh et al., 2012). Se ha observado que la vía de señalización de HER-2 juega un papel importante en el mantenimiento de las poblaciones de CSCs. La sobreexpresión de HER-2 está relacionada con la expresión de la enzima ALDH1, aumentando la proporción de CSCs (Ginestier et al., 2007). Trastuzumab disminuye la población de células madre tumorales en células sensibles (Korkaya et al., 2008).

Lapatinib (Tykerb) es una pequeña molécula, inhibidor lipofílico dual de quinasas que ejerce su efecto sobre EGFR y HER2 aprobado para el tratamiento de cáncer de mama metastásico HER2+ (Ryan et al., 2008). Por otra parte, estudios preclínicos han demostrado la actividad sinérgica de la utilización conjunta de Trastuzumab y Lapatinib en pacientes de cáncer de mama HER2+ (Blackwell et al., 2010).

b.) Terapias dirigidas a inhibir la angiogénesis

La angiogénesis es el proceso por el cual se forman nuevos vasos sanguíneos, originando en el caso del cáncer el paso de un estado preinvasivo y quiescente a una forma invasiva y metastásica (Li et al., 2012). La inhibición de este proceso es uno de los efectos buscados por algunas de las terapias selectivas en desarrollo. En este contexto, Bevacizumab, un anticuerpo monoclonal humanizado, está dirigido frente al VEGF, bloqueándolo y dando lugar a la alteración y destrucción del tejido vascular aberrante promovido por el tumor (Pavlidis and Pavlidis, 2013). Sin embargo, su utilización está siendo tema de debate al ser revocada su aprobación por la FDA, pero no por la comisión Europea, que aprobó su uso en combinación con paclitaxel y capacitabina (Miles et al., 2013). Otra molécula, Sunitinib, es capaz de inhibir varios receptores tirosina quinasa, tales como VEGFR, PDGFR, kit y Flt-3 (Mendel et al., 2003). Aunque su utilización en cáncer de mama avanzado está siendo estudiada, los resultados no muestran una mejora en la supervivencia media (Barrios et al., 2010).

Recientes estudios preclínicos sugieren que la utilización de agentes antiangiogénicos puede aumentar las propiedades invasivas y metastásicas de las células de cáncer de mama (Ebos et al., 2009; Paez-Ribes et al., 2009). Estos resultados pueden deberse a que la utilización de agentes antiangiogénicos provoca un estado de hipoxia que puede acelerar el crecimiento del tumor y la aparición de metástasis mediante el

aumento de la población de CSCs. Recientes estudios *in vivo* con células de cáncer de mama han demostrado que la administración de sunitinib y bevacizumab incrementaron la población de CSCs debido a la expresión del factor inducible por hipoxia (HIF-1α) a través de la activación de la vía de señalización Wnt (Conley et al., 2012).

c.) Terapias dirigidas frente a mTOR

La vía de señalización de mTOR juega un papel crucial como regulador del crecimiento celular y la proliferación. Esta treonin quinasa regula el crecimiento celular y la progresión del ciclo celular integrando señales provenientes de estímulos tales como nutrientes y factores de crecimiento (Advani, 2010). En este sentido, Everolimus es un compuesto que inhibe mTOR mediante su unión alostérica a mTORC1 (Efeyan and Sabatini, 2010). En estudios preclínicos, la utilización combinada de everolimus con inhibidores de aromatas resultan en una inhibición sinérgica de la proliferación e inducción de apoptosis (Boulay et al., 2005). Actualmente, la eficacia de Everolimus está siendo investigada en diversos ensayos clínicos (Perez and Spano, 2012). El efecto de Everolimus junto a docetaxel en CSCs de cáncer de mama se ha estudiado obteniéndose un efecto inhibidor sobre esta población (Zhang et al., 2012b).

8. INTERFERÓN

El interferón (IFN), molécula descubierta a mediados de los años 50 del siglo pasado, confiere a las células susceptibles de ser infectadas por virus resistencia a la infección por los mismos (Jonasch and Haluska, 2001). Las moléculas pertenecientes a la familia de los interferones son citoquinas que además de proteger a la célula de infecciones virales, también modulan el crecimiento y la diferenciación celular, siendo las primeras citoquinas en ser utilizadas en ensayos clínicos para tratar enfermedades infecciosas o desordenes de tipo neurológico. Actualmente, los interferones son utilizados como primera línea de terapia en enfermedades tales como hepatitis B y C, melanoma o esclerosis múltiple (Meyer, 2009).

Atendiendo a su unión al receptor, se pueden clasificar en tres clases diferentes (Hervas-Stubbs et al., 2011).

a.) Interferón tipo I:

Incluye 13 subtipos de IFN y el IFN-β. Ambos tipos presentan además de propiedades antivirales, un importante papel en el control del crecimiento celular y un potente efecto inmunomodulador y antiangiogénico (Figura 17). El efecto de inhibición del IFN sobre el crecimiento celular viene determinado por el control que ejerce sobre el ciclo celular, provocando una acumulación en la fase G_1, una prolongación de la fase S y un bloqueo de la transición a la fase G_2/M. Otros estudios han demostrado que la inhibición del crecimiento celular viene determinada por la inducción de apoptosis (Yanai et al., 2002).

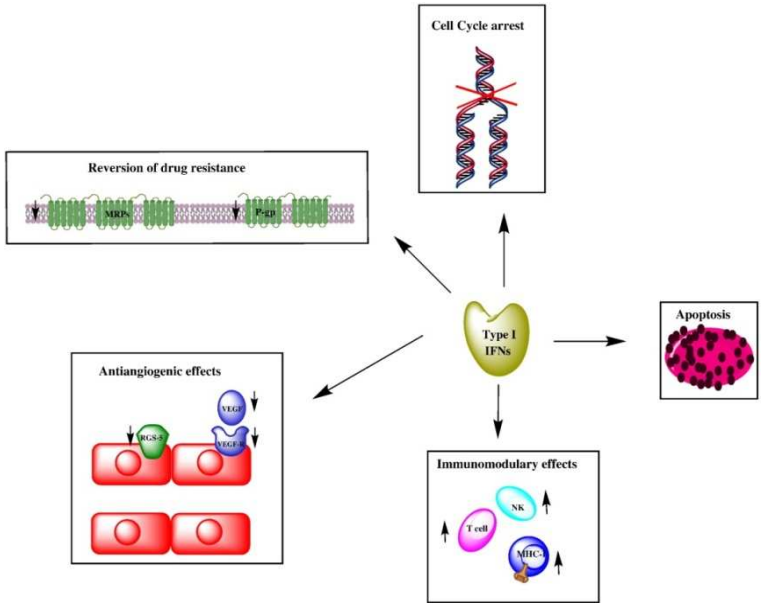

Figura 17. Mecanismos moleculares anticancerígenos del IFN-I: a) Parada del ciclo celular, b) inducción de apoptosis, c) efecto inmunomodulador, d) efectos antiangiogénicos, d) reversión de la resistencia a drogas. Fuente: (Dicitore et al., 2013).

La inducción de los genes IFN α/β está mediada por la activación de receptores de patrones de reconocimiento (PRRs), que incluyen TLRs, el gen-I inducible por ácido retinoico (RIG-I), y el gen 5 asociado a la diferenciación de melanoma (Mda5) (Takaoka et al., 2005; Gitlin et al., 2006; Ioannidis et al., 2013; Pothlichet et al., 2013). Además, se ha observado que la producción de IFN de tipo I puede ser inducida por virus o bacterias. Algunos potentes inductores de la producción de IFN incluyen a nivel

molecular el ARN de cadena doble (ARN_{ds}), ARN viral de cadena simple (ARN_{ss}), o el ADN de origen viral (Meyer, 2009).

La cascada de señalización dependiente de IFN I (Figura 18) comienza con su unión a un complejo de receptores denominado receptor IFN α/β (IFNAR), compuesto de dos subunidades, las cuales se encuentran asociadas a las proteínas tirosina quinasa Janus (Jak PTKs) y son las encargadas al activarse, de fosforilar STAT1 y STAT2, miembros de la familia de transductores de señales y activación de la transcripción (STATs) (Darnell et al., 1994; Stark et al., 1998). Tras esto, se forma un complejo activador de la transcripción, que también incluye al factor de transcripción IRF9/p48/ISGF3γ (Marie et al., 2000). Este complejo se transloca al núcleo y da lugar a la transcripción de genes inducidos por IFN (ISGs)(Darnell et al., 1994). Algunas de las proteínas inducidas están implicadas en procesos tales como la regulación de la composición de la membrana, señales de stress celular, apoptosis, ciclo celular o presentación de antígenos (Stark et al., 1998; Sen, 2001).

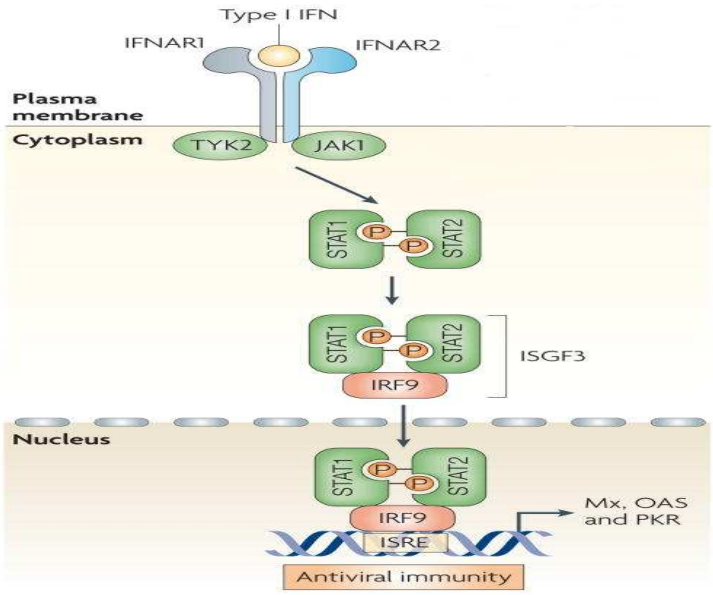

Figura 18. Ruta de señalización regulada por IFN de tipo I. Fuente: Takaoka Akinori and Yanai Hideyuki, 2006

Una de las moléculas inducidas por IFN de gran relevancia debido a sus funciones biológicas es la proteína quinasa dependiente de ARN_{ds} (PKR), una enzima que juega un papel fundamental en el mecanismo de defensa frente a la infección por virus (Okumura et al., 2013).

b.) Interferón tipo II:

Representado por el IFN de tipo γ. Posee propiedades antivirales e inmunomoduladoras. Este tipo de IFN no se encuentra relacionado estructuralmente con los IFNs de tipo I, además de unirse a un receptor diferente (Bach et al., 1997). Su producción se encuentra regulada por las citoquinas secretadas por las células presentadoras de antígenos, sobre todo interleukina (IL)-12 e IL-18 (Munder et al., 2001). El principal mecanismo por el cual el IFNγ ejerce su actividad antiviral, antiproliferativa e inmunomoduladora es mediante la inducción de la vía del catabolismo del triptófano, a través de la ruta de señalización de la kineurina, la cual se encuentra involucrada en numerosos procesos fisiológicos y patofisiológicos (Munn et al., 1999; Jusof et al., 2013).

Recientemente se está estudiando el efecto potenciador del IFNγ en la repuesta inmune a frente a las células cancerígenas como terapia, tratando de utilizar bajas dosis para evitar la toxicidad de este tipo de IFN en altas concentraciones (Radice et al., 2013).

c.) Interferón tipo III:

El interferón tipo III fue descrito por primera vez en 2003, describiéndose tres citoquinas altamente relacionadas, conocidas como IFNλ1, IFNλ2 y IFNλ3 (Kotenko et al., 2003). La expresión de este tipo de interferón se realiza en respuesta a la señalización mediada por TLR (Toll-like Receptors) provocada por infecciones virales y bacterianas, siendo más pronunciada en células plasmocíticas dendríticas y en células epiteliales (Coccia et al., 2004). Varios estudios preclínicos han demostrado los efectos antitumorales mediados por IFNλ en ratones y líneas tumorales de cáncer de mama, carcinoma esofágico o tumores neuroendocrinos (Sato et al., 2006; Zitzmann et al., 2006; Li et al., 2010).

8.1. Interferón y cáncer

A partir de los años 70 del siglo pasado, el perfeccionamiento de la técnica para producir IFN en cantidades suficientes permitieron la puesta en marcha de los primeros ensayos clínicos destinados a buscar la cura de determinados tipos de cáncer, tales como el osteosarcoma. A partir de aquí, se desarrolló la técnica de ADN recombinante que

permitió la producción de IFN para ser utilizado en ensayos clínicos (Goldstein and Laszlo, 1986). En los años 80, tanto el IFNα2a como el IFNα2b fueron aprobados por la FDA para su uso terapéutico en diferentes enfermedades, tales como la leucemia mielógena crónica, linfoma folicular, melanoma maligno o sarcoma de Kaposi (Bekisz et al., 2010).

8.2. Terapia combinada: interferón y fármacos antitumorales

Debido a la creciente necesidad de buscar tratamientos alternativos para el cáncer que potencien los efectos de los ya existentes y disminuyan su toxicidad se están realizando numerosos estudios en los que se potencia su uso combinado con IFN.

Existen diversos estudios donde la combinación de IFNα junto con quimioterapéuticos convencionales como el 5-FU ha mejorado la citotoxicidad en melanoma maligno y otros tipos de tumores, como el carcinoma renal, cáncer de páncreas o cáncer colorectal (Mulder et al., 1990; Bajetta et al., 1994; Evrard et al., 1999). Actualmente, el único agente aprobado tanto en Europa como en los EEUU como agente adyuvante en melanoma es el interferón alfa-2b (IFNα2b), donde se cree que actúa ejerciendo un papel inmunomodulador y antiproliferativo (Ascierto and Kirkwood, 2008) observándose en algunos ensayos clínicos una mejora en la supervivencia (Kirkwood et al., 1996) y unos resultados significativos en la supervivencia libre de recaída (Wheatley et al., 2003).

La aplicación simultánea de Gemcitabina, 5-Fluorouracilo e IFNα dio lugar a la curación completa de un caso clínico a 10 años de un carcinoma renal de células sarcomatoides metastásicas de bajo riesgo (Conter et al., 2013). .

Se ha demostrado en líneas tumorales de cáncer de mama y colon que el uso combinado de IFNα y nuevos derivados purínicos (Bozepinib) actúan de manera sinérgica, incrementando el efecto citotóxico, además de potenciar el efecto proapoptótico del compuesto. De igual manera, Bozepinib es capaz de inducir la formación de autofagosomas (mecanismo de muerte celular alternativo a la apoptosis, normalmente inactivada en células tumorales), viéndose potenciada en presencia de IFNα (Marchal et al., 2013).

9. PKR

PKR juega un papel crucial en la respuesta de las células eucariotas frente a las infecciones virales. Además, ha sido relacionado con procesos que incluyen diferenciación, apoptosis y respuesta a estrés. La inducción de la expresión de PKR resulta en la fosforilación del factor de transcripción eIF2a, inhibiendo la síntesis de proteínas (Barber et al., 1995; Samuel, 2001). PKR consta de un dominio de unión a ARN de doble cadena ($_{ds}$RBD), el cual comprende dos copias en tándem de motivos de unión a ARN de doble cadena ($_{ds}$RBM) y un dominio quinasa catalítico. El dominio $_{ds}$RBD interactúa con el ARN_{dc} en una secuencia no específica y no se une de forma apreciable al ADN_{dc} o a híbridos ARN-ADN (Hunter et al., 1975). La activación de PKR ocurre mediante la presencia de ARN_{dc} de 80 pb o de mayor longitud, sin requerimientos específicos en la secuencia, lo cual explica por qué PKR puede ser activado por ARN_{dc} de diversos orígenes (Garcia et al., 2007). La activación de PKR implica la fosforilación de eIF-2α. Esta fosforilación en el residuo S51 previene el reciclaje de este factor, necesario para la traducción, dando lugar a su inhibición. Debido a la acumulación de ARN_{dc}, PKR dispara la fosforilación de eIF-2α, inhibiendo de esta manera la traducción del ARN_m del virus, ejerciendo su actividad antiviral frente a un amplio espectro de virus que portan tanto ADN como ARN (Gale et al., 2000; Garcia et al., 2007).

En la ruta de señalización de PKR (Figura 19) también está implicada la familia de factores de transcripción NF-κβ, involucrados en la respuesta inmune e inflamatoria así como en procesos de diferenciación celular o apoptosis, entre otros (Donze et al., 2004). En este caso, la activación de esta ruta vendría determinada por la activación mediante PKR de IKK/NF-κβ (Ishii et al., 2001). El complejo IKK contiene una proteína estructural denominada IKKγ y dos subunidades quinasas, IKKα e IKKβ. Estudios realizados *in vivo* e *in vitro* indican que PKR sería la quinasa que fosforila Iκβα en respuesta a ARN_{ds}. Aunque PKR parece ser necesario para la transducción de la señal, evidencias posteriores indican que actuaría de forma indirecta en la activación de Iκβα (Garcia et al., 2007).

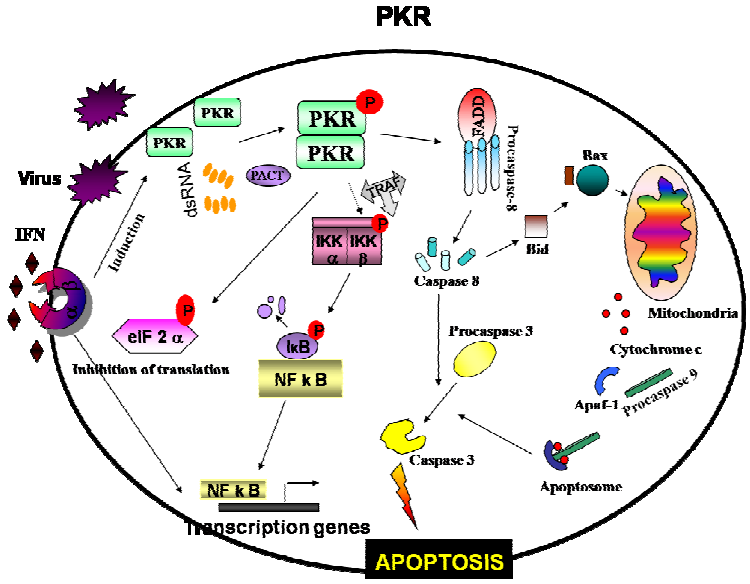

Figura 19: Ruta de señalización de PKR. Fuente: (Garcia et al., 2006; Garcia et al., 2007).

La inducción de apoptosis es una respuesta común a las infecciones por virus. Se ha demostrado que PKR esta implicada en la apoptosis inducida por un gran número de virus (Garcia et al., 2002). Sin embargo, PKR también está involucrado en la regulación de la apoptosis en ausencia de infección por virus, a través de la ruta de señalización FADD/caspasa 8. La inducción de apoptosis producida por PKR implica la activación tanto de la ruta intrínseca como de la ruta extrínseca de activación de caspasas, encontrándose por tanto activación de caspasa 8 y 9 de forma retro-alimentativa. La implicación del factor de transcripción NF-κβ en la inducción de apoptosis a través de la activación de PKR ha sido ampliamente discutida concluyendo que este factor puede actuar como pro-apoptotico o anti-apoptótico dependiendo del tipo de estímulo y de su intensidad (García MA et al. 2006, 2007).

II. JUSTIFICATION AND HYPOTHESIS

Recent studies have stimated that incidence of cancer for 2030 will be 20.3 million compared with 12.7 million stimated cases for 2008, being 13.2 predicted deaths related with cancer worldwide by 2030, compared with 7.6 million in 2008 (Bray et al., 2012). For this reason, improvement in cancer treatment is leading efforts worldwide.

At present, conventional anticancer therapies are aimed to target cancer cells limiting their proliferation or decreasing tumor size by killing them. So main efforts in drug industry have been to develop therapies based on compounds with cytotoxic and/or cytostatic effects either *in vitro* (established tumour cell lines) or *in vivo* (human cancer xenografts) assays (Kerbel, 2003; Zitvogel et al., 2008). Recently, there is an increased in cancer targeted therapies approaches based on the idea of limiting cytotoxic effects to tumour cells by improving drugs selectivity, resulting in a less harm to normal cells actuation, decreasing side effects and improving effectiveness. All this objectives are aimed to improve patient life quality and overall survival.

Our hypothesis is based in the following evidences:

1. Ultimately a great level of interest has arisen in the G_0/G_1 phase regulatory molecules such as cyclin D1, CdkIs, and p53 as potential therapeutic targets in diseases where control of inappropriate cellular proliferation would be a therapeutic benefit (Sherr, 1996). The use of cell-cycle-specific treatments in cancer therapy has greatly benefited from the major advances that have been recently made in the identification of the molecular actors regulating the cell cycle and from the better understanding of the connections between cell cycle and apoptosis (Marchal et al., 2004). Moreover, apoptotic defects in cancer cells are the primary obstacle that limits the therapeutic efficacy of anticancer agents, and hence the development of novel agents targeting programmed cell death pathways has become an imperative mission for clinical research. Although apoptosis has been considered as the typical mechanism for cell death, evidence currently available is accumulating that alternative cell death pathways such as autophagy process may play role in tumor response to chemotherapy (Mansilla et al., 2012). A potential mechanism of caspase-independent cell death is autophagy, which is defined as a controlled lysosomal degradation of macromolecules and organelles. In certain conditions, autophagy results in a form of cell death now described as type II programmed cell death, which is targeting as novel therapeutic strategies in cancer (Dalby et al., 2010). Moreover, senescence as a state of irreversible

growth arrest has important tumor suppression function by restricting cell proliferation and thereby impeding the accumulation of mutations. Furthermore, senescence induced by aberrant activation of oncogenes, oxidative stress, or DNA damage prevents cells at risk of malignant transformation from proliferating. Therefore, senescence offers an attractive therapeutic option if it can be induced in tumor cells (Kong et al., 2011).

2. Naturally occurring pyrimidine compounds have shown in vitro antiproliferative activities against the MCF-7 human breast cancer cell line in the micromolar range (Diaz-Gavilan et al., 2008), which suggests that these drugs may serve as prototypes for the development of even more potent structures, endowed with a new mechanism of action

3. Some of the most important signaling pathways involved in cancer are related with cell proliferation, differentiation and survival, which represent exciting targets for developing new antitumor drugs. Because signal transduction networks integrate multiple upstream inputs, targeting pathways downstream of the receptors could conceivably result in greater therapeutic efficacy and broader applicability. Moreover, kinase inhibitors that reduce the excessive proliferation signaling are revealed one of the most important emergent therapies against cancer (Janne et al., 2009; Neuzillet et al., 2014). For this reason, kinome profiling has arisen as an important tool to develop targeted therapies against kinases with aberrant expression directly involved in cancer pathology (Knight et al., 2010; Cho et al., 2012) and enables the discovery of novel targets for cancer therapy.

4. Although interferons are effective as single agents in certain clinical pathologic entities, increasing experience with these cytokines suggests that their greatest therapeutic potential may be realized in combination with other biological response modifiers, cytotoxic or antiviral agents 14. The apoptosis event has been well characterized during IFNα-combinations synergy; however, other mechanisms involved in the antitumor effectiveness of combinations have not been explored. PKR, which is induced by IFN type I, has been linked to normal cell growth and differentiation, inflammation, cytokine signalling, and apoptosis, and is involved in the antiviral and antitumor activities of these cytokines (Garcia et al., 2006). It has been recently suggested the major role of PKR in the induction of apoptosis by several chemotherapeutic drugs such as etoposide, doxorubicin and 5-fluorouracil (5-FU)

(Garcia et al., 2011; Peidis et al., 2011) with interesting expectative in the clinical use of this molecular target.

5. CSCs are a subpopulation of cells inside tumor with *stem cell* properties and have the ability to self renew, maintaining mass tumor by a combination of symmetric and asymmetric division (Boman et al., 2007) and are responsible of disease recurrence and metastasis (Clevers, 2011). Other CSCs properties include resistance to conventional chemo and radiotherapy (Moitra et al., 2011; Yang et al., 2013), a high tumorigenic potential when are transplanted into immunodeficient mice (Al-Hajj et al., 2004) or the possibility to identify then by superficial markers, sphere formation assays or intracellular activity such as aldehyde dehydrogenase activity assay (Li et al., 2009; Sun and Wang, 2010; Mannelli and Gallo, 2012). These properties make CSCs a valuable tool to develop targeted therapies against cancer. Actually, CSCs targeted therapies are aimed to inhibit CSCs deregulated pathways, involved in uncontrolled cell proliferation, anti-apoptotic properties, loss of cell cycle control or *stem* cell pathways (Feldmann et al., 2007; Korkaya et al., 2009; Kim et al., 2012; Kondratyev et al., 2012).

III. OBJECTIVES

MAIN OBJECTIVE:

To determine the anticancer activity, the molecular targets and signalling pathways regulated by new purine and 5-fluorouracil derivatives in differentiated cells and CSCs of breast and colon cancer.

SECONDARY OBJECTIVES:

1. To evaluate the antiproliferative and selective antitumour activity of new synthesized drugs on established tumour cell lines and CSCs.

2. To analyze the effect of compounds on cell cycle and apoptosis.

3. To establish the mechanism of action of Bozepinib by analyzing Kinome and gene expression profiling.

4. To explore the anti-angiogenic and anti-migratory activity of Bozepinib.

5. To determine the ability of Bozepinib to target CSCs signalling pathways.

6. To evaluate both the toxicity and tumor-regression *in vivo* effects of Bozepinib.

7. To study the efficacy of Bozepinib/IFNα combination to induce apoptosis, autophagy and senescence in cancer cells

IV. MATERIAL Y MÉTODOS

1. CULTIVO CELULAR

1.1. Líneas celulares

Las líneas celulares utilizadas fueron:

a.) Para el modelo de cáncer de mama:

- **Línea MCF-7:** Células de adenocarcinoma humano de mama caracterizada por ser ER^+, PR^+ y $HER2^-$ (ATCC HTB-22).

- **Línea MDA-MB 468:** Células de adenocarcinoma humano de mama, es $EGFR^+$ y $TGFR\alpha^+$ (ATCC HTB-132).

- **Línea SKBR-3:** Células de adenocarcinoma humano de mama, $HER\text{-}2^+$ (ATCC HTB-30).

- **Línea MCF-10A:** Células no tumorales, de carácter epitelial de la glándula mamaria humana (CRL-10317).

b.) Para el modelo de cáncer de colon:

- **Línea Caco-2:** Células de adenocarcinoma colorectal humano. Expresa EGF (ECACC: 86010202).

- **Línea T-84:** Células de carcinoma colorectal humano (ECACC: 8021101).

- **Línea SW-480:** Células de adenocarcinoma colorectal humano. Se caracterizan por tener una expresión positiva de los oncogenes c-myc, K-ras, H-ras, N-ras, Myb, sis y fos y sobreexpresar p53 (ECACC: 87092801).

- **Línea RKO:** Células de carcinoma de colon humano son $P53^+$ (ATCC: CRL-2577).

- **Línea HCT-116** $p53^{+/+}$**:** Células de carcinoma de colon humano, TGF-β 1, TGF-β 2 y p53 positivas y mutante para ras (ATCC CCL-247).

- **Línea HCT-116** $p53^{-/-}$**:** Suministrada por D. B. Vogelstein (Centro de Oncología Johns Hopkins, USA).

- **Línea HT-29:** Células de adenocarcinoma de colon humano (ATCC HTB-38). Se caracterizan por tener una expresión positiva de los oncogenes c-myc, K-ras, H-ras, N-ras, Myb, sis y fos y sobreexpresar p53.

- **Línea CCD18-Co:** Células no tumorales de colon humano (ATCC CRL-1459).

c.) Para el ensayo de formación de capilares:

- **Línea HUVEC**: Células procedentes de endotelio de cordón umbilical (ATCC CRL-1831).

d.) Otras líneas:

- Fibroblastos de embrión de ratón $PKR^{+/+}$ y $PKR^{-/-}$ (MEFs): Suministrados por D. M Esteban (Centro Nacional de Biotecnología, España).

1.2. Condiciones de cultivo

El cultivo celular se realizó bajo condiciones de esterilidad, en cabina de flujo laminar (Micro-V, Telstar, España). Para el crecimiento de las células se utilizaron frascos de cultivo de 75 o 25 cm^2, en incubador de CO_2 (Steri-Cult CO_2 Incubator, Thermo Electron Corporation, Waltham, MA, EEUU) a 37ºC y un 90% de humedad. Al alcanzar un 80-90% de confluencia, las células fueron despegadas de la superficie mediante una solución PBS-EDTA (0,02%) o tripsina-EDTA y posteriormente lavadas con medio de cultivo con FBS para inactivar la tripsina mediante centrifugación a 1500 rpm durante 5 min. A continuación fueron resembradas en nuevos frascos de cultivo.

Para el cultivo de las células tumorales MCF-7, MDA-MB 468, SKBR-3, Caco-2, T-84, HT-29, SW-480, HCT-116 así como para las células HCT-116 $p53^{+/+}$ y $p53^{-/-}$ se utilizó como medio de cultivo DMEM (Dulbecco´s Modified Eagles Medium; Sigma Chemical Co, St Luis, MO, EEUU), suplementado con un 10% de suero fetal bovino (FBS) (BioWhittaker, Lonza, Basel, Switzerland), inactivado a 56ºC durante 30 min y suplementado con 1% de una solución de penicilina/estreptomicina (10.000 U/ml penicilina G y 10mg/ml de estreptomicina; Sigma Chemical Co, St Luis, MO, EEUU).

La línea celular HUVEC fue cultivada con medio EGM-2 (Lonza).

Para el cultivo de las líneas celulares no tumorales de mama MCF-10A y colon CCD-18Co se utilizó como medio de cultivo DMEM/F12 enriquecido con 5% de suero de caballo descomplementado (HS), 1% de una solución de penicilina/estreptomicina (10.000 U/ml penicilina G y 10mg/ml de estreptomicina; Sigma Chemical Co, St Luis, MO, EEUU), 0,5 µg/ml de Hidrocortisona, 0,02 µg/ml de EGF, 0,01 µg/ml de Insulina y 100 ng/ml de Toxina Colérica.

Para el cultivo de las células madre tumorales (*medio de esferas)* se utilizó DMEM/F12 (Sigma Chemical Co, St Luis, MO, EEUU), suplementado con 1X de B27 (Gibco, Big Cavin, OK, EEUU), 1 µg/ml de hidrocortisona, 4ng/ml de heparina, 10 µg/ml de insulina, 10 ng/ml de Egf, 20 ng/ml de FGF y 1% de una solución de penicilina/estreptomicina (10.000 U/ml penicilina G y 10 mg/ml de estreptomicina; Sigma Chemical Co, St Luis, MO, EEUU).

1.3. Método de congelación celular

Para el mantenimiento de las líneas celulares (tanto tumorales como no tumorales) durante largos periodos de tiempo, las células fueron despegadas de los frascos de cultivo mediante una solución de tripsina-EDTA, centrifugadas a 1500 rpm durante 5 min en medio de cultivo suplementado con FBS y posteriormente el pellet celular fue resuspendido en Medio de Congelación a razón de 0,5 x 10^6 células, para luego ser introducidas inmediatamente en criotubos y éstos en el congelador a -80ºC durante 24h. Posteriormente, para su almacenaje a largo tiempo fueron trasladados a nitrógeno líquido a -196ºC.

Medio de congelación: Suero bovino fetal (FBS) inactivado mediante calor húmedo a 56ºC durante 30 min y dimetil sulfóxido (DMSO) al 5% (según recomendación de la ATCC).

1.4. Método de descongelación celular

Las líneas celulares conservadas a -80ºC (almacenamiento a corto plazo) o en nitrógeno líquido (almacenamiento a largo plazo) fueron descongeladas en calor húmedo a 37ºC e inmediatamente, resuspendidas en solución salina tamponada con fosfato (PBS) estéril y centrifugadas a 1500 rpm durante 5 min para eliminar los restos

de DMSO (dos lavados). El pellet fue resuspendido en medio de cultivo para finalmente realizar la siembra de las células en frascos de cultivo de 75 cm^2.

1.5. Contaje celular

Para el contaje de células, tras despegar y centrifugar las células, como se ha descrito previamente, el pellet fue resuspendido en medio de cultivo. Para conocer la densidad del cultivo se utilizó una cámara de Neubauer, las células que aparecían en cada cuadrante de la cámara fueron contadas, el número obtenido fue dividido entre cuatro, y multiplicado por 10.000 y finalmente se le fue aplicado el factor de dilución utilizado al tomar el volumen de muestra donde estaban resuspendidas las células.

2. AGENTES FARMACOLÓGICOS.

El diseño y síntesis de las (RS)- benzoxazepin-purinas y las 2,6-Dicloro-9- o 7-(Etoxycarbonylmetil)-9H- o 7H-Purinas fueron llevados a cabo por el grupo del profesor Dr. Joaquin Campos Rosa, del Departamento de Química Farmacéutica de la Universidad de Granada. Los compuestos fueron disueltos en DMSO a una concentración de mg/ml. Se preparó una solución "*stock"* que se almacenó a -20ºC y de ella se prepararon alícuotas que se utilizaron para los experimentos. Los compuestos utilizados se pueden clasificar en dos grupos (Tabla 1 y 2).

a.) Compuestos (RS)- benzoxazepin- purinas:

Compuesto	Estructura	Formula	Peso Molecular
ACG-812b-F3	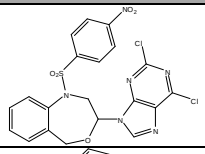	**$C_{20}H_{14}Cl_2N_6O_5S$**	**521.33**
FC-26c	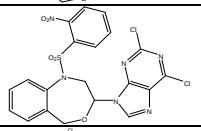	**$C_{20}H_{14}Cl_2N_6O_5S$**	**521.33**
ACG-812c-F1	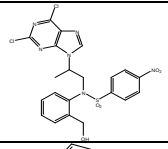	**$C_{21}H_{18}Cl_2N_6O_5S$**	**536.04**
FC-15d	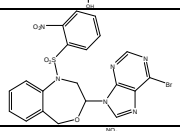	**$C_{20}H_{15}BrN_6O_5S$**	**531.33**
ACG-810e	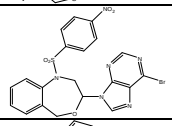	**$C_{20}H_{15}BrN_6O_5S$**	**531.33**
FC-29b	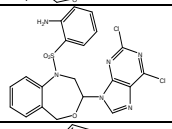	**$C_{20}H_{16}Cl_2N_6O_3S$**	**491.35**
FC-29d	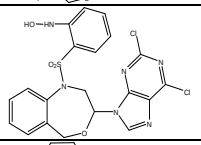	**$C_{20}H_{16}Cl_2N_6O_4S$**	**507.35**
FC-30b2	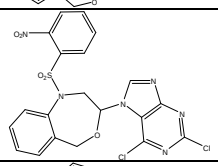	**$C_{20}H_{14}Cl_2N_6O_5S$**	**521.33**
FC-31	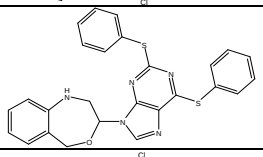	**$C_{26}H_{21}N_5OS_2$**	**409.89**
FC-34	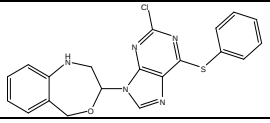	**$C_{20}H_{16}ClN_5OS$**	**409.89**
FC-35	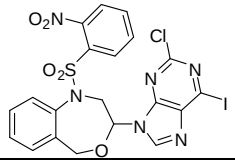	**$C_{20}H_{14}ClIN_6O_5S$**	**612.78**

Tabla 1. Resumen de las características de los compuestos (RS)- benzoxazepin- purinas.

b.) Compuestos 2,6-Dicloro-9- o 7-(Etoxycarbonylmetil)-9H- o 7H-Purinas:

Compuesto	Estructura	Formula	Peso Molecular
FMM298cF1	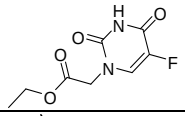	**$C_8H_9FN_2O_4$**	**216.17**
FMM 298dF1	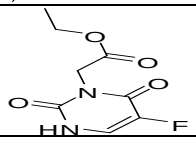	**$C_8H_9FN_2O_4$**	**216.17**
FMM262bf2	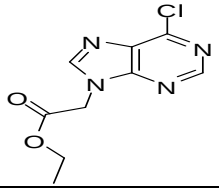	**$C_9H_9ClN_4O_2$**	**240.65**
FMM264bF1	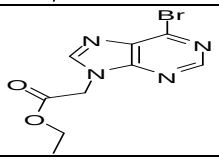	**$C_9H_9BrN_4O_2$**	**285.10**
FMM238bf2	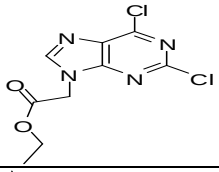	**$C_9H_8Cl_2N_4O_2$**	**275.09**
FMM262bf3	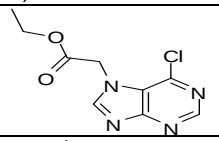	**$C_9H_9ClN_4O_2$**	**240.65**
FMM264c	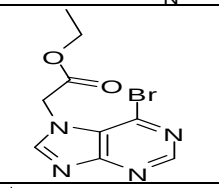	**$C_9H_9BrN_4O_2$**	**285.10**
FMM238bF3	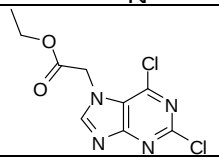	**$C_9H_8Cl_2N_4O_2$**	**275.09**

Tabla 2. Resumen de las características de los compuestos 2,6-Dicloro-9- o 7-(Etoxycarbonylmetil)-9H- o 7H-Purinas.

3. TRATAMIENTO DE LAS LÍNEAS CELULARES CON LOS COMPUESTOS ANTITUMORALES

Las células fueron despegadas de los frascos de cultivo utilizando una solución de tripsina-EDTA, centrifugadas en medio de cultivo a 1500 rpm durante 5 min y lavadas con PBS a 1500 rpm durante 5 min. Posteriormente, fueron contadas y sembradas a la densidad celular deseada en placas de 24 pocillos para su posterior tratamiento con los agentes farmacológicos a diferentes concentraciones. En cada experimento se utilizaron las diferentes líneas celulares en paralelo sin tratar con los agentes antitumorales como control. Cada 72 h se procedió al cambio de medio en las líneas celulares y además al tratamiento con los agentes antitumorales en las líneas celulares tratadas. La duración de los experimentos fue de seis días.

4. AISLAMIENTO DE CÉLULAS MADRE CANCERÍGENAS

El aislamiento de las células madre cancerígenas (CSCs) se llevó a cabo mediante la detección de la actividad aldehído deshidrogenasa (ALDH) por citometría de flujo, en las líneas celulares de mama SKBR-3 y MDA-MB 468, así como en la línea de cáncer colorrectal HCT-116. Para tal fin, se usó el kit Aldefluor (Stemcell Technologies, Vancouver, Canada) que mediante la metabolización de un sustrato, BODIPY-aminoacetaldehido (BAAA) gracias a la actividad de la enzima ALDH, da lugar a un producto fluorescente, el BODIPY-aminoacetato (BAA). Este último se acumula en el interior de la célula lo que permite su detección y posterior separación mediante citometría de flujo. Estas células $ALDH^+$ fueron separadas mediante un citómetro de flujo FACS Aria III, siendo seleccionadas las células que presentaban una mayor fluorescencia para el fluorocromo FITC. El dietilbenzaldehido (DEAB) es utilizado como control negativo, al ser un potente inhibidor de la actividad aldehído deshidrogenasa.

Tras la separación, las células fueron sembradas en placas de cultivo de baja adherencia (Corning Inc., Corning, NY, EEUU) y cultivadas en *medio de esferas*, para ser sometidas posteriormente a diferentes ensayos.

Para el aislamiento de las células madre cancerigenas se siguió el siguiente protocolo:

Las células fueron despegadas mediante la utilización de tripsina-EDTA y recogidas en tubos de citometría con una densidad de 10^6 células/ml. Posteriormente fueron resuspendidas en Aldefluor Assay Buffer, utilizándose un tubo como prueba y otro como control. Al tubo de prueba se le añadió 1ml de la suspensión celular mientras que al tubo control se le añadió 5µl de DEAB previo al inicio del ensayo. A continuación, se añadió 5 µl del sustrato BAAA, al tubo de prueba, se resuspendió bien con la pipeta y se transfirieron 500 µl al tubo control. Las células fueron incubadas a 37ºC durante 45 min, y centrifugadas. El pellet celular fue resuspendido en 500 µl de Aldefluor Assay Buffer y mantenido a 4ºC hasta su análisis.

4.1. Ensayo de formación de esferas

La capacidad de las células madre cancerígenas para formar esferas fue estudiada cultivando las células en placas de cultivo de baja adherencia de 6 pocillos (Corning Inc., Corning, NY, EEUU), utilizando un medio de cultivo que permite el mantenimiento de las características de células madre denominado *medio de esferas*, compuesto por DMEM/F12 (Sigma Chemical Co, St Luis, MO, EEUU), suplementado con 1X de B27 (Gibco, Big Cavin, OK, EEUU), 1 µg/ml de hidrocortisona, 4 ng/ml de heparina, 10 µg/ml de insulina, 10 ng/ml de EGF, 20 ng/ml de FGF y 1% de una solución de penicilina/estreptomicina (10.000 U/ml penicilina G y 10 mg/ml de estreptomicina (Sigma Chemical Co, St Luis, MO, EEUU).

Las células mantenidas en este tipo de cultivo fueron despegadas mediante tripsina-EDTA y lavadas dos veces con PBS, mediante centrifugación de 5 min a 1500 rpm. A continuación, el pellet celular fue resuspendido en *medio de esferas* y sembrado de nuevo en las placas de baja adherencia.

5. CITOTOXICIDAD *IN VITRO*

5.1. Determinación de la concentración inhibitoria 50 (CI_{50})

Para la determinación de la CI_{50}, las células fueron tratadas durante seis días con diferentes concentraciones de fármaco, para posteriormente llevar a cabo un ensayo colorimétrico con Sulforrodamina B. Para ello, se eliminó el medio de las placas de 24 pocillos y se procedió a añadir 300 µl de tricloroacético al 10% durante 20 min a 4ºC. Tras eliminar el tricloroacético, se dejaron secar las placas y se añadieron 500 µl de una

solución de Sulforrodamina B al 0,4%, dejando las placas en agitación durante veinte min a temperatura ambiente, para luego retirar el colorante que no se ha fijado y lavar tres veces con una solución de ácido acético 1%. A continuación, las placas se dejaron secar en oscuridad y finalmente la Sulforrodamina B se solubilizó con 500 µl de Tris-base 10 mM (pH 10,5) en agitación durante cinco min. Para proceder a la lectura de la absorbancia de una densidad óptica correspondiente a 492 nm se tomaron alícuotas de 100 µl que se transfirieron a placas de 96 pocillos para ser leídas en un colorímetro Titertek multiscan. De esta manera se obtuvieron los datos que se utilizaron para realizar las gráficas de Densidad óptica (D.O.) (eje y de la gráfica) y concentración (eje x) del fármaco. Mediante regresión mínimo cuadrática se calculó la ecuación de la curva y de aquí, la concentración del fármaco correspondiente a una D.O. (eje y)=50.

Para analizar el efecto sinérgico de Bozepinib en combinación con IFNα se determinó la CI_{50} tratando las células con diferentes concentraciones de Bozepinib en combinación con IFNα (50 IU/ml).

5.2. Determinación de la CI_{50} mediante ensayo con MTT

Las CSCs se sembraron a una concentración de 3000 células/pocillo en placas de baja adherencia de 96 pocillos (Corning Inc., Corning, NY, EEUU) y fueron tratadas con diferentes concentraciones de los compuestos antitumorales. Tras 72 h, se añadieron 10 µl de CellTiter 96® AQueous One Solution Cell Proliferation Assay (10 mg/ml) (Promega Corporation, Madison, USA) por pocillo y se incubaron a 37ºC durante 2-4 horas. Para la lectura de las placas se utilizó un colorímetro Titertek Multiscan apparatus (Flow, Irvine, CA, USA).

6. ENSAYO DE VIABILIDAD CELULAR BASADO EN LA ACTIVIDAD METABÓLICA

Las células en crecimiento exponencial, fueron sembradas en placas de 96 pocillos con una densidad de (5×10^3 células/pocillo) y mantenidas durante la noche en el incubador.

A continuación, las células fueron inducidas con 25 µM del inhibidor de caspasa Z-VAD-FMK o con 20 µM cloroquina (CQ) (Sigma) y 2 h después tratadas con 5 µM de Bozepinib y/o 500 IU/ml de IFNα. Tras 48h, la viabilidad celular fue medida

mediante ensayo colorimétrico (Cell counting kit-8 (CCK-8)-Dojindo) siguiendo las instrucciones del fabricante. CCK-8 está basado en la utilización de sales de tetrazolio, la cual es reducida a formazan en presencia de células vivas. Las placas de 96 pocillo fueron posteriormente leídas en un lector de microplacas Titertek Multiscan apparatus (Flow, Irvine, CA, USA).

7. DETERMINACIÓN DEL ÍNDICE TERAPÉUTICO (IT)

Para la determinación del índice terapéutico se calculó la CI_{50} tanto en las líneas celulares tumorales como en las no tumorales. El índice terapéutico vendría determinado por la siguiente expresión:

$$IT = CI_{50} \text{ línea no tumoral} / CI_{50} \text{ línea tumoral}$$

8. ANÁLISIS DEL CICLO CELULAR

Para el estudio del ciclo celular se sembraron $5x10^4$ células por pocillo en placas de seis pocillos y fueron tratadas con el compuesto durante 24 y 48 horas. A continuación, se centrifugó tanto el medio como las células despegadas con tripsina-EDTA en tubos de FACS a 1500 rpm durante 5 min. Se eliminó el sobrenadante y se realizó un lavado con PBS. Las células fueron fijadas con 700 µl de etanol al 70% a -20ºC durante 30 min. Para eliminar el etanol, se centrifugaron las células a 1800 rpm durante 5 min y posteriormente se lavaron con PBS, centrifugando a 1500 rpm durante 5 min. Tras esto, se preparó la solución de ioduro de propidio y RNAsa (el resto se completa con PBS hasta un ml).

El pelet celular fue resuspendido en 250 µl de la solución de ioduro de propidio y RNAsa. Las muestras fueron incubadas durante 30 min, en oscuridad a 37ºC y finalmente analizadas mediante FACSCsan.

Para los ensayos con Bozepinib e IFNα, las células fueron tratadas con 5 µM de Bozepinib y/o 500 IU/ml de IFNα durante 6 días (refrescandolo cada 72 h.) y analizadas siguiendo el protocolo anteriormente descrito.

9. ENSAYOS DE APOPTOSIS

Para detectar la inducción de apoptosis mediante el fármaco se utilizó el isocianato de fluoresceína (FITC) junto al ioduro de propidio. Para ello, se sembraron 300.000 células por pocillo en placas de seis pocillos y fueron tratadas con el compuesto durante 24 y 48 horas. Posteriormente, tanto el medio como las células despegadas con tripsina-EDTA en tubos de FACS fueron centrifugados a 1500 rpm durante 5 min. A continuación, y tras haber realizado un lavado con PBS, al pellet le fue añadido la solución de ANEXINA (10x binding buffer, ioduro de propidio, annexin V-FITC y agua miliQ). Las células fueron incubadas durante 30 min con esta solución a 37ºC en oscuridad. Finalmente se analizaron mediante citometría de flujo en un citómetro Becton Dickinson FACS Aria III.

Para el ensayo de apoptosis con Bozepinib e IFNα se sembraron 300.000 células por pocillo en placas de seis pocillos y fueron tratadas con Bozepinib solas o en combinación con IFNα (500 IU/ml) durante 48 horas. El IFNα fue añadido 8 horas antes de iniciarse el tratamiento con Bozepinib. Tras 48 h, las células fueron tripsinizadas y analizadas como se describe anteriormente. Las muestras se analizaron mediante citometría de flujo en un citómetro Becton Dickinson FACS Aria III.

10. ENSAYO RELACIONADO CON AUTOFAGIA

Las células fueron dispuestas en el cubreobjetos y transfectadas con el plásmido pCMV-GFP-LC3 y el plasmido control pCMV-GFP utilizando Lipofectamine 2000 (Invitrogen). Pasadas 24h tras la transfección, las células fueron tratadas con Bozepinib 5μM y/o IFNα 500 IU/ml durante 48h. Como control se usaron células tratadas con un volumen similar de DMSO. A continuación, se lavaron las células con PBS y se fijaron con paraformaldehido al 4%. Las imágenes fueron tomadas con un microscopio confocal laser Bio-Rad Radiance 2100.

11. MICROSCOPÍA ELECTRÓNICA DE TRANSMISIÓN

Las células tratadas con Bozepinib 5μM y/o IFNα 500 IU/ml fueron expuestas a sus respectivos tratamientos durante 48h. Como control se uraron células tratadas con un volumen similar de DMSO. A continuación, las células fueron lavadas tres veces con

PBS y luego fijadas con 0,5 ml de glutaraldehido (2,5% en tampón cacodilato 0,1 mol/l, pH 7,4) durante toda la noche a 4ºC. Posteriormente, fueron lavadas y fijadas en OsO_4 al 1% y embebidas en resina *polybed*. Finalmente, cortes ultrafinos fueron realizados y teñidos con acetato de uranilo y citrato de plomo para ser analizados mediante microscopía de transmisión de alta resolución (TEM PHILIPS CM20).

12. TINCIÓN CON β-GALACTOSIDASA

Las células fueron sembradas en placas de seis pocillos en su respectivo medio. Tras 7 días post-tratamiento, el medio fue eliminado y las células fijadas y teñidas utilizando el kit Senescence β-Galactosidase Staining Kit (Cell Signaling), siguiendo las instrucciones del fabricante, seguido de una incubación durante toda la noche a 37ºC en tampón pH 6. Las células senescentes teñidas de color azul fueron fotografiadas con un objetivo 10x.

13. ESTUDIO DE LA ACTIVIDAD DE KINASAS *IN VITRO*

El ensayo de inhibición de quinasas de Bozepinib se realizó en un panel de 36 quinasas. Los valores de la actividad residual fueron medidos utilizando el compuesto a dos concentraciones ($5x10^{-5}$M y $5x10^{-6}$M) para cada quinasa. Para disolver Bozepinib se utilizó DMSO al 100% para alcanzar concentraciones stock de $5x10^{-3}$M/100%DMSO y $5x10^{-4}$M/100%DMSO respectivamente. En el proceso se realizaron diluciones con agua hasta $5x10^{-4}$M/100%DMSO y $5x10^{-5}$M/100%DMSO en una placa de 96 pocillos directamente antes de ser utilizada. Para cada quinasa, 5 µl de cada una de las soluciones de $5x10^{-4}$M/100%DMSO y $5x10^{-5}$M/100%DMSO del compuesto se transfirieron a las placas de ensayo. El volumen final del ensayo fue de 50 µl. La concentración final del compuesto fue de 5×10^{-5} M y 5×10^{-6} M en 1% de DMSO.

Toda la actividad bioquímica del ensayo de las proteínas quinasas se desarrolló en una placa de 96 pocillos FlashPlatesTM (Perkin Elmer, Boston, USA) en un volumen de reacción de 50 ìl.

El cocktail de reacción contenía 25 µl del buffer de ensayo/[γ-33P]-ATP, 5 µl del compuesto (en DMSO, 10%), 10 µl de substrato y 10 µl de la proteína quinasa recombinante. La concentración final de ATP fue de 1 µM. El ensayo para cada enzima contenía HEPES-NaOH 60 mM; MgCl2 pH 7.5, 3 mM; MnCl2 3 mM; Na-

orthovanadate 3 μM; DTT 1.2 mM; PEG20000 ,50 μg/ml; ATP/[γ-33P]-ATP, 1 μM (approx. 7 x 1005 cpm por pocillo); diferentes concentraciones de proteínas quinasas y diferentes concentraciones de substrato. El ensayo de PKC-alpha contenía de forma adicional CaCl2, 1 mM; EDTA, 4 mM; 5 μg/ml de Fosfatidilserina y 1 μg/ml de 1.2-Dioleyl-glicerol.

Este cocktail se incubó a 30ºC durante 1 h. La reacción se detuvo mediante la adición de 50 μl de H3PO4 (v/v) al 2%. El contenido de los pocillos fue aspirado y lavado dos veces con 200 μl de NaCl (w/v) al 0.9%.

La incorporación de ^{33}Pi se determinó mediante un contador de centelleo de microplacas (Microbeta, Wallac). La actividad residual (en %) para cada pocillo con el compuesto se calculó mediante la siguiente fórmula:

Actividad residual (%) = 100 x [(cpm del compuesto-low control) / (high control-low control)].

14. ENSAYO DE FORMACIÓN DE CAPILARES

La capacidad para formar capilares de las células HUVEC en un medio semisólido fue comprobado mediante el cultivo de células tripsinizadas en placas de 96 pocillos recubiertas con Matrigel™ (BD Biosciences) en medio EGM-2. El Matrigel™ fue descongelado y utilizado para recubrir la superficie de los pocillos (50 μl/pocillo) y se dejó solidificar durante 1h a 37ºC. Las células fueron sembradas en las placas recubiertas con Matrigel™ a una densidad de 5-20 x 10^3 células/pocillo y cultivadas con medio EGM-2 durante 7 días. Se tomaro fotografías después de 4h, 24h y 7 días de cultivo, con microscopio Leica DM 5500B (Leica, Solms, Germany), equipado con el software Meta Systems. Las figuras fueron procesadas utilizando Adobe Photoshop 7.0. Las células fueron contadas para estudiar la formación de estructuras capilares. El número de estructuras parecidas a cordones fue determinado tras 24h y cada porción de cordón observado entre las ramificaciones se consideró como una unidad. Se realizó una medida semicuantitativa de la formación de cordones en Matrigel™ (índice de formación de túbulos).

15. ENSAYO DE CURACIÓN DE HERIDAS (WOUND HEALING)

La capacidad de migración de las células SKBR-3 y HCT-116 fue determinada utilizando el ensayo *in vitro* del *"wound healing" o curación de heridas*. Las células fueron sembradas en placas de seis pocillos hasta alcanzar una confluencia del 80%. Las heridas se realizaron utilizando puntas de 1000 µl para raspar la superficie de la monocapa de células SKBR-3 y 200 µl en el caso de las células HCT-116, lavando después los pocillos con medio para eliminar las células desprendidas. Posteriormente, el tamaño de la herida fue controlado mediante fotografías tomadas con un microscopio Axiovert 40 CFC Zeiss (Carl Zeiss meditec group, Germany) fotomicroscopio (objetivo 10x), durante 0, 24h y 48h. La distancia presente en la herida fue medida en cada punto de tiempo y se expresó como la media del cierre de la herida comparado con el tiempo inicial mediante el programa Image J software 1.47v (http://imagej.nih.gov/ij).

16. ANÁLISIS DE MICROARRAYS

Se trataron las células MDA-MB 468 con Bozepinib a una concentración de 5µM a 4 y 16h. Las células control no fueron tratadas con el compuesto. El ARN total fue extraido utilizando RNeasy Midi Kit (Qiagen), siguiendo las instrucciones del fabricante. El análisis de microarray fue llevado a cabo utilizando Affymetrix Human Gene 1.0 ST arrays, de acuerdo con el protocolo standard de Affymetrix. La lista de genes con un punto de corte en el fold change a partir de 1 fue subdividido en categorías funcionales mediante el recurso de análisis bioinformático DAVID (Database Annotation, Visualization and Integrated Discovery) del Centro Biomédico de computación Avanzada (NCI, Frederick,http://david.abcc.ncifcrf.gov). El análisis de las rutas de los genes fue también realizado utilizando DAVID.

16.1. Análisis de los datos pbtenidos mediante microarrays

Para realizar este análisis se escogieron los genes que presentaron un *fold change* mayor a 1,5 después del tratamiento de las células MDA-MB 468 con Bozepinib. Los datos obtenidos fueron importados y analizados con el programa Ingenuity Pathway Analysis (IPA, Ingenuity Systems; https://www.analysis. Ingenuity.com). IPA es una base de datos que actúa como repositorio de interacciones biológicas y anotaciones funcionales a partir de relaciones existentes entre proteínas, genes, células, tejidos, metabolitos, drogas y enfermedades.

17. OBTENCIÓN DE ARN

El ARN total se obtuvo de las células tras tratarlas con el fármaco durante 4 y 16h, a una concentración de 5 µM. La extracción de ARN se realizó mediante la utilización de trizol, Tri-Reagent (Life Technologies, Inc., Gaithersburg, MD). Para ello se descartó el medio y se lavaron las células con PBS. Tras esto, se añadió un mililitro de Tri-Reagent y se dejaron las células 15 min a temperatura ambiente. Se añadieron 200 µl de cloroformo a la muestra y se agitaron las células con un vortex. Posteriormente, se dejaron 10 min a temperatura ambiente. Tras esto se centrifugaron 15 min a 12000 g a 4ºC. La fase acuosa que contiene el ARN se transfirió a un eppendorf libre de nucleasas (Eppendorf Corp., Hamburg, Alemania), debajo queda una fase con restos celulares y ADN.

Para precipitar el ARN se añadieron 500 µl de isopropanol. Se agitó la muestra con un vortex y se dejó incubar a temperatura ambiente durante 10 min. A continuación, la muestra se centrifugó a 12000 g a 4ºC durante 10 min. Se descartó el isopropanol y se añadió 1 ml de etanol al 75% (diluido con agua miliQ). Tras agitar con el vortex se centrifugó la muestra a 12000 g durante 5 min a 4ºC. Se descartó el etanol y se dejó la muestra a temperatura ambiente para que el resto de etanol se evaporara. Tras añadir 50 ml de agua libre de RNasas (Qiagen, Valencia, CA, EEUU) se procedió a la cuantificación del ARN mediante un nanodrop (NanoDrop™ 2000/2000c Spectrophotometers, Thermo Scientific™). Finalmente, la muestra se guardó a -80ºC para su posterior utilización.

17.1. Cuantificación de ARN

Para la cuantificación del ARN, se procedió a la lectura de la absorbancia a 260 y 280 nm mediante un nanodrop (NanoDrop™ 2000/2000c Spectrophotometers, Thermo Scientific™). La relación $D.O._{.260}/D.O._{.280}$ nos permitió calcular la pureza de los ácidos nucleicos, considerando un rango óptimo los valores comprendidos entre 1,8 y 2. La concentración de ARN se calculo teniendo en cuenta que una unidad de D.O. a 260 nm se corresponde con una concentración de 40 mg/ml de ácidos nucleicos.

18. TRANSCRIPCIÓN REVERSA Y REACCIÓN EN CADENA DE LA POLIMERASA (RT-PCR).

18.1. Transcriptasa reversa

Para la reacción de la transcriptasa reversa se utilizó el ARN previamente extraído. El ARN se incubó a 70ºC durante 10 min y luego se mantuvo en hielo. Se utilizó el kit Reverse Transcription System (Promega, Madison, WI), para lo que se ajustó el volumen de cada reacción a 20 µl en cada eppendorf libre de nucleasas. Para cada reacción se utilizó 1 µg del ARN extraído y se añadieron 4 µl de $MgCl_2$, 2 µl de buffer 10x, 2 µl de la mezcla de dNTPs, 0,5 µl del inhibidor RNasin, 15 U de la enzima AMV y 0,5 µg de primers Oligo $(dT)_{15}$.

La reacción de la transcriptasa reversa se llevó a cabo en un termociclador (DOPPIO Thermal Cycler, VWR) with dual 48 well blocks. Los tubos de la reacción fueron calentados a 42ºC durante 15 min y posteriormente la temperatura subió hasta 95ºC durante 5 min. Finalmente, las muestras fueron mantenidas en hielo durante 5 min. El ADN_c fue guardado a -20ºC.

18.2. Reacción en cadena de la polimerasa cuantitativa

La Reacción en Cadena de la Polimerasa Cuantitativa en Tiempo Real se llevo a cabo para validar los datos obtenidos a partir de los microarrays de $_c$ADN de los genes seleccionados. El análisis se llevó a cabo con el sistema de "*PCR 7500 real-time PCR system*" (Applied Biosystems, Inc.), siguiendo las recomendaciones del distribuidor. Se utilizaron 2 µg totales de ARN, que fueron retrotranscritos a $_c$ADN utilizando el Kit Reverse Transcription System (Promega). Para realizar la Reacción en Cadena de la Polimerasa Cuantitativa en Tiempo Real se utilizó el kit GoTaq® RT-qPCR Master Mix (Promega). Se utilizó 1 µl de $_c$ADN en un volumen de 25 $_c$ADN que contenía agua libre de RNAsas, SYBR Green PCR Master Mix y los primers correspondientes (Tabla 3). Cada reacción fue llevada a cabo por triplicado.

Se utilizó el método de las Ct para calcular el factor de amplificación siguiendo las recomendaciones del distribuidor. Como control interno se utilizó GAPDH para normalizar las variaciones en la calidad y cantidad del $_c$ADN utilizado. La concentración del gen de interés y del gen de referencia endógeno se determinó

mediante la realización de una curva de calibrado para cada muestra, a partir de cinco diluciones seriadas de $_c$ADN

Genes	Secuencia de Primers	
CLAUDIN1	Forward	5´ GCGCGATATTTCTTCTTGCAGG-3´
	Reverse	5´TTCGTACCTGGCATTGACTGG-3´
CSE	Forward	5´ AGCCTTCATAATAGACTTCG 3´
	Reverse	5´ CAGCCCAGGATAAATAAC
CXCL10	Forward	5′ CCAGAATCGAAGGCCATCAA 3′
	Reverse	5′ CATTTCCTTGCTAACTGCTTTCAG 3′
E2F8	Forward	5´ GTGGATTACCTGAGGCCAAA 3´
	Reverse	5´ CTTCGTCAAGGCAGATGTCA 3´
MAML2	Forward	5´ ACATTTGTCAAGGCCACCTC 3´
	Reverse	5´ GTTTGCCAAAGCCTGGTTAG 3´
NOTCH3	Forward	5´ TGACCGTACTGGCGAGACT 3´
	Reverse	5´ CCGCTTGGCTGCATCAG 3´

Tabla 3. Secuencia de primers utilizada para validar los arrays realizados en la línea tumoral de cáncer de mama MDA-MB 468 tras el tratamiento con Bozepinib.

20. EXPRESIÓN DE PROTEÍNAS

20.1. Extracción de proteínas

La extracción de proteínas se realizó mediante la utilización de la siguiente solución: Tris al 6,05% y SDS al 0,4% (Sigma chemical Co., St Louis, MO, EEUU), diluidos en agua bidestilada, ajustándose el pH a 6,8. De la solución anteriormente preparada se tomaron 12,5 ml y se añadieron 2g de SDS, 10ml de glicerol (Sigma chemical Co., St Louis, MO, EEUU) y se disolvieron en agua bidestilada hasta un volumen final de 25 ml. A continuación, alícuotas de 800 µl fueron guardadas a -20ºC. A la hora de utilizar la solución, se descongeló la alícuota, se le añadieron 200 µl de 2-β-mercaptoetanol y se completó con agua bidestilada hasta un volumen final de 5 ml.

La extracción de proteínas se realizó mediante el cultivo de las células adherentes en placas de 6 pocillos, donde se realizaron los tratamientos con el

compuesto. Posteriormente, el medio de cultivo fue retirado y se procedió a lavar las células con PBS. A continuación, se añadieron 100 µl de la solución de extracción de proteínas y se despegaron las células de la superficie de la placa mediante la utilización de un scraper. La solución de lisis así obtenida fue recogida y guardada en un tubo eppendorf de 1,5 ml, para posteriormente ser hervida a 100ºC durante 10 min en un thermoblock ThermoStat plus (eppendorf Corp., Hamburg, Germany). Las muestras finalmente fueron almacenadas a -20ºC.

En el caso de las CSCs, al crecer en suspensión, se centrifugó el medio a 3000 rpm en tubos eppendorf de 1,5 ml. Se retiró el sobrenadante y se realizaron dos lavados con PBS. Posteriormente se añadió 100 µl de la solución de extracción de proteínas. La solución de lisis así obtenida fue hervida a 100ºC durante 10 min en un thermoblock ThermoStat plus (eppendorf Corp., Hamburg, Germany). Las muestras finalmente fueron almacenadas a -20ºC.

20.2. Electroforésis

Para la separación de las proteínas en base a su carga y tamaño, se utilizaron geles preparados que constaban de una zona superior denominada gel concentrador, y una zona inferior donde se iba a desarrollar la separación de las proteínas en función de su movilidad electroforética. Para la preparación de los cuatro geles (10% de acrilamida) se utilizaron los siguientes reactivos (Sigma chemical Co., St Louis, MO, EEUU):

Gel Superior	4 Geles
Acrilamida 30%	1,6 ml
Stacking Buffer 4X	4 ml
SDS 10%	1,8 ml
Agua	10,24 ml
APS 10%	100 µl
TEMED	10 µl

Gel Inferior	4 Geles
Acrilamida 30%	6,2 ml
Running Buffer 4X	4,6 ml
SDS 10%	180 µl
Glicerol 50%	1,8 ml
Agua	5,4 ml
APS 10%	100µl
TEMED	20 µl

En el proceso de preparación de los geles cabe resaltar la adición en último lugar del persulfato de amonio (APS) y la tetrametiletilendiamina (TEMED), ya que estos agentes provocan la polimerización de la acrilamida, dando lugar a su gelificación en unos 15 min.

Para la preparación de los geles se montaron los cristales en su soporte (Bio-Rad Laboratories, Inc., Hercules, CA, EEUU), tras lo cual se añadió en primer lugar el gel inferior a través de la ranura formada por los cristales de 1 mm de separación, hasta ocupar aproximadamente las ¾ partes del cristal. Se dejó solidificar y posteriormente se adicionó el gel superior hasta cubrir la totalidad del cristal, colocándose finalmente el peine de 10 pocillos. Tras la solidificación del gel, se retiró cuidadosamente el peine y se colocaron los cristales en una cubeta de electroforesis (Bio-Rad Laboratories, Inc., Hercules, CA, EEUU).

Para el desarrollo de la electroforesis se utilizó un "buffer de electoforésis", cuya composición se detalla a continuación:

5X	**1000 ml**
Tris	15 g
Glicina	72 g
SDS	5 g

Esta solución se utiliza a una concentración de 1X.

Finalmente, se procedió a la carga de las muestras en los pocillos de los geles junto con 10 µl de un patrón de peso molecular (Kaleidoscope Prestained Standards, Bio-Rad Laboratories, Inc., Hercules, CA, EEUU). La electroforesis se desarrolló mediante la aplicación de una diferencia de potencial de 100 V, observándose su avance mediante la presencia de azul de bromofenol existente en la solución de extracción de proteínas. Una vez alcanzado el frente la distancia deseada, se retiraron los geles de la cubeta.

20.3. Transferencia

La transferencia de las proteínas separadas electroforéticamente se realizó a una membrana de nitrocelulosa (Bio-Rad Laboratories, Inc., Hercules, CA, EEUU). Para

ello se retiraron los geles de los cristales y se eliminó el gel superior. Para el desarrollo de la transferencia de las proteínas a la membrana de nitrocelulosa se utilizó un "tampón de transferencia", cuya composición se detalla a continuación.

TRIS	5,82 g
Glicina	2,9 g
SDS	937 µl
Agua miliQ	Enrasar hasta 800 ml

Antes de la realización de la transferencia, se toman 200 ml de esta solución y se le añaden 50 ml de metanol.

El papel de filtro Whatman, previamente empapado en tampón de transferencia (al igual que la nitrocelulosa, durante unos 15 min), se utiliza para componer el sándwich, según el siguiente esquema:

PAPEL WHATMAN
GEL DE ACRILAMIDA
NITROCELULOSA
PAPEL WHATMAN

Tras esto, se colocó el sándwich en un aparato de transferencia Trans-Blot® Turbo™ Transfer System (Bio-Rad Laboratories, Inc., Hercules, CA, EEUU), aplicando 25V durante 30 min.

Tras la transferencia, las membranas fueron incubadas durante 5 min temperatura ambiente con un solución de Ponceau S (Sigma chemical Co., St Louis, MO, EEUU) para comprobar la correcta transferencia de las proteínas a la membrana de nitrocelulosa. Posteriormente, se realizaron tres lavados con PBS.

20.4. Marcaje de los anticuerpos y revelado

Una vez transferida la membrana de nitrocelulosa procedemos al bloqueo para evitar uniones inespecíficas con las proteínas. Para esto se utiliza leche desnatada al 5%

en PBS durante una hora en agitación a temperatura ambiente. Tras realizar tres lavados con PBS, se procedió al marcaje con los anticuerpos primarios (Tabla 4).

Anticuerpo	Casa comercial
p-HER2	Cell Signalling
p-SAP/JNK	Cell Signalling
p-ERK1/2	Cell Signalling
p-Akt	Cell Signalling
p-p53	Cell Signalling
Akt	Santa Cruz
VEGF	Santa Cruz
ERK1/2	Santa Cruz
JNK	Santa Cruz
Gli-3	Santa Cruz
Sox-2	Santa Cruz
C-Myc	Santa Cruz
β- catenina	Santa Cruz
PKR	Santa Cruz
Her-2/Neu	Santa Cruz
p-PKR	Sigma-Aldrich
β-actina	Sigma-Aldrich
p-Eif2α	Invitrogen

Tabla 4. Anticuerpos primarios utilizados para realizar la técnica de western blot.

La incubación con el anticuerpo primario se realizó durante todala noche en agitación a 4ºC. A continuación, las proteínas se marcaron con el correspondiente anticuerpo secundario (Tabla 5) mediante agitación durante una hora a temperatura

ambiente. Tras realizar tres lavados con PBS, se procedió al revelado de la membrana. Para ello, se utilizó el kit ECL (Bonus, Amersham, Little Chalfont, UK) y se incubó durante 5 min a temperatura ambiente en oscuridad.

Anticuerpo	Casa Comercial
Anti-rabbitIgG peroxidase conjugate	Sigma-Aldrich (A0545)
Anti-mouse IgG peroxidase conjugate	Sigma-Aldrich (A9044)

Tabla 5. Anticuerpos secundarios utilizados para realizar la técnica de western blot.

Finalmente, la membrana se reveló en un sistema de imagen LAS-4000, utilizando el software Image Reader LAS-4000. De esta manera se detectó la expresión de las proteínas.

21. ENSAYOS DE TUMORIGÉNESIS *IN VIVO*

22. TOXICIDAD AGUDA

La toxicidad aguda fue determinada en ratones BALB/c de seis semanas de edad, con una media de peso de 20 g, durante dos semanas. El fármaco fue disuelto en 0,25 ml de una mezcla de DMSO y NaCl al 0,9% y fue administrado a los ratones por vía intraperitoneal y oral (n=24) a dosis de 50; 5; 0,5 y 0,05 mg/kg. Los ratones control fueron inoculados con el mismo volumen de DMSO y NaCl al 0,9%. Tras 24h, no se observaron señales de toxicidad aguda. Finalmente, la dosis del fármaco fue incrementada a 75; 100; 150 y 200 mg/kg. Tras 24h, no fueron detectadas señales de toxicidad aguda. En todos los experimentos, los ratones se mantuvieron bajo condiciones controladas, fueron medidos y pesados y evaluados en busca de signos de toxicidad sistémica (pérdida de peso, pérdida de audición) y toxicidad local (alopecia, reacciones en la piel, pérdida de motilidad) durante 10 días.

22.1. Efecto antitumoral del fármaco

Células tumorales de cáncer de mama MDA-MB- 468 y cáncer de colon HT-29 en crecimiento exponencial fueron inoculadas de manera subcutánea en cada flanco de ratones desnudos ($2x10^6$ células/ratón) bajo condiciones asépticas. El crecimiento del tumor fue comprobado mediante la medida dos veces a la semana de los diámetros de los tumores con un calímetro vernier (longitud x profundidad). El peso de los tumores se calculó mediante la fórmula:

$$\text{Peso del tumor (mg)} = \text{Volumen del tumor } (mm^3) = d^2 \times D/2$$

Donde:

d = Diámetro menor.

D = Diámetro mayor.

Los tumores crecieron hasta alcanzar un volumen medio de 100 mm^3. A continuación, los animales fueron asignados al azar a los grupos control y tratamiento, para recibir metilcelulosa al 1% en el caso de los controles y el fármaco disuelto en metilcelulosa al 1% en el caso de los tratamientos mediante inyección intraperitoneal (20 mg/kg) una vez al día, tres veces a la semana durante 40 días en el caso de los tumores inducidos con células MDA-MB 468 y dos semanas en el caso de los tumores inducidos con las células HT-29.

V. RESULTS.

1. ANTIPROLIFERATIVE ACTIVITY OF NEW COMPOUNDS ON TUMORAL CELL LINES

We determined the antiproliferative activities of several novel compounds on different breast tumoral and non tumoral cell lines measuring the Inhibitory Concentration 50 (IC_{50}) as previously described in material and methods.

a.) Antiproliferative activities of (RS)-benzoxazepin-purines (Table 1). Results are showed below:

	IC_{50} (µM)		
Compound	**MCF-10A**	**MCF-7**	**MDA-MB 231**
ACG-812b-F3(Bozep)	1,82 ± 0,503	0,35 ± 0,011	0,16 ± 0,063
ACG-858E1(R-(14))	N.D.	0,19 ± 0,001	0,11 ± 0,001
ACG-858E2(S-(14))	N.D.	0,10 ± 0,001	0,11 ± 0,001
ACG-812c-F1	1,86 ± 0,050	0,35 ± 0,122	0,40 ± 0,074
ACG-810e	N.D.	1,22 ± 0,348	N.D.
ACG-630b-F1	N.D.	5,43 ± 0,321	N.D.
FC-29b	1,52 ± 0,498	0,82 ± 0,05	0,46 ± 0,017
FC-29d	1,23 ± 0,217	1,53 ± 0,04	0,48 ± 0,006
FC-30b2	1,26 ± 0,163	0,99 ± 0,9	0,31 ± 0,066
FC-35	0,35 ± 0,020	0,61 ± 0,043	0,25 ± 0,002
FC-26c	1,53 ± 0,198	0,38 ± 0,027	0,28 ± 0,006
FC-18b	N.D.	7,26 ± 2,291	N.D.
FC-15d	N.D.	3,61 ± 0,273	N.D.
FC-31	N.D.	9,71 ± 0,38	N.D.
FC-34	N.D.	13,85 ± 1,79	N.D.

Table 1. Antiproliferative activities of (RS)-benzoxazepin-purines against breast tumoral cell lines MCF-7, MDA-MB 231 and non tumoral MCF-10A cell line. N.D. Not determined.

The most active compounds were Fc-35 (IC_{50}=0,355) in MCF-10A non tumoral breast cell line and ACG-858-E2 (R-(14)) compound in MCF-7 (IC_{50}=0,19) and MDA-MB 231 (IC_{50}=0,11) breast cancer cell lines (Table 1, Figure 1).

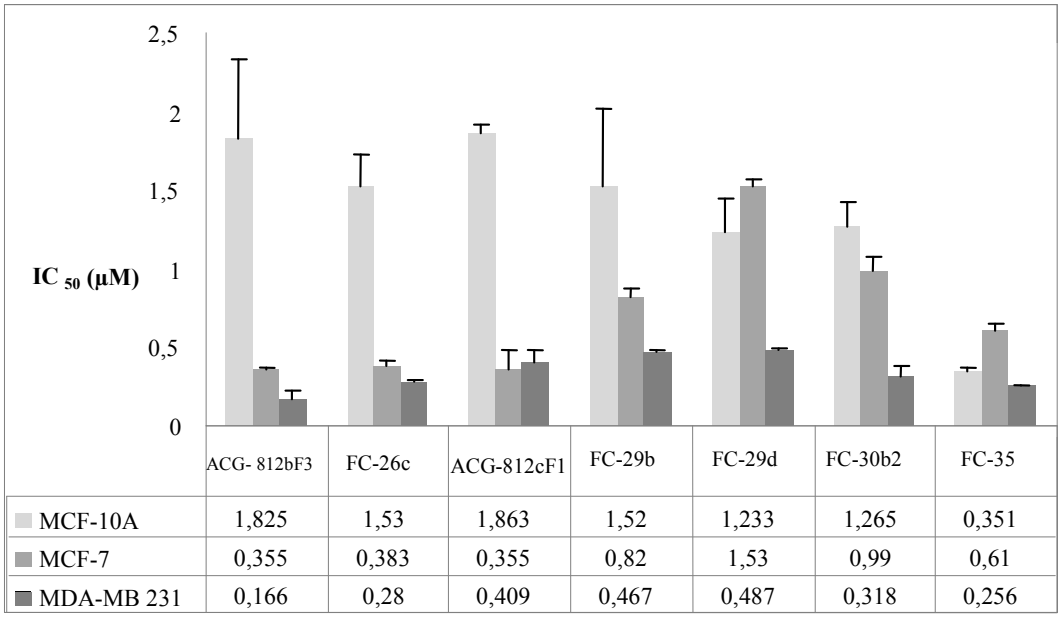

	ACG- 812bF3	FC-26c	ACG-812cF1	FC-29b	FC-29d	FC-30b2	FC-35
MCF-10A	1,825	1,53	1,863	1,52	1,233	1,265	0,351
MCF-7	0,355	0,383	0,355	0,82	1,53	0,99	0,61
MDA-MB 231	0,166	0,28	0,409	0,467	0,487	0,318	0,256

Figure 1: Comparison of antiproliferative activities for the most representative compounds against the breast cancer cell lines MCF-7 and MDA-MB 231, and the non tumoral MCF-10A cell line.

b.) Antiproliferative activities of 2,6-Dichloro-9- or 7-(Ethoxycarbonylmethyl)-9H-or 7H-Purines (Table 2). Results are showed below:

	IC_{50} (µM)	
	MCF-7	**HCT-116**
FMM 298cF1	25,20 ± 0,03	24,60 ± 0,01
FMM 298dF1	30,50 ± 0,03	22,60 ± 0,01
FMM 262bF2	35,10 ± 0,03	5,27 ± 0,04
FMM 262bF3	49,80 ± 0,03	68,00 ± 0,04
FMM 264b1	14,10 ± 0,06	23,50 ± 0,04
FMM 264c	20,20 ± 0,06	55,70 ± 0,04
FMM 238bF2	3,93 ± 0,04	6,20 ± 0,05
FMM 238b3	5,63 ± 0,03	6,36 ± 0,06

Table 2. Antiproliferative activities for 2,6-Dichloro-9- or 7-(Ethoxycarbonylmethyl)-9H-or 7H-Purines compounds against MCF-7 breast cancer and HCT-116 colon cancer cell lines.

The most active compounds against MCF-7 breast cancer cells were FMM238bF2 (IC_{50}=3,93) and FMM238b3 (IC_{50}=5,63) and in HCT-116 (colon cancer cell lines were FMM262bF2 (IC_{50}=5,27) and FMM238bF2 (IC_{50}=6,2).

2. SELECTIVE ANTITUMOUR ACTIVITY OF NEW COMPOUNDS

To determine the selective activity of (RS)-benzoxazepin-purines we determine the therapeutic index (TI) (Table 3) as previously described in material and methods.

	Therapeutic index (TI)	
Compound	**MCF-7**	**MDA-MB 231**
ACG-812b-F3(Bozep)	5,14	11,0
FC-26c	4,00	5,50
ACG-812c-F1	5,25	4,55
FC-29b	1,85	3,25
FC-29d	0,80	2,53
FC-30b2	1,27	4,00
FC-35	0,57	1,37

Table 3. Therapeutic index (TI) of (RS)-benzoxazepin-purines against breast tumoral cell lines MCF-7, MDA-MB 231 and non tumoral MCF-10A.

As ratio between tumoral IC_{50} cell line and the non tumoral IC_{50} cell line, the TI varies from values from 0,57 to 11. The best results correspond to the compound ACG-812b-F3 (Bozepinib), with a TI of 5,14 in MCF-7 and 11 in MDA-MB 231 breast cancer cell lines.

3. EFFECT OF COMPOUNDS ON CELL CYCLE

Once the antitumor activity of compounds was determined against the different breast and colon cancer cell lines with (RS)-benzoxazepin-purines and 2,6-Dichloro-9- or 7-(Ethoxycarbonylmethyl)-9H-or 7H-Purines, we carried out a selection between those that showed best antiproliferative effects in order to determine their influence on cell cycle phases. In this study we have included as control, drugs used in clinic against breast cancer, such 5-FU and paclitaxel, with a known action mechanism at cell cycle level (Yoshikawa et al., 2001; Hu et al., 2014).

In order to analyze if the antitumour effects of (RS)-benzoxazepin-purines involve changes in cell cycle distribution, the non tumoural cell line MCF-10A (Table 4) and the breast cancer cell lines MCF-7 (Table 5) and MDA-MB 231 (Table 6) were treated with the compounds at their respective IC_{50} values for 48 h and then analysed by flow cytometry.

	MCF-10A		
Compound	**G0/G1**	**G2/M**	**S**
MOCK	65,70+/-1,14	12,55+/-0,68	21,78+/-0,46
ACG-812b-F3(Bozep)	65,93+/-1,35	11,92+/-0,29	22,14+/-1,07
Fc-35	66,69+/-0,42	11,33+/-0,49	21,97+/-0,91
ACG-858E1(R-(14))	65,33+/-0,71	12,67+/-1,73	22,00+/-0,82
ACG-858E2(S-(14))	64,21+/-1,36	10,76+/-0,5	25,02+/-0,86
5-FU	34,20+/-1,43	9,56+/-1,39	55,73+/-2,11
Paclitaxel	36,70+/-1,56	23,49+/-0,94	39,75+/-2,50

Table 4. Cell cycle distribution of MCF-10A cells after (RS)-benzoxazepin-purines treatment for 48h.

	MCF-7		
Compound	**G0/G1**	**G2/M**	**S**
MOCK	89,88+/-1,73	1,57+/-2,12	8,55+/-0,40
ACG-812b-F3(Bozep)	87,20+/-2,69	1,57+/-1,12	8,55+/-0,40
Fc-35	84,09+/-3,85	6,38+/-2,93	9,53+/-0,93
ACG-858E1(R-(14))	87,22+/-0,54	1,22+/-1,32	11,06+/-1,48
ACG-858E2(S-(14))	89,02+/-0,76	3,10+/-0,74	7,87+/-0,02
5-FU	87,40+/-1,91	8,06+/-1,78	6,06+/-2,02
Paclitaxel	62,48+/-2,74	18,50+/-2,81	19,01+/-0,07

Table 5. Cell cycle distribution of MCF-7 cells after (RS)-benzoxazepin-purines treatment for 48h.

	MDA-MB 231		
Compound	**G0/G1**	**G2/M**	**S**
MOCK	42,06+/-0,00	31,59+/-0,00	26,35+/-0,00
ACG-812b-F3(Bozep)	45,40+/-0,00	25,40+/-0,00	29,36+/-0,00
Fc-35	40,37+/-3,95	30,30+/-3,94	28,82+/-7,18
ACG-858E1(R-(14))	50,78+/-0,57	46,23+/-1,11	2,985+/-0,54
ACG-858E2(S-(14))	39,97+/-0,00	30,67+/-0,00	29,37+/-0,00
5-FU	38,98+/-0,40	25,63+/-0,06	35,39+/-0,34
Paclitaxel	100+/-0,00	0,00	0,00

Table 6. Cell cycle distribution of MDA-MB 231 cells after (RS)-benzoxazepin-purines treatment for 48h.

No accumulation in a specific cell cycle phase was detected during treatment with the drugs in most of the cell lines analyzed in comparison with mock DMSO treated cells. Only ACG-858E2(R-(14)) enantiomer was able to induce an accumulation in both G0/G1 and G2/M phases in MDA-MB 231 cells with the consequently significant decreased in the S phase. Also an accumulation in the phase G2/M was detected in Fc-35 MCF-7 treated cells.

To study the mechanisms of the anti-tumour activity of 2,6-Dichloro-9- or 7-(Ethoxycarbonylmethyl)-9H-or 7H-Purines, we seleted the most active compounds (FMM238bF2 and FMM238bF3) to analyze the effects on the cell cycle distribution by flow cytometry (Tables 7 and 8). For this purpose we used MCF-7 and HCT-116 cell lines as representatives for breast and colon cancer, respectively.

	MCF-7		
Compound	**G0/G1**	**G2/M**	**S**
MOCK	34,58 ± 0,09	14,50 ± 1,06	50,91 ± 1,15
FMM238bF2	28,17 ± 1,37	15,39 ± 0,68	54,63 ± 1,18
FMM238bF3	34,54 ± 0,08	18,27 ± 0,79	47,19 ± 0,89

Table 7. Cell cycle distribution in MCF-7 breast cancer cell line after treatment for 24 h with the two most active compounds FMM238bF2 and FMM238bF3.

	HCT-116		
COMPOUND	**G0/G1**	**G2/M**	**S**
MOCK	44,70 ± 0,38	38,26 ± 1,40	17,02 ± 1,40
FMM238bF2	45,93 ± 1,11	36,75 ± 0,70	17,31 ± 0,44
FMM238bF3	33,58 ± 1,90	37,93 ± 1,92	28,47 ± 0,07

Table 8. Cell cycle distribution of HCT-116 colon cancer cell line after treatment for 24 h with the two most active compounds, FMM238bF2 and FMM238bF3.

The MCF-7 cells treated for 24 h with FMM238bF2 and FMM238bF3 did not show significant differences in the cell cycle progression compared with mock DMSO-

treated cells. We found a slight cell cycle arrest in the G_2/M and S-phases induced by FMM238bF2 (54,63 ± 1,18) and FMM238bF3 (18,27 ± 0,79), respectively (Table 7). In the HCT-116 treated cells FMM238bF2 did not modify the cell cycle profile and FMM238bF3 provoked a G_2/M cell cycle arrest (28,47 ± 0,07) at the expense of the G_0/G_1-phase (33,58 ± 1,90) (Table 8).

4. APOPTOSIS ASSAYS.

Apoptosis assays were accomplished by flow cytometry in the MCF-7 human breast cancer cell line treated cells with IC_{50} values of (RS)-benzoxazepin-purines family at 24 (Table 9) and 48 (Table 10) hours using Annexin V-FITC and propidium iodide (PI) staining. Simultaneous staining with annexin V-FITC and the PI non-vital dye made it possible to distinguish between early apoptosis (stained positive for annexin V-FITC and negative for PI), and late apoptosis or cell death (stained positive for both annexin V-FITC and PI).

Compounds	Viable cells	Necrotic cells	Early apoptosis	Late apoptosis
MOCK	90,42+/-0,63	9,55+/-0,21	0,00	0,03+/-0,01
ACG-812b-F3(Bozep)	94,16+/-0,64	4,93+/-0,23	0,66+/-0,22	0,23+/-0,20
ACG-810e	95,70+/-1,07	4,26+/-1,10	0,01+/-0,01	0,01+/-0,01
ACG-812c-F1	94,76+/-0,22	4,88+/-0,06	0,02+/-0,03	0,18+/-0,25
ACG-830b-F1	89,44+/-0,73	10,15+/-1,22	0,09+/-0,08	0,31+/-0,39
Fc-26c	91,65+/-4,40	8,33+/-4,40	0,01+/-0,02	0,01+/-0,01
Fc-15d	91,95+/-1,12	8,04+/-1,12	0,00	0,00
Fc-35	92,21+/-1,10	7,69+/-1,17	0,00	0,08+/-0,06
Fc-29d	90,86+/-0,23	9,11+/-0,13	0,00	0,11+/-0,10
Fc-31	87,29+/-3,76	12,68+/-3,74	0,00	0,07+/-0,05
Fc-34	83,09+/-13,15	7,55+/-0,04	0,07+/-0,05	0,07+/-0,05
Fc-30b2	95,03+/-1,96	4,94+/-0,92	0,02+-0,03	0,02+/-0,02
ACG-858E1(R-(14))	88,56+/-2,54	10,23+/-2,99	0,68+/-0,18	0,51+/-0,27
ACG-858E2(S-(14))	89,36+/-1,34	10,37+/-1,40	0,10+/-0,03	0,34+/-0,06
Fc-29b	82,09+/-6,99	17,61+/-7,27	0,01+/0,02	0,28+/-0,30

Table 9. Apoptosis induction on MCF-7 breast cancer cell line after treatment for 24h with the (RS)-benzoxazepin-purines.

Compounds	Viable cells	Necrotic cells	Early apoptosis	Late apoptosis
MOCK	86,26+/- 7,25	12,61+/-7,50	0,00	1,11+/-0,24
ACG-812b-F3(Bozep)	46,65+/-6,97	16,13+/-17,19	23,38+/-1,18	13,84+/-1,99
ACG-810e	51,04+/-24,77	10,92+/-4,48	35,64+/-1,44	2,40+/-0,88
ACG-812c-F1	49,71+/-0,38	4,81+/-0,25	43,30+/-0,26	2,17+/-0,39
ACG-830b-F1	62,62+/-1,53	5,56+/-2,13	28,06+/-0,73	3,75+/-0,12
Fc-26c	74,31+/-0,05	3,43+/-0,76	19,61+/-0,83	2,64+/-0,03
Fc-15d	67,60+/-2,64	3,76+/-1,03	24,43+/-1,02	4,19+/-0,59
Fc-35	58,32+/-6,60	8,085+/-3,50	24,27+/-0,49	9,33+/-2,62
Fc-29d	70,82+/-3,58	5,52+/-0,68	18,73+/-2,46	4,92+/-0,43
Fc-31	71,84+/-11,96	4,98+/-1,36	18,64+/-9,11	4,52+/-1,48
Fc-34	76,30+/-5,20	4,01+/-1,64	15,81+/-2,36	3,88+/-1,20
Fc-30b2	79,78+/-0,64	2,48+/-0,82	13,93+/-1,56	3,8+/-0,10
ACG-858E1(R-(14))	44,55+/-2,20	2,94+/-0,37	41,99+/-1,90	10,51+/-0,66
ACG-858E2(S-(14))	63,98+/-6,58	1,84+/-0,32	28,82+/-4,74	5,35+/-1,53
Fc-29b	76,34+/-0,52	1,99+/-0,44	18,89+/-0,70	2,77+/-0,77

Table 10. Apoptosis induction on MCF-7 breast cancer cell line after treatment for 48h with the (RS)-benzoxazepin-purines.

In MCF-7 mock DMSO treated cultures apoptosis was no detected after 24 h or 48 h (Table 9 and 10). Similarly, compounds did not induce apoptosis after 24 h of treatment (Table 9). In contrast, MCF-7 cells treated during 48 h (Table 10) with (RS)-benzoxazepin-purines showed a significant increase of early apoptotic cells in relation to the control culture with percentages varying from 13,93% in cells treated with Fc-30b2 to 43,30% after treatment with ACG-812-cF1 (Figure 2A). The percentage of late apoptotic cells also increased in MCF-7 cell line treated with drugs in comparison with mock-DMSO treated cells. It should be noted that levels of early apoptosis induced by ACG-858-E1(R-(14) (41,99%) (Figure 2A) were almost double in comparison with the corresponding racemic compound, ACG-812b-F3 (Bozepinib) (23,38%).

To confirm the presence of apoptosis in MCF-7 treated cells, we carried out confocal microscopy after staining with FITC-conjugated annexin V and the nuclear non-vital stain PI (Figure 2B). The presence of apoptosis was confirmated by the presence of tipycal staining pattern where annexin FITC is exposed at outer cell layer in

its attachment to phosphatidilserine residues exposed in this process. IP staining assessed the presence of both necrotic and later apoptotic cells.

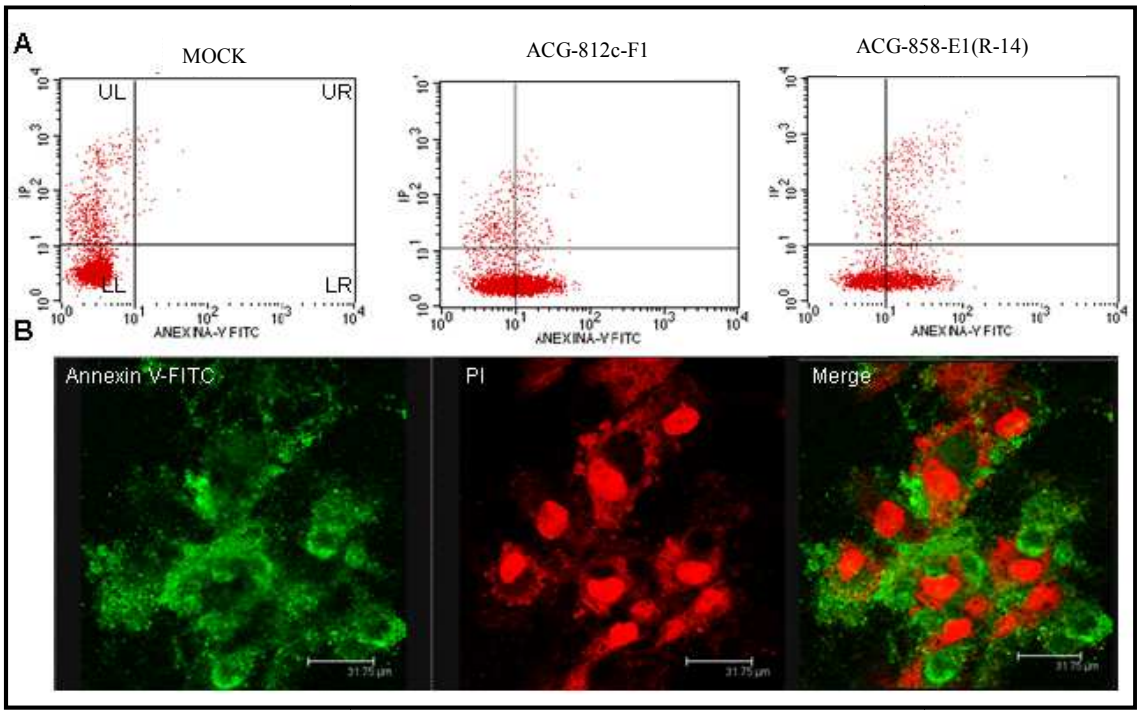

Figure 2. Apoptosis induction in MCF-7 breast cancer cell line after treatment for 48h with (RS)-benzoxazepin-purines. (**A**) Representative panels of cytometry analysis for mock treated cells with 0.5% DMSO alone, ACG-812c-F1 and ACG-858-E1(R-(14)). In each panel, lower left quadrant (LL) shows viable cells which are negative for both annexin V-FITC and PI, lower right (LR) shows annexin V positive cells which are in the early stage of apoptosis, upper left (UL) shows only PI positive cells which are dead, and upper right (UR) shows both annexin V and PI positive, which are in the stage of late apoptosis. (**B**) Confocal microscopy analysis using simultaneous staining with annexin V-FITC (green) and PI (red) in MCF-7 after treatment with ACG-812c-F1.

Also, we assayed apoptosis induction in MCF-7 breast cancer and HCT-116 colon cancer cell lines after treatment with the most active 2,6-Dichloro-9- or 7-(Ethoxycarbonylmethyl)-9H-or 7H-Purines compounds at IC_{50} values for 24 hours by flow cytometry (Table 11).

Compounds FMM238bF2 and FMM238bF3 at 24 h induced high levels of apoptosis in breast and colon cancer cells in comparison with mock DMSO treated cell cultures.

Compound	MCF-7	HCT-116
MOCK	10,80 ± 0,85	7,27 ± 1,57
FMM238bf2	20,53 ± 0,91	20,20 ± 3,18
FMM238bF3	24,10 ±4,37	17,03 ± 1,00

Table 11. Apoptosis induction in human MCF-7 breast cancer cell line and HCT-116 colon cancer cell line after treatment for 24 h with the two most active compounds, FMM238bF2 and FMM238bF3.

5. ANTIPROLIFERATIVE ACTIVITY OF BOZEPINIB ON ESTABLISHED CELL LINES

As result of data obtained in antiproliferative, cell cycle and apoptosis assays, as well as chemical properties based on feasibility synthesis, we select ACG-812-bF3 (Bozepinib) as the compound to carry out more detailed assays to know its action mechanism.

Antiproliferative assays were carried out on different tumoral and non tumoral breast and colon cell lines to determine IC_{50} (Table 12, Figure 3 and 4) as previously described in material and methods, with serial increased concentrations of Bozepinib. The results are showed below:

Cell line	IC50 (μM)
MCF-7	0,35 ± 0,01
MDA-MB 231	0,16 ± 0,06
SKBR-3	0,33 ± 0,00
MDA-MB 468	0,85 ± 0,00
MCF-10[a]	1,82 ± 0,00
Caco-2	0,63 ± 0,01
T-84	1,01 ± 0,28
HT-29	1,35 ± 0,28
SW-480	0,23 ± 0,01
HCT-116	0,57 ± 0,02
CCD-18Co	2,01 ± 0,01

Table 12. Antiproliferative activities of Bozepinib against breast cancer cell lines MCF-7, MDA-MB 231, SKBR 3, MDA-MB 468 and non tumoral MCF-10A cell line and colon cancer cell lines Caco-2, T-84, HT-29, SW-480, HCT-116 and non tumoral CCD-18Co cell line.

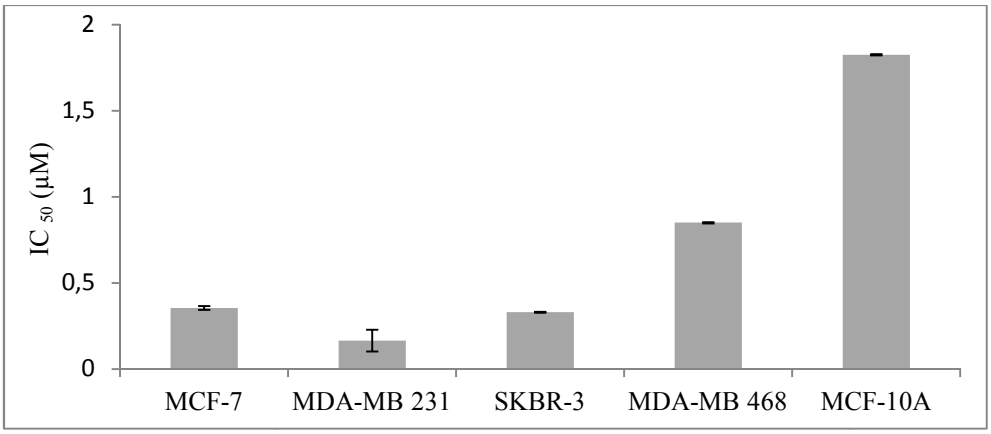

Figure 3. IC_{50} of Bozepinib in breast cancer cell lines and non tumoral cell line.

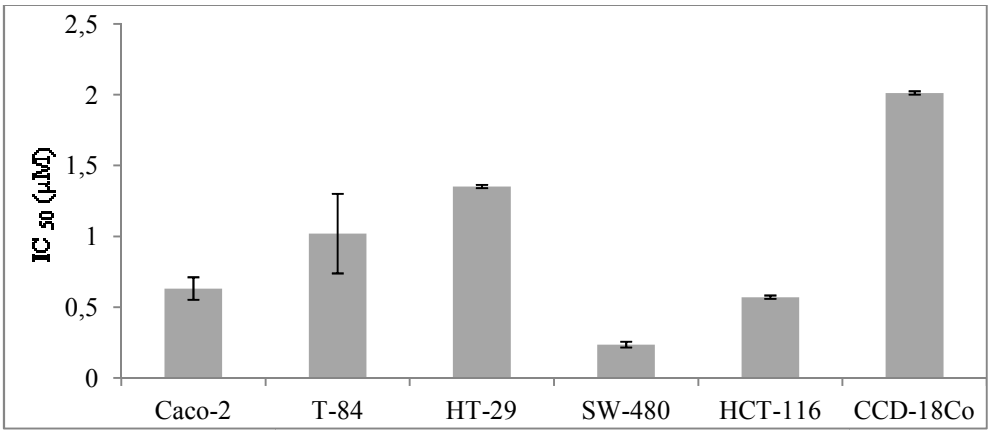

Figure 4. IC_{50} of Bozepinib in colon cancer cell lines and non tumoral cell line.

The IC_{50} value for the MCF-10A non tumoral cell line was almost double than the value determined for MDA-MB 468 cancer cells, and more than five times higher than IC_{50} value determined for MCF-7 and SKBR-3 breast cancer cell lines (Table 4, Figure 2).

Also IC_{50} values were determined in colon cancer cell lines Caco-2, T-84, HT-29, SW-480, HCT-116 and in the non tumoral cell line CCD-18Co (Table 4, Figure 3). IC_{50} value for colon non tumoral cell line was almost double than for the tumoral cell lines T-84 and HT-29 and more than triple for Caco-2 and SW-480 colon cancer cells lines.

6. SELECTIVE ACTIVITY OF BOZEPINIB ON ESTABLISHED CELL LINES.

To study the selective activity of Bozepinib we determine the therapeutic index (TI) as previously described in material and methods using IC_{50} calculated for the different tumoral and non tumoral breast and colon cell llines.

Cell line	TI
MCF-7	5,14
MDA-MB 231	11,00
SKBR-3	5,53
MDA-MB 468	2,14
Caco-2	3,18
T-84	1,97
HT-29	1,48
SW-480	8,56
HCT-116	3,52

Table 13. Therapeutic indexes (TI) for Bozepinib in MCF-7, MDA-MB 231, SKBR-3 and MDA-MB 468 breast cancer cell lines and Caco-2, T-84, HT-29, SW-480 and HCT-116 colon cancer cell lines.

Data showed a high selectivity level of Bozepinib for breast cancer cell line, with a TI value higher than 10 in MDA-MB 231 cancer cell line and 8,5 for SW-480 colon cancer cell line.

7. BOZEPINIB INHIBITS THE ACTIVATION OF SEVERAL KINASES INVOLVED IN CANCER CELLS PROLIFERATION

To study the effect of Bozepinib on cancer proliferation pathways, we carry out an *ex vivo* multikinase screening assay (described in Material and Methods). The inhibitory effect was assessed using two different Bozepinib concentrations, 5µM and 50µM. This effect was studied in a 36 kinases activity panel.

Compound	Bozepinib	
Assay conc. (μM)	**5**	**50**
AKT2	100	43
EGF-R wt	84	17
ERBB2	101	25
ERK2	104	50
JAK3	94	43
JNK1	45	29
JNK2	77	37
JNK3	81	43
p38-alpha	41	27
PDK1	86	24
RET	79	14
VEGF-R1	91	18
VEGF-R2	82	13
VEGF-R3	84	13

Table 14. Inhibitory effect of Bozepinib for an *ex vivo* assay for kinases with a residual activity under 50%, at two different concentrations, 5 μM and 50 μM.

Bozepinib treatment showed an inhibitory effect over numerous kinase activities at 50μM concentration, highlighting relevant kinases involved in cancer cells proliferation such as JNKs and ERKs and cellular signalling pathways such as EGFR and HER-2. Also, Akt protein and VEGF receptors were significantly inhibited in the screening assay (Table 14). In order to analyze whether Bozepinib inhibits the HER2 signaling pathways in breast cancer cells, we treated the HER2 positive SKBR-3 cell line with 5 μM of Bozepinib and we analyzed the expression and the activation of proteins involved in HER2 signalling at different times post-treatment (Figure 5A and Figure 6) by western blot analysis. Whereas the total level of HER2 receptor remained stable during treatment, the phosphorylated form was completely inhibited after 2 hours post-treatment. Consequently, p-Akt1 was also inhibited following a significant decrease in the total level of the VEGF production (Figure 5A). Moreover, we also detected the inhibition of Erk and JNK kinases in MCF-7 and MDA-MB 468 breast cancer cell lines when were treated with 5 μM of Bozepinib (Figure 5B and 5C, Figures 6 and 7). Both cell lines showed decreased levels of phosphorylation of JNK and Erk

proteins after treatment that were more accused in MCF-7 at 4 hours post-treatment and in MDA-MB 468 cell line after 8 hours post-treatment (Figure 5).

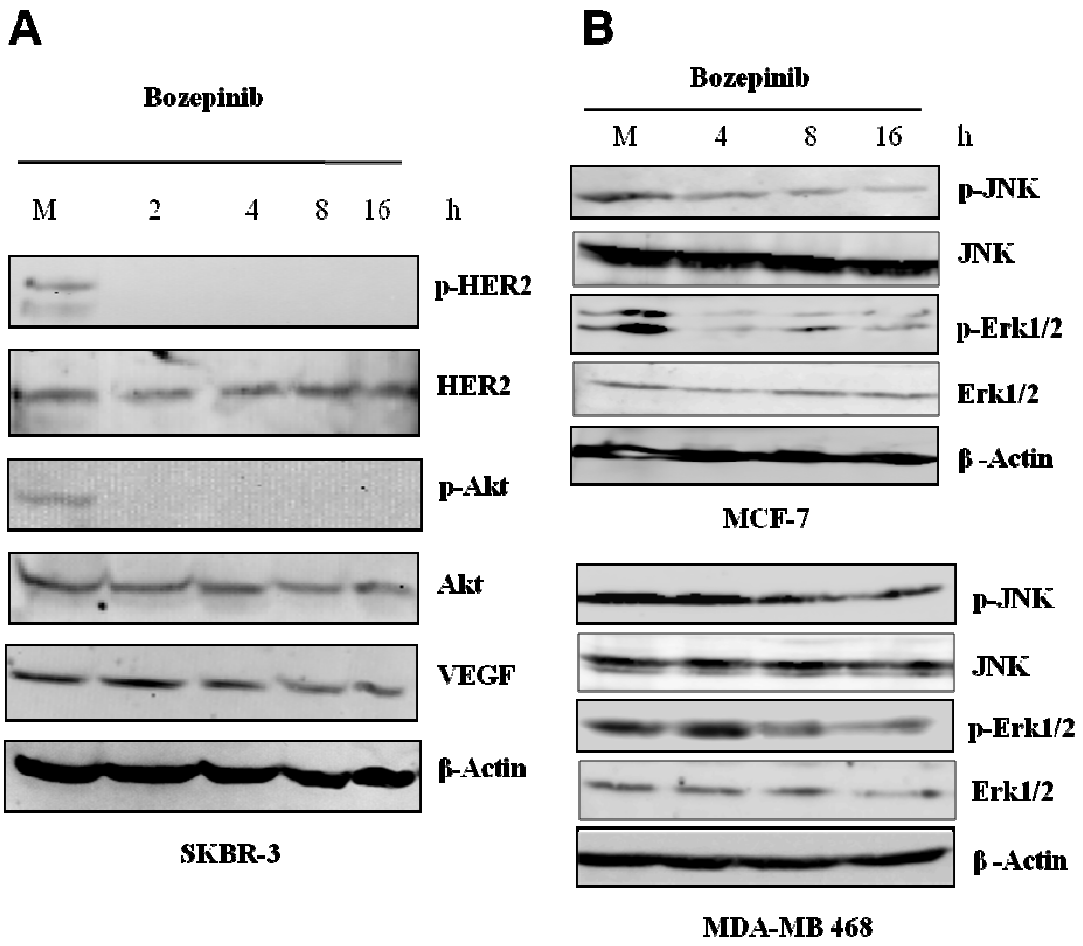

Figure 5. Western blot analysis of different proteins related with cancer cell proliferation after treatment with 5 µM of Bozepinib . p-HER2, HER-2, p-Akt, Akt, VEGF, p-JNK and p-Erk1/2 were analyzed after 2, 4, 8 and 16 h post-treatment in SKBR-3 (A), MCF-7 and MDA-MB 468 (B) cells and their respective mock treated cells. β-actin was used as housekeeping protein.

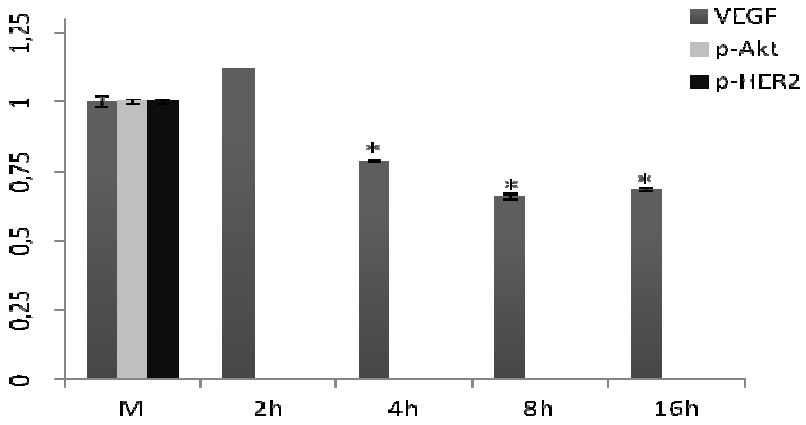

Figure 6. Western blot quantitation of VEGF, p-Akt and p-HER2 proteins on SKBR-3 breast cancer cells normalized with β-actin signal and relative to mock-treated cells (value 1) . Data were obtained from three independent experiments performed in duplicate and are expressed as mean ± SE (*p <0,05 vs control).

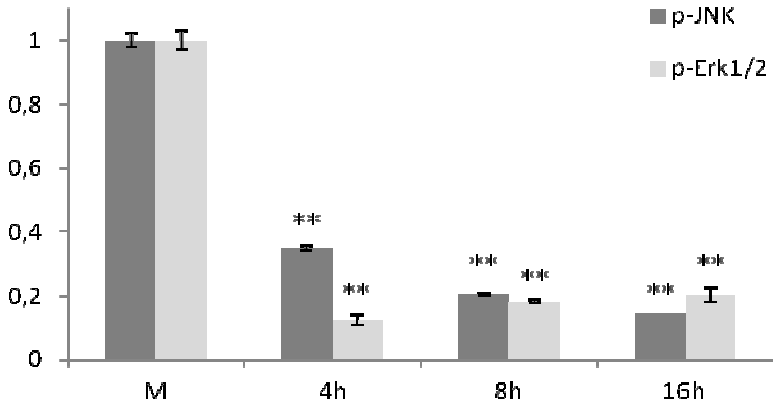

Figure 7. Western blot quantitation of p-JNK and p-Erk1/2 proteins on MCF-7 breast cancer cells normalized with β-actin signal and relative to mock-treated cells (value 1). Data were obtained from three independent experiments performed in duplicate and are expressed as mean ± SE (**p <0,01 vs control).

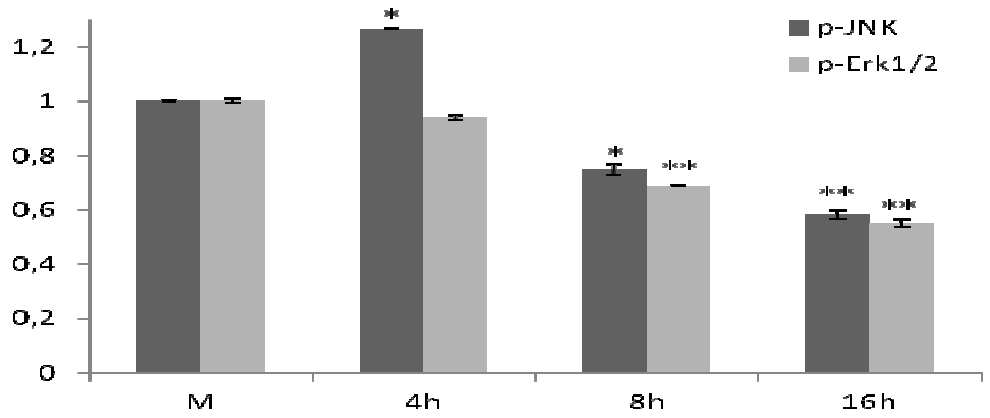

Figure 8. Western blot quantitation of p-JNK and p-Erk1/2 proteins on MDA-MB 468 breast cancer cells normalized with β-actin signal and relative to mock-treated cells (value 1). Data were obtained from three independent experiments performed in duplicate and are expressed as mean ± SE (**p <0,01 vs control; *p <0,05 vs control).

8. GENE EXPRESSION PROFILE CHANGES AFTER BOZEPINIB TREATMENT IN BREAST CANCER CELLS

Gene expression profile changes in MDA-MB 468 cells after Bozepinib treatment was used to understand the molecular changes underlying Bozepinib exposure. For this reason, a comparative cDNA microarray analysis was performed to investigate the differences in the expression profiles (close to 19000 gene) comparing the effect of Bozepinib (5 μM) in MDA-MB 468 cells at 4 and 16h.

Differentially expressed genes were identified (cut-off values >1.5 fold change and $p<0.05$). The overall gene expression response to Bozepinib treatment was time dependent. At 4h after Bozepinib treatment from 178 genes diferentially expressed, 115 genes were up-regulated whereas 64 genes were down-regulated. At 16h, about a total gene number of 471 were diferentially expressed; 143 were up-regulated and 328 were down-regulated (Figure 9).

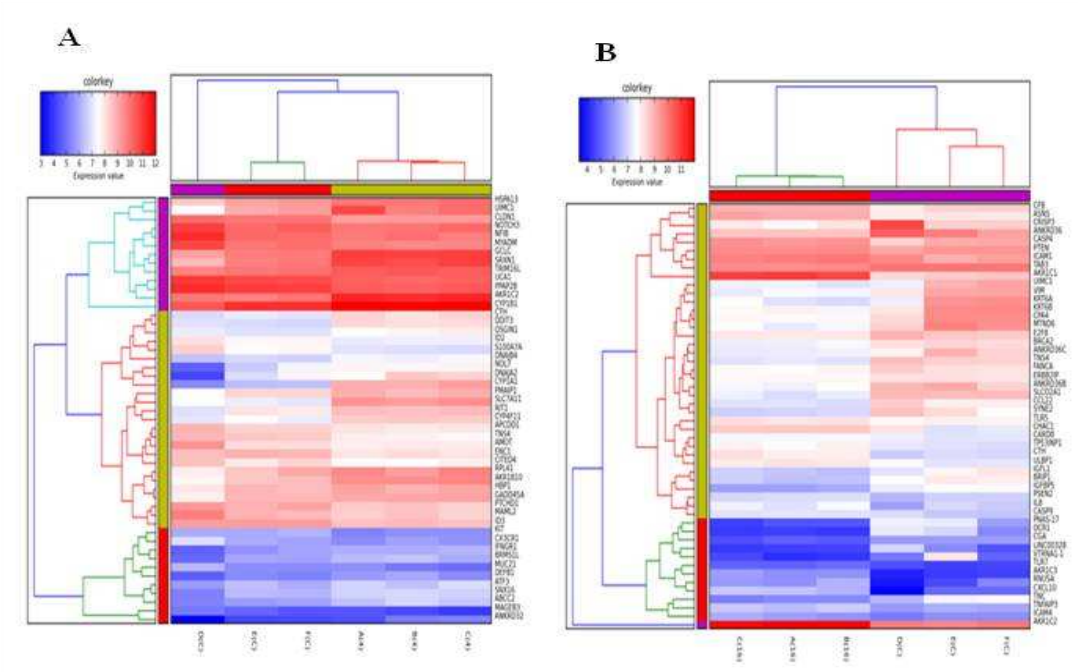

Figure 9. Gene expression profile heatmap of the 50 top fold change gene up and downregulated at 4 (A) and 16 (B) hours.

Our results show that differentially expressed genes belonged to several functional classes and pathways (Tables 15-18). We observed the down-regulation of genes involved in breast cancer tumourigenesis (*Brca1, Dkk1, Claudin1*), tumoral cells progression (*Notch3, Maml2, Vimentin*), multidrug resistance (*Vtrna1-1*), cell cycle progression (*E2f8A*), DNA reparation (*Brca1*), Metastasis (*Vimentin, Brms1l*) and upregulation of genes involved in inhibition of angiogenesis: *CXCL10*, apoptosis: *Casp4, Brms1l* (a metastasic repressor), *CSE* (involved in cell proliferation inhibition).

Representative examples of the top 25 up/down-regulated genes were listed in Tables 15, 16, 17 and 18.

Gene symbol	Gene description	Fold change
HMOX1	heme oxygenase (decycling) 1	15,55
CYP1A1	cytochrome P450, family 1, subfamily A, polypeptide 1	7,62
SLC7A11	solute carrier family 7, member 11	4,41
DNAJA2	DnaJ (Hsp40) homolog, subfamily A, member 2	3,52
AGPAT9	1-acylglycerol-3-phosphate O-acyltransferase 9	3,19
SCD	stearoyl-CoA desaturase (delta-9-desaturase)	3,18
UIMC1	ubiquitin interaction motif containing 1	3,14
UIMC1	ubiquitin interaction motif containing 1	3,14
LLPH	LLP homolog, long-term synaptic facilitation (Aplysia)	2,98
NOL7	nucleolar protein 7, 27kDa	2,80
AKR1C2	aldo-keto reductase family 1, member C2	2,69
ZC3H15	zinc finger CCCH-type containing 15	2,65
UFM1	ubiquitin-fold modifier 1	2,60
SRXN1	sulfiredoxin 1 homolog (S. cerevisiae)	2,53
GCLC	glutamate-cysteine ligase, catalytic subunit	2,47
AKR1C3	aldo-keto reductase family 1, member C3 (3-alpha hydroxysteroid dehydrogenase, type II)	2,44
DDIT3	DNA-damage-inducible transcript 3	2,44
GCLM	glutamate-cysteine ligase, modifier subunit	2,38
AKR1B10	aldo-keto reductase family 1, member B10 (aldose reductase)	2,37
CTH	cystathionase (cystathionine gamma-lyase)	2,29
CYP4F11	cytochrome P450, family 4, subfamily F, polypeptide 11	2,26
LOC644714	hypothetical protein LOC644714	2,24
ANKRD32	ankyrin repeat domain 32	2,20
FAM115A	family with sequence similarity 115, member A	2,18
TXNRD1	thioredoxin reductase 1	2,16

Table 15. List of the 25 first genes up-regulated in MDA-MB 468 cells after 4 hours of Bozepinib treatment.

Gene symbol	Gene description	Fold change
AKR1C2	aldo-keto reductase family 1, member C2	4,12
CXCL10	chemokine (C-X-C motif) ligand 10	4,00
AKR1C3	aldo-keto reductase family 1, member C3	3,01
RNU4-1	RNA, U4 small nuclear 1	2,82
RNU5E	RNA, U5E small nuclear	2,79
RNU5A	RNA, U5A small nuclear	2,59
RNU4-2	RNA, U4 small nuclear 2	2,41
RNU2-1	RNA, U2 small nuclear 1	2,30
STC2	stanniocalcin 2	2,25
SNORD116-6	small nucleolar RNA, C/D box 116-6	2,21
ASNS	asparagine synthetase (glutamine-hydrolyzing)	2,07
CTH	cystathionase (cystathionine gamma-lyase)	2,06
CHAC1	ChaC, cation transport regulator homolog 1 (E. coli)	2,05
DDIT4	DNA-damage-inducible transcript 4	1,94
ALDH1L2	aldehyde dehydrogenase 1 family, member L2	1,93
MUC15	mucin 15, cell surface associated	1,92
AKR1B10	aldo-keto reductase family 1, member B10 (aldose reductase)	1,90
PIR	pirin (iron-binding nuclear protein)	1,87
NUPR1	nuclear protein, transcriptional regulator, 1	1,86
CCL2	chemokine (C-C motif) ligand 2	1,83
CD209	CD209 molecule	1,80
DENND2D	DENN/MADD domain containing 2D	1,79
SCARNA10	small Cajal body-specific RNA 10	1,76
CYP39A1	cytochrome P450, family 39, subfamily A, polypeptide 1	1,75
LSM14B	LSM14B, SCD6 homolog B (S. cerevisiae)	1,73

Table 16. List of the 25 first genes up-regulated in MDA-MB 468 cells after 16 hours of Bozepinib treatment

Gene symbol	Gene description	Fold change
LOC100131541	hypothetical LOC100131541	2,12
S100A7A	S100 calcium binding protein A7A	1,85
EFCAB4B	EF-hand calcium binding domain 4B	1,82
TNS4	tensin 4	1,79
GJA5	gap junction protein, alpha 5, 40kDa	1,66
ENC1	ectodermal-neural cortex 1 (with BTB-like domain)	1,66
MAML2	mastermind-like 2 (Drosophila)	1,64
GRAMD2	GRAM domain containing 2	1,64
CLDN1	claudin 1	1,63
DLX3	distal-less homeobox 3	1,63
AMOT	angiomotin	1,63
LCN1	lipocalin 1 (tear prealbumin)	1,62
IKZF2	IKAROS family zinc finger 2 (Helios)	1,60
APBB3	amyloid beta (A4) precursor protein-binding, family B	1,59
LOC100134868	hypothetical LOC100134868	1,58
PTCHD1	patched domain containing 1	1,58
TAS2R14	taste receptor, type 2, member 14	1,58
CX3CR1	chemokine (C-X3-C motif) receptor 1	1,57
SLC10A5	solute carrier family 10 (sodium/bile acid cotransporter family)	1,57
CITED4	Cbp/p300-interacting transactivator, with Glu/Asp-rich carboxy-terminal domain,	1,57
IRX3	iroquois homeobox 3	1,57
P2RY2	purinergic receptor P2Y, G-protein coupled, 2	1,57
FMO6P	flavin containing monooxygenase 6 pseudogene	1,56
ATP6V0A4	ATPase, H+ transporting, lysosomal V0 subunit a4	1,55
PPAP2B	phosphatidic acid phosphatase type 2B	1,55

Table 17. List of the 25 first genes down-regulated in MDA-MB 468 cells after 4 hours of Bozepinib treatment

Gene symbol	Gene description	Fold change
OCR1	ovarian cancer-related protein 1	4,84
VTRNA1-1	vault RNA 1-1	3,57
OLFML3	olfactomedin-like 3	3,40
LOC100131541	hypothetical LOC100131541	2,93
ATP6V0D2	ATPase, H+ transporting, lysosomal 38kDa	2,88
TNC	tenascin C	2,88
SLCO2A1	solute carrier organic anion transporter family	2,87
KRT6A	keratin 6A	2,85
CPA4	carboxypeptidase A4	2,71
GPR21	G protein-coupled receptor 21	2,67
KRT6B	keratin 6B	2,64
IGFBP5	insulin-like growth factor binding protein 5	2,63
LOC51152	melanoma antigen	2,54
TNS4	tensin 4	2,51
C9orf131	chromosome 9 open reading frame 131	2,48
VIM	vimentin	2,47
SYNE2	spectrin repeat containing, nuclear envelope 2	2,44
ANKRD36B	ankyrin repeat domain 36B	2,42
LOC100130428	IGYY565	2,39
CRISP3	cysteine-rich secretory protein 3	2,38
DKK1	dickkopf homolog 1 (Xenopus laevis)	2,29
BRIP1	BRCA1 interacting protein C-terminal helicase 1	2,27
LOC100132099	FRSS1829	2,27
HIST1H2BM	histone cluster 1, H2bm	2,25
ANKRD36B	ankyrin repeat domain 36B	2,24

Table 18. List of the 25 first genes down-regulated in MDA-MB 468 tumours after 16 hours of Bozepinib treatment.

Data obtained by Affymetrix microarray were analyzed with DAVID (Database Annotation, Visualization and Integrated Discovery) of the Advanced Biomedical Computing Center (NCI, Frederick,http://david.abcc.ncifcrf.gov). Gene list was then subdivided into functional categories using clustering algorithms (by term enrichment score). A summary of functional gene clusters is showed in Figure 10.

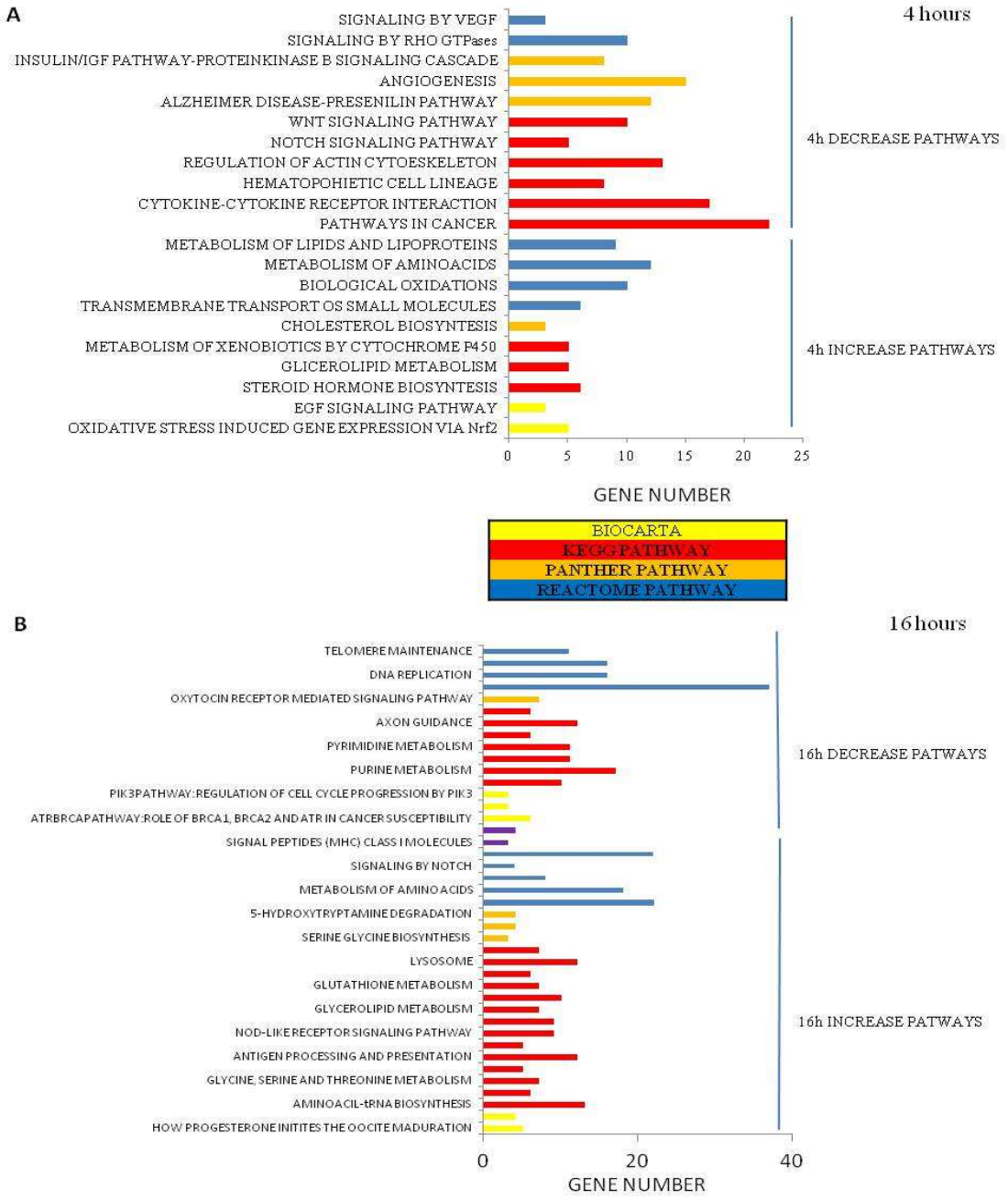

Figure 10. Gene clusters pathways affected by Bozepinib treatment after 4 hours (**A**) and 16 hours (**B**) on MDA-MB 468 breast cancer cells. Microarrays data were processed by DAVID.

Different types of analysis (functional, upstream regulator, and pathway analysis) were performed with the microarray data sets through the use of Ingenuity Pathways Analysis (IPA, IngenuityW Systems). IPA is a repository of biological interactions and functional annotations from many relationships between proteins, genes, complexes, cells, tissues, metabolites, drugs, and diseases. IPA selected sources and databases including major NCBI databases (EntrezGene, RefSeq, OMIM disease associations), microRNA-mRNA target databases, GWAS databases, and KEGG.

Genes from the dataset that met the log ratio cut-off of 1.5 were considered for analysis and to generate networks, which are graphical representation of molecular relationships between different genes. Ingenuity pathway analysis of gene expression profiles revealed several associated network functions (Figures 11 and 12).

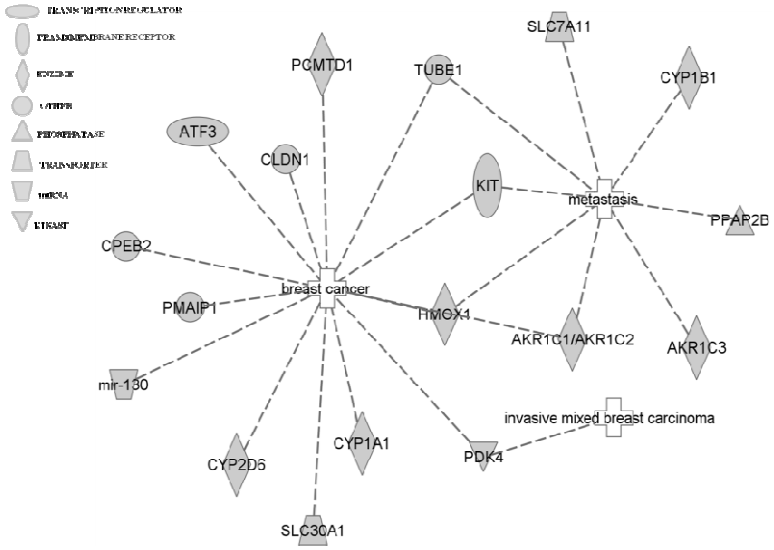

Figure 11. IPA network related with breast cancer at 4 hours in MDA-MB 468 cancer cell lines generated with microarray data gene. This network was classified as: Breast Cancer, Metastasis and Invasive Mixed Breast Carcinoma. Discontinuous lines are related with indirect interaction.

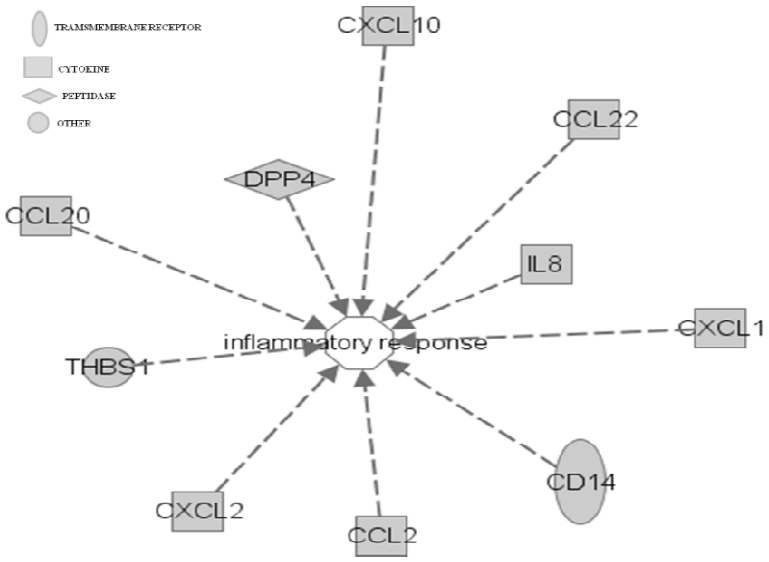

Figure 12. IPA network related with inflammatory response at 16 hours in MDA-MB 468 cancer cell lines generated with microarray data gene. This network was classified as Inflammatory Response. Discontinuous lines are related with indirect interaction.

9. VALIDATION OF GENE EXPRESSION CHANGES BY qRT-PCR.

Microarray data was validated by qRT-PCR. Data expression of selected genes (*CSE, CXCL10, MAML2, E2F8, NOTCH3 and CLAUDIN*1) was quantified by real time qRT-PCR. Genes that were found to be up- (Figure 13) or downregulated (Figure 14) by Bozepinib in the microarray data were confirmed by qRT-PCR assay.

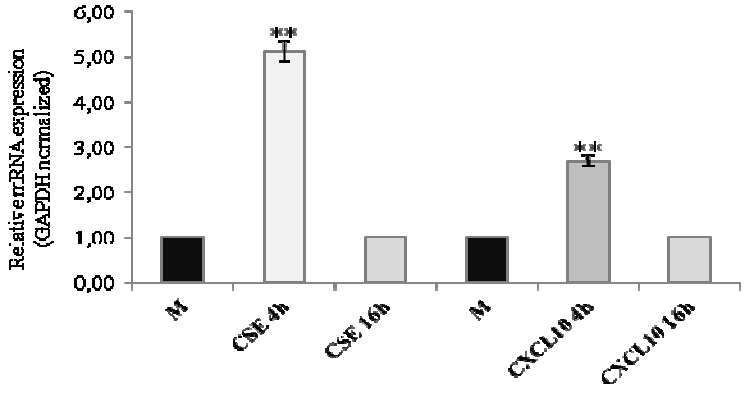

Figure 13. Relative mRNA expression quantified by qRT-PCR of selected genes upregulated after Bozepinib treatment in MDA-MB 468 cells compared with mock treated cells (value 1) and normalized with *GAPDH* reporter gene. Data were obtained from three independent experiments performed in duplicate and are expressed as mean ± SE (**p <0,01vs control).

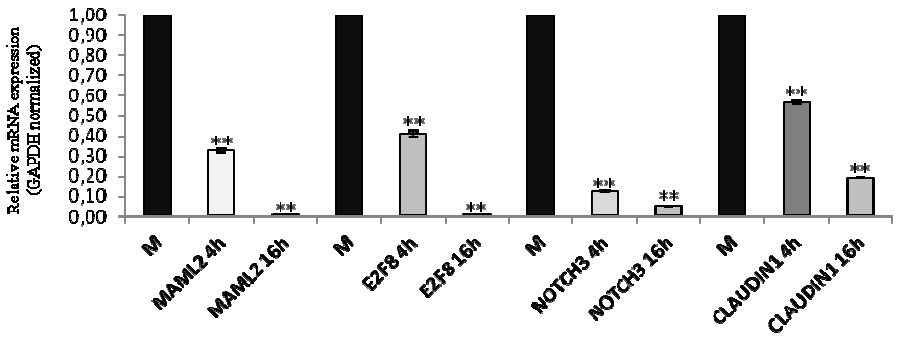

Figure 14. Relative mRNA expression quantified by qRT-PCR of selected genes downregulated after Bozepinib treatment in MDA-MB 468 cells compared with non treated cells and normalized with *GAPDH* reporter gene. Data were obtained from three independent experiments performed in duplicate and are expressed as mean ± SE (**p <0,01vs control).

10. BOZEPINIB HAS ANTIANGIOGENIC PROPERTIES AND INHIBITS CELL MIGRATION

The antiangiogenic properties of Bozepinib and its ability to suppress capillary-like structures was assessed by culturing HUVEC endothelial cell line on MATRIGEL^{TM}-coated wells as described in Material and Methods. As shown in Figure 15, HUVEC were able to form capillary-like structures after 4h and 8h. After treatment with Bozepinib at only 0,01 μM capillary-like structures were inhibited and this inhibition was dose dependent (Figures 15 and 16). This experiment confirms Bozepinib *in vitro* anti-angiogenic properties.

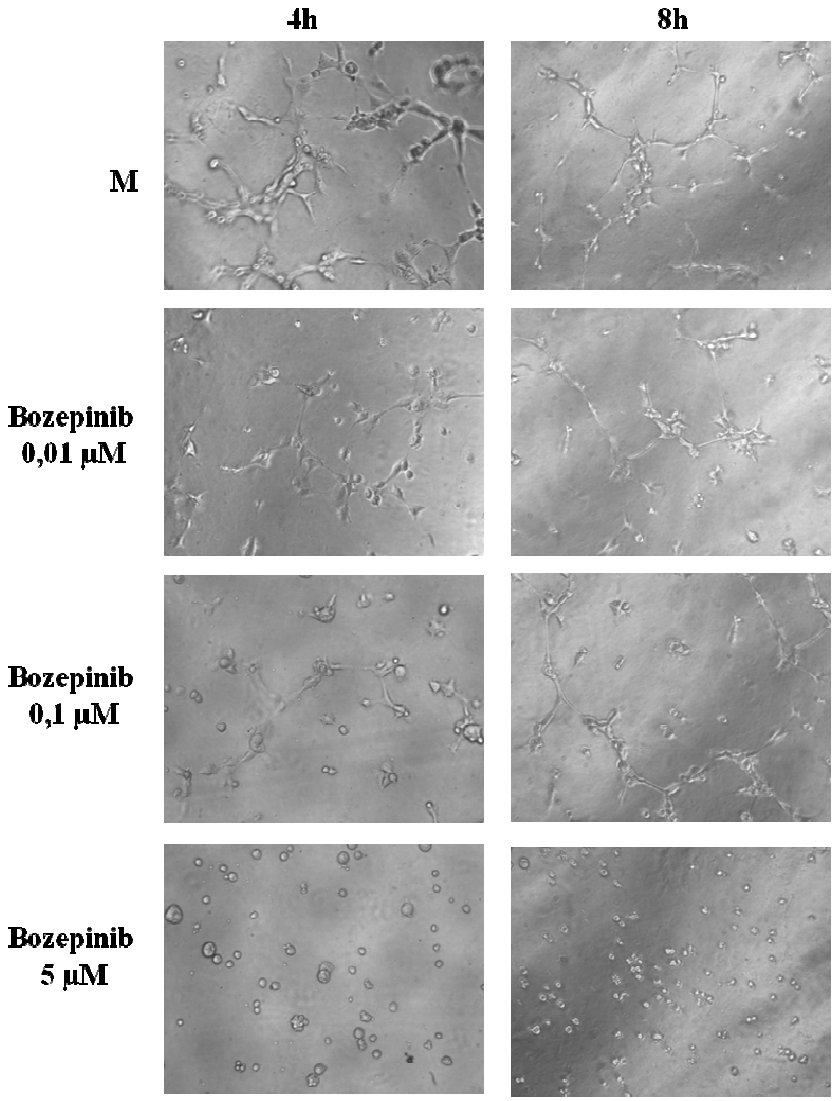

Figure 15. Inhibition of capillary network formation assay. Inhibition of capillary-like structures by Bozepinib at different concentrations (mock treated cells, 0,01µM, 0,1µM and 5 µM) and time (4 and 8 hours). Images of HUVEC cells cultured in EGM-2 medium were taken with light microscopy at 4 and 8h after Bozepinib treatment.

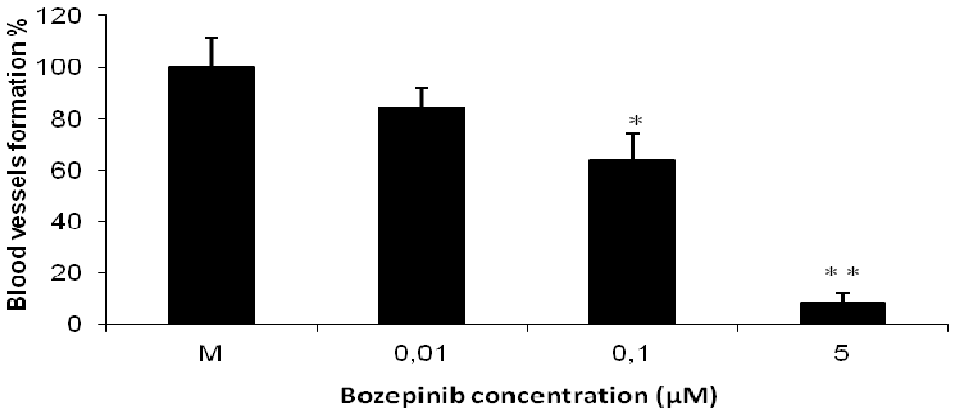

Figure 16. Semiquantification of Bozepinib capillary-like structure inhibition. Percentage of blood vessels inhibition after treatment with serveral Bozepinib concentrations compared with mock treated control cells at 4h. Data were obtained from three independent experiments performed in duplicate and are expressed as mean ± SE (**p <0,01 vs control).

11. WOUND HEALING ASSAY.

In order to evaluate Bozepinib treatment effect on cell migration we performed a cell migration assay (wound healing) on SKBR-3 breast cancer and HCT-116 colon cancer cell lines as previously described in Material and Methods. Data obtained from this assay showed a cell migration inhibition that was dose-dependent 48h after treatment with 0,2 µM, 2 µM and 5 µM compared with mock treated cells (Figures 17 and 18).

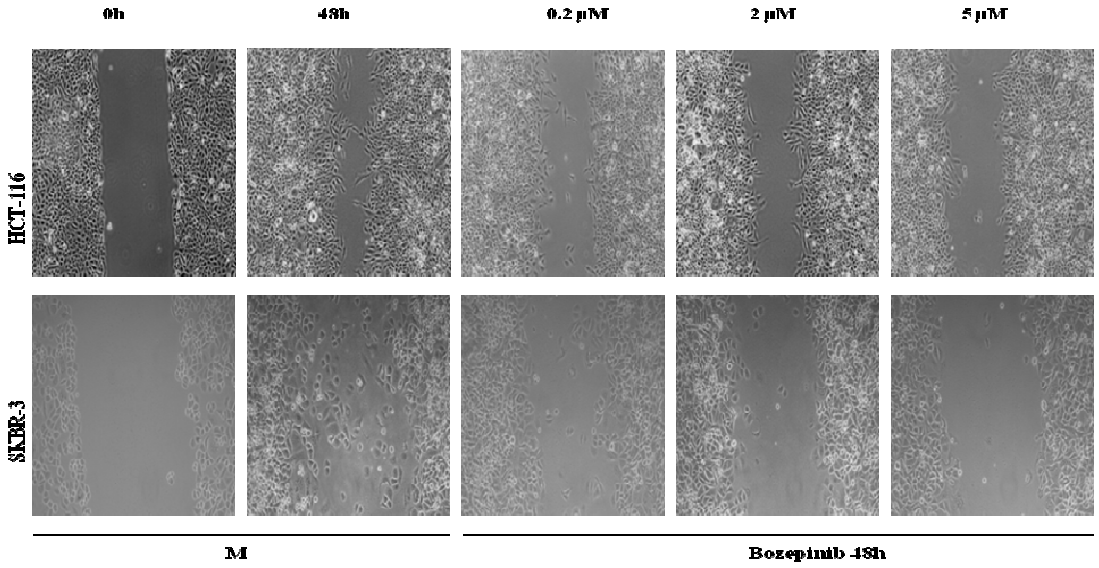

Figure 17. Bozepinib inhibits the invasiveness and cell migration of HCT-116 and SKBR-3 cells *in vitro*. Wound-healing assays were performed at 0 and 48 h with different concentrations of Bozepinib (Mock treated cells, 0,2 µM, 2 µM and 5 µM) observed under a phase-contrast microscope (10X objetive). The wound closure was illustrated by showing the area covered by cells 48 hours after wounding.

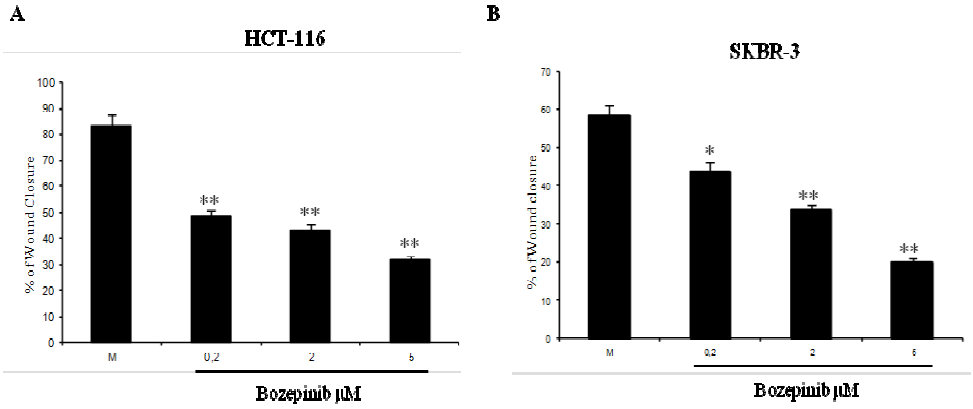

Figure 18. The panel represents the relative quantitation of the wound closure area calculated by measuring of the diminution of the wound bed surface upon time using Image J software 1.47v in HCT-116 (A) and SKBR-3 (B) cells. Data were obtained from three independent experiments performed in duplicate and are expressed as mean ± SE (**p <0,01; *p <0,05 vs control).

12. CYTOTOXICITY ACTIVITY OF BOZEPINIB ON BREAST AND COLON CANCER STEM CELL (CSCs) LINES

To determine the citotoxic activity on breast and colon CSCs lines isolated and grown as described in Material and Methods, we determine IC_{50} using serial increased concentrations of the compounds.

First of all, human breast and colon cell lines were enriched in CSCs by growing them into low attachment plates with *sphere medium* for 72h. After that, CSCs were isolated by flow cythometry by its ALDH activity as described in Material and Methods for SKBR-3 (Figure 19A), HCT-116 (Figure 19B) and MDA-MB 468 (Figure 19C).

We determined the Bozepinib IC_{50} values on the breast and colon cancer cells using two models of cells growing in sphere medium: one model consists in ALDH positive cells isolated by sorter (called ALDH+) and the other model consists in cells growing in sphere medium without previous sorter isolation (called “no sorter”). Moreover, we decided to use Salynomicin as control, one powerful anti CSCs drug (Gupta et al., 2009; Zhi et al., 2011). As showed in Table 19, IC_{50} value for Bozepinib in MDA-MB 468 and SKBR-3 cells growing in spheres was similar to Salynomicin. However, the IC_{50} value was lower for Salynomycin in the case of no sorter HCT-116 colon cancer cells. Different values were determined for sorter isolated ALDH+ and no sorter cells, and the positive cells did not show necessarily increased resistance in comparison with the no sorter isolated cells after both treatments (Table 19).

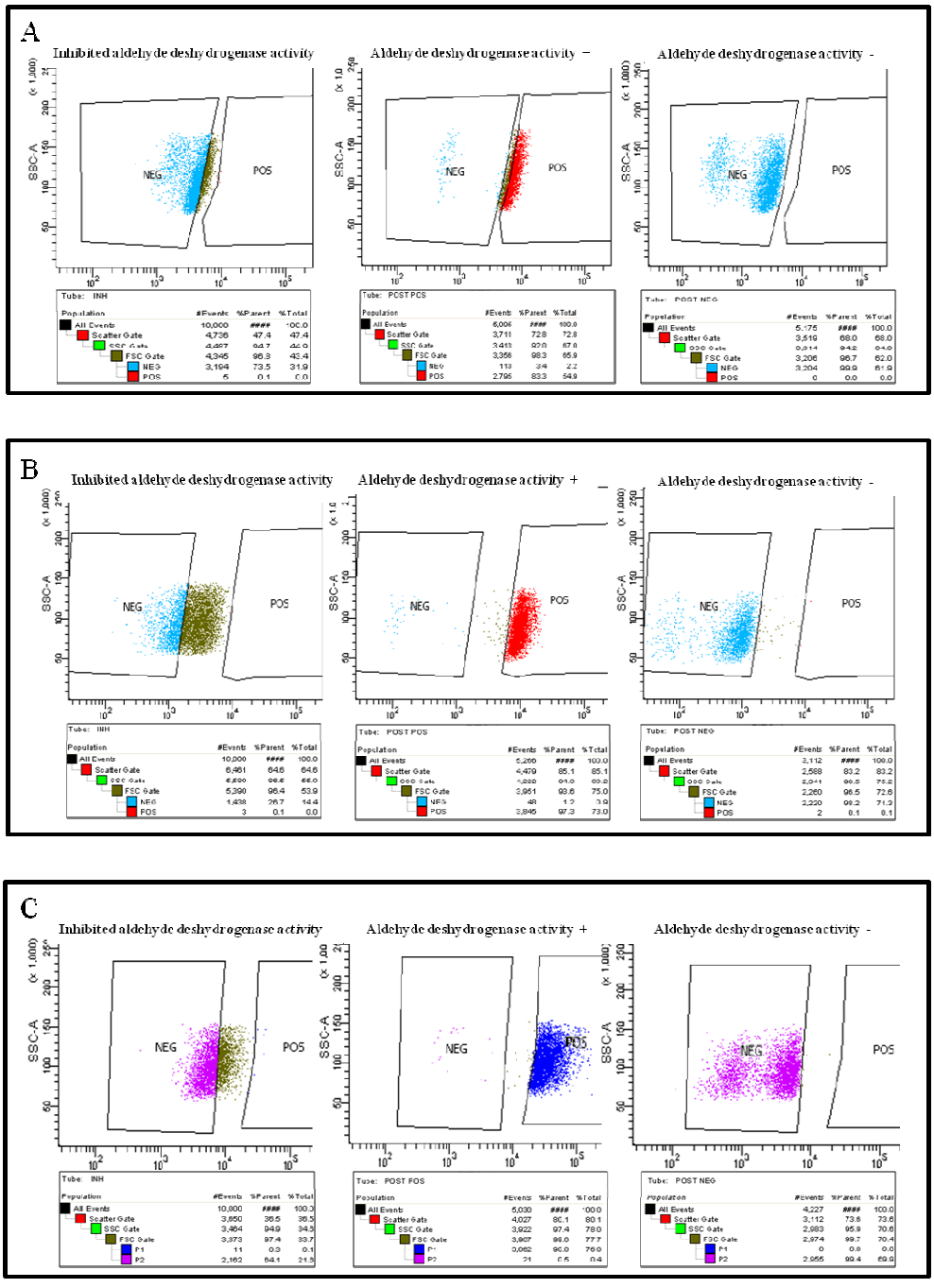

Figure 19. Breast cancer SKBR-3 (A) and MDA-MB 468 (B) CSCs and HCT-116 (C) colon CSCs isolation by flow cythometry based on aldehyde dehydrogenase activity.

	Bozepinib (µM)		Salinomycin (µM)	
Cell line	**ALDH +**	**NO SORTER**	**ALDH +**	**NO SORTER**
SKBR-3	15,78±0,023	15,06±0,002	9,67±0,07	10,05±0,005
MDA-MB 468	22,04±0,015	10,37±0,007	16,6±0,005	9,7±0,003
HCT-116	14,63±0,028	17,54±0,024	11,9±0,15	2,88±0,03

Table 19. Antiproliferative activities of Bozepinib and Salinomycin against SKBR-3 and MDA-MB 468 breast and HCT-116 colon CSCs enriched supopulations based on ALDH activity.

Although Bozepinib showed a higher IC_{50} value that Salynomicin in no sorter HCT-116 cells, it was able to considerably reduce the sphere formation at 8 µM and to inhibit the sphere formation after 20 µM after treatment (Figure20).

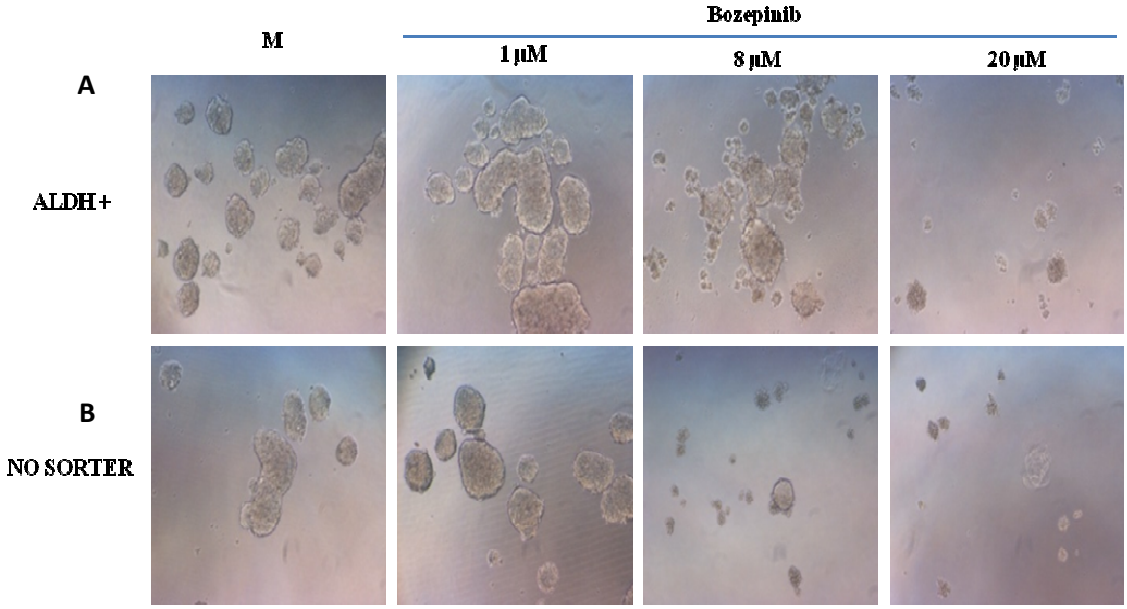

Figure 20. Antiproliferative activity of Bozepinib on positive aldheydo dehydrogenase activity (A, ALDH+) and non sorter CSCs sphere formation (B) on HCT-116 colon CSCs at 1, 8 and 20 µM concentrations, compared with mock-treated cells.

13. EFFECTS OF BOZEPINIB ON CSCs PATHWAYS

In correlation with the antitumor effect exerted by Bozepinib over CSCs and the gene data obtained by microarrays analysis we determined the modification of several described proteins involved in the *stem* phenotype of this subpopulations such as GLI-3,

SOX-2, c-myc, β-catenin. For this aim, both ALDH+ and ALDH- SKBR-3 breast and HCT-116 colon cancer subpopulations were treated with the IC_{50} and twice the IC_{50} of Bozepinib determined for every subpopulation (Figures 21 and 22).

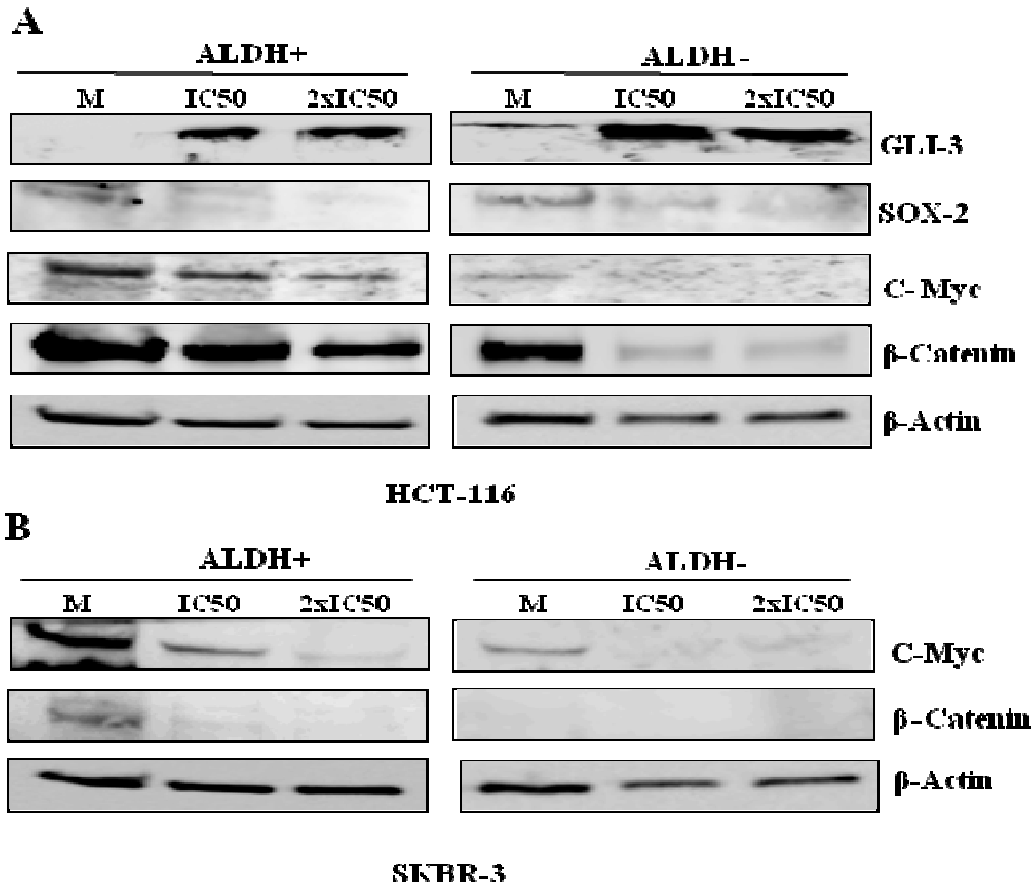

Figure 21. (**A**). Western blot analysis of GLI-3, SOX-2, c-Myc, β-Catenin and mock treated cells of ALDH+ and ALDH- HCT-116 CSCs after treatment with IC_{50} and $2xIC_{50}$ of Bozepinib. (**B**) Western blot analysis of c-Myc, β-Catenin and mock treated cells proteins of ALDH+ and ALDH- SKBR-3 breast CSCs after treatment with IC_{50} and $2xIC_{50}$ of Bozepinib. In both assays, β-actin was used as reference.

As shown in Figure 21, GLI-3, a described inhibitor of stem properties (Varnat et al., 2009) was detected in ALDH- HCT-116 cells and was absent in the HCT-116 ALDH+ subpopulation (Figures 21 and 22). Dramatically, this inhibitor was strongly induced in both subpopulations after Bozepinib treatment. However, no changes in GLI 3 protein level was detected in ALDH subpopulations isolated from SKBR-3 cell line (data not show). The stem cell transcription factor Sox2 was detected only in HCT-116 ALDH+ subpopulation but was reduced after treatment with IC_{50} and practically

disappeared after treatment with 2xIC_{50} concentration of Bozepinib (Figure 21 and 22). The oncogene c-myc was detected in both, HCT116 and SKBR-3 cell lines with high level of expression in ALDH+ subpopulations respect to the ALDH- subpopulations. Whereas a significant reduction of c-myc level was detected after bozepinib treatment in HCT-116 ALDH+ cells, c-myc was absent after treatment in the ALDH- cells of both HCT-116 and SKBR-3 subpopulations highlighting the absence of c-myc level even in SKBR-3 ALDH+ cells (Figure 23). Similar results were obtained for b-catenin expression where bozepinib was able to reduce its level in HCT-116 ALDH+ subpopulation and was able to inhibits its expression in ALDH- subpopulation of HCT-116 cell line and in both ALDH+/- subpopulations of SKBR-3 cell line.

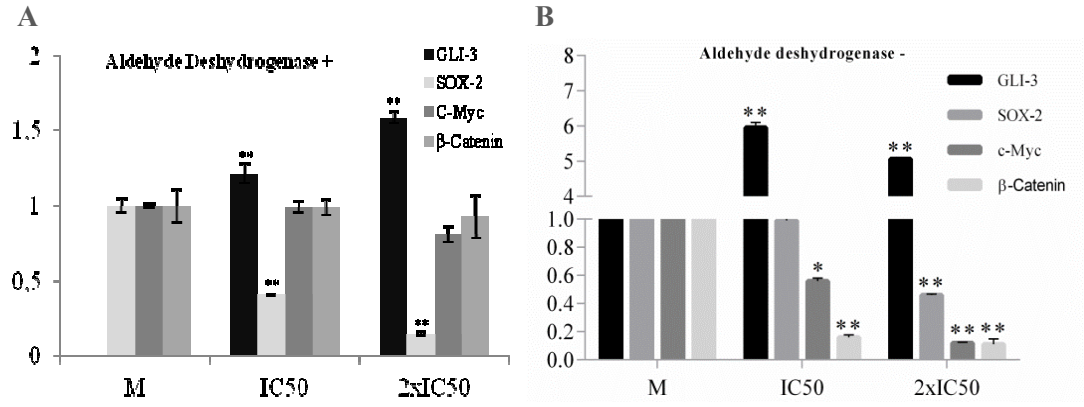

Figure 22. Relative western blot quantification of GLI-3, SOX-2, c-Myc and β-Catenin proteins on HCT-116 colon cancer cells normalized with β-actin signal and relative to mock-treated cells (value 1). (**A**) ALDH+ isolated cells and (**B**) ALDH– isolated cells. Data were obtained from three independent experiments performed in duplicate and are expressed as mean ± SE (**p<0,01 vs control, **p <0,05 vs control).

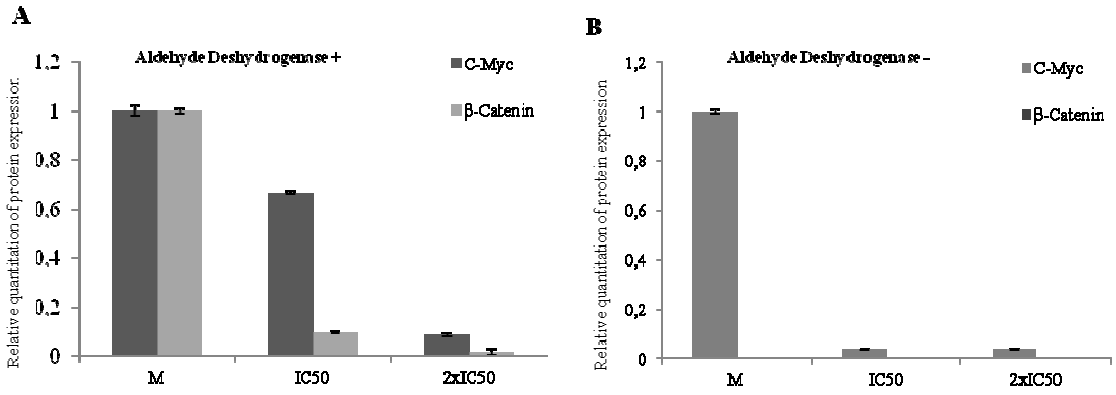

Figure 23. Relative western blot quantification of C-Myc and β-Catenin proteins on SKBR-3 breast cancer cells normalized with β-actin signal and relative to mock-treated cells (value 1) (**A**) ALDH+ isolated cells and (**B**) ALDH– isolated cells. Data were obtained from three independent experiments performed in duplicate and are expressed as mean ± SE (**p <0,01 vs control, *p <0,05 vs control).

14. *IN VIVO* TOXICITY AND ANTITUMOR EFFECT OF BOZEPINIB

To determine de toxicity of Bozepinib *in vivo***,** we examined both the acute and subacute toxicity profile of Bozepinib in BALB/c mice when it was administered in a single i.p. bolus injection (n = 25) at dose levels of 50, 75, 100, 150 and 200 mg/kg or *via* gavage (n = 25) in a single p.o. bolus at dose levels of 0.05, 0.5, 5 and 50 mg/kg. Bozepinib was nontoxic to BALB/c mice even at the highest i.p. bolus dose of 200 mg/kg and p.o. bolus dose of 50 mg/kg after 2 weeks. Control mice (n = 10; 5 mice for the i.p. group and 5 mice for the p.o. group) were treated with vehicle alone. All 50 Bozepinib-treated mice remained healthy and gained weight throughout the observation period, with no evidence of morbidity.

Moreover, we found that no signs of subacute toxicity appeared after 28 days of i.p. treatment with 100 mg /Kg twice a week (Figure 24). In fact, Bozepinib-treated mice showed no weight loss or unusual behavior and histopathologic examination also did not find any detectable toxicity in the liver or kidneys (data not shown), suggesting that Bozepinib at the concentration used did not cause any toxicity.

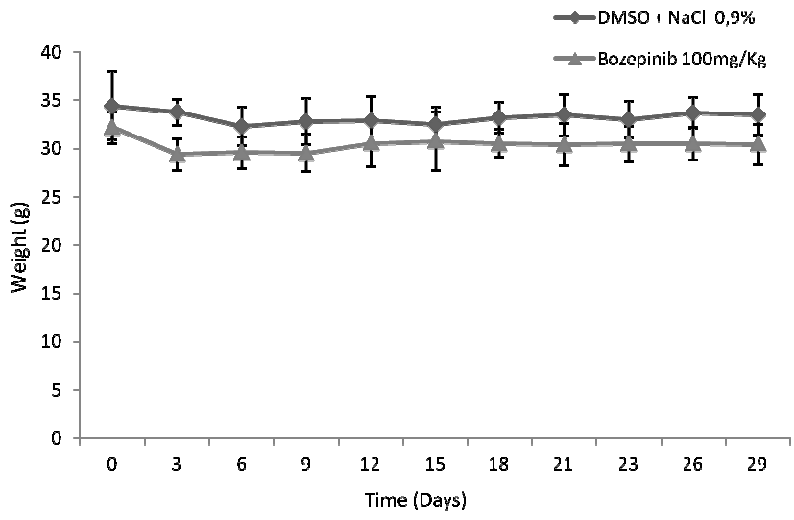

Figure 24. *In vivo* determination of Bozepinib subacute toxicity in BALB/c mice. Control mice were treated with a solution of DMSO+NaCl 0,9%. Bozepinib treatd mice were injected with a 100mg/kg dose.

To evaluate the effect of Bozepinib on tumour growth, heterotopic tumour xenografts were established using the MDA-MB-468 breast cancer cell line and the HT-29 colon cancer cell line. Nine days later, tumors reached a size superior of 100 mm3, and the mice received i.p. injection of Bozepinib or NaCl 0.9%, respectively. Bozepinib treatment significantly inhibited colon and breast cancer tumour growth when compared with control group ($P < 0.01$, $n = 8$). From day 3 for HT-29 cell line and day 18 for MDA-MB 468 after Bozepinib injection, the average of tumor volume was significantly lower in comparison with control group (Figures 25 and 26).

Inmunohistochemistry analysis showed that primary breast cancer tumours had a different morphological appearance between mice mock-treated and treated with 25 mg/kg of Bozepinib. Control group had a significant cell number indicative of a highly proliferative tissue; however, mice treated with Bozepinib displayed small size of tumours and with necrotic and non-viable tumour areas (Figure 27 A-D)

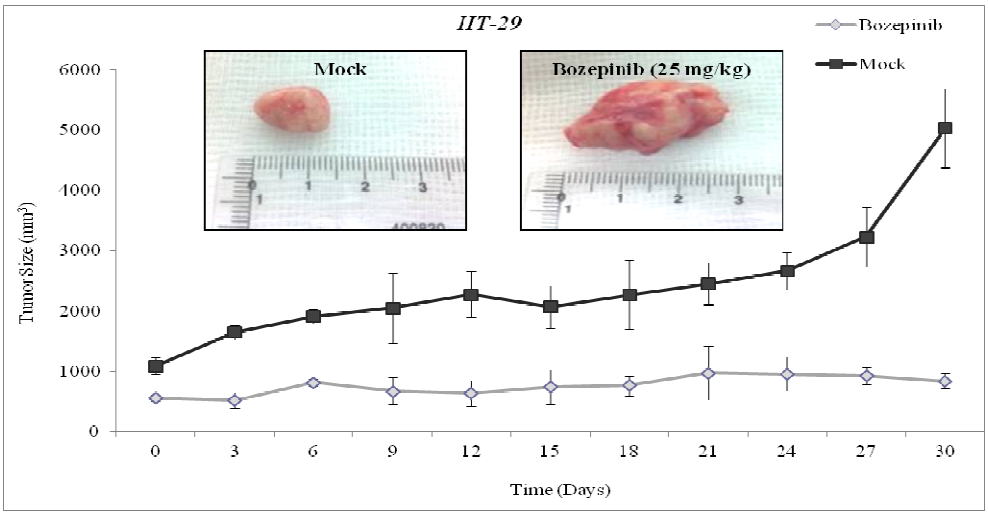

Figure 25. *In vivo* determination of Bozepinib antitumor activity in HT-29 colon cancer cells. Inserts represent tumor size of mock and Bozepzepinib treated mice.

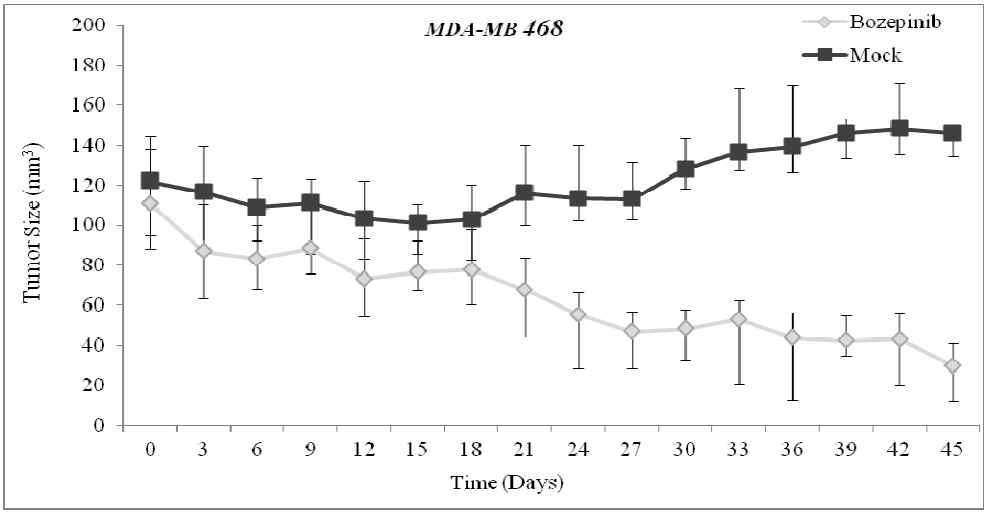

Figure 26. *In vivo* determination of Bozepinib antitumor activity in MDA-MB 468 breast cancer cells.

It has been described the ability of both HT-29 and MDA-MB 468 cells to form metastasis in nude mice (Price et al., 1989). We studied the spontaneous mestastatic potential in xenografts using MDA-MB-468 cell line. Lung metastasis ocurred in 5 of 6 (83.3%) mice in the control group (Figure 27 E) and, surprisingly, only in 1 of 6 mice (16.6%) treated with 25 mg/Kg of Bozepinib presented a metastatic nodule. Thse results demonstrate that Bozepinib have a potent antitumour and anti-metastatic activity.

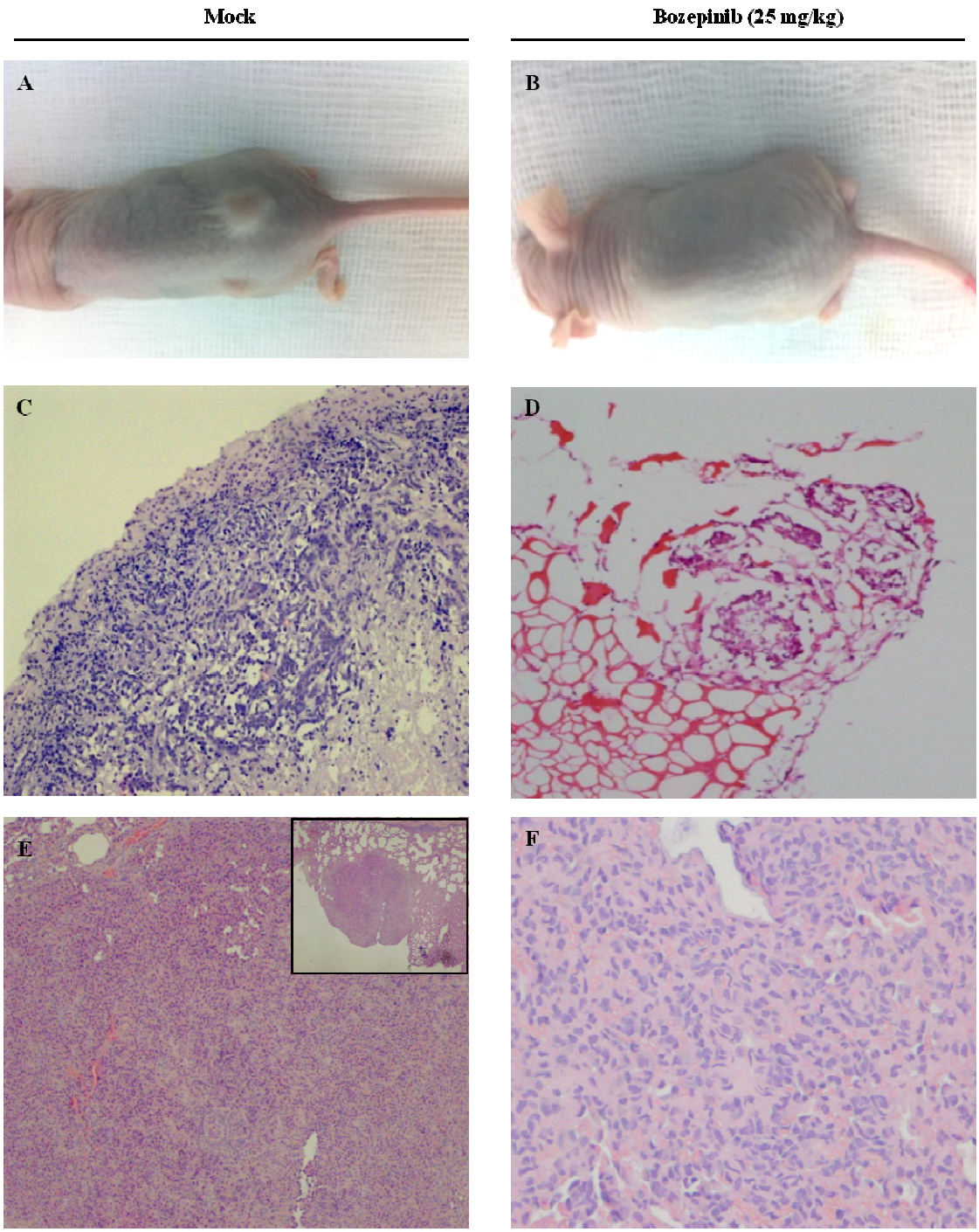

Figure 27. In vivo tumor induction of Balb/c nude mice with MDA-MB 468 cells. (A) Mock treated mice with vehicle alone and (B) treated with Bozepinib (25mg/kg). Representative hematoxylin and eosin (H&E)-stained section of tumour in mice mock-treated (C) (10x) and treated with Bozepinib (D) (4x). (E) Representative H&E-stained lung section from a metastasic nodule (10x) and insert (4x) in mock-treated mice. (F) Representative H&E-stained lung section from Bozepinib-treated mice (40x).

15. INTERFERON ENHANCES THE ANTITUMOUR EFECT OF BOZEPINIB IN COLON AND BREAST CANCER CELLS.

We have previously described the antitumor effect of Bozepinib in breast and colon cancer cell line (Table 12). In order to analyze if Bozepinib plus IFNα had also a synergistic cytotoxic effect in breast and colon cancer cells, we determined the IC_{50} value in several cancer cell lines and RKO cell line as described in Material and methods (Table 20).

	IC_{50} (μM)	
Cell line	**Bozepinib**	**Bozepinib+IFNα**
RKO	0,13 ± 0,01	0,09± 0,01
MCF-7	0,78 ± 0,06	0,44 ± 0,03
HCT-116	0,48 ± 0,08	0,31 ± 0,02
MEFsPKR $^{+/+}$	1,12 ± 0,18	0,89 ± 0,08
MEFsPKR $^{-/-}$	1,74 ± 0,28	1,77 ± 0,18

Table 20. Antiproliferative effects on several cell lines for Bozepinib and Bozepinib+IFNα.

Colon cancer cell lines were more sensible to Bozepinib cytotoxic effect showing lower IC_{50} values than MCF-7 breast cancer cell line (Table 20). Moreover, we analyzed if IFNα was able to improve the cytotoxic effect of Bozepinib by the addition of low dose (50 IU/mL of IFNα). This low dose by itself was not able to induce significant anti-proliferative effect in RKO and MCF-7 cancer cell lines, while slightly affected cell viability of HCT-116 cells (Figure 28).

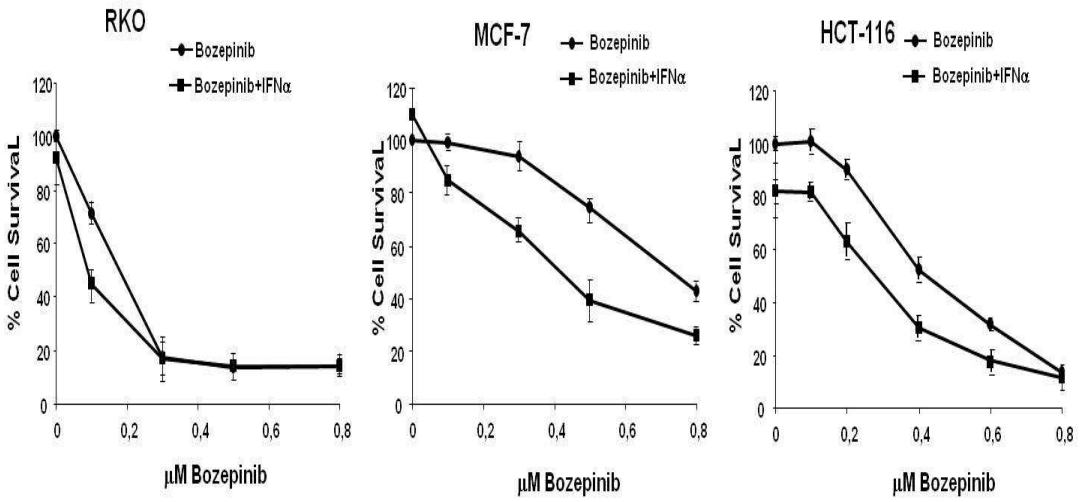

Figure 28. Cytotoxic effect of Bozepinib and the Bozepinib/IFNα combined therapy. MCF-7, HCT-116 and RKO cell lines were treated with increasing amounts of Bozepinib alone (circle) or in combination with 50 IU/ml of IFNα (square) during 6 days as described in Material and Methods. The curve of cell survival is represented as percentage referred to mock-treated cells. Values showed represent the mean of the triplicate determinations calculated from a single experiment. Experiments were repeated at least three times.

However, both compounds synergistically induced the death of cancer cell lines analyzed (Figure 28), and consequently, the IC_{50} value of Bozepinib was reduced when was combined with IFNα (Table 20).

15.1 Apoptosis assays of Bozepinib/IFNα effect on breast and colon cancer

In order to analyze if the effectiveness of the Bozepinib/IFNα combination is due in part, to an improvement in the apoptosis phenomenon, we treated MCF-7, HCT-116, and RKO cell lines with Bozepinib alone or in combination with 500 IU/mL of IFNα. We found that the apoptosis induced by Bozepinib at 48 h was significantly increased when IFNα was added in all the cell lines analyzed (Figures 29, 30).

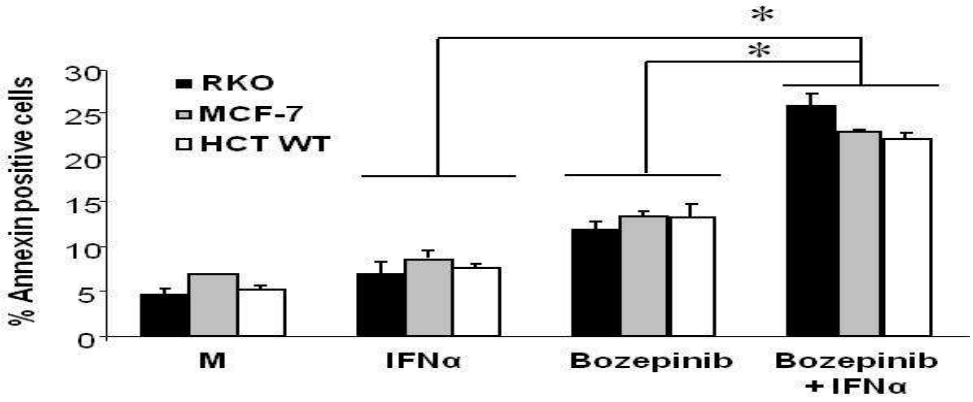

Figure 29. Apoptosis is enhanced after Bozepinib and IFNα combination. MCF-7, HCT-116 and RKO cell lines were mock-treated, treated with 5 μM of Bozepinib or treated with 500 IU/mL of IFNα or treated with the combination of Bozepinib/IFNα for 48 hours. Treated cells were thereafter trypsinized and analyzed by flow cytometry using the Annexin V-FITC detection kit. [a.] Data are expressed as mean ±S.E.M. of three independent experiments,*p<0,05 (t-test).

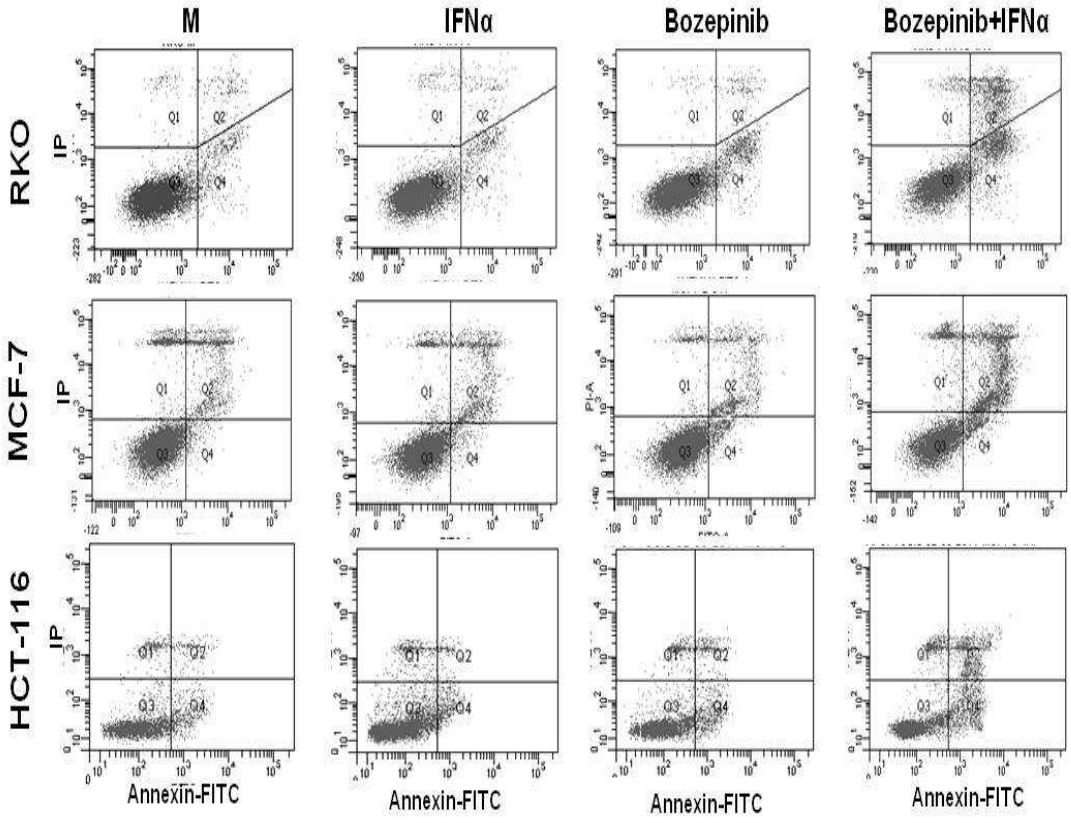

Figure 30. Representative images of the flow cytometry analysis with Annexin V-FITC staining for HCT-116, MCF-7 and RKO cells, mock treated, treated with Bozepinib, IFNα or both.

15.2. The Bozepinib induced apoptosis and efectiveness of IFNα combined therapy is related with PKR but not with p53

PKR phosphorylation and its natural substrate eIF2α were analyzed in MCF-7 and HCT-116 cell lines. Bozepinib treatment induced PKR and eIF2α phosphorylation in both tumor cell lines. Importantly, it was also observed an increase in the PKR levels after Bozepinib treatment that was more evident in HCT-116 cell line, where the PKR basal level (total and phosphorylated) was lower than the PKR basal level of the MCF-7 cells. In contrast, total and phospho-p53 levels were not affected during Bozepinib treatment in both cell lines (Figure 31).

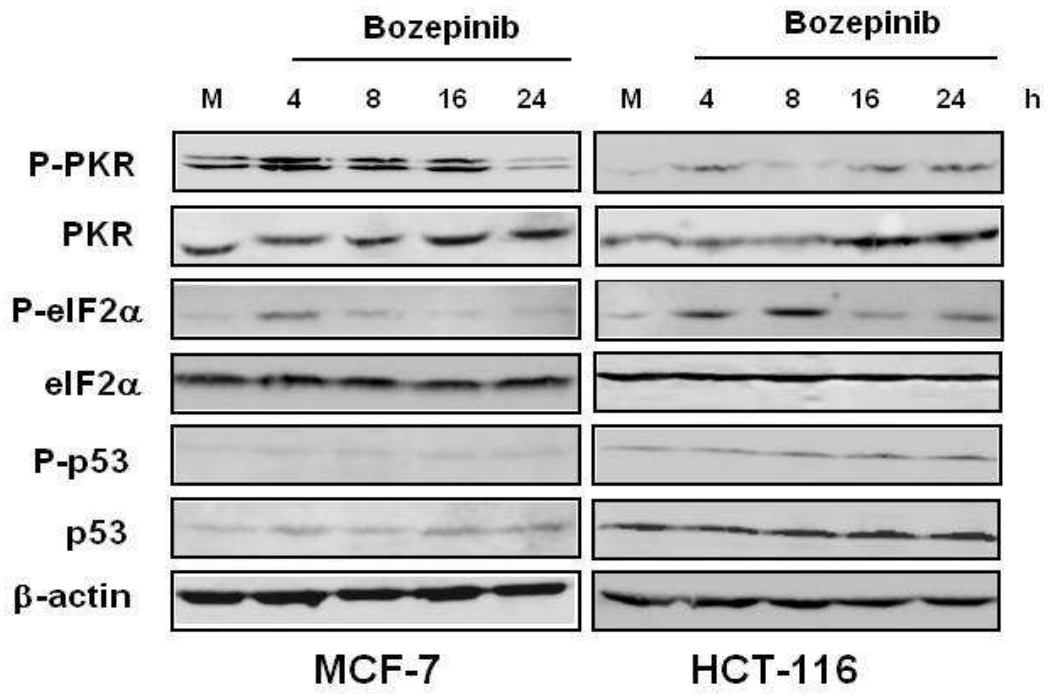

Figure 31. MCF-7 and HCT-116 cell lines were mock-treated or treated with 5 μM of Bozepinib during 4, 8, 16 and 24 hours. Total proteins were extracted for immunoblot analysis using anti-phospho PKR, anti- whole PKR, anti-phospho eIF2α, anti-whole eIF2α, anti-phospho p53, anti-whole p53 and anti-β-actin antibodies.

We analyzed next the contribution of PKR and p53 in apoptosis induction by Bozepinib. We also analyzed the effect of PKR absence in the effectiveness of the Bozepinib/IFNα combination. In fact, Bozepinib and IFNα separately were able to

induce important level of apoptosis in PKR$^{+/+}$ MEFs that was enhanced when both compounds were combined. However, low levels of apoptosis were induced in the absence of the PKR protein in PKR$^{-/-}$ MEFs even when Bozepinib and IFNα were combined (Figure 32, A).

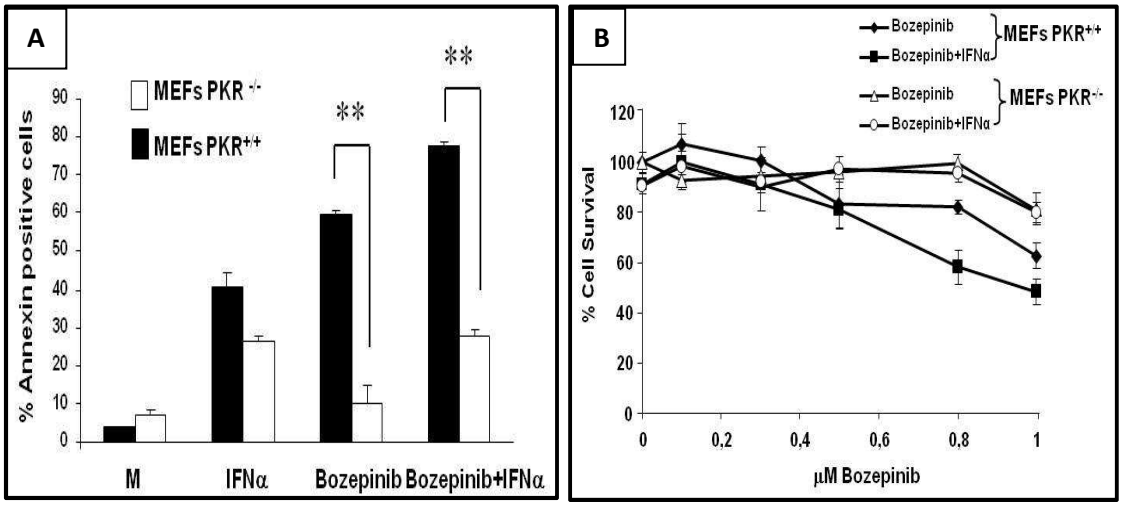

Figure 32. A. MCF-7 and HCT-116 cell lines were mock-treated or treated with 5 µM of Bozepinib during 4, 8, 16 and 24 hours. Total proteins were extracted for immunoblot analysis using anti-phospho PKR, anti- whole PKR, anti-phospho eIF2α, anti-whole eIF2α, anti-phospho p53, anti-whole p53 and anti-β-actin antibodies. B. PKR$^{+/+}$ and PKR$^{-/-}$ MEFs were mock treated or treated with 2,5 µM of Bozepinib or treated with 500 IU/ml of mouse IFNα or treated with Bozepinib/IFNα during 48 hours, **p<0,01 (*t*-test) (upper panel). Subsequently, cells were trypsinized and analyzed by flow cytometry to AnnexinV positive determination. Cells were treated with increasing amounts of Bozepinib alone or in combination with 50 IU/ml of mouse IFNα during 6 days as described in Material and Methods. The curve of cell survival was represented as percentage referred to mock-treated cells. Values showed represent the mean of the triplicate determinations calculated from a single experiment. Experiments were repeated at least three times.

To demonstrate the role of PKR in the cytotoxic effect of Bozepinib and Bozepinib /IFNα combination, we analyzed the cell survival in PKR$^{+/+}$ and PKR$^{-/-}$ MEFs treated with increasing amounts of Bozepinib , showing that the cytotoxic effect of Bozepinib is higher in PKR$^{+/+}$ MEFs in comparison with PKR$^{-/-}$ MEFs (Figure 32B, Table 20). Moreover, our results show that whereas cell viability was significantly reduced when IFNα was added to Bozepinib in PKR$^{+/+}$ MEFs, cell viability was not affected by the Bozepinib/IFNα combination in PKR$^{-/-}$ MEFs.

Although p53 modification was not detected by western blot after Bozepinib treatment (Figure 31), we finally analyzed the effect of Bozepinib, IFNα and the Bozepinib/IFNα combination in the presence or absence of p53 protein in HCT-116 WT cells and HCT-116-p53 KO cells. In fact, the levels of apoptosis after treatments were similar in both cell lines; however, when PKR was down-regulated expressing sh-PKR interference, apoptosis was significantly reduced (Figure 33).

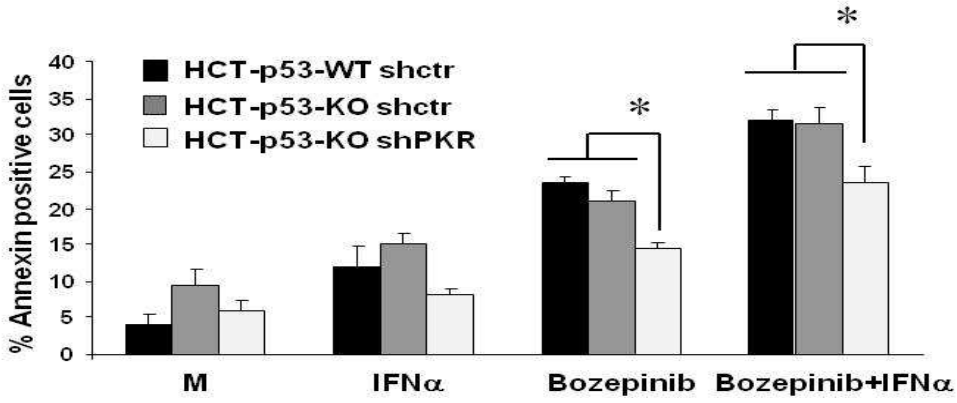

Figure 33. HCT-116 p53 WT cell line and HCT-116 p53 KO cell line expressing shRNA against PKR (shRNA-PKR) or expressing a control shRNA (shRNAc) were mock-treated or treated with 5 μM of Bozepinib or treated with 500 IU/ml of human IFNα or treated with the combination of Bozepinib/IFNα during 48 hours, *p<0,05 (t-test).

All together these results suggest that in part, PKR but not p53 contributes to the response of the cancer cells to the effects of Bozepinib and Bozepinib/IFNα combination.

15.3. Synergystic effect of Bozepinib/IFNα is related with autophagy proces

We analyzed the ability of Bozepinib to induce autophagy, and the regulation of this process by IFNα in MCF-7 cell line which is deficient in caspase 3-activation (Yang et al., 2001). Despite the low level of endogenous LC3 protein, LC3-II level was weakly detected at 48 hours after Bozepinib treatment and was more evident when IFNα was added (Figure 34). Confocal microscopy was used to analyze the redistribution of LC3 protein into autophagosomes in MCF-7 cells transfected with pCMV-GFP-LC3

vector and pCMV-GFP control vector and then, cells were mock-treated or treated with Bozepinib, IFNα and the Bozepinib/IFNα combination.

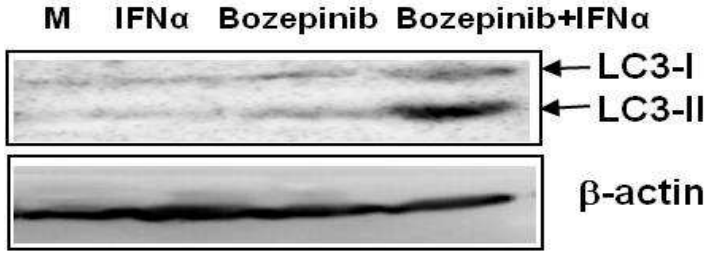

Figure 34. Bozepinib induced LC3-autophagosomed formation that was strongly enhanced when combined with IFNα. MCF-7 cells were mock-treated or treated with 5 μM of Bozepinib or treated with 500 IU/ml of human IFNα or with the combination of Bozepinib/IFNα for 48 hours. Total proteins were extracted for immunoblot analysis using anti-LC3 and anti-α-actin antibodies.

As shown Figure 35, after 48 hours post-treatment, mock-treated cells displayed a diffuse staining. However, an evident speckled fluorescent staining pattern was detected in almost all cells analyzed after the Bozepinib/IFNα treatment, indicating the redistribution of LC3 to autophagosomes. The speckled fluorescent stained was less pronounced after treatment with both Bozepinib or IFNα added separately, and detected in less than half of the cells analyzed (Figure 35). Cells expressing the control vector pCMV-GFP displayed the diffuse staining even in the presence of the Bozepinib/IFNα treatment (Figure 35).

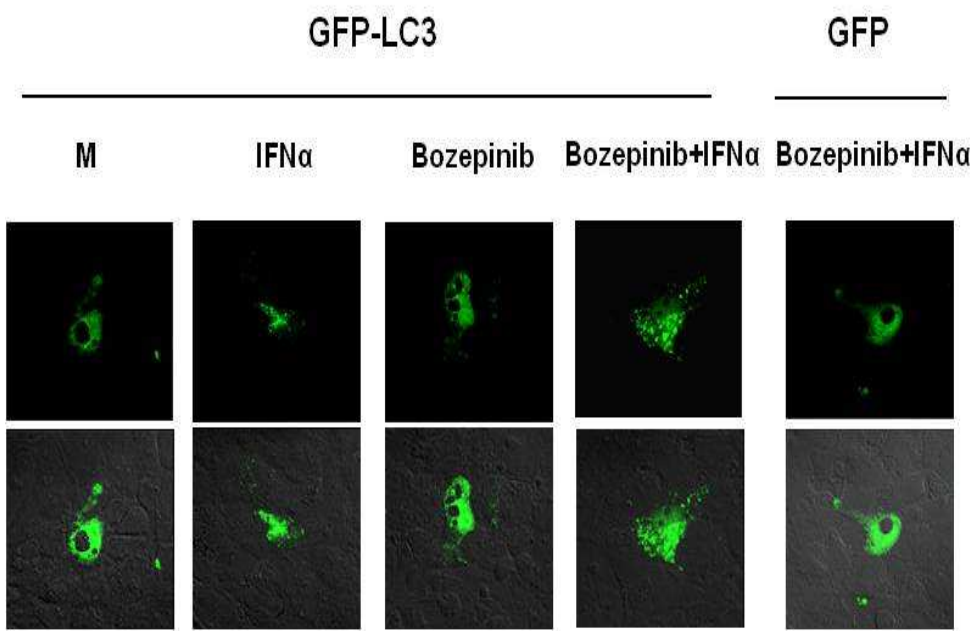

Figure 35. MCF-7 cells were plated in cover slips supported in 6wells plates and transfected with 5 μg of GFP-LC3 or GFP-control plasmids using as described in Materials and Methods. After 24 hours cells were treated with 5 μM of Bozepinib or treated with 500 IU/ml of human IFNα or treated with the combination of Bozepinib/IFNα for 48 hours. Cells were fixed and visualized using a Radiance 2000 confocal microscopy.

Moreover we analyzed cell morphology using TEM after 48 hours post-treatment. The most spectacular morphological effects were observed when IFNα is combined with Bozepinib (Figure 36). As showed in Figure 36, autophagic vacuoles surrounded by a double layered membrane and containing cytoplasmic constituents were observed after the Bozepinib/IFNα treatment. Similar to MCF-7 cell line, colon cancer HCT-116 cells also presented autophagic vacuoles after treatments as is observed by the TEM images (Figure 36).

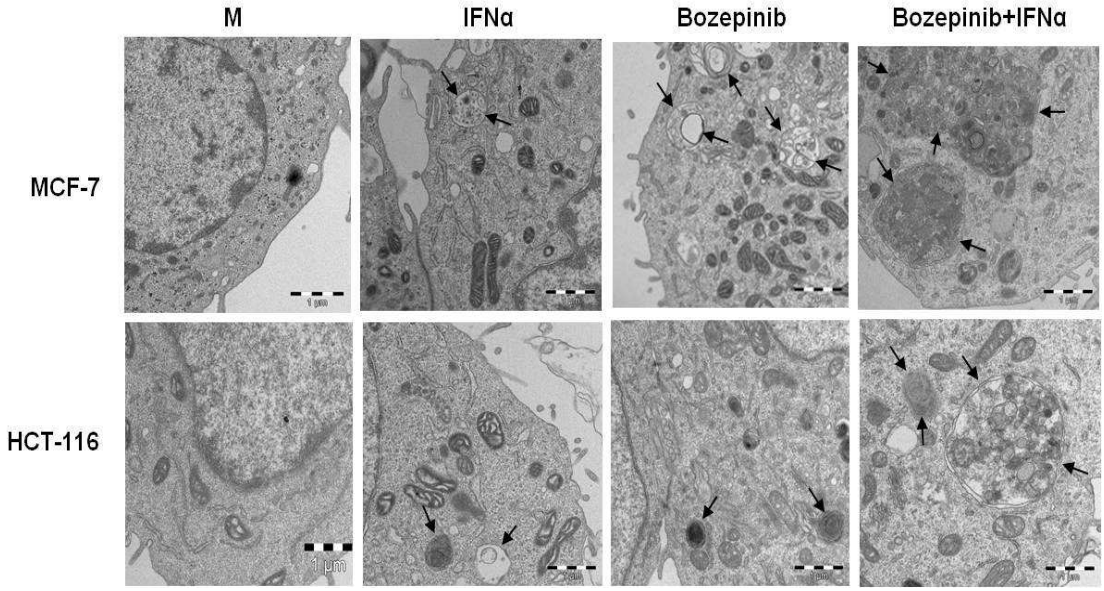

Figure 36. Bozepinib induced LC3-autophagosomed formation that was strongly enhanced when combined with IFNα. MCF-7 and HCT-116 cells were mock-treated or treated with 5 µM of Bozepinib or treated with 500 IU/ml of human IFNα or with the combination of Bozepinib/IFNα for 48 hours. Cells were fixed and prepared for TEM visualization as described in Materials and Methods. TEM images show that treated cells contained typical autophagolysosomes (arrows) containing organelles and lamellar structures.

In order to analyze the involvement of the autophagy process induced by Bozepinib and IFNα combination on cell viability, MCF-7 cells were treated 2 hours before of Bozepinib, IFNα and Bozepinib/IFNα treatment with the autophagy inhibitor CQ and the caspase 3 inhibitor Z-VAD (Figure 37). Whereas Z-VAD did not affect the cell death induced by both Bozepinib or Bozepinib/IFNα combination, the cell viability after Bozepinib/IFNα treatment was significantly higher in cells pre-treated with the autophagy inhibitor CQ. The treatment with CQ caused the described LC3-II accumulation that has been suggested as the result of CQ-induced inhibition of the fusion between autophagosome and lysosomes (Geng et al., 2010; Yoon et al., 2010) that was more evident after Bozepinib/IFNα treatment (Figure 37).

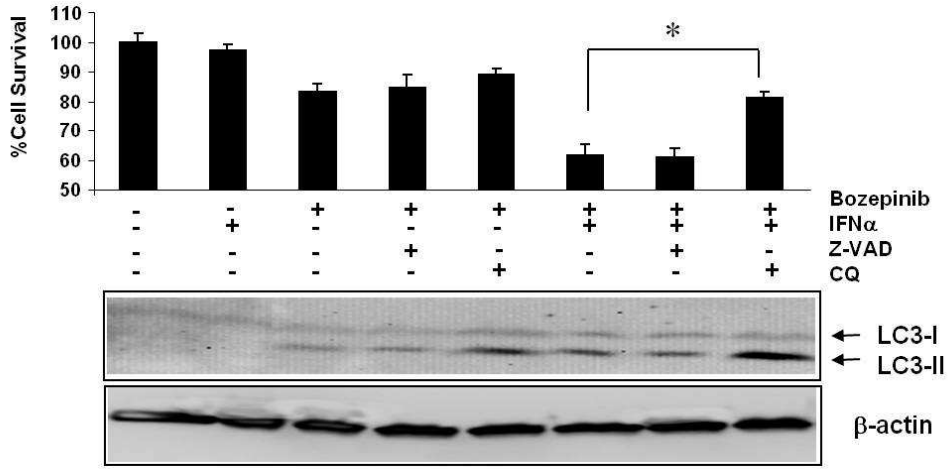

Figure 37. MCF-7 cells were treated 2 hours before of 5 μM Bozepinib, 500 IU/ml IFNα or Bozepinib/IFNα treatments with 20 μM of CQ or 25 μM of Z-VAD inhibitors. After 48 hours, cells were treated with CCK-8, measured at 450 nm O.D. and represented as described in Materials and Methods, and total proteins were extracted for immunoblot analysis using anti-LC3 and anti-β-actin antibodies. *p<0,05 (*t*-test). Western blot signals were quantified with Image J software and relative β-actin-normalized values have been assigned referred to non-treated cells.

These results demonstrate that Bozepinib is able to induce the autophagy process in cancer cells that is clearly evidenced when is combined with the IFNα cytokine, and suggest the contribution of autophagy process in the cell death induced by Bozepinib/IFNα combination.

15.4 Bozepinib ability to induce lysosomal senescence-associated to β-Gal activity is enhanced by IFNα

We observed that during long time treatment of Bozepinib and the Bozepinib/IFNα combination at low doses, there remains a minority population in all cell lines analyzed, which is more evident in the MCF-7 cell line. In order to characterize this population we analyzed the β-gal activity and cell cycle in MCF-7 cells. β-gal activity was detected in the residual surviving population after 7 days with the Bozepinib treatment as showed in Figure 38.

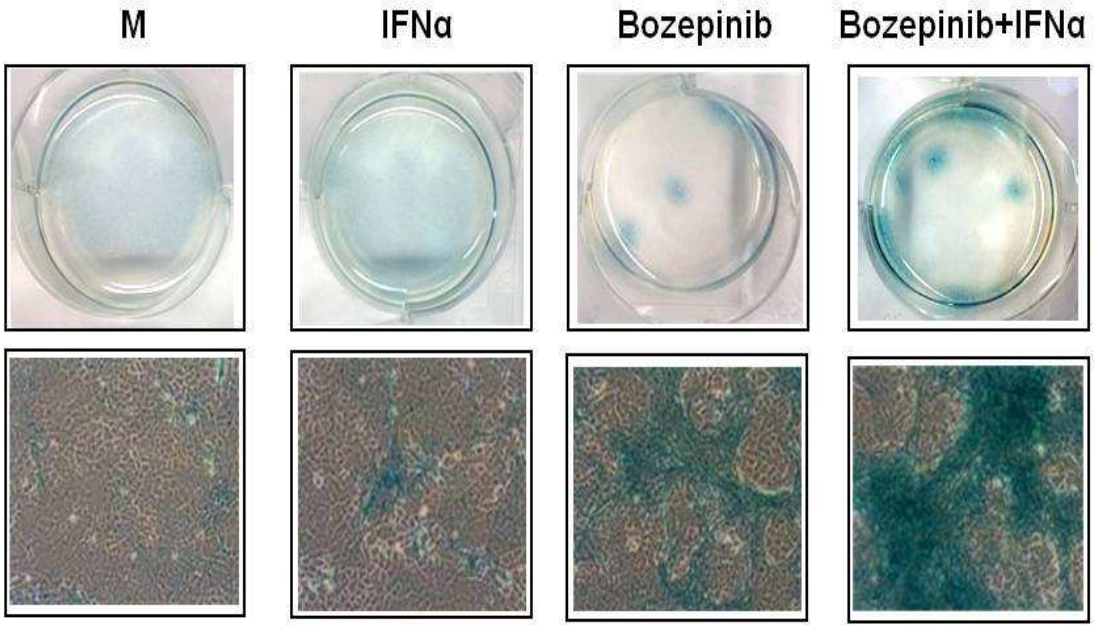

Figure 38. IFNα enhanced the ability of Bozepinib drug to induce the ß-galactosidase (SA-ß-gal) enzymatic activity. MCF-7 cells were mock treated or treated with 2.5 μM of Bozepinib or treated with 500 IU/ml of human IFNα or treated with the combination of Bozepinib/IFNα during 7 days. Cells were fixed and stained using the Senescence β-Galactosidase Staining Kit as described in Materials and Methods and photographed under a 10× objective with a microscopy (Leica) using visible light (lower panel) and the corresponding p6 wells were photographed under 1x objective with a standard camera

However, although this population was minority after 7 days of the Bozepinib/IFNα treatment, the β-gal activity was more evident. Moreover, the percentage of cells arrested in the S phase after the Bozepinib/IFNα treatment was around 30%, whereas the Bozepinib or the mock-treated cells showed 11-13% of the cells in the S phase (Figure 39) after 7 days of treatment.

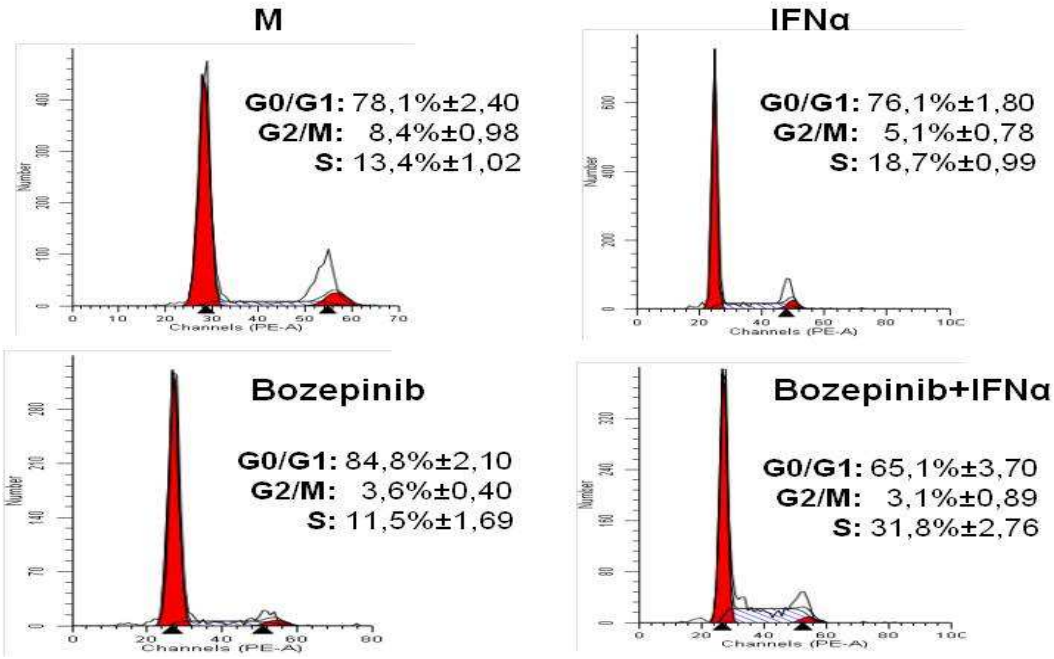

Figure 39. IFNα enhanced the ability of Bozepinib to induce the β-galactosidase (SA-β-gal) enzymatic activity. Cells were fixed and analyzed by flow cytometry after staining with PI. Values represent the mean of the triplicate determinations calculated from a single experiment. Experiments were repeated at least three times.

Therefore, these results show that Bozepinib and IFNα alone are able to induce senescence in the residual surviving population, which is more evident after the Bozepinib/IFNα combination.

VI. DISCUSSION

Cancer represents the second cause of death by disease in the world, being the colorectal and breast cancer two neoplasias with important incidence in most of worldwide countries. This disease is characterized by an uncontrolled cell proliferation due to the accumulation of DNA damage and because of properties of tumoral cells to evade programmed cell death (Fernald and Kurokawa, 2013) and the cell cycle checkpoints regulation (Williams and Stoeber, 2012). In recent studies, a new approach to understand the complex mechanism underlying cancer is described. Cancer stem cells have emerged to explain the carcinogenic process and the reason of resistance to classsic antitumoral treatments. The understanding of the characteristic properties of these CSCs has helped to explain the problems associated with efficacy of conventional therapies used to fight against cancer.

Conventional anticancer drugs are based mainly in the cytotoxic activity, but normally this effect is associated with a poor selectivity, affecting both cancer cells and normal cells, limiting its therapeutical effectiveness by inducing damage to normal proliferating cells and resulting on undesirable side effects (Monsuez et al., 2010). For this reason there is an emerging need in the design of new therapeutic approaches that target tumour and cancer stem cells to avoid undesirable side effects and relapses in cancer due to CSCs resistance (Ma et al., 2008; Shervington and Lu, 2008). As part of this main objective, we tested several new sinthethized pharmacological compounds in stablished breast and colon tumour cell lines.

In our research the compounds used were synthetyzed in basis to increase its lipophilic properties. One of the main problems of conventional chemotherapeutical drugs are solubility and lipolhilicity. Lipophilicity has been related with drugs properties, such as absorption, permeability, distribution, plasma protein binding elimination or toxicity (Di et al., 2009). In this way, a good approach to achieve this is the use of Lipinski rules. Lipinski and cols analysed the physic-chemical properties of more than 2000 drugs and candidate drugs in clinical trials, concluding that permeability and absortion properties of a compound were related with the following properties:

a. Molecular weight of the compound is less than 500.

b. Lipophilicity, expressed as a quantity known as log*P* (the logarithm of the partition coefficient between water and 1-octanol), is less than 5.

c. The number of groups in the molecule that can donate hydrogen atoms to hydrogen bonds (usually the sum of of hydroxyl and amine groups in a drug molecule) is less than 5.

d. The number of groups that can accept hydrogen atoms to form hydrogen bonds (estimated by the sum of oxygen and nitrogen atoms) is less than 10.

e. Compound classes that are substrates for biological transporters are exceptions to the rule.

These rules (based on the 90-percentile values of the drugs property distributions) are related to absorption by passive diffusion of compounds through cell membranes; but not to compounds that are actively transported through cell membranes by transporter proteins (Lipinski et al., 2001).

Several classifications such as biopharmaceutics classification system (BCS) and the development classification system (DCS) make a classification with oral drugs substances in four groups based on solubility and permeability properties. Traditionally, only drug candidates with a good solubility in water made it to the development phase; however, since the pharmaceutical industry adjusted the "rational drug design" in the screening phase, poorly water-soluble drug candidates are also becoming more prevalent in drug research A benefit of poorly water-soluble drugs could be lipophilicity. Despite restricting the solubility, lipophilicity can provide an efficient interaction with the target receptor and gives a possibility to pass the lipidic domain of natural membranes (Stuurman et al., 2013).

Previous studies report the synthesis and anticancer activities of compounds where the linkage between the 5-fluorouracil (5-FU) moiety and the seven-membered ring was carried out through its *N*-1 atom and *trans*-**7** (Saniger et al., 2003). Moreover, the antiprolifaerative activities of a compound where the thymine (T) linked to a seven-membered ring compounds exhibited an *in vitro* antiproliferative activities (12.74 ± 4.79 and 30.05 ± 0.71 μM, respectively) against the MCF-7 cell line was reported (Nuñez et el., 2005).

The uracil (U) *O,N*-acetals derived from the tetrahydrobenzoxazepine moiety, (Diaz-Gavilan et al., 2006) showed *in vitro* antiproliferative activities against the MCF-7 human breast cancer cell line in the submicromolar range (Diaz-Gavilan et al., 2008).

These compounds may serve as prototypes for the development of more potent structures.

Once the alkylated pyrimidine derivatives were studied, the shift was made to the more lipophilic purine ones. These purine derivatives showed potent antitumor activities in the different tumour cell lines assayed. It must be pointed out that from all IC_{50} against cell lines the majority below 1 μM and high TI values, which indicates the selective citotoxicity against cancer cells (Nunez et al., 2008).

In our work, we reported the synthesis and antiproliferative activities of purine derivatives against the cancerous MCF-7 and MDA-MB 231 human breast cancer cell lines and the corresponding normal one (MCF-10A) to define the *in vitro* TI as a measure of the selectivity. The in vitro therapeutic index (TI) of drug is defined as the ratio of the toxic dose to the therapeutic dose (In vitro TI= IC_{50} non-tumour cell line/IC_{50} tumour cell line). Finally the most active racemic compound was resolved and the antiproliferative activity of its enantiomers was measured.

Moreover, we select the benzo-fused seven- and six-membered scaffolds linked to the pyrimidine or purine moieties as leader compounds, and decided to maintain the double-ringed nitrogenous bases and, as a first approach, connect the other components to the ethyl acetate. We reported the synthesis and anti-proliferative activity against human breast and colon cancer cells of two 5-FU derivatives and six purine scaffolds.

After all these studies, we select the most active compound, known as Bozepinib, with an IC_{50} of 166 μM and no acute toxicity *in vivo*. Inasmuch as Bozepinib had potent antiproliferative activities, this encouraged us to carry out studies to determine the mechanism of action at the molecular level.

ANTIPROLIFERATIVE EFFECTS OF THE NEW ANTITUMOUR COMPOUNDS

We evaluated the *in vitro* antiproliferative effect of new synthesized antitumoral compounds in several stablished tumour cell lines. In the efforts to look for more potent antitumoral drugs, we reported a serie of modifications in the structure of these

compounds to increase its lipophilic properties and increase its antiproliferative activities.

In (RS)-benzoxazepin-purines family, 6 of 9 compounds (ACG-812b-F3, FC-26c, ACG-812c-F1, FC-29b, FC-30b2, FC-35) showed IC_{50} values lower than 1 μM on MCF-7 and MDA-MB 231 breast cancer cell lines. On the other hand, in non cancerous MCF-10A cell line, the IC_{50} for these compounds was higher than 1 μM (except for compound Fc-35, IC_{50} is less than 1 μM). In this case, *N*-9''-*O,N*-acetals showed the most potent antiproliferative effect, being the di-chloro purines derivates more powerfull than di-bromo purines derivates. These data revealed that the inhibition of cell proliferation induced by (RS)-benzoxazepin-purines family was dose dependent and that di-chloro purines derivates have more potent antiproliferative effect than its di-bromo derivate.

Interestingly, 12 of 15 compounds tested on MCF-7 cells (ACG-812b-F3, ACG-858E1, ACG-858E2, ACG-812c-F1, ACG-810e, ACG-630b-F1, FC-29b, FC-29d, FC-30b2, FC-35, FC-26c, FC-15d) showed a lower IC_{50} than 5-fluorouracil, one of the commonest chemotherapeuthic drug used in cancer. In all of the nine compounds tested on MDA-MB 231 cancer cells this difference was higher compared with 5-FU (Nunez et al., 2008) .

Non selective effect of conventional cytotoxic anticancer therapy is one of the problems that must be overcomed. This problem is due to the poor selectivity of anticancer drugs which kill both tumour and normal cells, resulting on side effects in patients under these treatments. For this pourpuse we use the MCF-10A non tumour breast cancer cell line to determine the *in vitro* therapeutic index (TI). Compound ACG-812-bF3 **(**known as Bozepinib**)** was the most selective against the human breast adenocarcinoma MCF-7 and MDA-MB 231 cancer cell lines (TIs = 5.1 and 11.0, respectively) in relation to the normal one MCF-10A.

Encouraged with these results, we test one of the most active (RS)-benzoxazepin-purines copound (Bozepinib) in colon cancer cell lines, obtaining IC_{50} values varying from 0,235 μM in SW-480 tumoral cell line to 2,012 μM in CCD-18Co non tumoral cell line. According with these results we were able to determine the *in vitro* TI for SW-480 cell line, obtaining a result of a TI= 8,56. This TI value, according with results obtained in MCF-7 and MDA-MB 231 confirms the selective properties of

compound Bozepinib in *in vitro* assays. These results offer a new perspective in selection of a new antitumor compound with a selective action against tumoral cells and encourage us to further study the molecular mechanism underlying this selective property.

In 2,6-Dichloro-9- or 7-(Ethoxycarbonylmethyl)-9H-or 7H-Purines families, the 2,6-dichloropurine derivatives (FMM238bF2, FMM238bF3) were the most active compounds, showing single-digit micromolar IC_{50} values against MCF-7 breast cancer cell line and HCT-116 colon cancer cell line. The *N*-9 derivative FMM238bF2 elicits improved activities in all cancerous cell lines than its *N*-7 regioisomer FMM238bF3. Generally, the *N*-9 purine derivatives present an augmented activity than that of their *N*-7 regioisomers. The 5-FU derivatives evidence intermediate potencies ($IC_{50} \approx 22$ and 50 μM), being the *N*-1 isomer FMM298cF1 more active than *N*-3 FMM298dF1 against MCF-7, except in the case of HCT-116. In this case, IC_{50} value suggests that a correlation with the lipophilicity of the target compounds may exist. These data revealed that exist a proliferation inhibition due to 2,6-dichloropurine derivatives on MCF-7 and HCT-116 cancer cell lines in a dose dependent manner.

Once antiproliferative activity of compounds belonging to both groups was demonstrated, we focused our investigation to elucidate the mechanism of action of them by cell cycle and apoptosis assays.

NEW ANTITUMOUR COMPOUNDS INDUCE CELL CYCLE MODIFICATIONS AND APOPTOSIS

Dysregulation of the cell cycle engine underlies the uncontrolled cell proliferation that characterizes cancer. Mitogens release the brakes of cell cycle progression by stimulating G_1–S CDK activities, which trigger the phosphorylation of pRB proteins, leading to disruption of their interaction with the E2F family of transcription factors. In cancer cells, the pRB brakes are often defective, resulting in E2F-dependent G_1–S gene expression even in the absence of mitogens (Harbour and Dean, 2000). This may arise as a result of activating tumourigenic mutations, which have been identified in diverse tumours at all levels in the mitogenic signalling pathways from ligands and receptors (eg HER2/ErbB2/neu receptor mutations or *HER2*

gene amplification) to downstream signalling networks (eg Ras–Raf–MAPK or PI3K–Akt signalling pathways), and also for the cell cycle-regulated genes themselves (eg *CYCLIND1* and *CDK4* gene amplification) (Williams and Stoeber, 2012). Cell cycle regulation by chemotherapeutic drugs is one of the most important actuation mechanisms in the treatment of cancer. In recent years, many studies have showed an association between cell cycle regulation and cancer inasmuch as the cell cycle inhibitors are being considered as a weapon for the management of cancer (Wesierska-Gadek et al., 2004).

To focus our studies on the effect of the compounds on cell cycle stages regulation we carried out the analysis by flow cytometry of the most representative (RS)-benzoxazepin-purines compounds (ACG-812-bF3, FC-26c, Fc-35, Fc-29b, Fc-29d, ACG-812c-F1, Fc-30b2) on MCF-7 and MDA-MB 231 breast cancer cell lines and MCF-10A non tumour cell line. The non-accumulation in a specific phase was detected during treatment with the drugs in most of the cell lines analyzed in comparison with control-DMSO-treated cells. Only the (R)-14 (ACG-858E1) enantiomer was able to induce in MDA-MB 231 cells an accumulation in both G0/G1 and G2/M phases with the consequently significant decreased in the S phase. Also, an accumulation in the phase G2/M was detected with compound Fc-35 treatment in MCF-7 cells. Treatment with 5-FU and paclitaxel, as have been described previously, induced accumulation in the S or G2/M phases depending on the cell line analyzed (Grem et al., 1999). These results indicate that compounds inhibited all phases of the cell cycle, probably through the inhibition of protein synthesis as it has been proved with other antitumour drugs (Duncan et al., 2009).

The cell cycle analysis of the most representative compounds of 2,6-Dichloro-9- or 7-(Ethoxycarbonylmethyl)-9H-or 7H-Purines in MCF-7 and HCT-116 cell lines dysplayed that MCF-7 cells treated for 24 h with FMM238bF2 and FMM238bF3 did not show significant differences in the cell cycle progression compared with DMSO-treated control cells. We found a slight cell cycle arrest in the G2/M and S-phases induced by FMM238bF2 (54.63 ± 1.18) and 33 (18.27 ± 0.79), respectively. In HCT-116 colon cancer cells, FMM238bF2 did not modify the cell cycle profile and FMM238bF3 provoked a G2/M cell cycle arrest (28.47 ± 0.07) at the expense of the G0/G1-phase (33.58 ± 1.90). Previously, we have demonstrated that potent anti-tumour

drugs did not modify the cell cycle in comparison with control cells, due to a translational block and consequently inhibition of the protein synthesis by the activation and phosphorylation of the initiation factor eIF2α (Conejo-Garcia et al., 2011).

Apoptosis is a highly regulated cell death program and is related to the regulation of development and homeostasis. Typically this phenomenon displays biochemical and morphological changes. Morphologically it is characterized by nuclear condensation, plasma membrane blebbing, cell shrinkage, formation of apoptotic bodies and chromosomal DNA fragmentation. The shrunken remainders are phagocytosed and their constituents are recycled. Apoptotic cell death concerns a single cell rather than groups of adjacent cells, and it can be induced by various treatments, such as DNA-damaging agents, anticancer drugs, ROS, UV irradiation, TNF-α, bacterial toxins, and Fas ligand (Kroemer et al., 2009; Deng et al., 2010b). Apoptosis, and nor necrosis, is the desired effect of an antitumor drug, which represent a selective property of the pharmacological compound. Although the major apoptotic pathway of anticancer drugs acts through the loss of mitochondrial membrane integrity (Kaufmann and Earnshaw, 2000), the apoptotic pathway involves in our purine derivates is still no well known.

In our research, we selected compounds with higher antitumor activity and higher TI to determine the ability to induce programmed cell death in breast and colon cancer cell lines. Apoptosis induction in the most representative (RS)-benzoxazepin-purines compounds (ACG-812b-F3, FC-26c, FC-35, FC-29b, FC-29d, ACG-812c-F1, FC-30b2, ACG858E1, ACG858E2) was assessed on MCF-7 breast cancer cell line where the demonstration of programmed cell death by known apoptosis-inducing agents has proven difficult and only few cytotoxic agents act preferentially through an apoptotic mechanism in human breast cancer cells. In fact, Paclitaxel (Taxol®) induced programmed cell death of up to 47% of the cell population (Li et al., 2013). Compared with non treated cells, where no apoptosis induction was detected after treatment for 24 or 48 hours, (RS)-benzoxazepin-purines compounds did not induce apoptosis after 24 h of treatment. In contrast, apoptosis induction was detected after 48 hours treatment with all compounds in a variably percentage, most of all represented by early apoptosis instead later apoptosis. The most potent apoptosis induction compound was ACG-858E1. It should be noted that levels of early apoptosis induced by ACG-858E1 were almost double in comparison with the corresponding racemic compound Bozepinib, which may explain the enantioselective antiproliferative activity shown by this

enantiomer. These high apoptotic percentages shown by ACG-858E1 are consistent with the G1 and G2/M arrest since cells exposed to specific agents typically enter apoptosis from a given phase of the cell cycle. Differences in cytotoxicity, cell-cycle analysis or apoptotic levels between ACG-858E1 and ACG-858E2 suggest distinct signalling pathways as has been shown with other antitumour enantiomers (de Fatima et al., 2008). Other compound, FC-30b2, showed a high total apoptosis induction (45,47%, mostly early apoptosis).

The effects of compounds on the pattern of cell death were also confirmed by confocal microscopy after staining with FITC-conjugated annexin V and the nuclear non-vital stain PI. MCF-7 cells treated with compounds showed several staining patterns. Some cells displayed an intense FITC staining located at the plasma membrane and a nucleus with intensely PI-labeled marginated chromatin, suggesting that they were in the course of apoptosis. Other cells showed a peculiar staining pattern, because they exhibited nuclei with the same features observed in true apoptotic cells and, at the same time, cytoplasms homogeneously stained for annexin V. In fact, the FITC staining was located not only at the cell surface, but also within the cytoplasm. Therefore, these cells were considered as aponecrotic cells as previously has been established (Gooch and Yee, 1999). In addition, patches of localised partially condensed chromatin were found in other cells abutted along the inner part of the nuclear membrane. In the control cultures, most of the cells turned out to be negative for both stainings except for some dying cells with the staining features of apoptosis. The present data support the effect of the compounds in some of the series of steps of the apoptotic process where a wide range of intermediate morphological and biochemical types of cell death occurs (Marchal et al., 2004).

Also we assayed apotosis induction in the 2,6-dichloropurine derivatives FMM238bF2 and FMM238bF3. Although both compounds showed different cell cycle profiles that were dependent upon the cell line studied, however, at 24 h induced high levels of apoptosis in all cancer cells in comparison with DMSO-treated cell cultures.

This apoptosis was induced even in the MCF-7 breast cancer cells that have shown deficiency in the caspase-activation mechanisms (Kagawa et al., 2001). Moreover, the fact that FMM238bF2 and FMM238bF3 gathered cells at S and G2/M phases respectively in breast and colon cancer cells accompanied by high levels of

programmed death cell indicates that these compounds have different cytotoxic effects on each tumour cell type.

Based on these results, we select Bozepinib, one of the most potent antiproliferative compounds with the best selective activity and properties that allow us to syntetise it to perform more complex assays and to understand the molecular basis underlying its antiotumour properties.

BOZEPINIB IBHIBITS PROLIFERATION PATHWAYS INVOLVED IN CANCER

Cancer is a multistep disease where an accumulation of mutations are necessary, multiple pathways involved in proliferation are often affected by this process, wich affects both cell membrane receptors and protein signalling pathways. In this way we found the importance of design pharmacological compounds that selectively target these dysregulated pathways. Bozepinib showed IC_{50} values in both colon and breast cells significantly higher in the non-tumor cell lines than in all tumor cell lines analyzed, presenting high TI levels. Moreover, this novel compound showed null *in vivo* toxicity verified using mouse xenograft models of breast and colon cancer, which indicates its clinical potential.

In order to identify the mechanism of action of Bozepinib we performed a kinome assays that resulted in an inhibitory *ex vivo* effect on proteins related with critical proliferation pathways involved in cancer tumourigenesis process. Among these proteins we found membrane cell receptors such as EGFR, HER2 or VEGF and proteins kinases belonging to downstream cell proliferation pathways such as JNK or ERK, among others. These data were confirmed by inmunoblot assays in breast cancer cell lines. Bozepinib was a selective inhibitor of HER2 positive the SKBR-3 breast cancer cells (Tseng et al., 2006; Do et al., 2013; Sahlberg et al., 2013) as we verified with inmunoblot analysis and in an *in vivo* xenotrasplant of HER 2 positive HT-29 (Pohl et al., 2009; LaBonte et al., 2011) cells in nude mice. Approximately 25-30% of all primary breast tumors overexpress HER2 receptors, (Liu et al., 2013; Tang et al., 2013) which makes this receptor a clinically relevant molecular constituent of breast cancer

associated with a poor prognosis and a decreasing overall survival (Lower et al., 2009; Arteaga et al., 2012).

Trastuzumab (Herceptin®), a humanized anti-HER2 monoclonal antibody is actually used in first line clinical treatment for metastasic HER2 positive breast tumors (Awada et al., 2012), showing an improvement on patients overall survival (Fiteni et al., 2013; Swain et al., 2013) and prognosis (Dawood et al., 2010). Despite these encourage results, trastuzumab response rates are low and with an average of 9 months. Moreover, the majority of HER2 overexpressing tumours demonstrated *de novo* or intrinsic resistance to trastuzumab monotherapy in metastatic breast cancer (Nahta et al., 2006).

For this reason, there is an increasing interest in looking for novel targeted therapies which overcomes treatment resistance. In this way is important to target not only the proliferating related receptors but also downstream signalling proteins involved in this process. Furthermore, current therapies are aimed to target both HER2 receptor and downstream signalling pathways. Lapatinib, a small molecule tyrosine kinase inhibitor is an example of this approach, wich used in combination with anti-HER2 antibodies improve the effect of the treatment (Xia et al., 2005). Different treatments with other antibodies and different drugs such as tyrosine kinase and mammalian target of rapamycin (mTOR) inhibitors, among others, are also currently under investigation (Nielsen et al., 2013). Selectivity of Bozepinib for HER2-positive breast cancer cells was attributable to its inhibitory effects on HER2 phosphorylation levels as well as AKT, JNKs, ERK2 and VEGF signalling pathways, which were established by the kinome assay and by inmunoblotting of lysed cancer cells treated with Bozepinib. The inhibition of AKT phosphorilation, induced by Bozepinib treatment would be involved in downregulation of constitutively active PI3K/Akt/mTOR pathway in cancer (Kumar et al., 2013), and related with apoptosis inhibition in cancerous proliferating cells. AKT is an important part of PI3K signalling, and its activation is involved in tumor progression throught increased cell proliferation, invasion and angiogenesis (Datta et al., 1999). AKT aberrant activation is in relatioship with diverse types of cancer such as colon, breast or prostate cacinoma (Roy et al., 2002; Stal et al., 2003; Cherrin et al., 2010). The importance of the alteration of this pathway is envidenced by the development of targeted therapies focused on AKT. AZD5363 is a novel pyrrolopyrimidine-derived compound able to inhibit AKT substrates phosphorylation in

LNCaP and BT474c cell lines and the growth of human xenographts *in vivo* (Davies et al., 2012).

On the other hand, although an inhibition on EGF-R activity was detected by the kinoma assay, we were not able to detect changes in the phosphorylation of the receptor in EGF-R positive MDA-MB 468 cells induced with EGF factor and treated with Bozepinib (data not shown). However, we detected an inhibition in the phosphorylation of JNK and ERK1/2 kinases in both, MCF7 cells expressing basal EGF-R level (Knowlden et al., 2003) and MDA-MB 468 cells expressing high level of EGF-R. ERK inhibitors are currently considered as a therapeutic option for the treatment of patients with *BRAF* -, *KRAS* -, or *NRAS* -mutant tumors, including patients who relapse on BRAF or MEK inhibitor therapy (Morris et al., 2013). In this sense, the selective effect of Bozepinib over tumors expressing these mutations opens a new via to be investigated with this novel drug. It has been described that the therapeutic effect of JNK inhibitors depends on suppression of proliferation with antitumor consequences and several JNK inhibitors are currently also in preclinical analysis. All these data suggest that Bozepinib is a selective inhibitor of HER2 signalling, but its antitumor activity involves several mechanisms of action.

ANTIANGIOGENIC AND ANTIMIGRATORY EFFECT OF BOZEPINIB

Considering the intrincating network represented by signalling pathways affected by cancer and tumorigenesis process, the inhibition of several pathways such HER2 or JNK and Erk1/2 involves an inhibition of related pathways such as angiogenesis and migration (Meadows et al., 2004; Ennis et al., 2005). In our case, the inhibition of these pathways seems to affect angiogenic and migratory invasive properties.

Bozepinib treatment was able to reduce the VEGF basal level in SKBR-3 breast cancer cells and showed inhibitory effects against VEGFR-1, VEGFR-2 and VEGFR-3 in the kinome assay. VEGF, the main ligand of VEGFR-1 and VEGFR-2, plays a crucial role on angiogenesis and metastasis (Roberts et al., 2013) by the activation of endothelial cells and the induction of new blood vessels formation that, thereby, facilitates local tumour growth (Ferrara, 2004). For this reason, there are several studies

involving targeted therapies against VEGF, but despite of initial success, advanced tumours are becoming resistant to antiangiogenic therapies (Loges et al., 2010).

Moreover, the antiangiogenic properties of Bozepininb were assessed by the inhibition of the capillary tube formation assay carried out in HUVEC cells, where the ability of these cells to form capillary-like structures is widely used to test antiangiogenic properties of different compounds (Aranda and Owen, 2009). In our study, Bozepinib was able to inhibit capillary-like tube structures at μM doses. In adittion, the antimigratory effect of Bozepinib was demonstrated by the *wound healing* assay in both SKBR-3 breast cancer and HCT-116 colon cancer cell line. According with this effect showed in cancer cell lines, the metastatic capacity of MDA-MB 468 cells xenotransplanted in nude mice was also inhibited after intraperitoneal treatment with Bozepinib (25 mg/kg), which suggests the clinical potential of this promising anitumour drug.

BOZEPINIB TREATMENT INDUCES GENE PROFILLING CHANGES IN BREAST CANCER CELLS.

Changes induced by Bozepinib treatment were studied by microarray assay in MDA-MB 468 breast cancer cell line to assess the effect of the compound on different signalling pathway involved in tumorigenesis and cancer. With this assay we evaluated the diferences in gene profiling expression between cells before and after Bozepinib treatment.

Bozepinib treatment up-regulated several genes involved in metabolic routes, such us cytochrome p450 family genes and glutathione metabolism related genes, both routes involved in the metabolism of drugs (Akhdar et al., 2009) but also in anti-tumor process such as detoxification (Bernhardt, 2006; Arellanes-Robledo et al., 2010), also playing critical role in stress response, apoptosis and proliferation (Gilot et al., 2002; Wu et al., 2006). Moreover, the messenger of Cysthiathionine-Lyase CSE an enzyme with anti proliferative properties that engages ERK1/2 and JNK signalling (Yang et al., 2004a) was upregulated after Bozepinib treatment. In addition, we found up regulation of genes involved in immune and inflammatory processes such us the chemokine CXCL10, associated with increased immune infiltration and improved survival in

patients with solid malignancies (Kondo et al., 2004; Kryczek et al., 2009), including breast cancer (Datta et al., 2006; Bronger et al., 2012). CXCL10 is a member of the ELR⁻CXC chemokine family. It is a potent chemoattractant for natural killer and activated T cells, acting through the CXCR3 receptor (Taub et al., 1993). This chemokine is able to elicit potent antitumor effect (Luster and Leder, 1993) and is a potent inhibitor of angiogenesis *in vivo*, suppressing endothelial cell differentiation into tubular capillary structures *in vitro* (Angiolillo et al., 1995). So the upregulation of CXCL10 after Bozepinib treatment could be involved in the antiangiogenic effects exerted by Bozepinib.

On the other hand, genes involved in breast cancer tumourigenesis such us claudin 1 and E2F8 among others, were downregulated after Bozepinib-treatment. The claudins belong to a family of tight junction proteins crucial for the organization of epithelial cell polarity, capable of recruiting signalling proteins regulating various cellular processes including cell growth, differentiation and tumourigenesis (Hewitt et al., 2006). In human lung carcinoma A549 cells it was demonstrated that the expression of claudin 1 was increased in response to TNFα, suggesting that plays a critical role in cell migration related with TNFα induction (Shiozaki et al., 2012). Moreover, in gastric carcinoma, overexpression of claudin 1 was negatively related with the differentiation but positively with the invasiveness and metastasis of gastric cancer (Wu et al., 2008). Although claudin 1 has been suggested that acts as a tumour suppressor, however, it directly participates in promoting breast cancer progression, possibly through the alteration of expression of EMT genes. Moreover, recently it has been described that its downregulation contribute to inhibit breast cancer migration (Blanchard et al., 2013). According with this data, the downregulation of *claudin1* observed in our study in MDA-MB 468 breast cancer cell line after Bozepinib treatment could be related with the migration inhibition observed by this drug.

The dysregulation of E2F family member of transcription factors including the E2F8 atypical member contributes to oncogenesis and progression. Ectopic overexpression of E2F8 promoted cell proliferation, colony formation, and tumorigenicity, whereas E2F8 knockdown inhibited these phenotypes (Deng et al., 2010a), suggesting that the downregulation of E2F8 induced by Bozepinib could contribute to its anti-tumor effect. Moreover, the downregulation of E2F8 after Bozepinib treatment could be involved in tumourigenicity disminution as observed in

hepatocellular carcinoma, where E2F8 is strongly upregulated and, in contrast, its suppression inhibits cell proliferation, colony formation, and tumourigenicity (Deng et al., 2010a). In addition, recently it has been showed that HER2 tumourigenesis and metastasis is regulated by E2F activator transcription factors (Andrechek, 2013), highlighting the need to investigate the involvement of this factor en the mechanism of action of Bozepinib.

Curiously, Bozepinib induced the downregulation of important genes involved in Notch and Wnt signalling, mechanisms that has been described that promote human stem cell expansion and contribute to CSCs phenotype when are dysregulated (Van Camp et al., 2013) For example, we detected a downregulation of the coactivator Mastermind-like MAML-2 protein that is essential for Notch-mediated transcriptional activation (Fryer et al., 2002; Nam et al., 2003, 2006; Maillard et al., 2004). It has been described that its downregulation decreases Notch signalling, inducing strong inhibition of proliferation of lymphoma cells (Kochert et al., 2011) and reducing the primary tumor sphere formation and side population in MCF-7 cell line, contributing to decrease the number of CSCs populations (Wong et al., 2012). We also detected an evident downregulation of Notch 3 gene. The oncogenic functions of Notch signalling involve the inhibition of apoptosis and the promotion of cell proliferation. Notch 3 is a gene wich encodes a protein involved in Notch signalling pathway and inhibits the tumor suppressor E2A through the ERK pathway, leading to a decrease in apoptosis and increased proliferation (Talora et al., 2003). *In vivo* experiments showed that Notch 3 induced expression in transgenic mice promotes tumour development (Hu et al., 2006). Recently, it has been demonstrated that Notch3 transgene induction promotes a highly migratory phenotype in neuroblastoma cells and enhances mesenchymal marker gene expression (van Nes et al., 2013). Moreover, Notch 3 signalling aberrations or over-exppression, have been implicated in various types of cancers and, recently, Notch3 has been involved in the proliferation of HER2 positive and negative breast cancer cells, suggesting that targeted suppression of this signalling pathway may be a promising strategy for the treatment of determined HER2 related breast cancers (Yamaguchi et al., 2008; Pradeep et al., 2012).

BOZEPINIB EFFECTS ON CSCs

The discovery of CSCs has been converted in one of the most important achievements in the fight against cancer. This subpopulation presents inside tumor has unlimited proliferation potential, ability to self-renew, and capacity to generate a differentiated lineage that form the major tumor population (Clevers, 2005). Characteristically, CSCs present radio and chemotherapy resistance and, in contrast to differentiated tumor cells, they are relatively quiescent and have a slow cycling rate (Abdullah and Chow, 2013). These properties make CSCs responsible of relapse in a majority of cancer cases, making them an objective for targeted therapies of cancer. The diferential properties of CSCs make them good candidates for isolation for further studies. Actually, different assays has been developed to isolate CSCs, such as flow cytometry based on CSCs-specific cell surface markers (Chen et al., 2013), detection of side-population (SP) phenotypes by Hoechst 33342 exclusion (Moserle et al., 2008) and the ability to grow as floating spheres in serum-free medium (Rybak et al., 2011).

In this study, we used the ALDH activity present in CSCs to isolate them after enrichment in *stem* properties using a specific culture medium to stimulate sphere formation (*sphere media*). Sphere formation assay is increasingly used to enrich stem cell populations in a cell culture based on their anchorage-independent growth. By this method, CSCs are able to form spheres *in vitro* in serum-free suspension cultures. CSCs isolation based on ALDH is a widely used method in breast (Ginestier et al., 2007; Charafe-Jauffret et al., 2010) and colon (Hou et al., 2013) cancer, being the Aldefluor® assay the most popular method, since high ALDH activity is associated with metastasis, resistance to chemotherapies, and poor prognosis in human cancer. Moreover, it has been identified as one of the most specific markers of human CSCs (Charafe-Jauffret et al., 2010; Marcato et al., 2011; Tirino et al., 2013).

According with the proteomic and genomic results obtained after Bozepinib treatment and considering the recent works relating HER2 positivity with CSC phenotype in breast cancer cells with high ALDH activity (Korkaya et al., 2008; Duru et al., 2012), we decided to analyze the efficacy of Bozeopinib on CSCs enriched subpopulations. Our results showed that Bozepinib was able to inhibit both, mamo and colono-spheres formation and was able to eliminate CSCs subpopulations isolated by ALDH activity. Previously, ALDH1 activity was used to select SKBR-3 radioresistant

cells *in vitro*, and to study *stem cell* markers (Mihatsch et al., 2011). In HCT-116 cells, isolation of $ALDH1^+/CD133^+$ subpopulation and transplantation into mice assessed the tumourigenicity potential of the CSC subpopulation, showing the enrichment in CSCs by this method (Lin et al., 2011). All these data support our study based on ALDH1 isolation and enrichment for the analysis of Bozepinib efficacy against breast and colon CSCs models.

The new field of study opened by CSCs discovering offers new tools to test novel antitumor treatments focused on target CSCs. In this way there a lot of studies based on this therapeutic strategy. *Stem cell* properties showed by CSCs are mainly enhanced by disregulation of signalling pathways such as Wnt, Notch and Hedgehog (Takebe et al., 2011) and the overexpression of other *stemness* markers related with pluripotence such as Sox2, β-catenin or c-Myc (Botchkina et al., 2010; Neumann et al., 2011). Bozepinib displayed IC_{50} values that were higher in the spheres enriched ALDH+ subpopulation in comparison with cells growing in spheres without previous enrichment selection. Similar results have been shown for salinomycin drug, which has been described as a selective anti CSC drug. However its use is limited in human by considerable toxicity (Gupta et al., 2009; Naujokat and Steinhart, 2012; Ojo et al., 2013).

In order to deep in the mechanism of action of Bozepinib over CSCs we analyzed a panel of proteins involved in CSC phenotype by western blot analysis. Since the level of expression of these proteins vary between cell lines, different patterns of proteins were detected for every cell line, SKBR-3 and HT-116. Whereas no considerable differences were detected in the expression level of analyzed proteins in both cells lines treated with Bozepinib, interesting changes were detected in ALDH+-enriched subpopulation. We detected interesting changes in the level of the Gli 3 protein expression, a described target gene transcription repressor of Hedgehog signaling pathway (Takebe et al., 2011). Whereas Gli 3 expression was detected in HCT-116 ALDH- isolated cells, this protein was not detected in the ALDH+ isolated cells, suggesting that Hedgehog signalling pathways is involved in CSC phenotype, as it has been described (Varnat et al., 2009; Merchant and Matsui, 2010). The treatment with Bozepinib induced a strong expression in Gli 3 protein in both ALDH+ and ALDH- cells in colon cancer cells. Since Gli 3 overexpression reduced tumor cell proliferation and induced apoptosis in colon CSCs (Varnat et al., 2009), the Gli 3 induction by

Bozepinib could be the mechanism by which this drug exerts its antitumor activity in colon CSCs that must to be deeply explored. We also detected a significant reduction in the level of Sox 2 expression, c-myc and β-catenin in both ALDH+ and ALDH- isolated cells after Bozepinib treatment. However, according with the high level of stem signalling proteins described for CSCs, we detected lower levels of these proteins in the ALDH- subpopulation, in comparison with ALDH+ cells. The transcription factor SOX2 is involved together with c-Myc, KLF4 and Oct3/4 in the induction and maintenance of pluripotenvy in stem cells and, recently, it has been associated the expression of both SOX2 and β-catenin with metastases and poor prognosis in colon cancer (Neumann et al., 2011).

SOX2 (Sex-determining region Y (SRY)-Box2) is a member of the SOX family of transcription factors responsible of coordinating disparate functions such as maintaining stem cell properties and differentiation restriction. In particular, SOX2 is involved in the regulation of stem cell fate during embryonic development and its expression levels need to be tightly regulated to ensure normal embryonic development (Herreros-Villanueva et al., 2013) Extensive studies revealed that SOX2 regulates the complex transcriptional network to maintain the unique characteristics of stem cells and the anti-apoptosis property of CSCs (Jia et al., 2011; Brafman et al., 2013). Recently, increasing Sox2 level was reported in Tamoxifen breast cancer cells, related with an activation of Wnt signaling and an enrichment in ALDH+ CSCs (Piva et al., 2013). These data support the SOX2 inhibition detected by inmunoblot assays in HCT-116 ALDH+ cells after Bozepinib treatment compared with mock treated cells, and the downregulation of related Wnt pathway gene found in the microarray assay.

c-Myc is a regulator gene that encodes for a transcription factor. A mutated version of Myc is found in many cancers, which causes Myc to be constitutively expressed. This further induces an unregulated expression of several genes, some of which are involved in cell proliferation. Recent studies showed the inhibition of cancer cell lines proliferation, invasion and cell migration when expression of c-Myc is inhibited (Zhao et al., 2013; Zhou et al., 2013b). The inhibition of c-Myc by Bozepinib treatment in both colon HCT-116 and breast SKBR-3 CSCs highlights the interesting actuation mechanism of the compound. Moreover, recently was reported the cooperation of c-Myc and HER2 to drive *stem like* properties in breast cancer (Nair et al., 2013).

According with previous data, activation of Gli3 in both cell lines is related with an inactivation of β-catenin expression in both CSC lines (Ulloa et al., 2007). Wnt/β-catenin signaling plays a critical role in CSCs (Reya and Clevers, 2005), being β-catenin the key mediator in Wnt signalling. This protein is found in multiple subcellular localizations, including junctions where it contributes to stabilize cell to cell contacts, while in cytoplasm is involved in transcriptional regulation (Voronkov and Krauss, 2013). So, the inhibition of β-catenin suggests the disruption of the Wnt signalling pathway by Bozepinib, affecting one of the key pathways involved in related *stem* properties of CSCs.

Although we show promising data proving the efficacy of Bozepinib against CSCs, the specific mechanism by which Bozepinib inhibits CSCs growth require more investigation. However, the low toxicity, the specific HER2, JNK and ERKs inhibition, the anti-angiogenic and anti-migration activity together the *in vivo* antitumur effect supports further studies on the therapeutic potential of Bozepinib in breast and colon cancer patients.

INTERFERONα (IFNα) ENHANCES THE CYTOTOXIC EFECT OF BOZEPINIB IN COLON AND BREAST CANCER CELLS IMPROVING PKR-MEDIATED APOPTOSIS, AUTOPHAGY AND SENESCENCE PROCESSES

Our results showed that Bozepinib is able to exert a potent antitumor activity also in colon cancer cell lines, with IC_{50} values lower than described for breast cancer cell lines, suggesting a great potential to be used as cancer antiproliferative compound. For this reason, we aimed our efforts to identify the molecular targets involved in the Bozepinib-mediated apoptosis through the study of activation and induction of PKR and the tumour suppressor p53 pro-apoptotic proteins.

PKR but not p53 was surprisingly induced and activated during Bozepinib treatment against breast and colon cancer cell lines, triggering eIF2α phosphorylation. It is well established that eIF2α phosphorylation correlates with a translational block and consequently leads to an inhibition of protein synthesis, providing the cell with the opportunity to elict adaptative responses to stress that finally could trigger cell death by apoptosis (Holcik and Sonenberg, 2005). The analysis of the PKR mRNA levels after

Bozepinib treatment suggested that PKR protein up-regulation was not due to a transcriptional phenomenon similar to previously described for the 5-FU treatment (Garcia et al., 2011). It is widely known that p53 is critical for the apoptosis response to DNA damage agents and cytotoxic agents such us 5-FU, etoposide, paclitaxel, cisplatin among others (Martinez-Rivera and Siddik, 2012). However, the loss of p53 function is frequently involved in tumour resistance to chemotherapeutic agents. Moreover, apoptosis can also occur in mutant p53 cell lines in response to some of these chemotherapeutic drugs, suggesting that more targets are involved in the apoptosis induction in response to chemotherapy (Backus et al., 2003; Konstantakou et al., 2009; Garcia et al., 2011). Recently, it has been showed that PKR protein plays an important role in the induction of apoptosis by doxorubicin, etoposide and 5-FU chemotherapeuticdrugs, being both proteins, p53 and PKR necessary for the cancer cell death by apoptosis in response to the chemotherapy treatments (Yoon et al., 2009; Garcia et al., 2011; Peidis et al., 2011)

In our efforts to determinate apoptosis induction mechanism, we found the first evidence that PKR but not p53 is involved in the apoptosis induction by a purine-derivative antitumor drug. In fact, the levels of apoptosis induced by Bozepinib are similar in HCT-116 colon cancer cells despite of the p53 protein presence or absence. However, the absence or down-regulation of PKR expression in MEFs knockout cells or in human colon cancer cells expressing PKR interference, decreased significantly the apoptosis induced by the Bozepinib compound. Since p53 is mutated in more than 50% of tumours, drugs inducing apoptosis through molecular targets different of p53 are of great clinical interest.

In order to improve the efficacy of Bozepinib we have combined this drug with interferon-α cytokine (IFNα). Several studies have demonstrated that IFNα enhances the chemosensitivity of cancer cells to several drugs, mainly through apoptosis improvement. Our results showed that Bozepinib and IFNα act synergistically to suppress breast and colon cancer cell viability over treatments with the agent alone, reducing the cell viability more than 20% in MCF-7 breast cancer cell line and RKO and HCT-116 colon cancer cell lines. Recently, it has been described that the combination of 9-cis-retinoic acid and IFNα induced marked anti-proliferative and proapoptotic effects in cancer cells through the modulation of critical targets such us p27Kip1 and p21WAF1/Cip1 proteins (Dal Col et al., 2012). Moreover, several studies

show the *in vitro* and *in vivo* effectiveness of the combined therapy with IFNα and diverse chemotherapeutic drugs such as 5-FU (Nakamura et al., 2007), where p27Kip1, Fas/FasL and TRAIL have been involved through triggering apoptosis enhancement. Recently, PKR protein was discovered as an interesting molecular target key for the effectiveness of the 5-FU/IFNα combination (Garcia et al., 2011).

Our data demonstrate that one of the mechanisms related to IFNα improvement of the cytotoxic effect of Bozepinib was through apoptosis enhancement and the synergistic apoptotic effect induced by the Bozepinib/IFNα combination was also affected by the absence or down-regulation of the interferon-induced PKR protein. In fact, the cytotoxic effect of Bozepinib was higher in $PKR^{+/+}$ MEFs in comparison with $PKR^{-/-}$ MEFs and cell viability was significantly reduced when IFNα is combined with Bozepinib in $PKR^{+/+}$ MEFs. In contrast, cell viability was not affected by Bozepinib/IFNα combination in $PKR^{-/-}$ MEFs. These data suggest that PKR, in part, contributes to the effectiveness of the Bozepinib/IFNα combination, and therefore we hypothesize that its deregulation in tumours could affect the response of patients to combined therapies.

Drugs combinations in cancer therapy that enhance efficacy have great success in a variety of therapeutic applications (Dal Col et al., 2012). Since it has been described that most of cancer cells show low level of active caspases or mutations that inactive the apoptosis effectors (Philchenkov et al., 2004; Soung et al., 2005; Ghavami et al., 2009), antitumor drugs inducing additional or alternative cell death are of great interest. It has been described that autophagy could constitute an alternative cell death pathway in cells with a disrupted apoptoticpathway (Dalby et al., 2010; Laha et al., 2014). In this way, MCF-7 cells are a good model system to study drug-cell death induction by autophagy due to its defect in caspases activation (Janicke et al., 1998; Akar et al., 2008). Moreover, alternative effects different to apoptosis induced by IFNα-combined antitumor-therapies have been not yet explored. Bozepinib was able to induce autophagosomes that were showed by the LC3-I to LC 3-II conversion, and re-localization of the GFP-LC3 protein. Surprisingly, the addition of IFNα clearly increased autophagosomes in MCF-7 cells. Moreover, previous treatment with low dose of the autophagy inhibitor CQ was able to reduce significantly the Bozepinib/IFNα-induced cell death suggesting that similarly as described for several anti-cancer compounds such as rottlerin and etoposide (Xue et al., 1999; Akar et al., 2008),

autophagy leads to cell death in response to Bozepinib/IFNα treatment. In correlation with the inability of MCF-7 cells to induce activation of caspase 3 (Yang et al., 2001; Hattangadi et al., 2004) pre-treatment with the pan caspase inhibitor Z-VAD did not affect cell viability showed after the treatments. Although it is known that autophagy is required for the production of IFNα by plasmacytoid dendritic cells during viral infections (Lee et al., 2007) and it has been recently showed that type I IFN induces autophagic trafficking of viral proteins of hepatitis C viruses (Desai et al., 2011), however, the role of IFNα in autophagy process is still unclear and is restricted to its antiviral function. Our results show for the first time the evidence that IFNα is involved in the autophagy process in combination with an antitumor agent. The mechanism of action in this process needs to be further investigated, and might have important therapeutic implications.

Finally, we observed that during a long time treatment with even lower doses of Bozepinib and Bozepinib/IFNα combination, a minority population persists in the MCF-7 cells that shows β-gal enzymatic activity being once again more evident in surviving cells treated with the Bozepinib/IFNα combination. Moreover this population showed a high percentage of cells arrested in phase S in comparison with cells untreated or treated with Bozepinib or IFNα separately. As tumors often develop resistance to apoptosis induced by anticancer treatment (Fulda, 2010), induction of senescence in tumour cells could be an alternative approach in cancer therapy, and especially effective in the treatment of cancer cells in which apoptotic pathways are disabled (Kong et al., 2011). Although the exact mechanism by IFNα regulates senescence is under investigation, it have been suggested that IFNα downregulates telomerase activity along with the growth inhibition of lymphoma Daudi cells (Akiyama et al., 1999) or by repression of hTERT related with a decreasing telomerase activity in human malignant hematopoietic cell lines (Xu et al., 2000). Moreover, it has been suggested that the overexpression of two IFN-regulatory transcription factors (IRF5 and IRF7) are able to induce a senescence-related phenotype in immortal cells (Li et al., 2008a). More recently was suggested the first evidence that the IFNα combination with a chemotherapeutic agent, vinblastine, triggers senescence; however, the authors showed this effect in endothelial cells in the context of angiogenesis process in the tumour (Upreti et al., 2010). Our results show that IFNα enhances the senescence in tumour

cells provoked by Bozepinib, which suggest that this cytokine could act directly in this process when combined with other antitumor drugs.

VII. CONCLUSIONS

1. Both (RS)-benzoxazepin-purines and 2,6-Dichloro-9- or 7-(Ethoxycarbonylmethyl)-9H-or 7H-Purines showed a potent antiproliferative activity in a micromolar range and in a dose dependent manner in breast and colon cancer cell lines.

2. The main mechanism of cell death induced by (RS)-benzoxazepin-purines and 2,6-Dichloro-9- or 7-(Ethoxycarbonylmethyl)-9H-or 7H-Purines is based on apoptosis induction, mostly early apoptosis in (RS)-benzoxazepin-purines in breast and colon cancer cell lines.

3. The most selective compound in (RS)-benzoxazepin-purines is ACG-812-bF3, also known as Bozepinib in breast and colon cancer cell lines.

4. Bozepinib is able to inhibit several kinases related with cancer proliferation pathways in *in vitro* kinase assay.

5. Bozepinib treatment of SKBR-3 breast cancer overexpressing HER2 inhibits HER2 receptor phosphorilation and downstream kinase protein phosphorilation of Akt, following by a decrease of VEGF levels. Moreover and indepently of the effect on HER2 receptor is able to inhibit phosphorilation of proteins involved in cancer proliferation pathways such as Erk and JNK in MCF-7 and MDA-MB 468 non overexpressing HER2 breast cancer cell lines.

6. Bozepinib treatment of MDA-MB 468 breast cancer cell line induce changes in gene profiling expression related with pathways involved in cancer progression and *stem like* properties.

7. Bozepinib treatment negatively regulates angiogenesis by inhibition of capillary like structures formation in HUVEC and inhibits migration in SKBR-3 breast and HCT-116 colon cancer cell lines

8. Bozepinib showed antiproliferative activity on both aldheyde dehydrogenase + isolated SKBR-3 and MDA-MB 468 breast CSCs and also in aldheyde dehydrogenase + isolated HCT-116 colon CSCs in a micromolar range and in a dose dependent manner. This effect is also showed by inhibition of sphere forming colonies in HCT-116 colon CSCs.

9. The selective antitumor activity of Bozepinib against CSCs is showed in inhibition of *stem like* properties related proteins on breast and colon CSCs.

10. PKR but not p53 is involved in the apoptosis induced by Bozepinib.

11. The combination of Bozepinib with natural cytokines such us IFNα is able to potentiate the apoptosis induced effect. The synergyc effect of Bozepinib and IFNα also enhances autophagy and senescence, processes that have been suggested of being of great importance especially in tumour cells that show resistance to conventional chemotherapy.

12. Bozepinib posseses *in vivo* antitumor activity in MDA-MB 468 breast and colon HCT-116 cancer cell lines transplanted in inmunodeficient mice.

VIII. REFERENCES

Abdullah LN, Chow EK. 2013. Mechanisms of chemoresistance in cancer stem cells. Clin Transl Med 2:3.

Abubaker K, Latifi A, Luwor R, Nazaretian S, Zhu H, Quinn MA, Thompson EW, Findlay JK, Ahmed N. 2013. Short-term single treatment of chemotherapy results in the enrichment of ovarian cancer stem cell-like cells leading to an increased tumor burden. Mol Cancer 12:24.

Advani SH. 2010. Targeting mTOR pathway: A new concept in cancer therapy. Indian J Med Paediatr Oncol 31:132-136.

Ahmed RL, Schmitz KH, Anderson KE, Rosamond WD, Folsom AR. 2006. The metabolic syndrome and risk of incident colorectal cancer. Cancer 107:28-36.

Akar U, Chaves-Reyez A, Barria M, Tari A, Sanguino A, Kondo Y, Kondo S, Arun B, Lopez-Berestein G, Ozpolat B. 2008. Silencing of Bcl-2 expression by small interfering RNA induces autophagic cell death in MCF-7 breast cancer cells. Autophagy 4:669-679.

Akhdar H, Loyer P, Rauch C, Corlu A, Guillouzo A, Morel F. 2009. Involvement of Nrf2 activation in resistance to 5-fluorouracil in human colon cancer HT-29 cells. Eur J Cancer 45:2219-2227.

Akiyama M, Iwase S, Horiguchi-Yamada J, Saito S, Furukawa Y, Yamada O, Mizoguchi H, Ohno T, Yamada H. 1999. Interferon-alpha repressed telomerase along with G1-accumulation of Daudi cells. Cancer Lett 142:23-30.

Al-Hajj M, Becker MW, Wicha M, Weissman I, Clarke MF. 2004. Therapeutic implications of cancer stem cells. Curr Opin Genet Dev 14:43-47.

Al-Hajj M, Wicha MS, Benito-Hernandez A, Morrison SJ, Clarke MF. 2003. Prospective identification of tumorigenic breast cancer cells. Proc Natl Acad Sci U S A 100:3983-3988.

Alvarez P, Marchal JA, Boulaiz H, Carrillo E, Velez C, Rodriguez-Serrano F, Melguizo C, Prados J, Madeddu R, Aranega A. 2012. 5-Fluorouracil derivatives: a patent review. Expert Opin Ther Pat 22:107-123.

Alvite Canosa M, Alonso Fernandez L, Seoane Vigo M, Berdeal Diaz M, Perez Grobas J, Carral Freire M, Bouzon Alejandro A, Gomez Dovigo A, Maceira Quintian F, Gomez Freijoso C. 2009. [Leiomyosarcoma of the colon with lung metastases as the first manifestation]. Rev Esp Enferm Dig 101:145-146.

Andersen V, Holst R, Vogel U. 2013. Systematic review: diet-gene interactions and the risk of colorectal cancer. Aliment Pharmacol Ther 37:383-391.

Andrechek ER. 2013. HER2/Neu tumorigenesis and metastasis is regulated by E2F activator transcription factors. Oncogene.

Angiolillo AL, Sgadari C, Taub DD, Liao F, Farber JM, Maheshwari S, Kleinman HK, Reaman GH, Tosato G. 1995. Human interferon-inducible protein 10 is a potent inhibitor of angiogenesis in vivo. J Exp Med 182:155-162.

Arai F, Hirao A, Ohmura M, Sato H, Matsuoka S, Takubo K, Ito K, Koh GY, Suda T. 2004. Tie2/angiopoietin-1 signaling regulates hematopoietic stem cell quiescence in the bone marrow niche. Cell 118:149-161.

Aranda E, Owen GI. 2009. A semi-quantitative assay to screen for angiogenic compounds and compounds with angiogenic potential using the EA.hy926 endothelial cell line. Biol Res 42:377-389.

Arellanes-Robledo J, Salcido-Neyoy ME, Marquez-Quinones A, Garcia-Roman R, Beltran-Ramirez O, Le Berre V, Sokol S, Francois JM, Villa-Trevino S. 2010. Celecoxib activates Stat5 and restores or increases the expression of growth hormone-regulated genes in hepatocarcinogenesis. Anticancer Drugs 21:411-422.

Arteaga CL, Sliwkowski MX, Osborne CK, Perez EA, Puglisi F, Gianni L. 2012. Treatment of HER2-positive breast cancer: current status and future perspectives. Nat Rev Clin Oncol 9:16-32.

Ascierto PA, Kirkwood JM. 2008. Adjuvant therapy of melanoma with interferon: lessons of the past decade. J Transl Med 6:62.

Aschele C, Debernardis D, Bandelloni R, Cascinu S, Catalano V, Giordani P, Barni S, Turci D, Drudi G, Lonardi S, Gallo L, Maley F, Monfardini S. 2002. Thymidylate synthase

protein expression in colorectal cancer metastases predicts for clinical outcome to leucovorin-modulated bolus or infusional 5-fluorouracil but not methotrexate-modulated bolus 5-fluorouracil. Ann Oncol 13:1882-1892.

Awada A, Bozovic-Spasojevic I, Chow L. 2012. New therapies in HER2-positive breast cancer: a major step towards a cure of the disease? Cancer Treat Rev 38:494-504.

Aytes A, Mitrofanova A, Kinkade CW, Lefebvre C, Lei M, Phelan V, Lekaye HC, Koutcher JA, Cardiff RD, Califano A, Shen MM, Abate-Shen C. 2013. ETV4 promotes metastasis in response to activation of PI3-kinase and Ras signaling in a mouse model of advanced prostate cancer. Proc Natl Acad Sci U S A.

Babiera GV, Rao R, Feng L, Meric-Bernstam F, Kuerer HM, Singletary SE, Hunt KK, Ross MI, Gwyn KM, Feig BW, Ames FC, Hortobagyi GN. 2006. Effect of primary tumor extirpation in breast cancer patients who present with stage IV disease and an intact primary tumor. Ann Surg Oncol 13:776-782.

Backus HH, Wouters D, Ferreira CG, van Houten VM, Brakenhoff RH, Pinedo HM, Peters GJ. 2003. Thymidylate synthase inhibition triggers apoptosis via caspases-8 and -9 in both wild-type and mutant p53 colon cancer cell lines. Eur J Cancer 39:1310-1317.

Bach EA, Aguet M, Schreiber RD. 1997. The IFN gamma receptor: a paradigm for cytokine receptor signaling. Annu Rev Immunol 15:563-591.

Bafford AC, Burstein HJ, Barkley CR, Smith BL, Lipsitz S, Iglehart JD, Winer EP, Golshan M. 2009. Breast surgery in stage IV breast cancer: impact of staging and patient selection on overall survival. Breast Cancer Res Treat 115:7-12.

Bajetta E, Di Leo A, Zampino MG, Sertoli MR, Comella G, Barduagni M, Giannotti B, Queirolo P, Tribbia G, Bernengo MG, et al. 1994. Multicenter randomized trial of dacarbazine alone or in combination with two different doses and schedules of interferon alfa-2a in the treatment of advanced melanoma. J Clin Oncol 12:806-811.

Barber GN, Jagus R, Meurs EF, Hovanessian AG, Katze MG. 1995. Molecular Mechanisms Responsible for Malignant Transformation by Regulatory and Catalytic Domain Variants of the Interferon-Induced Enzyme Rna-Dependent Protein-Kinase. Journal of Biological Chemistry 270:17423-17428.

Barrios CH, Liu MC, Lee SC, Vanlemmens L, Ferrero JM, Tabei T, Pivot X, Iwata H, Aogi K, Lugo-Quintana R, Harbeck N, Brickman MJ, Zhang K, Kern KA, Martin M. 2010. Phase III randomized trial of sunitinib versus capecitabine in patients with previously treated HER2-negative advanced breast cancer. Breast Cancer Res Treat 121:121-131.

Bekisz J, Baron S, Balinsky C, Morrow A, Zoon KC. 2010. Antiproliferative Properties of Type I and Type II Interferon. Pharmaceuticals (Basel) 3:994-1015.

Bergamaschi A, Hjortland GO, Triulzi T, Sorlie T, Johnsen H, Ree AH, Russnes HG, Tronnes S, Maelandsmo GM, Fodstad O, Borresen-Dale AL, Engebraaten O. 2009. Molecular profiling and characterization of luminal-like and basal-like in vivo breast cancer xenograft models. Mol Oncol 3:469-482.

Bernhardt R. 2006. Cytochromes P450 as versatile biocatalysts. J Biotechnol 124:128-145.

Bertoncello I, Williams B. 2004. Hematopoietic stem cell characterization by Hoechst 33342 and rhodamine 123 staining. Methods Mol Biol 263:181-200.

Bezemer ID, Rinaldi S, Dossus L, Gils CH, Peeters PH, Noord PA, Bueno-de-Mesquita HB, Johnsen SP, Overvad K, Olsen A, Tjonneland A, Boeing H, Lahmann PH, Linseisen J, Nagel G, Allen N, Roddam A, Bingham S, Khaw KT, Kesse E, Tehard B, Clavel-Chapelon F, Agudo A, Ardanaz E, Quiros JR, Amiano P, Martinez-Garcia C, Tormo MJ, Pala V, Panico S, Vineis P, Palli D, Tumino R, Trichopoulou A, Baibas N, Zilis D, Hemon B, Norat T, Riboli E, Kaaks R. 2005. C-peptide, IGF-I, sex-steroid hormones and adiposity: a cross-sectional study in healthy women within the European Prospective Investigation into Cancer and Nutrition (EPIC). Cancer Causes Control 16:561-572.

Bingham SA, Day NE, Luben R, Ferrari P, Slimani N, Norat T, Clavel-Chapelon F, Kesse E, Nieters A, Boeing H, Tjonneland A, Overvad K, Martinez C, Dorronsoro M, Gonzalez CA, Key TJ, Trichopoulou A, Naska A, Vineis P, Tumino R, Krogh V, Bueno-de-Mesquita HB, Peeters PH, Berglund G, Hallmans G, Lund E, Skeie G, Kaaks R, Riboli

E. 2003. Dietary fibre in food and protection against colorectal cancer in the European Prospective Investigation into Cancer and Nutrition (EPIC): an observational study. Lancet 361:1496-1501.

Bishop JF, Dewar J, Toner GC, Smith J, Tattersall MH, Olver IN, Ackland S, Kennedy I, Goldstein D, Gurney H, Walpole E, Levi J, Stephenson J, Canetta R. 1999. Initial paclitaxel improves outcome compared with CMFP combination chemotherapy as front-line therapy in untreated metastatic breast cancer. J Clin Oncol 17:2355-2364.

Blackwell KL, Burstein HJ, Storniolo AM, Rugo H, Sledge G, Koehler M, Ellis C, Casey M, Vukelja S, Bischoff J, Baselga J, O'Shaughnessy J. 2010. Randomized study of Lapatinib alone or in combination with trastuzumab in women with ErbB2-positive, trastuzumab-refractory metastatic breast cancer. J Clin Oncol 28:1124-1130.

Blanchard AA, Ma X, Dueck KJ, Penner C, Cooper SC, Mulhall D, Murphy LC, Leygue E, Myal Y. 2013. Claudin 1 expression in basal-like breast cancer is related to patient age. BMC Cancer 13:268.

Bodor M, Kelly EJ, Ho RJ. 2005. Characterization of the human MDR1 gene. AAPS J 7:E1-5.

Bolos V, Mira E, Martinez-Poveda B, Luxan G, Canamero M, Martinez AC, Manes S, de la Pompa JL. 2013. Notch activation stimulates migration of breast cancer cells and promotes tumor growth. Breast Cancer Res 15:R54.

Boman BM, Wicha MS, Fields JZ, Runquist OA. 2007. Symmetric division of cancer stem cells--a key mechanism in tumor growth that should be targeted in future therapeutic approaches. Clin Pharmacol Ther 81:893-898.

Bosco EE, Knudsen ES. 2007. RB in breast cancer: at the crossroads of tumorigenesis and treatment. Cell Cycle 6:667-671.

Botchkina GI, Zuniga ES, Das M, Wang Y, Wang H, Zhu S, Savitt AG, Rowehl RA, Leyfman Y, Ju J, Shroyer K, Ojima I. 2010. New-generation taxoid SB-T-1214 inhibits stem cell-related gene expression in 3D cancer spheroids induced by purified colon tumor-initiating cells. Mol Cancer 9:192.

Botchkina IL, Rowehl RA, Rivadeneira DE, Karpeh MS, Jr., Crawford H, Dufour A, Ju J, Wang Y, Leyfman Y, Botchkina GI. 2009. Phenotypic subpopulations of metastatic colon cancer stem cells: genomic analysis. Cancer Genomics Proteomics 6:19-29.

Boulay A, Rudloff J, Ye J, Zumstein-Mecker S, O'Reilly T, Evans DB, Chen S, Lane HA. 2005. Dual inhibition of mTOR and estrogen receptor signaling in vitro induces cell death in models of breast cancer. Clin Cancer Res 11:5319-5328.

Bourgier C, Aimard L, Bodez V, Bollet MA, Cutuli B, Franck D, Hennequin C, Kirova YM, Azria D. 2013. Adjuvant radiotherapy in the management of axillary node negative invasive breast cancer: a qualitative systematic review. Crit Rev Oncol Hematol 86:33-41.

Bouwman P, Aly A, Escandell JM, Pieterse M, Bartkova J, van der Gulden H, Hiddingh S, Thanasoula M, Kulkarni A, Yang Q, Haffty BG, Tommiska J, Blomqvist C, Drapkin R, Adams DJ, Nevanlinna H, Bartek J, Tarsounas M, Ganesan S, Jonkers J. 2010. 53BP1 loss rescues BRCA1 deficiency and is associated with triple-negative and BRCA-mutated breast cancers. Nat Struct Mol Biol 17:688-695.

Brafman DA, Moya N, Allen-Soltero S, Fellner T, Robinson M, McMillen ZL, Gaasterland T, Willert K. 2013. Analysis of SOX2-Expressing Cell Populations Derived from Human Pluripotent Stem Cells. Stem Cell Reports 1:464-478.

Brand TM, Iida M, Wheeler DL. 2011. Molecular mechanisms of resistance to the EGFR monoclonal antibody cetuximab. Cancer Biol Ther 11:777-792.

Bray F, Jemal A, Grey N, Ferlay J, Forman D. 2012. Global cancer transitions according to the Human Development Index (2008-2030): a population-based study. Lancet Oncol 13:790-801.

Bronger H, Kraeft S, Schwarz-Boeger U, Cerny C, Stockel A, Avril S, Kiechle M, Schmitt M. 2012. Modulation of CXCR3 ligand secretion by prostaglandin E2 and cyclooxygenase inhibitors in human breast cancer. Breast Cancer Res 14:R30.

Buczacki S, Davies RJ, Winton DJ. 2011. Stem cells, quiescence and rectal carcinoma: an unexplored relationship and potential therapeutic target. Br J Cancer 105:1253-1259.

Buikema JW, Mady AS, Mittal NV, Atmanli A, Caron L, Doevendans PA, Sluijter JP, Domian IJ. 2013. Wnt/beta-catenin signaling directs the regional expansion of first and second heart field-derived ventricular cardiomyocytes. Development.

Campbell LL, Polyak K. 2007. Breast tumor heterogeneity: cancer stem cells or clonal evolution? Cell Cycle 6:2332-2338.

Cao L, Zhou Y, Zhai B, Liao J, Xu W, Zhang R, Li J, Zhang Y, Chen L, Qian H, Wu M, Yin Z. 2011. Sphere-forming cell subpopulations with cancer stem cell properties in human hepatoma cell lines. BMC Gastroenterol 11:71.

Capper D, Gaiser T, Hartmann C, Habel A, Mueller W, Herold-Mende C, von Deimling A, Siegelin MD. 2009. Stem-cell-like glioma cells are resistant to TRAIL/Apo2L and exhibit down-regulation of caspase-8 by promoter methylation. Acta Neuropathol 117:445-456.

Carey LA, Perou CM, Livasy CA, Dressler LG, Cowan D, Conway K, Karaca G, Troester MA, Tse CK, Edmiston S, Deming SL, Geradts J, Cheang MC, Nielsen TO, Moorman PG, Earp HS, Millikan RC. 2006. Race, breast cancer subtypes, and survival in the Carolina Breast Cancer Study. JAMA 295:2492-2502.

Cavalieri E, Chakravarti D, Guttenplan J, Hart E, Ingle J, Jankowiak R, Muti P, Rogan E, Russo J, Santen R, Sutter T. 2006. Catechol estrogen quinones as initiators of breast and other human cancers: implications for biomarkers of susceptibility and cancer prevention. Biochim Biophys Acta 1766:63-78.

Cavalieri EL, Rogan EG. 2004. A unifying mechanism in the initiation of cancer and other diseases by catechol quinones. Ann N Y Acad Sci 1028:247-257.

Cavalieri EL, Rogan EG. 2011. Unbalanced metabolism of endogenous estrogens in the etiology and prevention of human cancer. J Steroid Biochem Mol Biol 125:169-180.

Celis JE, Moreira JM, Cabezon T, Gromov P, Friis E, Rank F, Gromova I. 2005. Identification of extracellular and intracellular signaling components of the mammary adipose tissue and its interstitial fluid in high risk breast cancer patients: toward dissecting the molecular circuitry of epithelial-adipocyte stromal cell interactions. Mol Cell Proteomics 4:492-522.

Center MM, Jemal A, Ward E. 2009. International trends in colorectal cancer incidence rates. Cancer Epidemiol Biomarkers Prev 18:1688-1694.

Ciatto S, Rosselli Del Turco M, Ambrogetti D, Bravetti P, Catarzi S, Morrone D, Cariaggi MP. 1997. Solid nonpalpable breast lesions. Success and failure of guided fine-needle aspiration cytology in a consecutive series of 2444 cases. Acta Radiol 38:815-820.

Citri A, Yarden Y. 2006. EGF-ERBB signalling: towards the systems level. Nat Rev Mol Cell Biol 7:505-516.

Clemons M, Danson S, Howell A. 2002. Tamoxifen ("Nolvadex"): a review. Cancer Treat Rev 28:165-180.

Clevers H. 2005. Stem cells, asymmetric division and cancer. Nat Genet 37:1027-1028.

Clevers H. 2011. The cancer stem cell: premises, promises and challenges. Nat Med 17:313-319.

Cobrinik D, Lee MH, Hannon G, Mulligan G, Bronson RT, Dyson N, Harlow E, Beach D, Weinberg RA, Jacks T. 1996. Shared role of the pRB-related p130 and p107 proteins in limb development. Genes Dev 10:1633-1644.

Coccia EM, Severa M, Giacomini E, Monneron D, Remoli ME, Julkunen I, Cella M, Lande R, Uze G. 2004. Viral infection and Toll-like receptor agonists induce a differential expression of type I and lambda interferons in human plasmacytoid and monocyte-derived dendritic cells. Eur J Immunol 34:796-805.

Compton MM. 1992. A biochemical hallmark of apoptosis: internucleosomal degradation of the genome. Cancer Metastasis Rev 11:105-119.

Conejo-Garcia A, Garcia-Rubino ME, Marchal JA, Nunez MC, Ramirez A, Cimino S, Garcia MA, Aranega A, Gallo MA, Campos JM. 2011. Synthesis and anticancer activity of (RS)-9-(2,3-dihydro-1,4-benzoxaheteroin-2-ylmethyl)-9H-purines. Eur J Med Chem 46:3795-3801.

Conley SJ, Gheordunescu E, Kakarala P, Newman B, Korkaya H, Heath AN, Clouthier SG, Wicha MS. 2012. Antiangiogenic agents increase breast cancer stem cells via the generation of tumor hypoxia. Proc Natl Acad Sci U S A 109:2784-2789.

Conter HJ, Lim ZD, Ng CS, Millikan RE, Tannir NM. 2013. Curability of poor-risk metastatic sarcomatoid renal cell carcinoma with the combination of gemcitabine, 5-fluorouracil, and interferon-alfa: a case report of a 55-year-old man with a 10-year complete remission. Clin Genitourin Cancer 11:370-373.

Cooper MK, Porter JA, Young KE, Beachy PA. 1998. Teratogen-mediated inhibition of target tissue response to Shh signaling. Science 280:1603-1607.

Croce CM. 2008. Oncogenes and cancer. N Engl J Med 358:502-511.

Crystal P, Koretz M, Shcharynsky S, Makarov V, Strano S. 2005. Accuracy of sonographically guided 14-gauge core-needle biopsy: results of 715 consecutive breast biopsies with at least two-year follow-up of benign lesions. J Clin Ultrasound 33:47-52.

Curry CL, Reed LL, Golde TE, Miele L, Nickoloff BJ, Foreman KE. 2005. Gamma secretase inhibitor blocks Notch activation and induces apoptosis in Kaposi's sarcoma tumor cells. Oncogene 24:6333-6344.

Charafe-Jauffret E, Ginestier C, Iovino F, Tarpin C, Diebel M, Esterni B, Houvenaeghel G, Extra JM, Bertucci F, Jacquemier J, Xerri L, Dontu G, Stassi G, Xiao Y, Barsky SH, Birnbaum D, Viens P, Wicha MS. 2010. Aldehyde dehydrogenase 1-positive cancer stem cells mediate metastasis and poor clinical outcome in inflammatory breast cancer. Clin Cancer Res 16:45-55.

Charehbili A, Fontein DB, Kroep JR, Liefers GJ, Mieog JS, Nortier JW, van de Velde CJ. 2013. Neoadjuvant hormonal therapy for endocrine sensitive breast cancer: A systematic review. Cancer Treat Rev.

Chau I, Norman AR, Cunningham D, Tait D, Ross PJ, Iveson T, Hill M, Hickish T, Lofts F, Jodrell D, Webb A, Oates JR. 2005. A randomised comparison between 6 months of bolus fluorouracil/leucovorin and 12 weeks of protracted venous infusion fluorouracil as adjuvant treatment in colorectal cancer. Ann Oncol 16:549-557.

Chen HJ, Hsu LS, Shia YT, Lin MW, Lin CM. 2012. The beta-catenin/TCF complex as a novel target of resveratrol in the Wnt/beta-catenin signaling pathway. Biochem Pharmacol 84:1143-1153.

Chen JK, Taipale J, Cooper MK, Beachy PA. 2002a. Inhibition of Hedgehog signaling by direct binding of cyclopamine to Smoothened. Genes Dev 16:2743-2748.

Chen JK, Taipale J, Young KE, Maiti T, Beachy PA. 2002b. Small molecule modulation of Smoothened activity. Proc Natl Acad Sci U S A 99:14071-14076.

Chen W, Zhang X, Chu C, Cheung WL, Ng L, Lam S, Chow A, Lau T, Chen M, Li Y, Nie Y, Wong BC, Pang R. 2013. Identification of CD44+ cancer stem cells in human gastric cancer. Hepatogastroenterology 60:949-954.

Chen YC, Hsu HS, Chen YW, Tsai TH, How CK, Wang CY, Hung SC, Chang YL, Tsai ML, Lee YY, Ku HH, Chiou SH. 2008. Oct-4 expression maintained cancer stem-like properties in lung cancer-derived CD133-positive cells. PLoS One 3:e2637.

Cherrin C, Haskell K, Howell B, Jones R, Leander K, Robinson R, Watkins A, Bilodeau M, Hoffman J, Sanderson P, Hartman G, Mahan E, Prueksaritanont T, Jiang G, She QB, Rosen N, Sepp-Lorenzino L, Defeo-Jones D, Huber HE. 2010. An allosteric Akt inhibitor effectively blocks Akt signaling and tumor growth with only transient effects on glucose and insulin levels in vivo. Cancer Biol Ther 9:493-503.

Chikazawa N, Tanaka H, Tasaka T, Nakamura M, Tanaka M, Onishi H, Katano M. 2010. Inhibition of Wnt signaling pathway decreases chemotherapy-resistant side-population colon cancer cells. Anticancer Res 30:2041-2048.

Cho NL, Lin CI, Du J, Whang EE, Ito H, Moore FD, Jr., Ruan DT. 2012. Global tyrosine kinome profiling of human thyroid tumors identifies Src as a promising target for invasive cancers. Biochem Biophys Res Commun 421:508-513.

Christmann M, Kaina B. 2012. O(6)-methylguanine-DNA methyltransferase (MGMT): impact on cancer risk in response to tobacco smoke. Mutat Res 736:64-74.

D'Incalci M, Colombo T, Ubezio P, Nicoletti I, Giavazzi R, Erba E, Ferrarese L, Meco D, Riccardi R, Sessa C, Cavallini E, Jimeno J, Faircloth GT. 2003. The combination of yondelis and cisplatin is synergistic against human tumor xenografts. Eur J Cancer 39:1920-1926.

Dal Col J, Mastorci K, Fae DA, Muraro E, Martorelli D, Inghirami G, Dolcetti R. 2012. Retinoic acid/alpha-interferon combination inhibits growth and promotes apoptosis in mantle cell lymphoma through Akt-dependent modulation of critical targets. Cancer Res 72:1825-1835.

Dalby KN, Tekedereli I, Lopez-Berestein G, Ozpolat B. 2010. Targeting the prodeath and prosurvival functions of autophagy as novel therapeutic strategies in cancer. Autophagy 6:322-329.

Dalerba P, Dylla SJ, Park IK, Liu R, Wang X, Cho RW, Hoey T, Gurney A, Huang EH, Simeone DM, Shelton AA, Parmiani G, Castelli C, Clarke MF. 2007. Phenotypic characterization of human colorectal cancer stem cells. Proc Natl Acad Sci U S A 104:10158-10163.

Damgaard OE, Jensen MB, Kroman N, Tvedskov TF. 2013. Quantifying the number of lymph nodes identified in one-stage versus two-stage axillary dissection in breast cancer. Breast 22:44-46.

Danforth HD, Ruff MD, Reid WM, Miller RL. 1977. Anticoccidial activity of salinomycin in battery raised broiler chickens. Poult Sci 56:926-932.

Darby S, McGale P, Correa C, Taylor C, Arriagada R, Clarke M, Cutter D, Davies C, Ewertz M, Godwin J, Gray R, Pierce L, Whelan T, Wang Y, Peto R. 2011. Effect of radiotherapy after breast-conserving surgery on 10-year recurrence and 15-year breast cancer death: meta-analysis of individual patient data for 10,801 women in 17 randomised trials. Lancet 378:1707-1716.

Darnell JE, Jr., Kerr IM, Stark GR. 1994. Jak-STAT pathways and transcriptional activation in response to IFNs and other extracellular signaling proteins. Science 264:1415-1421.

Datta D, Flaxenburg JA, Laxmanan S, Geehan C, Grimm M, Waaga-Gasser AM, Briscoe DM, Pal S. 2006. Ras-induced modulation of CXCL10 and its receptor splice variant CXCR3-B in MDA-MB-435 and MCF-7 cells: relevance for the development of human breast cancer. Cancer Res 66:9509-9518.

Datta SR, Brunet A, Greenberg ME. 1999. Cellular survival: a play in three Akts. Genes Dev 13:2905-2927.

Davies BR, Greenwood H, Dudley P, Crafter C, Yu DH, Zhang J, Li J, Gao B, Ji Q, Maynard J, Ricketts SA, Cross D, Cosulich S, Chresta CC, Page K, Yates J, Lane C, Watson R, Luke R, Ogilvie D, Pass M. 2012. Preclinical pharmacology of AZD5363, an inhibitor of AKT: pharmacodynamics, antitumor activity, and correlation of monotherapy activity with genetic background. Mol Cancer Ther 11:873-887.

Dawood S, Broglio K, Buzdar AU, Hortobagyi GN, Giordano SH. 2010. Prognosis of women with metastatic breast cancer by HER2 status and trastuzumab treatment: an institutional-based review. J Clin Oncol 28:92-98.

de Fatima A, Zambuzzi WF, Modolo LV, Tarsitano CA, Gadelha FR, Hyslop S, de Carvalho JE, Salgado I, Ferreira CV, Pilli RA. 2008. Cytotoxicity of goniothalamin enantiomers in renal cancer cells: involvement of nitric oxide, apoptosis and autophagy. Chem Biol Interact 176:143-150.

de Gramont A, Figer A, Seymour M, Homerin M, Hmissi A, Cassidy J, Boni C, Cortes-Funes H, Cervantes A, Freyer G, Papamichael D, Le Bail N, Louvet C, Hendler D, de Braud F, Wilson C, Morvan F, Bonetti A. 2000. Leucovorin and fluorouracil with or without oxaliplatin as first-line treatment in advanced colorectal cancer. J Clin Oncol 18:2938-2947.

De Laurentiis M, Cancello G, D'Agostino D, Giuliano M, Giordano A, Montagna E, Lauria R, Forestieri V, Esposito A, Silvestro L, Pennacchio R, Criscitiello C, Montanino A, Limite G, Bianco AR, De Placido S. 2008. Taxane-based combinations as adjuvant chemotherapy of early breast cancer: a meta-analysis of randomized trials. J Clin Oncol 26:44-53.

Delaney G, Jacob S, Featherstone C, Barton M. 2005. The role of radiotherapy in cancer treatment: estimating optimal utilization from a review of evidence-based clinical guidelines. Cancer 104:1129-1137.

Dembinski JL, Krauss S. 2009. Characterization and functional analysis of a slow cycling stem cell-like subpopulation in pancreas adenocarcinoma. Clin Exp Metastasis 26:611-623.

Deng Q, Wang Q, Zong WY, Zheng DL, Wen YX, Wang KS, Teng XM, Zhang X, Huang J, Han ZG. 2010a. E2F8 contributes to human hepatocellular carcinoma via regulating cell proliferation. Cancer Res 70:782-791.

Deng YT, Huang HC, Lin JK. 2010b. Rotenone induces apoptosis in MCF-7 human breast cancer cell-mediated ROS through JNK and p38 signaling. Mol Carcinog 49:141-151.

Desai MM, Gong B, Chan T, Davey RA, Soong L, Kolokoltsov AA, Sun J. 2011. Differential, type I interferon-mediated autophagic trafficking of hepatitis C virus proteins in mouse liver. Gastroenterology 141:674-685, 685 e671-676.

Di L, Kerns EH, Carter GT. 2009. Drug-like property concepts in pharmaceutical design. Curr Pharm Des 15:2184-2194.

Diaz-Gavilan M, Gomez-Vidal JA, Entrena A, Gallo MA, Espinosa A, Campos JM. 2006. Study of the factors that control the ratio of the products between 5-fluorouracil, uracil, and tetrahydrobenzoxazepine O,O-acetals bearing electron-withdrawing groups on the nitrogen atom. J Org Chem 71:1043-1054.

Diaz-Gavilan M, Gomez-Vidal JA, Rodriguez-Serrano F, Marchal JA, Caba O, Aranega A, Gallo MA, Espinosa A, Campos JM. 2008. Anticancer activity of (1,2,3,5-tetrahydro-4,1-benzoxazepine-3-yl)-pyrimidines and -purines against the MCF-7 cell line: Preliminary cDNA microarray studies. Bioorg Med Chem Lett 18:1457-1460.

Dicitore A, Caraglia M, Gaudenzi G, Manfredi G, Amato B, Mari D, Persani L, Arra C, Vitale G. 2013. Type I interferon-mediated pathway interacts with peroxisome proliferator activated receptor-gamma (PPAR-gamma): At the cross-road of pancreatic cancer cell proliferation. Biochim Biophys Acta 1845:42-52.

Dick FA. 2007. Structure-function analysis of the retinoblastoma tumor suppressor protein - is the whole a sum of its parts? Cell Div 2:26.

Dick JE. 2008. Stem cell concepts renew cancer research. Blood 112:4793-4807.

Diggs DL, Huderson AC, Harris KL, Myers JN, Banks LD, Rekhadevi PV, Niaz MS, Ramesh A. 2011. Polycyclic aromatic hydrocarbons and digestive tract cancers: a perspective. J Environ Sci Health C Environ Carcinog Ecotoxicol Rev 29:324-357.

Dontu G, Abdallah WM, Foley JM, Jackson KW, Clarke MF, Kawamura MJ, Wicha MS. 2003. In vitro propagation and transcriptional profiling of human mammary stem/progenitor cells. Genes Dev 17:1253-1270.

Donze O, Deng J, Curran J, Sladek R, Picard D, Sonenberg N. 2004. The protein kinase PKR: a molecular clock that sequentially activates survival and death programs. EMBO J 23:564-571.

Dowlati A, Nethery D, Kern JA. 2004. Combined inhibition of epidermal growth factor receptor and JAK/STAT pathways results in greater growth inhibition in vitro than single agent therapy. Mol Cancer Ther 3:459-463.

Drygin D, O'Brien SE, Hannan RD, McArthur GA, Von Hoff DD. 2013. Targeting the nucleolus for cancer-specific activation of p53. Drug Discov Today.

Du W, Pogoriler J. 2006. Retinoblastoma family genes. Oncogene 25:5190-5200.

Dumay A, Feugeas JP, Wittmer E, Lehmann-Che J, Bertheau P, Espie M, Plassa LF, Cottu P, Marty M, Andre F, Sotiriou C, Pusztai L, de The H. 2013. Distinct tumor protein p53 mutants in breast cancer subgroups. Int J Cancer 132:1227-1231.

Duncan KJ, Eckert KA, Clawson GA. 2009. Mechanisms of growth inhibition in human papillomavirus positive and negative cervical cancer cells by the chloromethyl ketone protease inhibitor, succinyl-alanine-alanine-proline-phenylalanine chloromethyl ketone. J Pharmacol Exp Ther 330:359-366.

Duru N, Fan M, Candas D, Menaa C, Liu HC, Nantajit D, Wen Y, Xiao K, Eldridge A, Chromy BA, Li S, Spitz DR, Lam KS, Wicha MS, Li JJ. 2012. HER2-associated radioresistance

of breast cancer stem cells isolated from HER2-negative breast cancer cells. Clin Cancer Res 18:6634-6647.

Ebos JM, Lee CR, Cruz-Munoz W, Bjarnason GA, Christensen JG, Kerbel RS. 2009. Accelerated metastasis after short-term treatment with a potent inhibitor of tumor angiogenesis. Cancer Cell 15:232-239.

Efeyan A, Sabatini DM. 2010. mTOR and cancer: many loops in one pathway. Curr Opin Cell Biol 22:169-176.

Elliott RL, Blobe GC. 2005. Role of transforming growth factor Beta in human cancer. J Clin Oncol 23:2078-2093.

Ellisen LW, Bird J, West DC, Soreng AL, Reynolds TC, Smith SD, Sklar J. 1991. TAN-1, the human homolog of the Drosophila notch gene, is broken by chromosomal translocations in T lymphoblastic neoplasms. Cell 66:649-661.

Ennis BW, Fultz KE, Smith KA, Westwick JK, Zhu D, Boluro-Ajayi M, Bilter GK, Stein B. 2005. Inhibition of tumor growth, angiogenesis, and tumor cell proliferation by a small molecule inhibitor of c-Jun N-terminal kinase. J Pharmacol Exp Ther 313:325-332.

Eramo A, Lotti F, Sette G, Pilozzi E, Biffoni M, Di Virgilio A, Conticello C, Ruco L, Peschle C, De Maria R. 2008. Identification and expansion of the tumorigenic lung cancer stem cell population. Cell Death Differ 15:504-514.

Evans TR, Yellowlees A, Foster E, Earl H, Cameron DA, Hutcheon AW, Coleman RE, Perren T, Gallagher CJ, Quigley M, Crown J, Jones AL, Highley M, Leonard RC, Mansi JL. 2005. Phase III randomized trial of doxorubicin and docetaxel versus doxorubicin and cyclophosphamide as primary medical therapy in women with breast cancer: an anglo-celtic cooperative oncology group study. J Clin Oncol 23:2988-2995.

Evrard A, Cuq P, Ciccolini J, Vian L, Cano JP. 1999. Increased cytotoxicity and bystander effect of 5-fluorouracil and 5-deoxy-5-fluorouridine in human colorectal cancer cells transfected with thymidine phosphorylase. Br J Cancer 80:1726-1733.

Federman DG, Kravetz JD, Kirsner RS. 2002. Skin cancer screening by dermatologists: prevalence and barriers. J Am Acad Dermatol 46:710-714.

Feinberg AP, Ohlsson R, Henikoff S. 2006. The epigenetic progenitor origin of human cancer. Nat Rev Genet 7:21-33.

Feldmann G, Dhara S, Fendrich V, Bedja D, Beaty R, Mullendore M, Karikari C, Alvarez H, Iacobuzio-Donahue C, Jimeno A, Gabrielson KL, Matsui W, Maitra A. 2007. Blockade of hedgehog signaling inhibits pancreatic cancer invasion and metastases: a new paradigm for combination therapy in solid cancers. Cancer Res 67:2187-2196.

Ferlay J, Shin HR, Bray F, Forman D, Mathers C, Parkin DM. 2010. Estimates of worldwide burden of cancer in 2008: GLOBOCAN 2008. Int J Cancer 127:2893-2917.

Fernald K, Kurokawa M. 2013. Evading apoptosis in cancer. Trends Cell Biol 23:620-633.

Ferrara N. 2004. Vascular endothelial growth factor: basic science and clinical progress. Endocr Rev 25:581-611.

Fisher B, Anderson S, Bryant J, Margolese RG, Deutsch M, Fisher ER, Jeong JH, Wolmark N. 2002. Twenty-year follow-up of a randomized trial comparing total mastectomy, lumpectomy, and lumpectomy plus irradiation for the treatment of invasive breast cancer. N Engl J Med 347:1233-1241.

Fiteni F, Villanueva C, Bazan F, Perrin S, Chaigneau L, Dobi E, Montcuquet P, Cals L, Meneveau N, Nerich V, Limat S, Pivot X. 2013. Long-term follow-up of patients with metastatic breast cancer treated by trastuzumab: Impact of institutions. Breast.

Fraile RJ, Baker LH, Buroker TR, Horwitz J, Vaitkevicius VK. 1980. Pharmacokinetics of 5-fluorouracil administered orally, by rapid intravenous and by slow infusion. Cancer Res 40:2223-2228.

Frangioni JV. 2008. New technologies for human cancer imaging. J Clin Oncol 26:4012-4021.

Friday BB, Adjei AA. 2005. K-ras as a target for cancer therapy. Bba-Rev Cancer 1756:127-144.

Fuchs D, Daniel V, Sadeghi M, Opelz G, Naujokat C. 2010. Salinomycin overcomes ABC transporter-mediated multidrug and apoptosis resistance in human leukemia stem cell-like KG-1a cells. Biochem Biophys Res Commun 394:1098-1104.

Fulda S. 2010. Evasion of apoptosis as a cellular stress response in cancer. Int J Cell Biol 2010:370835.

Gale M, Jr., Tan SL, Katze MG. 2000. Translational control of viral gene expression in eukaryotes. Microbiol Mol Biol Rev 64:239-280.

Gao MQ, Choi YP, Kang S, Youn JH, Cho NH. 2010. CD24+ cells from hierarchically organized ovarian cancer are enriched in cancer stem cells. Oncogene 29:2672-2680.

Garcia MA, Carrasco E, Aguilera M, Alvarez P, Rivas C, Campos JM, Prados JC, Calleja MA, Esteban M, Marchal JA, Aranega A. 2011. The chemotherapeutic drug 5-fluorouracil promotes PKR-mediated apoptosis in a p53-independent manner in colon and breast cancer cells. PLoS One 6:e23887.

Garcia MA, Gil J, Ventoso I, Guerra S, Domingo E, Rivas C, Esteban M. 2006. Impact of protein kinase PKR in cell biology: from antiviral to antiproliferative action. Microbiol Mol Biol Rev 70:1032-1060.

Garcia MA, Guerra S, Gil J, Jimenez V, Esteban M. 2002. Anti-apoptotic and oncogenic properties of the dsRNA-binding protein of vaccinia virus, E3L. Oncogene 21:8379-8387.

Garcia MA, Meurs EF, Esteban M. 2007. The dsRNA protein kinase PKR: virus and cell control. Biochimie 89:799-811.

Gasco M, Shami S, Crook T. 2002. The p53 pathway in breast cancer. Breast Cancer Res 4:70-76.

Geng Y, Kohli L, Klocke BJ, Roth KA. 2010. Chloroquine-induced autophagic vacuole accumulation and cell death in glioma cells is p53 independent. Neuro Oncol 12:473-481.

Ghavami S, Hashemi M, Ande SR, Yeganeh B, Xiao W, Eshraghi M, Bus CJ, Kadkhoda K, Wiechec E, Halayko AJ, Los M. 2009. Apoptosis and cancer: mutations within caspase genes. J Med Genet 46:497-510.

Gianni L, Dafni U, Gelber RD, Azambuja E, Muehlbauer S, Goldhirsch A, Untch M, Smith I, Baselga J, Jackisch C, Cameron D, Mano M, Pedrini JL, Veronesi A, Mendiola C, Pluzanska A, Semiglazov V, Vrdoljak E, Eckart MJ, Shen Z, Skiadopoulos G, Procter M, Pritchard KI, Piccart-Gebhart MJ, Bell R. 2011. Treatment with trastuzumab for 1 year after adjuvant chemotherapy in patients with HER2-positive early breast cancer: a 4-year follow-up of a randomised controlled trial. Lancet Oncol 12:236-244.

Giard RWM, Hermans J. 1992. The Value of Aspiration Cytologic Examination of the Breast - a Statistical Review of the Medical Literature. Cancer 69:2104-2110.

Gilot D, Loyer P, Corlu A, Glaise D, Lagadic-Gossmann D, Atfi A, Morel F, Ichijo H, Guguen-Guillouzo C. 2002. Liver protection from apoptosis requires both blockage of initiator caspase activities and inhibition of ASK1/JNK pathway via glutathione S-transferase regulation. J Biol Chem 277:49220-49229.

Ginestier C, Hur MH, Charafe-Jauffret E, Monville F, Dutcher J, Brown M, Jacquemier J, Viens P, Kleer CG, Liu S, Schott A, Hayes D, Birnbaum D, Wicha MS, Dontu G. 2007. ALDH1 is a marker of normal and malignant human mammary stem cells and a predictor of poor clinical outcome. Cell Stem Cell 1:555-567.

Giovannucci E, Harlan DM, Archer MC, Bergenstal RM, Gapstur SM, Habel LA, Pollak M, Regensteiner JG, Yee D. 2010. Diabetes and cancer: a consensus report. Diabetes Care 33:1674-1685.

Gitlin L, Barchet W, Gilfillan S, Cella M, Beutler B, Flavell RA, Diamond MS, Colonna M. 2006. Essential role of mda-5 in type I IFN responses to polyriboinosinic:polyribocytidylic acid and encephalomyocarditis picornavirus. Proc Natl Acad Sci U S A 103:8459-8464.

Glaysher S, Bolton LM, Johnson P, Atkey N, Dyson M, Torrance C, Cree IA. 2013. Targeting EGFR and PI3K pathways in ovarian cancer. Br J Cancer.

Goldstein D, Laszlo J. 1986. Interferon therapy in cancer: from imaginon to interferon. Cancer Res 46:4315-4329.

Gong C, Yao H, Liu Q, Chen J, Shi J, Su F, Song E. 2010. Markers of tumor-initiating cells predict chemoresistance in breast cancer. PLoS One 5:e15630.

Gonzalez CA, Riboli E. 2010. Diet and cancer prevention: Contributions from the European Prospective Investigation into Cancer and Nutrition (EPIC) study. Eur J Cancer 46:2555-2562.

Gooch JL, Yee D. 1999. Strain-specific differences in formation of apoptotic DNA ladders in MCF-7 breast cancer cells. Cancer Lett 144:31-37.

Goodell MA. 2005. Stem cell identification and sorting using the Hoechst 33342 side population (SP). Curr Protoc Cytom Chapter 9:Unit9 18.

Gottschling S, Schnabel PA, Herth FJ, Herpel E. 2012. Are we missing the target? Cancer stem cells and drug resistance in non-small cell lung cancer. Cancer Genomics Proteomics 9:275-286.

Gou HF, Zang J, Jiang M, Yang Y, Cao D, Chen XC. 2012. Clinical prognostic analysis of 116 patients with primary intestinal non-Hodgkin lymphoma. Med Oncol 29:227-234.

Grem JL. 2000. 5-Fluorouracil: forty-plus and still ticking. A review of its preclinical and clinical development. Invest New Drugs 18:299-313.

Grem JL, Nguyen D, Monahan BP, Kao V, Geoffroy FJ. 1999. Sequence-dependent antagonism between fluorouracil and paclitaxel in human breast cancer cells. Biochem Pharmacol 58:477-486.

Gross E, L'Faqihi-Olive FE, Ysebaert L, Brassac M, Struski S, Kheirallah S, Fournie JJ, Laurent G, Quillet-Mary A. 2010. B-chronic lymphocytic leukemia chemoresistance involves innate and acquired leukemic side population cells. Leukemia 24:1885-1892.

Groth C, Fortini ME. 2012. Therapeutic approaches to modulating Notch signaling: current challenges and future prospects. Semin Cell Dev Biol 23:465-472.

Gschwendt M, Muller HJ, Kielbassa K, Zang R, Kittstein W, Rincke G, Marks F. 1994. Rottlerin, a novel protein kinase inhibitor. Biochem Biophys Res Commun 199:93-98.

Gupta PB, Onder TT, Jiang G, Tao K, Kuperwasser C, Weinberg RA, Lander ES. 2009. Identification of selective inhibitors of cancer stem cells by high-throughput screening. Cell 138:645-659.

Hahn WC, Weinberg RA. 2002. Rules for making human tumor cells. N Engl J Med 347:1593-1603.

Hanahan D, Weinberg RA. 2000. The hallmarks of cancer. Cell 100:57-70.

Harbeck N, Salem M, Nitz U, Gluz O, Liedtke C. 2010. Personalized treatment of early-stage breast cancer: present concepts and future directions. Cancer Treat Rev 36:584-594.

Harbour JW, Dean DC. 2000. The Rb/E2F pathway: expanding roles and emerging paradigms. Genes Dev 14:2393-2409.

Hassan KA, Wang L, Korkaya H, Chen G, Maillard I, Beer DG, Kalemkerian GP, Wicha MS. 2013. Notch pathway activity identifies cells with cancer stem cell-like properties and correlates with worse survival in lung adenocarcinoma. Clin Cancer Res 19:1972-1980.

Hattangadi DK, DeMasters GA, Walker TD, Jones KR, Di X, Newsham IF, Gewirtz DA. 2004. Influence of p53 and caspase 3 activity on cell death and senescence in response to methotrexate in the breast tumor cell. Biochem Pharmacol 68:1699-1708.

Heeg S, Doebele M, von Werder A, Opitz OG. 2006. In vitro transformation models: modeling human cancer. Cell Cycle 5:630-634.

Heidenreich A, Bellmunt J, Bolla M, Joniau S, Mason M, Matveev V, Mottet N, Schmid HP, van der Kwast T, Wiegel T, Zattoni F. 2011. [EAU guidelines on prostate cancer. Part I: screening, diagnosis, and treatment of clinically localised disease]. Actas Urol Esp 35:501-514.

Helleday T, Lo J, van Gent DC, Engelward BP. 2007. DNA double-strand break repair: from mechanistic understanding to cancer treatment. DNA Repair (Amst) 6:923-935.

Hermann PC, Huber SL, Herrler T, Aicher A, Ellwart JW, Guba M, Bruns CJ, Heeschen C. 2007. Distinct populations of cancer stem cells determine tumor growth and metastatic activity in human pancreatic cancer. Cell Stem Cell 1:313-323.

Herreros-Villanueva M, Zhang JS, Koenig A, Abel EV, Smyrk TC, Bamlet WR, de Narvajas AA, Gomez TS, Simeone DM, Bujanda L, Billadeau DD. 2013. SOX2 promotes dedifferentiation and imparts stem cell-like features to pancreatic cancer cells. Oncogenesis 2:e61.

Hervas-Stubbs S, Perez-Gracia JL, Rouzaut A, Sanmamed MF, Le Bon A, Melero I. 2011. Direct effects of type I interferons on cells of the immune system. Clin Cancer Res 17:2619-2627.

Hewitt KJ, Agarwal R, Morin PJ. 2006. The claudin gene family: expression in normal and neoplastic tissues. BMC Cancer 6:186.

Hilton J. 1984. Role of aldehyde dehydrogenase in cyclophosphamide-resistant L1210 leukemia. Cancer Res 44:5156-5160.

Hiraga T, Ito S, Nakamura H. 2011. Side population in MDA-MB-231 human breast cancer cells exhibits cancer stem cell-like properties without higher bone-metastatic potential. Oncol Rep 25:289-296.

Hodge LS, Taub ME, Tracy TS. 2011. Effect of its deaminated metabolite, 2',2'-difluorodeoxyuridine, on the transport and toxicity of gemcitabine in HeLa cells. Biochem Pharmacol 81:950-956.

Holcik M, Sonenberg N. 2005. Translational control in stress and apoptosis. Nat Rev Mol Cell Biol 6:318-327.

Hollande F, Pannequin J, Joubert D. 2010. The long road to colorectal cancer therapy: searching for the right signals. Drug Resist Updat 13:44-56.

Homann N, Konig IR, Marks M, Benesova M, Stickel F, Millonig G, Mueller S, Seitz HK. 2009. Alcohol and colorectal cancer: the role of alcohol dehydrogenase 1C polymorphism. Alcohol Clin Exp Res 33:551-556.

Hori YS, Kuno A, Hosoda R, Horio Y. 2013. Regulation of FOXOs and p53 by SIRT1 Modulators under Oxidative Stress. PLoS One 8:e73875.

Hou Y, Liu YY, Zhao XK. 2013. Expression of aldehyde dehydrogenase 1 in colon cancer. Asian Pac J Trop Med 6:574-577.

Hu C, Dievart A, Lupien M, Calvo E, Tremblay G, Jolicoeur P. 2006. Overexpression of activated murine Notch1 and Notch3 in transgenic mice blocks mammary gland development and induces mammary tumors. Am J Pathol 168:973-990.

Hu P, Huang Q, Li Z, Wu X, Ouyang Q, Chen J, Cao Y. 2014. Silencing MAP3K1 expression through RNA interference enhances paclitaxel-induced cell cycle arrest in human breast cancer cells. Mol Biol Rep 41:19-24.

Hu W, Liu W. 2010. Side populations of glioblastoma cells are less sensitive to HSV-TK/GCV suicide gene therapy system than the non-side population. In Vitro Cell Dev Biol Anim 46:497-501.

Hunter T, Hunt T, Jackson RJ, Robertson HD. 1975. The characteristics of inhibition of protein synthesis by double-stranded ribonucleic acid in reticulocyte lysates. J Biol Chem 250:409-417.

Hurt EM, Kawasaki BT, Klarmann GJ, Thomas SB, Farrar WL. 2008. CD44+ CD24(-) prostate cells are early cancer progenitor/stem cells that provide a model for patients with poor prognosis. Br J Cancer 98:756-765.

Hwang RF, Moore TT, Hattersley MM, Scarpitti M, Yang B, Devereaux E, Ramachandran V, Arumugam T, Ji B, Logsdon CD, Brown JL, Godin R. 2012. Inhibition of the hedgehog pathway targets the tumor-associated stroma in pancreatic cancer. Mol Cancer Res 10:1147-1157.

Hwangbo W, Lee JH, Ahn S, Kim S, Park KH, Kim CH, Kim I. 2013. EGFR Gene Amplification and Protein Expression in Invasive Ductal Carcinoma of the Breast. Korean J Pathol 47:107-115.

Ioannidis I, Ye F, McNally B, Willette M, Flano E. 2013. Toll-like receptor expression and induction of type I and type III interferons in primary airway epithelial cells. J Virol 87:3261-3270.

Ishii T, Kwon H, Hiscott J, Mosialos G, Koromilas AE. 2001. Activation of the I kappa B alpha kinase (IKK) complex by double-stranded RNA-binding defective and catalytic inactive mutants of the interferon-inducible protein kinase PKR. Oncogene 20:1900-1912.

Issa MM, Zasada W, Ward K, Hall JA, Petros JA, Ritenour CW, Goodman M, Kleinbaum D, Mandel J, Marshall FF. 2006. The value of digital rectal examination as a predictor of

prostate cancer diagnosis among United States Veterans referred for prostate biopsy. Cancer Detect Prev 30:269-275.

Izumi Y, Xu L, di Tomaso E, Fukumura D, Jain RK. 2002. Tumour biology: herceptin acts as an anti-angiogenic cocktail. Nature 416:279-280.

Jacks T, Weinberg RA. 1996. Cell-cycle control and its watchman. Nature 381:643-644.

Jacobson JA, Danforth DN, Cowan KH, d'Angelo T, Steinberg SM, Pierce L, Lippman ME, Lichter AS, Glatstein E, Okunieff P. 1995. Ten-year results of a comparison of conservation with mastectomy in the treatment of stage I and II breast cancer. N Engl J Med 332:907-911.

Janicke RU, Ng P, Sprengart ML, Porter AG. 1998. Caspase-3 is required for alpha-fodrin cleavage but dispensable for cleavage of other death substrates in apoptosis. J Biol Chem 273:15540-15545.

Janne PA, Gray N, Settleman J. 2009. Factors underlying sensitivity of cancers to small-molecule kinase inhibitors. Nat Rev Drug Discov 8:709-723.

Jemal A, Bray F, Center MM, Ferlay J, Ward E, Forman D. 2011. Global cancer statistics. CA Cancer J Clin 61:69-90.

Jia X, Li X, Xu Y, Zhang S, Mou W, Liu Y, Lv D, Liu CH, Tan X, Xiang R, Li N. 2011. SOX2 promotes tumorigenesis and increases the anti-apoptotic property of human prostate cancer cell. J Mol Cell Biol 3:230-238.

Jiang F, Qiu Q, Khanna A, Todd NW, Deepak J, Xing L, Wang H, Liu Z, Su Y, Stass SA, Katz RL. 2009. Aldehyde dehydrogenase 1 is a tumor stem cell-associated marker in lung cancer. Mol Cancer Res 7:330-338.

Jiang J, Hui CC. 2008. Hedgehog signaling in development and cancer. Dev Cell 15:801-812.

Jonasch E, Haluska FG. 2001. Interferon in oncological practice: review of interferon biology, clinical applications, and toxicities. Oncologist 6:34-55.

Jorgensen TJ, Ruczinski I, Yao Shugart Y, Wheless L, Berthier Schaad Y, Kessing B, Hoffman-Bolton J, Helzlsouer KJ, Kao WH, Francis L, Alani RM, Strickland PT, Smith MW, Alberg AJ. 2012. A population-based study of hedgehog pathway gene variants in relation to the dual risk of basal cell carcinoma plus another cancer. Cancer Epidemiol 36:e288-293.

Jusof FF, Khaw LT, Ball HJ, Hunt NH. 2013. Improved spectrophotometric human interferon-gamma bioassay. J Immunol Methods 394:115-120.

Kaaks R, Berrino F, Key T, Rinaldi S, Dossus L, Biessy C, Secreto G, Amiano P, Bingham S, Boeing H, Bueno de Mesquita HB, Chang-Claude J, Clavel-Chapelon F, Fournier A, van Gils CH, Gonzalez CA, Gurrea AB, Critselis E, Khaw KT, Krogh V, Lahmann PH, Nagel G, Olsen A, Onland-Moret NC, Overvad K, Palli D, Panico S, Peeters P, Quiros JR, Roddam A, Thiebaut A, Tjonneland A, Chirlaque MD, Trichopoulou A, Trichopoulos D, Tumino R, Vineis P, Norat T, Ferrari P, Slimani N, Riboli E. 2005. Serum sex steroids in premenopausal women and breast cancer risk within the European Prospective Investigation into Cancer and Nutrition (EPIC). J Natl Cancer Inst 97:755-765.

Kagawa S, Gu J, Honda T, McDonnell TJ, Swisher SG, Roth JA, Fang B. 2001. Deficiency of caspase-3 in MCF7 cells blocks Bax-mediated nuclear fragmentation but not cell death. Clin Cancer Res 7:1474-1480.

Kar S, Deb M, Sengupta D, Shilpi A, Bhutia SK, Patra SK. 2012. Intricacies of hedgehog signaling pathways: a perspective in tumorigenesis. Exp Cell Res 318:1959-1972.

Kataoka Y, Mukohara T, Shimada H, Saijo N, Hirai M, Minami H. 2010. Association between gain-of-function mutations in PIK3CA and resistance to HER2-targeted agents in HER2-amplified breast cancer cell lines. Ann Oncol 21:255-262.

Kaufmann M, von Minckwitz G, Mamounas EP, Cameron D, Carey LA, Cristofanilli M, Denkert C, Eiermann W, Gnant M, Harris JR, Karn T, Liedtke C, Mauri D, Rouzier R, Ruckhaeberle E, Semiglazov V, Symmans WF, Tutt A, Pusztai L. 2012. Recommendations from an international consensus conference on the current status and future of neoadjuvant systemic therapy in primary breast cancer. Ann Surg Oncol 19:1508-1516.

Kaufmann SH, Earnshaw WC. 2000. Induction of apoptosis by cancer chemotherapy. Exp Cell Res 256:42-49.

Kerbel RS. 2003. Human tumor xenografts as predictive preclinical models for anticancer drug activity in humans: better than commonly perceived-but they can be improved. Cancer Biol Ther 2:S134-139.

Kerr JF, Wyllie AH, Currie AR. 1972. Apoptosis: a basic biological phenomenon with wide-ranging implications in tissue kinetics. Br J Cancer 26:239-257.

Kim JH, Yoo HI, Kang HS, Ro J, Yoon S. 2012. Salinomycin sensitizes antimitotic drugs-treated cancer cells by increasing apoptosis via the prevention of G2 arrest. Biochem Biophys Res Commun 418:98-103.

Kim KY, Yu SN, Lee SY, Chun SS, Choi YL, Park YM, Song CS, Chatterjee B, Ahn SC. 2011. Salinomycin-induced apoptosis of human prostate cancer cells due to accumulated reactive oxygen species and mitochondrial membrane depolarization. Biochem Biophys Res Commun 413:80-86.

King KM, Lupichuk S, Baig L, Webster M, Basi S, Whyte D, Rix S. 2009. Optimal use of taxanes in metastatic breast cancer. Curr Oncol 16:8-20.

Kinzler KW, Nilbert MC, Su LK, Vogelstein B, Bryan TM, Levy DB, Smith KJ, Preisinger AC, Hedge P, McKechnie D, et al. 1991. Identification of FAP locus genes from chromosome 5q21. Science 253:661-665.

Kirkwood JM, Strawderman MH, Ernstoff MS, Smith TJ, Borden EC, Blum RH. 1996. Interferon alfa-2b adjuvant therapy of high-risk resected cutaneous melanoma: the Eastern Cooperative Oncology Group Trial EST 1684. J Clin Oncol 14:7-17.

Knight ZA, Lin H, Shokat KM. 2010. Targeting the cancer kinome through polypharmacology. Nat Rev Cancer 10:130-137.

Knowlden JM, Hutcheson IR, Jones HE, Madden T, Gee JM, Harper ME, Barrow D, Wakeling AE, Nicholson RI. 2003. Elevated levels of epidermal growth factor receptor/c-erbB2 heterodimers mediate an autocrine growth regulatory pathway in tamoxifen-resistant MCF-7 cells. Endocrinology 144:1032-1044.

Knudson AG, Jr. 1971. Mutation and cancer: statistical study of retinoblastoma. Proc Natl Acad Sci U S A 68:820-823.

Kochert K, Ullrich K, Kreher S, Aster JC, Kitagawa M, Johrens K, Anagnostopoulos I, Jundt F, Lamprecht B, Zimber-Strobl U, Stein H, Janz M, Dorken B, Mathas S. 2011. High-level expression of Mastermind-like 2 contributes to aberrant activation of the NOTCH signaling pathway in human lymphomas. Oncogene 30:1831-1840.

Komatsu T, Yamazaki H, Shimada N, Nakajima M, Yokoi T. 2000. Roles of cytochromes P450 1A2, 2A6, and 2C8 in 5-fluorouracil formation from tegafur, an anticancer prodrug, in human liver microsomes. Drug Metab Dispos 28:1457-1463.

Kondo T, Ito F, Nakazawa H, Horita S, Osaka Y, Toma H. 2004. High expression of chemokine gene as a favorable prognostic factor in renal cell carcinoma. J Urol 171:2171-2175.

Kondratyev M, Kreso A, Hallett RM, Girgis-Gabardo A, Barcelon ME, Ilieva D, Ware C, Majumder PK, Hassell JA. 2012. Gamma-secretase inhibitors target tumor-initiating cells in a mouse model of ERBB2 breast cancer. Oncogene 31:93-103.

Konecny GE, Pegram MD, Venkatesan N, Finn R, Yang G, Rahmeh M, Untch M, Rusnak DW, Spehar G, Mullin RJ, Keith BR, Gilmer TM, Berger M, Podratz KC, Slamon DJ. 2006. Activity of the dual kinase inhibitor lapatinib (GW572016) against HER-2-overexpressing and trastuzumab-treated breast cancer cells. Cancer Res 66:1630-1639.

Kong Y, Cui H, Ramkumar C, Zhang H. 2011. Regulation of senescence in cancer and aging. J Aging Res 2011:963172.

Konstantakou EG, Voutsinas GE, Karkoulis PK, Aravantinos G, Margaritis LH, Stravopodis DJ. 2009. Human bladder cancer cells undergo cisplatin-induced apoptosis that is associated with p53-dependent and p53-independent responses. Int J Oncol 35:401-416.

Korinek V, Barker N, Morin PJ, van Wichen D, de Weger R, Kinzler KW, Vogelstein B, Clevers H. 1997. Constitutive transcriptional activation by a beta-catenin-Tcf complex in APC-/- colon carcinoma. Science 275:1784-1787.

Korkaya H, Paulson A, Charafe-Jauffret E, Ginestier C, Brown M, Dutcher J, Clouthier SG, Wicha MS. 2009. Regulation of mammary stem/progenitor cells by PTEN/Akt/beta-catenin signaling. PLoS Biol 7:e1000121.

Korkaya H, Paulson A, Iovino F, Wicha MS. 2008. HER2 regulates the mammary stem/progenitor cell population driving tumorigenesis and invasion. Oncogene 27:6120-6130.

Kotenko SV, Gallagher G, Baurin VV, Lewis-Antes A, Shen M, Shah NK, Langer JA, Sheikh F, Dickensheets H, Donnelly RP. 2003. IFN-lambdas mediate antiviral protection through a distinct class II cytokine receptor complex. Nat Immunol 4:69-77.

Krauss RM, Deckelbaum RJ, Ernst N, Fisher E, Howard BV, Knopp RH, Kotchen T, Lichtenstein AH, McGill HC, Pearson TA, Prewitt TE, Stone NJ, Horn LV, Weinberg R. 1996. Dietary guidelines for healthy American adults. A statement for health professionals from the Nutrition Committee, American Heart Association. Circulation 94:1795-1800.

Kroemer G, Galluzzi L, Vandenabeele P, Abrams J, Alnemri ES, Baehrecke EH, Blagosklonny MV, El-Deiry WS, Golstein P, Green DR, Hengartner M, Knight RA, Kumar S, Lipton SA, Malorni W, Nunez G, Peter ME, Tschopp J, Yuan J, Piacentini M, Zhivotovsky B, Melino G. 2009. Classification of cell death: recommendations of the Nomenclature Committee on Cell Death 2009. Cell Death Differ 16:3-11.

Kryczek I, Banerjee M, Cheng P, Vatan L, Szeliga W, Wei S, Huang E, Finlayson E, Simeone D, Welling TH, Chang A, Coukos G, Liu R, Zou W. 2009. Phenotype, distribution, generation, and functional and clinical relevance of Th17 cells in the human tumor environments. Blood 114:1141-1149.

Kubo M, Nakamura M, Tasaki A, Yamanaka N, Nakashima H, Nomura M, Kuroki S, Katano M. 2004. Hedgehog signaling pathway is a new therapeutic target for patients with breast cancer. Cancer Res 64:6071-6074.

Kumar D, Shankar S, Srivastava RK. 2013. Rottlerin induces autophagy and apoptosis in prostate cancer stem cells via PI3K/Akt/mTOR signaling pathway. Cancer Lett.

Kushi LH, Doyle C, McCullough M, Rock CL, Demark-Wahnefried W, Bandera EV, Gapstur S, Patel AV, Andrews K, Gansler T. 2012. American Cancer Society Guidelines on nutrition and physical activity for cancer prevention: reducing the risk of cancer with healthy food choices and physical activity. CA Cancer J Clin 62:30-67.

LaBonte MJ, Wilson PM, Fazzone W, Russell J, Louie SG, El-Khoueiry A, Lenz HJ, Ladner RD. 2011. The dual EGFR/HER2 inhibitor lapatinib synergistically enhances the antitumor activity of the histone deacetylase inhibitor panobinostat in colorectal cancer models. Cancer Res 71:3635-3648.

Laha D, Pramanik A, Maity J, Mukherjee A, Pramanik P, Laskar A, Karmakar P. 2014. Interplay between autophagy and apoptosis mediated by copper oxide nanoparticles in human breast cancer cells MCF7. Biochim Biophys Acta 1840:1-9.

Lanz TA, Wood KM, Richter KE, Nolan CE, Becker SL, Pozdnyakov N, Martin BA, Du P, Oborski CE, Wood DE, Brown TM, Finley JE, Sokolowski SA, Hicks CD, Coffman KJ, Geoghegan KF, Brodney MA, Liston D, Tate B. 2010. Pharmacodynamics and pharmacokinetics of the gamma-secretase inhibitor PF-3084014. J Pharmacol Exp Ther 334:269-277.

Lauffer JM, Zhang T, Modlin IM. 1999. Review article: current status of gastrointestinal carcinoids. Aliment Pharmacol Ther 13:271-287.

Laurent-Puig P, Lievre A, Blons H. 2009. Mutations and response to epidermal growth factor receptor inhibitors. Clin Cancer Res 15:1133-1139.

Le XF, Pruefer F, Bast RC, Jr. 2005. HER2-targeting antibodies modulate the cyclin-dependent kinase inhibitor p27Kip1 via multiple signaling pathways. Cell Cycle 4:87-95.

Lee HK, Lund JM, Ramanathan B, Mizushima N, Iwasaki A. 2007. Autophagy-dependent viral recognition by plasmacytoid dendritic cells. Science 315:1398-1401.

Lee SH, Nam HJ, Kang HJ, Kwon HW, Lim YC. 2013. Epigallocatechin-3-gallate attenuates head and neck cancer stem cell traits through suppression of Notch pathway. Eur J Cancer 49:3210-3218.

Leibovici D, Shilo Y, Raz O, Stav K, Sandbank J, Segal M, Zisman A. 2011. Is the diagnostic yield of prostate needle biopsies affected by prostate volume? Urol Oncol.

Leonard GD, Fojo T, Bates SE. 2003. The role of ABC transporters in clinical practice. Oncologist 8:411-424.

Levine AJ. 1997. p53, the cellular gatekeeper for growth and division. Cell 88:323-331.

Li C, Lee CJ, Simeone DM. 2009. Identification of human pancreatic cancer stem cells. Methods Mol Biol 568:161-173.

Li FY, Lai MD. 2009. Colorectal cancer, one entity or three. J Zhejiang Univ Sci B 10:219-229.

Li L, Berger SH, Wyatt MD. 2004a. Involvement of base excision repair in response to therapy targeted at thymidylate synthase. Mol Cancer Ther 3:747-753.

Li Q, Kawamura K, Ma G, Iwata F, Numasaki M, Suzuki N, Shimada H, Tagawa M. 2010. Interferon-lambda induces G1 phase arrest or apoptosis in oesophageal carcinoma cells and produces anti-tumour effects in combination with anti-cancer agents. Eur J Cancer 46:180-190.

Li Q, Tang L, Roberts PC, Kraniak JM, Fridman AL, Kulaeva OI, Tehrani OS, Tainsky MA. 2008a. Interferon regulatory factors IRF5 and IRF7 inhibit growth and induce senescence in immortal Li-Fraumeni fibroblasts. Mol Cancer Res 6:770-784.

Li R, Hao Z, Liu KX. 2004b. Analysis of the quality of coding for tumors in line with International Classification of Diseases. Di Yi Jun Yi Da Xue Xue Bao 24:187, 191.

Li T, Wen H, Brayton C, Das P, Smithson LA, Fauq A, Fan X, Crain BJ, Price DL, Golde TE, Eberhart CG, Wong PC. 2007. Epidermal growth factor receptor and notch pathways participate in the tumor suppressor function of gamma-secretase. J Biol Chem 282:32264-32273.

Li WW, Li VW, Hutnik M, Chiou AS. 2012. Tumor angiogenesis as a target for dietary cancer prevention. J Oncol 2012:879623.

Li X, Lewis MT, Huang J, Gutierrez C, Osborne CK, Wu MF, Hilsenbeck SG, Pavlick A, Zhang X, Chamness GC, Wong H, Rosen J, Chang JC. 2008b. Intrinsic resistance of tumorigenic breast cancer cells to chemotherapy. J Natl Cancer Inst 100:672-679.

Li Z, Tian T, Hu X, Zhang X, Nan F, Chang Y, Lv F, Zhang M. 2013. Six1 mediates resistance to paclitaxel in breast cancer cells. Biochem Biophys Res Commun 441:538-543.

Licciulli S, Avila JL, Hanlon L, Troutman S, Cesaroni M, Kota S, Keith B, Simon MC, Pure E, Radtke F, Capobianco AJ, Kissil JL. 2013. Notch1 Is Required for Kras-Induced Lung Adenocarcinoma and Controls Tumor Cell Survival via p53. Cancer Res.

Lin L, Liu A, Peng Z, Lin HJ, Li PK, Li C, Lin J. 2011. STAT3 is necessary for proliferation and survival in colon cancer-initiating cells. Cancer Res 71:7226-7237.

Lin SS, Lai KC, Hsu SC, Yang JS, Kuo CL, Lin JP, Ma YS, Wu CC, Chung JG. 2009. Curcumin inhibits the migration and invasion of human A549 lung cancer cells through the inhibition of matrix metalloproteinase-2 and -9 and Vascular Endothelial Growth Factor (VEGF). Cancer Lett 285:127-133.

Lipinski CA, Lombardo F, Dominy BW, Feeney PJ. 2001. Experimental and computational approaches to estimate solubility and permeability in drug discovery and development settings. Adv Drug Deliv Rev 46:3-26.

Liu D, Shi M, Duan C, Chen H, Hu Y, Yang Z, Duan H, Guo N. 2013. Downregulation of Erbin in Her2-overexpressing breast cancer cells promotes cell migration and induces trastuzumab resistance. Mol Immunol 56:104-112.

Liu G, Yuan X, Zeng Z, Tunici P, Ng H, Abdulkadir IR, Lu L, Irvin D, Black KL, Yu JS. 2006. Analysis of gene expression and chemoresistance of CD133+ cancer stem cells in glioblastoma. Mol Cancer 5:67.

Liu WD, Zhang T, Wang CL, Meng HM, Song YW, Zhao Z, Li ZM, Liu JK, Pan SH, Wang WB. 2012. Sphere-forming tumor cells possess stem-like properties in human fibrosarcoma primary tumors and cell lines. Oncol Lett 4:1315-1320.

Loges S, Schmidt T, Carmeliet P. 2010. Mechanisms of resistance to anti-angiogenic therapy and development of third-generation anti-angiogenic drug candidates. Genes Cancer 1:12-25.

Lower EE, Glass E, Blau R, Harman S. 2009. HER-2/neu expression in primary and metastatic breast cancer. Breast Cancer Res Treat 113:301-306.

Lu W, de Bock GH, Schaapveld M, Baas PC, Wiggers T, Jansen L. 2011. The value of routine physical examination in the follow up of women with a history of early breast cancer. Eur J Cancer 47:676-682.

Luster AD, Leder P. 1993. IP-10, a -C-X-C- chemokine, elicits a potent thymus-dependent antitumor response in vivo. J Exp Med 178:1057-1065.

Lynch HT, de la Chapelle A. 2003. Hereditary colorectal cancer. N Engl J Med 348:919-932.

Ma J, Xia J, Miele L, Sarkar FH, Wang Z. 2013. Notch Signaling Pathway in Pancreatic Cancer Progression. Pancreat Disord Ther 3.

Ma S, Chan KW, Hu L, Lee TK, Wo JY, Ng IO, Zheng BJ, Guan XY. 2007. Identification and characterization of tumorigenic liver cancer stem/progenitor cells. Gastroenterology 132:2542-2556.

Ma S, Lee TK, Zheng BJ, Chan KW, Guan XY. 2008. CD133+ HCC cancer stem cells confer chemoresistance by preferential expression of the Akt/PKB survival pathway. Oncogene 27:1749-1758.

MacDonald BT, Tamai K, He X. 2009. Wnt/beta-catenin signaling: components, mechanisms, and diseases. Dev Cell 17:9-26.

Magee PJ, Rowland IR. 2004. Phyto-oestrogens, their mechanism of action: current evidence for a role in breast and prostate cancer. Brit J Nutr 91:513-531.

Manne U, Srivastava RG, Srivastava S. 2005. Recent advances in biomarkers for cancer diagnosis and treatment. Drug Discov Today 10:965-976.

Mannelli G, Gallo O. 2012. Cancer stem cells hypothesis and stem cells in head and neck cancers. Cancer Treat Rev 38:515-539.

Mansilla S, Llovera L, Portugal J. 2012. Chemotherapeutic targeting of cell death pathways. Anticancer Agents Med Chem 12:226-238.

Manzano A, Perez-Segura P. 2012. Colorectal cancer chemoprevention: is this the future of colorectal cancer prevention? ScientificWorldJournal 2012:327341.

Marcato P, Dean CA, Pan D, Araslanova R, Gillis M, Joshi M, Helyer L, Pan L, Leidal A, Gujar S, Giacomantonio CA, Lee PW. 2011. Aldehyde dehydrogenase activity of breast cancer stem cells is primarily due to isoform ALDH1A3 and its expression is predictive of metastasis. Stem Cells 29:32-45.

Marchal JA, Boulaiz H, Suarez I, Saniger E, Campos J, Carrillo E, Prados J, Gallo MA, Espinosa A, Aranega A. 2004. Growth inhibition, G(1)-arrest, and apoptosis in MCF-7 human breast cancer cells by novel highly lipophilic 5-fluorouracil derivatives. Invest New Drugs 22:379-389.

Marchal JA, Carrasco E, Ramirez A, Jimenez G, Olmedo C, Peran M, Agil A, Conejo-Garcia A, Cruz-Lopez O, Campos JM, Garcia MA. 2013. Bozepinib, a novel small antitumor agent, induces PKR-mediated apoptosis and synergizes with IFNalpha triggering apoptosis, autophagy and senescence. Drug Des Devel Ther 7:1301-1313.

Marie I, Smith E, Prakash A, Levy DE. 2000. Phosphorylation-induced dimerization of interferon regulatory factor 7 unmasks DNA binding and a bipartite transactivation domain. Mol Cell Biol 20:8803-8814.

Markman B, Dienstmann R, Tabernero J. 2010. Targeting the PI3K/Akt/mTOR pathway--beyond rapalogs. Oncotarget 1:530-543.

Maron R, Schechter B, Mancini M, Mahlknecht G, Yarden Y, Sela M. 2013. Inhibition of pancreatic carcinoma by homo- and heterocombinations of antibodies against EGF-receptor and its kin HER2/ErbB-2. Proc Natl Acad Sci U S A 110:15389-15394.

Martinez-Rivera M, Siddik ZH. 2012. Resistance and gain-of-resistance phenotypes in cancers harboring wild-type p53. Biochem Pharmacol 83:1049-1062.

Maugeri-Sacca M, Zeuner A, De Maria R. 2011. Therapeutic targeting of cancer stem cells. Front Oncol 1:10.

Mavaddat N, Antoniou AC, Easton DF, Garcia-Closas M. 2010. Genetic susceptibility to breast cancer. Mol Oncol 4:174-191.

McAuliffe PF, Meric-Bernstam F, Mills GB, Gonzalez-Angulo AM. 2010. Deciphering the role of PI3K/Akt/mTOR pathway in breast cancer biology and pathogenesis. Clin Breast Cancer 10 Suppl 3:S59-65.

McCullough MJ, Prasad G, Farah CS. 2010. Oral mucosal malignancy and potentially malignant lesions: an update on the epidemiology, risk factors, diagnosis and management. Aust Dent J 55 Suppl 1:61-65.

McDermott SP, Wicha MS. 2010. Targeting breast cancer stem cells. Mol Oncol 4:404-419.

McDonagh CF, Huhalov A, Harms BD, Adams S, Paragas V, Oyama S, Zhang B, Luus L, Overland R, Nguyen S, Gu J, Kohli N, Wallace M, Feldhaus MJ, Kudla AJ, Schoeberl B, Nielsen UB. 2012. Antitumor activity of a novel bispecific antibody that targets the ErbB2/ErbB3 oncogenic unit and inhibits heregulin-induced activation of ErbB3. Mol Cancer Ther 11:582-593.

Meadows KN, Bryant P, Vincent PA, Pumiglia KM. 2004. Activated Ras induces a proangiogenic phenotype in primary endothelial cells. Oncogene 23:192-200.

Mekenkamp LJ, Heesterbeek KJ, Koopman M, Tol J, Teerenstra S, Venderbosch S, Punt CJ, Nagtegaal ID. 2012. Mucinous adenocarcinomas: poor prognosis in metastatic colorectal cancer. Eur J Cancer 48:501-509.

Mendel DB, Laird AD, Xin X, Louie SG, Christensen JG, Li G, Schreck RE, Abrams TJ, Ngai TJ, Lee LB, Murray LJ, Carver J, Chan E, Moss KG, Haznedar JO, Sukbuntherng J, Blake RA, Sun L, Tang C, Miller T, Shirazian S, McMahon G, Cherrington JM. 2003. In vivo antitumor activity of SU11248, a novel tyrosine kinase inhibitor targeting vascular endothelial growth factor and platelet-derived growth factor receptors: determination of a pharmacokinetic/pharmacodynamic relationship. Clin Cancer Res 9:327-337.

Meng RD, Shelton CC, Li YM, Qin LX, Notterman D, Paty PB, Schwartz GK. 2009. gamma-Secretase inhibitors abrogate oxaliplatin-induced activation of the Notch-1 signaling pathway in colon cancer cells resulting in enhanced chemosensitivity. Cancer Res 69:573-582.

Merchant AA, Matsui W. 2010. Targeting Hedgehog--a cancer stem cell pathway. Clin Cancer Res 16:3130-3140.

Meyer O. 2009. Interferons and autoimmune disorders. Joint Bone Spine 76:464-473.

Mihatsch J, Toulany M, Bareiss PM, Grimm S, Lengerke C, Kehlbach R, Rodemann HP. 2011. Selection of radioresistant tumor cells and presence of ALDH1 activity in vitro. Radiother Oncol 99:300-306.

Miles DW, Dieras V, Cortes J, Duenne AA, Yi J, O'Shaughnessy J. 2013. First-line bevacizumab in combination with chemotherapy for HER2-negative metastatic breast cancer: pooled and subgroup analyses of data from 2447 patients. Ann Oncol 24:2773-2780.

Miller WR, Bartlett J, Brodie AM, Brueggemeier RW, di Salle E, Lonning PE, Llombart A, Maass N, Maudelonde T, Sasano H, Goss PE. 2008. Aromatase inhibitors: are there differences between steroidal and nonsteroidal aromatase inhibitors and do they matter? Oncologist 13:829-837.

Mitchison TJ. 2012. The proliferation rate paradox in antimitotic chemotherapy. Mol Biol Cell 23:1-6.

Miyamoto S, Nakanishi M, Rosenberg DW. 2013. Suppression of colon carcinogenesis by targeting Notch signaling. Carcinogenesis.

Miyazaki Y, Shibuya M, Sugawara H, Kawaguchi O, Hirsoe C. 1974. Salinomycin, a new polyether antibiotic. J Antibiot (Tokyo) 27:814-821.

Mizoue T, Inoue M, Wakai K, Nagata C, Shimazu T, Tsuji I, Otani T, Tanaka K, Matsuo K, Tamakoshi A, Sasazuki S, Tsugane S. 2008. Alcohol drinking and colorectal cancer in Japanese: a pooled analysis of results from five cohort studies. Am J Epidemiol 167:1397-1406.

Moitra K, Lou H, Dean M. 2011. Multidrug efflux pumps and cancer stem cells: insights into multidrug resistance and therapeutic development. Clin Pharmacol Ther 89:491-502.

Monsuez JJ, Charniot JC, Vignat N, Artigou JY. 2010. Cardiac side-effects of cancer chemotherapy. Int J Cardiol 144:3-15.

Moore N, Lyle S. 2011. Quiescent, slow-cycling stem cell populations in cancer: a review of the evidence and discussion of significance. J Oncol 2011.

Morin PJ, Sparks AB, Korinek V, Barker N, Clevers H, Vogelstein B, Kinzler KW. 1997. Activation of beta-catenin-Tcf signaling in colon cancer by mutations in beta-catenin or APC. Science 275:1787-1790.

Morris EJ, Jha S, Restaino CR, Dayananth P, Zhu H, Cooper A, Carr D, Deng Y, Jin W, Black S, Long B, Liu J, Dinunzio E, Windsor W, Zhang R, Zhao S, Angagaw MH, Pinheiro EM, Desai J, Xiao L, Shipps G, Hruza A, Wang J, Kelly J, Paliwal S, Gao X, Babu BS, Zhu L, Daublain P, Zhang L, Lutterbach BA, Pelletier MR, Philippar U, Siliphaivanh P, Witter D, Kirschmeier P, Bishop WR, Hicklin D, Gilliland DG, Jayaraman L, Zawel L, Fawell S, Samatar AA. 2013. Discovery of a novel ERK inhibitor with activity in models of acquired resistance to BRAF and MEK inhibitors. Cancer Discov 3:742-750.

Moserle L, Indraccolo S, Ghisi M, Frasson C, Fortunato E, Canevari S, Miotti S, Tosello V, Zamarchi R, Corradin A, Minuzzo S, Rossi E, Basso G, Amadori A. 2008. The side population of ovarian cancer cells is a primary target of IFN-alpha antitumor effects. Cancer Res 68:5658-5668.

Moskal A, Norat T, Ferrari P, Riboli E. 2007a. Alcohol intake and colorectal cancer risk: A dose-response meta-analysis of published cohort studies. International Journal of Cancer 120:664-671.

Moskal A, Norat T, Ferrari P, Riboli E. 2007b. Alcohol intake and colorectal cancer risk: a dose-response meta-analysis of published cohort studies. Int J Cancer 120:664-671.

Mulder NH, Willemse PH, Schraffordt Koops H, de Vries EG, Sleijfer DT. 1990. Dacarbazine (DTIC) and human recombinant interferon alpha 2a (Roferon) in the treatment of disseminated malignant melanoma. Br J Cancer 62:1006-1007.

Munder M, Mallo M, Eichmann K, Modolell M. 2001. Direct stimulation of macrophages by IL-12 and IL-18 - a bridge built on solid ground. Immunol Lett 75:159-160.

Munn DH, Shafizadeh E, Attwood JT, Bondarev I, Pashine A, Mellor AL. 1999. Inhibition of T cell proliferation by macrophage tryptophan catabolism. J Exp Med 189:1363-1372.

Murkies AL, Wilcox G, Davis SR. 1998. Clinical review 92 - Phytoestrogens. J Clin Endocr Metab 83:297-303.

Nagata Y, Lan KH, Zhou X, Tan M, Esteva FJ, Sahin AA, Klos KS, Li P, Monia BP, Nguyen NT, Hortobagyi GN, Hung MC, Yu D. 2004. PTEN activation contributes to tumor inhibition by trastuzumab, and loss of PTEN predicts trastuzumab resistance in patients. Cancer Cell 6:117-127.

Nahta R, Yu D, Hung MC, Hortobagyi GN, Esteva FJ. 2006. Mechanisms of disease: understanding resistance to HER2-targeted therapy in human breast cancer. Nat Clin Pract Oncol 3:269-280.

Nair R, Roden DL, Teo WS, McFarland A, Junankar S, Ye S, Nguyen A, Yang J, Nikolic I, Hui M, Morey A, Shah J, Pfefferle AD, Usary J, Selinger C, Baker LA, Armstrong N, Cowley MJ, Naylor MJ, Ormandy CJ, Lakhani SR, Herschkowitz JI, Perou CM, Kaplan W, O'Toole SA, Swarbrick A. 2013. c-Myc and Her2 cooperate to drive a stem-like phenotype with poor prognosis in breast cancer. Oncogene.

Najar AG, Pashaei-Asl R, Omidi Y, Farajnia S, Nourazarian AR. 2013. EGFR antisense oligonucleotides encapsulated with nanoparticles decrease EGFR, MAPK1 and STAT5 expression in a human colon cancer cell line. Asian Pac J Cancer Prev 14:495-498.

Nakamura M, Nagano H, Sakon M, Yamamoto T, Ota H, Wada H, Damdinsuren B, Noda T, Marubashi S, Miyamoto A, Takeda Y, Umeshita K, Nakamori S, Dono K, Monden M. 2007. Role of the Fas/FasL pathway in combination therapy with interferon-alpha and fluorouracil against hepatocellular carcinoma in vitro. J Hepatol 46:77-88.

Naujokat C, Steinhart R. 2012. Salinomycin as a drug for targeting human cancer stem cells. J Biomed Biotechnol 2012:950658.

Neumann J, Bahr F, Horst D, Kriegl L, Engel J, Luque RM, Gerhard M, Kirchner T, Jung A. 2011. SOX2 expression correlates with lymph-node metastases and distant spread in right-sided colon cancer. BMC Cancer 11:518.

Neumann J, Wehweck L, Maatz S, Engel J, Kirchner T, Jung A. 2013. Alterations in the EGFR pathway coincide in colorectal cancer and impact on prognosis. Virchows Arch.

Neuzillet C, Tijeras-Raballand A, de Mestier L, Cros J, Faivre S, Raymond E. 2014. MEK in cancer and cancer therapy. Pharmacol Ther 141:160-171.

Nielsen DL, Kumler I, Palshof JA, Andersson M. 2013. Efficacy of HER2-targeted therapy in metastatic breast cancer. Monoclonal antibodies and tyrosine kinase inhibitors. Breast 22:1-12.

Noda E, Maeda K, Inoue T, Nishihara T, Nishiguchi Y, Ohira M, Hirakawa K. 2006. Expression of genes for 5-FU-metabolizing enzymes and response to irinotecan plus 5-FU-leucovorin in colorectal cancer. Anticancer Res 26:4653-4658.

Noguchi M. 2007. Role of breast surgeons in evolution of the surgical management of breast cancer. Breast Cancer 14:1-8.

Noordhuis P, Holwerda U, Van der Wilt CL, Van Groeningen CJ, Smid K, Meijer S, Pinedo HM, Peters GJ. 2004. 5-Fluorouracil incorporation into RNA and DNA in relation to thymidylate synthase inhibition of human colorectal cancers. Ann Oncol 15:1025-1032.

Nordling CO. 1953. A new theory on cancer-inducing mechanism. Br J Cancer 7:68-72.

Nourazarian AR, Najar AG, Farajnia S, Khosroushahi AY, Pashaei-Asl R, Omidi Y. 2012. Combined EGFR and c-Src antisense oligodeoxynucleotides encapsulated with PAMAM Denderimers inhibit HT-29 colon cancer cell proliferation. Asian Pac J Cancer Prev 13:4751-4756.

Nowell PC. 1976. The clonal evolution of tumor cell populations. Science 194:23-28.

Nunez MC, Diaz-Gavilan M, Conejo-Garcia A, Cruz-Lopez O, Gallo MA, Espinosa A, Campos JM. 2008. Design, synthesis and anticancer activity against the MCF-7 cell line of benzo-fused 1,4-dihetero seven- and six-membered tethered pyrimidines and purines. Curr Med Chem 15:2614-2631.

O'Brien CA, Pollett A, Gallinger S, Dick JE. 2007. A human colon cancer cell capable of initiating tumour growth in immunodeficient mice. Nature 445:106-110.

Ojo OO, Bhadauria S, Rath SK. 2013. Dose-dependent adverse effects of salinomycin on male reproductive organs and fertility in mice. PLoS One 8:e69086.

Okumura F, Okumura AJ, Uematsu K, Hatakeyama S, Zhang DE, Kamura T. 2013. Activation of double-stranded RNA-activated protein kinase (PKR) by interferon-stimulated gene 15 (ISG15) modification down-regulates protein translation. J Biol Chem 288:2839-2847.

Ott JJ, Ullrich A, Miller AB. 2009. The importance of early symptom recognition in the context of early detection and cancer survival. Eur J Cancer 45:2743-2748.

Ottevanger PB, De Mulder PH. 2005. The quality of chemotherapy and its quality assurance. Eur J Surg Oncol 31:656-666.

Ozben T. 2006. Mechanisms and strategies to overcome multiple drug resistance in cancer. FEBS Lett 580:2903-2909.

Paez-Ribes M, Allen E, Hudock J, Takeda T, Okuyama H, Vinals F, Inoue M, Bergers G, Hanahan D, Casanovas O. 2009. Antiangiogenic therapy elicits malignant progression of tumors to increased local invasion and distant metastasis. Cancer Cell 15:220-231.

Pajonk F, Vlashi E, McBride WH. 2010. Radiation resistance of cancer stem cells: the 4 R's of radiobiology revisited. Stem Cells 28:639-648.

Palacios Eito A, Cabezas SG, Ugalde PF, del Campo ER, Romero AO, Martin Mdel M, Arjona JM, Paredes MM. 2013. Characterization and adequacy of the use of radiotherapy and its trend in time. Radiother Oncol 106:260-265.

Palmieri C, Krell J, James CR, Harper-Wynne C, Misra V, Cleator S, Miles D. 2010. Rechallenging with anthracyclines and taxanes in metastatic breast cancer. Nat Rev Clin Oncol 7:561-574.

Parkin DM, Bray F, Ferlay J, Pisani P. 2005. Global cancer statistics, 2002. CA Cancer J Clin 55:74-108.

Pasche B. 2001. Role of transforming growth factor beta in cancer. J Cell Physiol 186:153-168.

Pastrana E, Silva-Vargas V, Doetsch F. 2011. Eyes wide open: a critical review of sphere-formation as an assay for stem cells. Cell Stem Cell 8:486-498.

Patrawala L, Calhoun-Davis T, Schneider-Broussard R, Tang DG. 2007. Hierarchical organization of prostate cancer cells in xenograft tumors: the CD44+alpha2beta1+ cell population is enriched in tumor-initiating cells. Cancer Res 67:6796-6805.

Patrawala L, Calhoun T, Schneider-Broussard R, Zhou J, Claypool K, Tang DG. 2005. Side population is enriched in tumorigenic, stem-like cancer cells, whereas ABCG2+ and ABCG2- cancer cells are similarly tumorigenic. Cancer Res 65:6207-6219.

Pavlidis ET, Pavlidis TE. 2013. Role of bevacizumab in colorectal cancer growth and its adverse effects: a review. World J Gastroenterol 19:5051-5060.

Pece S, Tosoni D, Confalonieri S, Mazzarol G, Vecchi M, Ronzoni S, Bernard L, Viale G, Pelicci PG, Di Fiore PP. 2010. Biological and molecular heterogeneity of breast cancers correlates with their cancer stem cell content. Cell 140:62-73.

Peidis P, Papadakis AI, Muaddi H, Richard S, Koromilas AE. 2011. Doxorubicin bypasses the cytoprotective effects of eIF2alpha phosphorylation and promotes PKR-mediated cell death. Cell Death Differ 18:145-154.

Peltomaki P, Vasen H. 2004. Mutations associated with HNPCC predisposition -- Update of ICG-HNPCC/INSiGHT mutation database. Dis Markers 20:269-276.

Perez EA, Romond EH, Suman VJ, Jeong JH, Davidson NE, Geyer CE, Jr., Martino S, Mamounas EP, Kaufman PA, Wolmark N. 2011. Four-year follow-up of trastuzumab plus adjuvant chemotherapy for operable human epidermal growth factor receptor 2-positive breast cancer: joint analysis of data from NCCTG N9831 and NSABP B-31. J Clin Oncol 29:3366-3373.

Perez EA, Spano JP. 2012. Current and emerging targeted therapies for metastatic breast cancer. Cancer 118:3014-3025.

Perrot CY, Javelaud D, Mauviel A. 2013. Overlapping activities of TGF-beta and Hedgehog signaling in cancer: therapeutic targets for cancer treatment. Pharmacol Ther 137:183-199.

Petit T, Wilt M, Velten M, Rodier JF, Fricker JP, Dufour P, Ghnassia JP. 2010. Semi-quantitative evaluation of estrogen receptor expression is a strong predictive factor of pathological complete response after anthracycline-based neo-adjuvant chemotherapy in hormonal-sensitive breast cancer. Breast Cancer Res Treat 124:387-391.

Philchenkov A, Zavelevich M, Kroczak TJ, Los M. 2004. Caspases and cancer: mechanisms of inactivation and new treatment modalities. Exp Oncol 26:82-97.

Pierre FH, Martin OC, Santarelli RL, Tache S, Naud N, Gueraud F, Audebert M, Dupuy J, Meunier N, Attaix D, Vendeuvre JL, Mirvish SS, Kuhnle GC, Cano N, Corpet DE. 2013. Calcium and alpha-tocopherol suppress cured-meat promotion of chemically induced colon carcinogenesis in rats and reduce associated biomarkers in human volunteers. Am J Clin Nutr.

Pietras RJ, Poen JC, Gallardo D, Wongvipat PN, Lee HJ, Slamon DJ. 1999. Monoclonal antibody to HER-2/neureceptor modulates repair of radiation-induced DNA damage and enhances radiosensitivity of human breast cancer cells overexpressing this oncogene. Cancer Res 59:1347-1355.

Piva M, Domenici G, Iriondo O, Rabano M, Simoes BM, Comaills V, Barredo I, Lopez-Ruiz JA, Zabalza I, Kypta R, Vivanco MD. 2013. Sox2 promotes tamoxifen resistance in breast cancer cells. EMBO Mol Med.

Plumb JA, Finn PW, Williams RJ, Bandara MJ, Romero MR, Watkins CJ, La Thangue NB, Brown R. 2003. Pharmacodynamic response and inhibition of growth of human tumor xenografts by the novel histone deacetylase inhibitor PXD101. Mol Cancer Ther 2:721-728.

Pohl M, Stricker I, Schoeneck A, Schulmann K, Klein-Scory S, Schwarte-Waldhoff I, Hasmann M, Tannapfel A, Schmiegel W, Reinacher-Schick A. 2009. Antitumor activity of the HER2 dimerization inhibitor pertuzumab on human colon cancer cells in vitro and in vivo. J Cancer Res Clin Oncol 135:1377-1386.

Poplin EA, Benedetti JK, Estes NC, Haller DG, Mayer RJ, Goldberg RM, Weiss GR, Rivkin SE, Macdonald JS. 2005. Phase III Southwest Oncology Group 9415/Intergroup 0153 randomized trial of fluorouracil, leucovorin, and levamisole versus fluorouracil continuous infusion and levamisole for adjuvant treatment of stage III and high-risk stage II colon cancer. J Clin Oncol 23:1819-1825.

Portillo I, Idigoras I, Ojembarrena E, Arana-Arri E, Zubero MB, Pijoan JI, Lopez Urrutia A, Marques ML. 2013. [Main results of the colorectal cancer screening program in the Basque Country (Spain)]. Gac Sanit 27:358-361.

Pothlichet J, Meunier I, Davis BK, Ting JP, Skamene E, von Messling V, Vidal SM. 2013. Type I IFN triggers RIG-I/TLR3/NLRP3-dependent inflammasome activation in influenza A virus infected cells. PLoS Pathog 9:e1003256.

Pradeep CR, Kostler WJ, Lauriola M, Granit RZ, Zhang F, Jacob-Hirsch J, Rechavi G, Nair HB, Hennessy BT, Gonzalez-Angulo AM, Tekmal RR, Ben-Porath I, Mills GB, Domany E, Yarden Y. 2012. Modeling ductal carcinoma in situ: a HER2-Notch3 collaboration enables luminal filling. Oncogene 31:907-917.

Prasad CP, Rath G, Mathur S, Bhatnagar D, Ralhan R. 2009. Potent growth suppressive activity of curcumin in human breast cancer cells: Modulation of Wnt/beta-catenin signaling. Chem Biol Interact 181:263-271.

Prat A, Perou CM. 2011. Deconstructing the molecular portraits of breast cancer. Mol Oncol 5:5-23.

Price JE, Daniels LM, Campbell DE, Giavazzi R. 1989. Organ distribution of experimental metastases of a human colorectal carcinoma injected in nude mice. Clin Exp Metastasis 7:55-68.

Prince ME, Sivanandan R, Kaczorowski A, Wolf GT, Kaplan MJ, Dalerba P, Weissman IL, Clarke MF, Ailles LE. 2007. Identification of a subpopulation of cells with cancer stem cell properties in head and neck squamous cell carcinoma. Proc Natl Acad Sci U S A 104:973-978.

Puig-Vives M, Pollan M, Rue M, Osca-Gelis G, Saez M, Izquierdo A, Marcos-Gragera R. 2012. Rapid increase in incidence of breast ductal carcinoma in situ in Girona, Spain 1983-2007. Breast 21:646-651.

Puig-Vives M, Sanchez MJ, Sanchez-Cantalejo J, Torrella-Ramos A, Martos C, Ardanaz E, Chirlaque MD, Perucha J, Diaz JM, Mateos A, Machon M, Marcos-Gragera R. 2013. Distribution and prognosis of molecular breast cancer subtypes defined by immunohistochemical biomarkers in a Spanish population-based study. Gynecol Oncol 130:609-614.

Purow B. 2012. Notch inhibition as a promising new approach to cancer therapy. Adv Exp Med Biol 727:305-319.

Purton LE, Scadden DT. 2007. Limiting factors in murine hematopoietic stem cell assays. Cell Stem Cell 1:263-270.

Qiu X, Wang Z, Li Y, Miao Y, Ren Y, Luan Y. 2012. Characterization of sphere-forming cells with stem-like properties from the small cell lung cancer cell line H446. Cancer Lett 323:161-170.

Qualtrough D, Buda A, Gaffield W, Williams AC, Paraskeva C. 2004. Hedgehog signalling in colorectal tumour cells: induction of apoptosis with cyclopamine treatment. Int J Cancer 110:831-837.

Radice E, Miranda V, Bellone G. 2013. Low-doses of sequential-kinetic-activated interferon-gamma enhance the ex vivo cytotoxicity of peripheral blood natural killer cells from patients with early-stage colorectal cancer. A preliminary study. Int Immunopharmacol.

Radtke F, Clevers H. 2005. Self-renewal and cancer of the gut: two sides of a coin. Science 307:1904-1909.

Reese DM, Slamon DJ. 1997. HER-2/neu signal transduction in human breast and ovarian cancer. Stem Cells 15:1-8.

Reya T, Clevers H. 2005. Wnt signalling in stem cells and cancer. Nature 434:843-850.

Reya T, Morrison SJ, Clarke MF, Weissman IL. 2001. Stem cells, cancer, and cancer stem cells. Nature 414:105-111.

Rich JN, Bao S. 2007. Chemotherapy and cancer stem cells. Cell Stem Cell 1:353-355.

Riker AI, Glass F, Perez I, Cruse CW, Messina J, Sondak VK. 2005. Cutaneous melanoma: methods of biopsy and definitive surgical excision. Dermatol Ther 18:387-393.

Rivlin N, Brosh R, Oren M, Rotter V. 2011. Mutations in the p53 Tumor Suppressor Gene: Important Milestones at the Various Steps of Tumorigenesis. Genes Cancer 2:466-474.

Roberts E, Cossigny DA, Quan GM. 2013. The Role of Vascular Endothelial Growth Factor in Metastatic Prostate Cancer to the Skeleton. Prostate Cancer 2013:418340.

Roesch A, Fukunaga-Kalabis M, Schmidt EC, Zabierowski SE, Brafford PA, Vultur A, Basu D, Gimotty P, Vogt T, Herlyn M. 2010. A temporarily distinct subpopulation of slow-cycling melanoma cells is required for continuous tumor growth. Cell 141:583-594.

Rohan TE, Soskolne CL, Carroll KK, Kreiger N. 2007. The Canadian Study of Diet, Lifestyle, and Health: design and characteristics of a new cohort study of cancer risk. Cancer Detect Prev 31:12-17.

Roy HK, Olusola BF, Clemens DL, Karolski WJ, Ratashak A, Lynch HT, Smyrk TC. 2002. AKT proto-oncogene overexpression is an early event during sporadic colon carcinogenesis. Carcinogenesis 23:201-205.

Rusnak DW, Lackey K, Affleck K, Wood ER, Alligood KJ, Rhodes N, Keith BR, Murray DM, Knight WB, Mullin RJ, Gilmer TM. 2001. The effects of the novel, reversible epidermal growth factor receptor/ErbB-2 tyrosine kinase inhibitor, GW2016, on the growth of human normal and tumor-derived cell lines in vitro and in vivo. Mol Cancer Ther 1:85-94.

Rutkowski P, Wozniak A, Debiec-Rychter M, Kakol M, Dziewirski W, Zdzienicki M, Ptaszynski K, Jurkowska M, Limon J, Siedlecki JA. 2011. Clinical utility of the new American Joint Committee on Cancer staging system for gastrointestinal stromal tumors: current overall survival after primary tumor resection. Cancer 117:4916-4924.

Rutman RJ, Cantarow A, Paschkis KE. 1954. Studies in 2-acetylaminofluorene carcinogenesis. III. The utilization of uracil-2-C14 by preneoplastic rat liver and rat hepatoma. Cancer Res 14:119-123.

Ryan Q, Ibrahim A, Cohen MH, Johnson J, Ko CW, Sridhara R, Justice R, Pazdur R. 2008. FDA drug approval summary: lapatinib in combination with capecitabine for previously treated metastatic breast cancer that overexpresses HER-2. Oncologist 13:1114-1119.

Rybak AP, He L, Kapoor A, Cutz JC, Tang D. 2011. Characterization of sphere-propagating cells with stem-like properties from DU145 prostate cancer cells. Biochim Biophys Acta 1813:683-694.

Sainsbury R. 2013. The development of endocrine therapy for women with breast cancer. Cancer Treat Rev 39:507-517.

Samuel CE. 2001. Antiviral actions of interferons. Clin Microbiol Rev 14:778-809, table of contents.

Sanchez MJ, Payer T, De Angelis R, Larranaga N, Capocaccia R, Martinez C. 2010. Cancer incidence and mortality in Spain: estimates and projections for the period 1981-2012. Ann Oncol 21 Suppl 3:iii30-36.

Sanchez P, Hernandez AM, Stecca B, Kahler AJ, DeGueme AM, Barrett A, Beyna M, Datta MW, Datta S, Ruiz i Altaba A. 2004. Inhibition of prostate cancer proliferation by interference with SONIC HEDGEHOG-GLI1 signaling. Proc Natl Acad Sci U S A 101:12561-12566.

Santiago RJ, Wu L, Harris E, Fox K, Schultz D, Glick J, Solin LJ. 2004. Fifteen-year results of breast-conserving surgery and definitive irradiation for Stage I and II breast carcinoma: the University of Pennsylvania experience. Int J Radiat Oncol Biol Phys 58:233-240.

Sarasin A, Kauffmann A. 2008. Overexpression of DNA repair genes is associated with metastasis: a new hypothesis. Mutat Res 659:49-55.

Sato A, Ohtsuki M, Hata M, Kobayashi E, Murakami T. 2006. Antitumor activity of IFN-lambda in murine tumor models. J Immunol 176:7686-7694.

Scaltriti M, Rojo F, Ocana A, Anido J, Guzman M, Cortes J, Di Cosimo S, Matias-Guiu X, Ramon y Cajal S, Arribas J, Baselga J. 2007. Expression of p95HER2, a truncated form

of the HER2 receptor, and response to anti-HER2 therapies in breast cancer. J Natl Cancer Inst 99:628-638.

Schellens JH. 2007. Capecitabine. Oncologist 12:152-155.

Schueller G, Schueller-Weidekamm C, Helbich TH. 2008. Accuracy of ultrasound-guided, large-core needle breast biopsy. Eur Radiol 18:1761-1773.

Sellers AH. 1971. The clinical classification of malignant tumours: the TNM system. Can Med Assoc J 105:836 passim.

Sen GC. 2001. Viruses and interferons. Annu Rev Microbiol 55:255-281.

Seshasai SR, Kaptoge S, Thompson A, Di Angelantonio E, Gao P, Sarwar N, Whincup PH, Mukamal KJ, Gillum RF, Holme I, Njolstad I, Fletcher A, Nilsson P, Lewington S, Collins R, Gudnason V, Thompson SG, Sattar N, Selvin E, Hu FB, Danesh J. 2011. Diabetes mellitus, fasting glucose, and risk of cause-specific death. N Engl J Med 364:829-841.

Shannon J, Douglas-Jones AG, Dallimore NS. 2001. Conversion to core biopsy in preoperative diagnosis of breast lesions: is it justified by results? J Clin Pathol 54:762-765.

Sharma S. 2009. Tumor markers in clinical practice: General principles and guidelines. Indian J Med Paediatr Oncol 30:1-8.

Sherr CJ. 1996. Cancer cell cycles. Science 274:1672-1677.

Shervington A, Lu C. 2008. Expression of multidrug resistance genes in normal and cancer stem cells. Cancer Invest 26:535-542.

Shiozaki A, Bai XH, Shen-Tu G, Moodley S, Takeshita H, Fung SY, Wang Y, Keshavjee S, Liu M. 2012. Claudin 1 mediates TNFalpha-induced gene expression and cell migration in human lung carcinoma cells. PLoS One 7:e38049.

Sigal A, Rotter V. 2000. Oncogenic mutations of the p53 tumor suppressor: the demons of the guardian of the genome. Cancer Res 60:6788-6793.

Singh BN, Kumar D, Shankar S, Srivastava RK. 2012. Rottlerin induces autophagy which leads to apoptotic cell death through inhibition of PI3K/Akt/mTOR pathway in human pancreatic cancer stem cells. Biochem Pharmacol 84:1154-1163.

Singh SK, Hawkins C, Clarke ID, Squire JA, Bayani J, Hide T, Henkelman RM, Cusimano MD, Dirks PB. 2004. Identification of human brain tumour initiating cells. Nature 432:396-401.

Skof E, Rebersek M, Hlebanja Z, Ocvirk J. 2009. Capecitabine plus Irinotecan (XELIRI regimen) compared to 5-FU/LV plus Irinotecan (FOLFIRI regimen) as neoadjuvant treatment for patients with unresectable liver-only metastases of metastatic colorectal cancer: a randomised prospective phase II trial. BMC Cancer 9:120.

Smith I, Procter M, Gelber RD, Guillaume S, Feyereislova A, Dowsett M, Goldhirsch A, Untch M, Mariani G, Baselga J, Kaufmann M, Cameron D, Bell R, Bergh J, Coleman R, Wardley A, Harbeck N, Lopez RI, Mallmann P, Gelmon K, Wilcken N, Wist E, Sanchez Rovira P, Piccart-Gebhart MJ. 2007. 2-year follow-up of trastuzumab after adjuvant chemotherapy in HER2-positive breast cancer: a randomised controlled trial. Lancet 369:29-36.

Soung YH, Lee JW, Kim SY, Jang J, Park YG, Park WS, Nam SW, Lee JY, Yoo NJ, Lee SH. 2005. CASPASE-8 gene is inactivated by somatic mutations in gastric carcinomas. Cancer Res 65:815-821.

Stal O, Perez-Tenorio G, Akerberg L, Olsson B, Nordenskjold B, Skoog L, Rutqvist LE. 2003. Akt kinases in breast cancer and the results of adjuvant therapy. Breast Cancer Res 5:R37-44.

Stanton BZ, Peng LF, Maloof N, Nakai K, Wang X, Duffner JL, Taveras KM, Hyman JM, Lee SW, Koehler AN, Chen JK, Fox JL, Mandinova A, Schreiber SL. 2009. A small molecule that binds Hedgehog and blocks its signaling in human cells. Nat Chem Biol 5:154-156.

Stark GR, Kerr IM, Williams BR, Silverman RH, Schreiber RD. 1998. How cells respond to interferons. Annu Rev Biochem 67:227-264.

Storms RW, Trujillo AP, Springer JB, Shah L, Colvin OM, Ludeman SM, Smith C. 1999. Isolation of primitive human hematopoietic progenitors on the basis of aldehyde dehydrogenase activity. Proc Natl Acad Sci U S A 96:9118-9123.

Stuurman FE, Nuijen B, Beijnen JH, Schellens JH. 2013. Oral anticancer drugs: mechanisms of low bioavailability and strategies for improvement. Clin Pharmacokinet 52:399-414.

Su HM, Hsieh PH, Chen HF. 2010. A maternal high n-6 fat diet with fish oil supplementation during pregnancy and lactation in rats decreases breast cancer risk in the female offspring. J Nutr Biochem 21:1033-1037.

Sun S, Wang Z. 2010. ALDH high adenoid cystic carcinoma cells display cancer stem cell properties and are responsible for mediating metastasis. Biochem Biophys Res Commun 396:843-848.

Swain SM, Kim SB, Cortes J, Ro J, Semiglazov V, Campone M, Ciruelos E, Ferrero JM, Schneeweiss A, Knott A, Clark E, Ross G, Benyunes MC, Baselga J. 2013. Pertuzumab, trastuzumab, and docetaxel for HER2-positive metastatic breast cancer (CLEOPATRA study): overall survival results from a randomised, double-blind, placebo-controlled, phase 3 study. Lancet Oncol 14:461-471.

Takaoka A, Yanai H, Kondo S, Duncan G, Negishi H, Mizutani T, Kano S, Honda K, Ohba Y, Mak TW, Taniguchi T. 2005. Integral role of IRF-5 in the gene induction programme activated by Toll-like receptors. Nature 434:243-249.

Takebe N, Harris PJ, Warren RQ, Ivy SP. 2011. Targeting cancer stem cells by inhibiting Wnt, Notch, and Hedgehog pathways. Nat Rev Clin Oncol 8:97-106.

Talora C, Campese AF, Bellavia D, Pascucci M, Checquolo S, Groppioni M, Frati L, von Boehmer H, Gulino A, Screpanti I. 2003. Pre-TCR-triggered ERK signalling-dependent downregulation of E2A activity in Notch3-induced T-cell lymphoma. EMBO Rep 4:1067-1072.

Tang Y, Mackey J, Lai R, Ghosh S, Santos C, Graham K, Damaraju S, Pasdar M, Li L. 2013. Quantitative proteomic analysis of HER2 normal and overexpressing MCF-7 breast cancer cells revealed proteomic changes accompanied with HER2 gene amplification. J Proteomics 91:200-209.

Taub DD, Lloyd AR, Conlon K, Wang JM, Ortaldo JR, Harada A, Matsushima K, Kelvin DJ, Oppenheim JJ. 1993. Recombinant human interferon-inducible protein 10 is a chemoattractant for human monocytes and T lymphocytes and promotes T cell adhesion to endothelial cells. J Exp Med 177:1809-1814.

Tirino V, Desiderio V, Paino F, De Rosa A, Papaccio F, La Noce M, Laino L, De Francesco F, Papaccio G. 2013. Cancer stem cells in solid tumors: an overview and new approaches for their isolation and characterization. FASEB J 27:13-24.

Todaro M, Alea MP, Di Stefano AB, Cammareri P, Vermeulen L, Iovino F, Tripodo C, Russo A, Gulotta G, Medema JP, Stassi G. 2007. Colon cancer stem cells dictate tumor growth and resist cell death by production of interleukin-4. Cell Stem Cell 1:389-402.

Tostar U, Malm CJ, Meis-Kindblom JM, Kindblom LG, Toftgard R, Unden AB. 2006. Deregulation of the hedgehog signalling pathway: a possible role for the PTCH and SUFU genes in human rhabdomyoma and rhabdomyosarcoma development. J Pathol 208:17-25.

Ulloa F, Itasaki N, Briscoe J. 2007. Inhibitory Gli3 activity negatively regulates Wnt/beta-catenin signaling. Curr Biol 17:545-550.

Upreti M, Koonce NA, Hennings L, Chambers TC, Griffin RJ. 2010. Pegylated IFN-alpha sensitizes melanoma cells to chemotherapy and causes premature senescence in endothelial cells by IRF-1 mediated signaling. Cell Death Dis 1:e67.

Van Camp JK, Beckers S, Zegers D, Van Hul W. 2013. Wnt Signaling and the Control of Human Stem Cell Fate. Stem Cell Rev.

van Dongen JA, Bartelink H, Fentiman IS, Lerut T, Mignolet F, Olthuis G, van der Schueren E, Sylvester R, Winter J, van Zijl K. 1992. Randomized clinical trial to assess the value of breast-conserving therapy in stage I and II breast cancer, EORTC 10801 trial. J Natl Cancer Inst Monogr:15-18.

van Nes J, Chan A, van Groningen T, van Sluis P, Koster J, Versteeg R. 2013. A NOTCH3 transcriptional module induces cell motility in neuroblastoma. Clin Cancer Res 19:3485-3494.

Varnat F, Duquet A, Malerba M, Zbinden M, Mas C, Gervaz P, Ruiz i Altaba A. 2009. Human colon cancer epithelial cells harbour active HEDGEHOG-GLI signalling that is essential for tumour growth, recurrence, metastasis and stem cell survival and expansion. EMBO Mol Med 1:338-351.

Veeck J, Dahl E. 2012. Targeting the Wnt pathway in cancer: the emerging role of Dickkopf-3. Biochim Biophys Acta 1825:18-28.

Vivanco I, Sawyers CL. 2002. The phosphatidylinositol 3-Kinase AKT pathway in human cancer. Nat Rev Cancer 2:489-501.

Vogel CL, Cobleigh MA, Tripathy D, Gutheil JC, Harris LN, Fehrenbacher L, Slamon DJ, Murphy M, Novotny WF, Burchmore M, Shak S, Stewart SJ, Press M. 2002. Efficacy and safety of trastuzumab as a single agent in first-line treatment of HER2-overexpressing metastatic breast cancer. J Clin Oncol 20:719-726.

Voronkov A, Krauss S. 2013. Wnt/beta-catenin signaling and small molecule inhibitors. Curr Pharm Des 19:634-664.

Vriens BE, Aarts MJ, de Vries B, van Gastel SM, Wals J, Smilde TJ, van Warmerdam LJ, de Boer M, van Spronsen DJ, Borm GF, Tjan-Heijnen VC. 2013. Doxorubicin/cyclophosphamide with concurrent versus sequential docetaxel as neoadjuvant treatment in patients with breast cancer. Eur J Cancer 49:3102-3110.

Walsh N, Kennedy S, Larkin A, Corkery B, O'Driscoll L, Clynes M, Crown J, O'Donovan N. 2013. EGFR and HER2 inhibition in pancreatic cancer. Invest New Drugs 31:558-566.

Wang Z, Sicinski P, Weinberg RA, Zhang Y, Ravid K. 1996. Characterization of the mouse cyclin D3 gene: exon/intron organization and promoter activity. Genomics 35:156-163.

Wang Z, Wang T, Bian J. 2013. Association between MDR1 C3435T polymorphism and risk of breast cancer. Gene.

Warnakulasuriya S, Sutherland G, Scully C. 2005. Tobacco, oral cancer, and treatment of dependence. Oral Oncol 41:244-260.

Watters JW, Cheng C, Majumder PK, Wang R, Yalavarthi S, Meeske C, Kong L, Sun W, Lin J, Heyer J, Ware C, Winter C, Reilly JF, Demuth T, Clark S, Chiu MI, Robinson MO, Kohl N, Kannan K. 2009. De novo discovery of a gamma-secretase inhibitor response signature using a novel in vivo breast tumor model. Cancer Res 69:8949-8957.

Wei P, Walls M, Qiu M, Ding R, Denlinger RH, Wong A, Tsaparikos K, Jani JP, Hosea N, Sands M, Randolph S, Smeal T. 2010. Evaluation of selective gamma-secretase inhibitor PF-03084014 for its antitumor efficacy and gastrointestinal safety to guide optimal clinical trial design. Mol Cancer Ther 9:1618-1628.

Weinberg RA. 1989. Oncogenes, antioncogenes, and the molecular bases of multistep carcinogenesis. Cancer Res 49:3713-3721.

Weinberg RA. 1996a. How cancer arises. Sci Am 275:62-70.

Weinberg RA. 1996b. The molecular basis of carcinogenesis: understanding the cell cycle clock. Cytokines Mol Ther 2:105-110.

Weng AP, Ferrando AA, Lee W, Morris JPt, Silverman LB, Sanchez-Irizarry C, Blacklow SC, Look AT, Aster JC. 2004. Activating mutations of NOTCH1 in human T cell acute lymphoblastic leukemia. Science 306:269-271.

Wesierska-Gadek J, Gueorguieva M, Wojciechowski J, Horky M. 2004. Cell cycle arrest induced in human breast cancer cells by cyclin-dependent kinase inhibitors: a comparison of the effects exerted by roscovitine and olomoucine. Pol J Pharmacol 56:635-641.

Wheatley K, Ives N, Hancock B, Gore M, Eggermont A, Suciu S. 2003. Does adjuvant interferon-alpha for high-risk melanoma provide a worthwhile benefit? A meta-analysis of the randomised trials. Cancer Treat Rev 29:241-252.

Wicha MS, Liu S, Dontu G. 2006. Cancer stem cells: an old idea--a paradigm shift. Cancer Res 66:1883-1890; discussion 1895-1886.

Williams GH, Stoeber K. 2012. The cell cycle and cancer. J Pathol 226:352-364.

Williams JA, Guicherit OM, Zaharian BI, Xu Y, Chai L, Wichterle H, Kon C, Gatchalian C, Porter JA, Rubin LL, Wang FY. 2003. Identification of a small molecule inhibitor of the hedgehog signaling pathway: effects on basal cell carcinoma-like lesions. Proc Natl Acad Sci U S A 100:4616-4621.

Winau F, Westphal O, Winau R. 2004. Paul Ehrlich--in search of the magic bullet. Microbes Infect 6:786-789.

Winzer KJ, Sauer R, Sauerbrei W, Schneller E, Jaeger W, Braun M, Dunst J, Liersch T, Zedelius M, Brunnert K, Guski H, Schmoor C, Schumacher M. 2004. Radiation therapy after breast-conserving surgery; first results of a randomised clinical trial in patients with low risk of recurrence. Eur J Cancer 40:998-1005.

Wong NK, Fuller M, Sung S, Wong F, Karsan A. 2012. Heterogeneity of breast cancer stem cells as evidenced with Notch-dependent and Notch-independent populations. Cancer Med 1:105-113.

Wong RS. 2011. Apoptosis in cancer: from pathogenesis to treatment. J Exp Clin Cancer Res 30:87.

Wright MH, Calcagno AM, Salcido CD, Carlson MD, Ambudkar SV, Varticovski L. 2008. Brca1 breast tumors contain distinct CD44+/CD24- and CD133+ cells with cancer stem cell characteristics. Breast Cancer Res 10:R10.

Wu WK, Wang XJ, Cheng AS, Luo MX, Ng SS, To KF, Chan FK, Cho CH, Sung JJ, Yu J. 2013. Dysregulation and crosstalk of cellular signaling pathways in colon carcinogenesis. Crit Rev Oncol Hematol 86:251-277.

Wu X, Pandolfi PP. 2001. Mouse models for multistep tumorigenesis. Trends Cell Biol 11:S2-9.

Wu Y, Fan Y, Xue B, Luo L, Shen J, Zhang S, Jiang Y, Yin Z. 2006. Human glutathione S-transferase P1-1 interacts with TRAF2 and regulates TRAF2-ASK1 signals. Oncogene 25:5787-5800.

Wu YL, Zhang S, Wang GR, Chen YP. 2008. Expression transformation of claudin-1 in the process of gastric adenocarcinoma invasion. World J Gastroenterol 14:4943-4948.

Wyman C, Kanaar R. 2006. DNA double-strand break repair: all's well that ends well. Annu Rev Genet 40:363-383.

Xia W, Gerard CM, Liu L, Baudson NM, Ory TL, Spector NL. 2005. Combining lapatinib (GW572016), a small molecule inhibitor of ErbB1 and ErbB2 tyrosine kinases, with therapeutic anti-ErbB2 antibodies enhances apoptosis of ErbB2-overexpressing breast cancer cells. Oncogene 24:6213-6221.

Xu D, Erickson S, Szeps M, Gruber A, Sangfelt O, Einhorn S, Pisa P, Grander D. 2000. Interferon alpha down-regulates telomerase reverse transcriptase and telomerase activity in human malignant and nonmalignant hematopoietic cells. Blood 96:4313-4318.

Xu JW, Li QQ, Tao LL, Cheng YY, Yu J, Chen Q, Liu XP, Xu ZD. 2011. Involvement of EGFR in the promotion of malignant properties in multidrug resistant breast cancer cells. Int J Oncol 39:1501-1509.

Xue L, Fletcher GC, Tolkovsky AM. 1999. Autophagy is activated by apoptotic signalling in sympathetic neurons: an alternative mechanism of death execution. Mol Cell Neurosci 14:180-198.

Yabuuchi S, Pai SG, Campbell NR, de Wilde RF, De Oliveira E, Korangath P, Streppel MM, Rasheed ZA, Hidalgo M, Maitra A, Rajeshkumar NV. 2013. Notch signaling pathway targeted therapy suppresses tumor progression and metastatic spread in pancreatic cancer. Cancer Lett 335:41-51.

Yamaguchi N, Oyama T, Ito E, Satoh H, Azuma S, Hayashi M, Shimizu K, Honma R, Yanagisawa Y, Nishikawa A, Kawamura M, Imai J, Ohwada S, Tatsuta K, Inoue J, Semba K, Watanabe S. 2008. NOTCH3 signaling pathway plays crucial roles in the proliferation of ErbB2-negative human breast cancer cells. Cancer Res 68:1881-1888.

Yanai Y, Sanou O, Yamamoto K, Yamauchi H, Ikegami H, Kurimoto M. 2002. The anti-tumor activities of interferon (IFN)-alpha in chronic myelogenous leukaemia (CML)-derived cell lines depends on the IFN-alpha subtypes. Cancer Lett 185:173-179.

Yang CF, Peng LX, Huang TJ, Yang GD, Chu QQ, Liang YY, Cao X, Xie P, Zheng LS, Huang HB, Cai MD, Huang JL, Liu RY, Zhu ZY, Qian CN, Huang BJ. 2013. Cancer stem-like

cell characteristics induced by EB virus-encoded LMP1 contribute to radioresistance in nasopharyngeal carcinoma by suppressing the p53-mediated apoptosis pathway. Cancer Lett.

Yang G, Cao K, Wu L, Wang R. 2004a. Cystathionine gamma-lyase overexpression inhibits cell proliferation via a H2S-dependent modulation of ERK1/2 phosphorylation and p21Cip/WAK-1. J Biol Chem 279:49199-49205.

Yang X, Klein R, Tian X, Cheng HT, Kopan R, Shen J. 2004b. Notch activation induces apoptosis in neural progenitor cells through a p53-dependent pathway. Dev Biol 269:81-94.

Yang XH, Sladek TL, Liu X, Butler BR, Froelich CJ, Thor AD. 2001. Reconstitution of caspase 3 sensitizes MCF-7 breast cancer cells to doxorubicin- and etoposide-induced apoptosis. Cancer Res 61:348-354.

Yarden Y. 2001. The EGFR family and its ligands in human cancer. signalling mechanisms and therapeutic opportunities. Eur J Cancer 37 Suppl 4:S3-8.

Yin W, Jiang Y, Shen Z, Shao Z, Lu J. 2011. Trastuzumab in the adjuvant treatment of HER2-positive early breast cancer patients: a meta-analysis of published randomized controlled trials. PLoS One 6:e21030.

Yoon CH, Lee ES, Lim DS, Bae YS. 2009. PKR, a p53 target gene, plays a crucial role in the tumor-suppressor function of p53. Proc Natl Acad Sci U S A 106:7852-7857.

Yoon YH, Cho KS, Hwang JJ, Lee SJ, Choi JA, Koh JY. 2010. Induction of lysosomal dilatation, arrested autophagy, and cell death by chloroquine in cultured ARPE-19 cells. Invest Ophthalmol Vis Sci 51:6030-6037.

Yoshikawa R, Kusunoki M, Yanagi H, Noda M, Furuyama JI, Yamamura T, Hashimoto-Tamaoki T. 2001. Dual antitumor effects of 5-fluorouracil on the cell cycle in colorectal carcinoma cells: a novel target mechanism concept for pharmacokinetic modulating chemotherapy. Cancer Res 61:1029-1037.

Youlden DR, Cramb SM, Dunn NA, Muller JM, Pyke CM, Baade PD. 2012. The descriptive epidemiology of female breast cancer: an international comparison of screening, incidence, survival and mortality. Cancer Epidemiol 36:237-248.

Yu H, Rohan T. 2000. Role of the insulin-like growth factor family in cancer development and progression. J Natl Cancer Inst 92:1472-1489.

Yuan SS, Lee SY, Chen G, Song M, Tomlinson GE, Lee EY. 1999. BRCA2 is required for ionizing radiation-induced assembly of Rad51 complex in vivo. Cancer Res 59:3547-3551.

Zeng ZJ, Li JH, Zhang YJ, Zhao ST. 2013. Optimal combination of radiotherapy and endocrine drugs in breast cancer treatment. Cancer Radiother 17:208-214.

Zhang L, Li L, Jiao M, Wu D, Wu K, Li X, Zhu G, Yang L, Wang X, Hsieh JT, He D. 2012a. Genistein inhibits the stemness properties of prostate cancer cells through targeting Hedgehog-Gli1 pathway. Cancer Lett 323:48-57.

Zhang M, Rosen JM. 2006. Stem cells in the etiology and treatment of cancer. Curr Opin Genet Dev 16:60-64.

Zhang X, Zhang S, Liu Y, Liu J, Ma Y, Zhu Y, Zhang J. 2012b. Effects of the combination of RAD001 and docetaxel on breast cancer stem cells. Eur J Cancer 48:1581-1592.

Zhao Y, Jian W, Gao W, Zheng YX, Wang YK, Zhou ZQ, Zhang H, Wang CJ. 2013. RNAi silencing of c-Myc inhibits cell migration, invasion, and proliferation in HepG2 human hepatocellular carcinoma cell line: c-Myc silencing in hepatocellular carcinoma cell. Cancer Cell Int 13:23.

Zhi QM, Chen XH, Ji J, Zhang JN, Li JF, Cai Q, Liu BY, Gu QL, Zhu ZG, Yu YY. 2011. Salinomycin can effectively kill ALDH(high) stem-like cells on gastric cancer. Biomed Pharmacother 65:509-515.

Zhou J, Li P, Xue X, He S, Kuang Y, Zhao H, Chen S, Zhi Q, Guo X. 2013a. Salinomycin induces apoptosis in cisplatin-resistant colorectal cancer cells by accumulation of reactive oxygen species. Toxicol Lett 222:139-145.

Zhou S, Schuetz JD, Bunting KD, Colapietro AM, Sampath J, Morris JJ, Lagutina I, Grosveld GC, Osawa M, Nakauchi H, Sorrentino BP. 2001. The ABC transporter Bcrp1/ABCG2

is expressed in a wide variety of stem cells and is a molecular determinant of the side-population phenotype. Nat Med 7:1028-1034.

Zhou X, Hao Q, Liao JM, Liao P, Lu H. 2013b. Ribosomal protein S14 negatively regulates c-Myc activity. J Biol Chem 288:21793-21801.

Zitvogel L, Apetoh L, Ghiringhelli F, Kroemer G. 2008. Immunological aspects of cancer chemotherapy. Nat Rev Immunol 8:59-73.

Zitzmann K, Brand S, Baehs S, Goke B, Meinecke J, Spottl G, Meyer H, Auernhammer CJ. 2006. Novel interferon-lambdas induce antiproliferative effects in neuroendocrine tumor cells. Biochem Biophys Res Commun 344:1334-1341.

IX. GLOSSARY

5-FU: 5-fluorouracilo

ADH: Alcohol Deshidrogenasa

ADN: Acido Desoxirribonucleico

AJCC: American Joint Committee on Cancer

ALDH: Aldehído Deshidrogenasa

AMV: Avian Myeloblastosis Virus

APBI: Accelerated Partial Breast Irradiation

APC: Adenomatous Polyposis Coli

APS: Ammonium Persulfate

ARN_m: Acido Ribonucleico Mensajero

ATCC: American Type Culture Collection

ATP: Adenosin Trifosfato

BAA: BODIPY-aminoacetato

BAAA: BODIPY-aminoacetaldehido

CI_{50}: Inhibitory Concentration 50

CQ: Cloroquina

CSCs: Cancer Stem Cells

CT: Tomografía Computerizada

D.O: Densidad Optica

DAVID: Database Annotation, Visualization and Integrated Discovery

DEAB: Dietilbenzaldehido

DHH: Desert HH

DMEM: Dulbecco's Modified Eagle's Medium

DMN: Dimetilnitrosamina

DMSO: Dimetilsulfoxido

DVL: Dishevelled

EDTA: Ethylenediaminetetraacetic Acid

EGF: Epidermal Growth Factor

EGFR: Epidermal Growth Factor Receptor

EPIC: European Prospective Investigation into Cancer and Nutrition

ER: Receptores de Estrógenos

ERK: Extracellular Signal-RegulatedKinases

FACS: Fluorescence-activated Cell Sorting

FBS: Foetal Bovine Serum

FDA: Food and Drug Administration

FdUMP: 5´-fluoro-2´-desoxiuridina-5´-monofosfato

FdUTP: 5-fluoro-2´-desoxiuridina-5´-trifosfato

FGF: Fibroblast Growth Factor

FITC: Fluorescein Isothiocyanate

FLIP: FLICE-like Inhibitory Protein

FUTP: 5-fluorouridina-5´-trifosfato

Fz: Frizzled

Fz: Frizzled

GFP: Green Fluorescent Protein

GSK-3β: Glycogen Synthase Kinase- 3β

HER-2: Human Epidermal Growth Factor Receptor 2

Hh: Hedgehog

HIF-1: Hypoxia-Inducible Factor 1

HNPCC: Cáncer de Colon Hereditario sin Poliposis

HS: Horse Serum

IAPs: Inhibitor of Apoptosis Proteins

IFN: Interferon

IGF: Factor de Crecimiento Relacionado con la Insulina

IGF-1: Insulin-Like Growth Factor-1

IHH: Indian HH

ILN: Interleukina

INE: Instituto Nacional de Estadística

IPA: Ingenuity Pathway Analysis

IT: Indice Terapeutico

IU: Internationa Unit

JAK: Janus Kinases

JNK: c-Jun N-terminal Kinase

LC3: Microtubule-associated protein 1A/1B-light chain 3

LRP: Low Density Lipoprotein Receptor Related Protein

M: Mock

MAPK: Mitogen Activated Protein Kinase

MEFs: Mouse embryonic fibroblasts

mTOR: Mammalian Target of Rapamycin

NNAL: 4-(metilnitrosamino)-1-(3-piridil)-1-butanol

NNK: 4-(metilnitrosamino)-1-(3-piridil)-1-butanona

NNN: N´-nitrosonornicotina

OMS: Organizacion Mundial de la Salud

PAF: Poliposis Adenomatosa Familiar

PARP-1:Poly(ADP-Ribose) Polymerase1

PBS: Phosphate-Buffered Saline

PCR: Polymerase Chain Reaction

PET: Tomografía mediante Emisión de Positrones

Pgp: Glicoproteína P

PI: Propidium Iodide

PI3K: Phosphatidylinositol 3-Kinase

PKC: Protein Kinase C

PKC-δ: Proteína Quinasa C-delta

PKR: Proteína Quinasa dependiente de ARN_{ds}

PLCγ: Phospholipase C Gamma

Ptch: Patched

PTEN: Phosphatase and Tensin homolog

RMN: Resonancia Magnética Nuclear

ROS: Especies Reactivas del Oxígeno

Rpm: Revoluciones por minuto

RT-qPCR: Real-time Reverse-Transcription PCR

SC: Stem Cells

SDS: Sodium Dodecyl Sulfate

SHBG: Hormona Sexual de Unión a la Globulina

SHH: Sonic HH

Smo: Smoothened

SNPs: Single Nucleotide Polymorphisms

SPECT: Tomografía Computarizada de Emisión Monofotónica

STAT: Signal Transducers and Activators of Transcription

TCF4: T Cell Transcription Factor 4

TEMED:N,N,N′,N′Tetramethylethylene diamine

TGF-β: Transforming Growth Factor-β

TLRs: Toll-Like Receptors

UE: Union Europea

US: Ultrasonidos

UVA: Ultraviolet Radiation A

UVA: Ultraviolet Radiation B

VEGF: Vascular Endothelial Growth Factor

WBI: Whole breast irradiation

WHO: World Health Organization

OTHER STUDIES IN WHICH THE PHD STUDENT HAS PARTICIPATED

- María A. García, Esther Carrasco, Alberto Ramírez, Gema Jiménez, Elena López-Ruiz, Macarena Perán, Manuel Picón, Joaquín Campos, Houria Boulaiz and Juan Antonio Marchal. Apoptosis as a Therapeutic Target in Cancer and Cancer Stem Cells: Novel Strategies and Futures Perspectives. Libro: Apoptosis and Medicine. ISBN: 978-953-51-0701-9. InTech - Open Access Company. 2012

- Boulaiz H, Alvarez PJ, Prados J, Marchal J, Melguizo C, Carrillo E, Peran M, Rodriguez F, Ramirez A, Ortiz R, Aranega A. 2011. gef Gene Expression in MCF-7 Breast Cancer Cells is Associated with a Better Prognosis and Induction of Apoptosis by p53-Mediated Signaling Pathway. Int J Mol Sci 12:7445-7458.

- Kimatrai M, Conejo-Garcia A, Ramirez A, Andreolli E, Da Silveira-Gomes A, Garcia MA, Aranega A, Marchal JA, Campos JM. 2011. Synthesis and anticancer activity of the (R,S)-benzofused 1,5-oxathiepine moiety tethered to purines through alkylidenoxy linkers. ChemMedChem 6:1854-1859.

- Conejo-Garcia A, Garcia-Rubino ME, Marchal JA, Nunez MC, Ramirez A, Cimino S, Garcia MA, Aranega A, Gallo MA, Campos JM. 2011. Synthesis and anticancer activity of (RS)-9-(2,3-dihydro-1,4-benzoxaheteroin-2-ylmethyl)-9H-purines. Eur J Med Chem 46:3795-3801.

- Boulaiz H, Alvarez PJ, Ramirez A, Marchal JA, Prados J, Rodriguez-Serrano F, Peran M, Melguizo C, Aranega A. 2011. Nanomedicine: application areas and development prospects. Int J Mol Sci 12:3303-3321.

- Macarena Peran, Fernando Rodriguez-Serrano, Houria Boulaiz, Juan Antonio Marchal, Elena Lopez, Manuel Picón, Ana R. Rama, Raúl Ortiz, Alberto Ramirez and Antonia Aranega. Fluorescence Recovery after Photobleaching. Libro: Cell Movement: New Research Trends. ISBN: 978-1-60692-570-6. Nova Science Publishers, Inc., 2009.

-.

ANNEX OF ARTICLES INCLUDED IN THIS THESIS

Supplementary information

Anti-proliferative Activity of 2,6-Dichloro-9- or 7-(Ethoxycarbonylmethyl)-9*H*-or 7*H*-Purines against Several Human Solid Tumour Cell Lines

Fátima Morales,[a,1] Alberto Ramirez,[b,c,1] Ana Conejo-García,[a] Cynthia Morata,[b] Juan A. Marchal,[b] Joaquín M. Campos,[a,*]

[a]*Departamento de Química Farmacéutica y Orgánica, Facultad de Farmacia, c/ Campus de Cartuja s/n, 18071 Granada (Spain).*

[b]*Instituto de Biopatología y Medicina Regenerativa (IBIMER); Departamento de Anatomía y Embriología Humana, Facultad de Medicina, Avenida de Madrid s/n, 18071 Granada (Spain).*

[c]*Departamento de Ciencias de la Salud, Facultad de Ciencias Experimentales y de la Salud, Paraje de las Lagunillas s/n, 23071 Jaén (Spain).*

[1]*These authors contributed equally to this work*

Contents

European Journal of Medicinal Chemistry 46 (2011) 249–258

Contents lists available at ScienceDirect

European Journal of Medicinal Chemistry

journal homepage: http://www.elsevier.com/locate/ejmech

Original article

New (*RS*)-benzoxazepin-purines with antitumour activity: The chiral switch from (*RS*)-2,6-dichloro-9-[1-(*p*-nitrobenzenesulfonyl)-1,2,3,5-tetrahydro-4,1-benzoxazepin-3-yl]-9*H*-purine

Luisa C. López-Cara [a], Ana Conejo-García [a], Juan A. Marchal [b], Giuseppe Macchione [a], Olga Cruz-López [a], Houria Boulaiz [b], María A. García [b,c], Fernando Rodríguez-Serrano [b], Alberto Ramírez [b], Carlos Cativiela [d], Ana I. Jiménez [d], Juan M. García-Ruiz [e], Duane Choquesillo-Lazarte [e], Antonia Aránega [b], Joaquín M. Campos [a,*]

[a] *Departamento de Química Farmacéutica y Orgánica, Facultad de Farmacia, c/ Campus de Cartuja s/n, 18071 Granada, Spain*
[b] *Instituto de Biopatología y Medicina Regenerativa (IBIMER), Departamento de Anatomía y Embriología Humana, Facultad de Medicina, Avenida de Madrid s/n, 18071 Granada, Spain*
[c] *Unidad de Investigación, Hospital Universitario Virgen de las Nieves, Granada, Spain*
[d] *Departamento de Química Orgánica y Química Física, Facultad de Ciencias, Universidad de Zaragoza, 50009 Zaragoza, Spain*
[e] *Laboratorio de Estudios Cristalográficos, IACT, CSIC-Universidad de Granada, Av. del Conocimiento s/n, P.T. Ciencias de la Salud, 18100 Armilla, Granada, Spain*

ARTICLE INFO

Article history:
Received 14 September 2010
Received in revised form
27 October 2010
Accepted 8 November 2010
Available online 3 December 2010

Keywords:
Antitumour
Benzoxazepine
2,6-Disubstituted purine
Homochiral
MCF-7
Microwave
Seven-membered ring

ABSTRACT

Completing an SAR study, a series of (*RS*)-6-substituted-7- or 9-(1,2,3,5-tetrahydro-4,1-benzoxazepine-3-yl)-7*H* or 9*H*-purines has been prepared under microwave-assisted conditions. Their antiproliferative activities on MCF-7 and MDA-MB-231 cancerous cell lines are presented, being the majority of the IC_{50} values below 1 μM. The most active compound (*RS*)-2,6-dichloro-9-[1-(*p*-nitrobenzenesulfonyl)-1,2,3,5-tetrahydro-4,1-benzoxazepin-3-yl]-9*H*-purine (**14**) presents an IC_{50} of 0.166 μM against the human cancerous cell line MDA-MB-231. Compound **14** was the most selective against the human breast adenocarcinoma MCF-7 and MDA-MB-231 cancer cell lines (Therapeutic Indexes, TIs = 5.1 and 11.0, respectively) in relation to the normal one MCF-10A. (*RS*)-**14** was resolved into its enantiomers. Both enantiomers are equally potent, but more potent than the corresponding racemic mixture. (*R*)-**14** induces apoptosis against MCF-7 up to 52.50% of cell population after 48 h, being more potent than the clinical-used drug paclitaxel (43%). (*RS*)-**14** induces no acute toxicity in mice after two weeks of treatment.

1. Introduction

With more than 10 million new cases each year cancer is at present one of the most devastating diseases worldwide with an immense affliction burden not only for affected individuals, their relatives and friends but also representing heavy challenges to health care systems [1]. In the year 2000, cancer was responsible for 12% of the nearly 56 million deaths worldwide and in many countries this percentage is even higher with more than a quarter of deaths attributable to cancer. Moreover, it is expected that cancer rates can further increase by 50% to 15 million new cases in the year 2020, mainly due to steadily ageing populations in both developed and developing countries [2].

In recent years, many studies have shown an association between cell-cycle regulation and cancer inasmuch as the cell-cycle inhibitors are being considered as a weapon for the management of cancer [3]. Ultimately a great level of interest has arisen in the G_0/G_1 phase regulatory molecules such as cyclin D1, CdkIs, and p53 as potential therapeutic targets in diseases where control of inappropriate cellular proliferation would be a therapeutic benefit [4].

Apoptosis is an essential physiological process throughout the life of multi-cellular organisms important in the development and in the maintenance of tissue homeostasis. Apoptosis is involved in controlling the cell number and proliferation during embryogenesis, deletion of activated lymphocytes at the end of the immune response, elimination of self-reactive lymphocytes, in controlled destruction of damaged, aged, infected, transformed, and other harmful cells [5,6]. Zivny et al. have recently reviewed the apoptotic pathways, molecules involved in the cross-talk between individual apoptosis pathways,

* Corresponding author. Tel.: +34 958 243848; fax: +34 958 243845.
E-mail address: jmcampos@ugr.es (J.M. Campos).

0223-5234/$ – see front matter © 2010 Elsevier Masson SAS. All rights reserved.
doi:10.1016/j.ejmech.2010.11.011

apoptosis regulation as well as mechanisms of action of conventional anticancer drugs and new promising agents, which trigger directly or indirectly apoptosis of hematologic cancer cells [7].

We have reported the synthesis and anticancer activities of compounds **1**–**3**, **5**–**6** [8] and *trans*-**7** [9] (Chart 1). In all the cases, the linkage between the 5-fluorouracil (5-FU) moiety and the seven-membered ring was carried out through its $N-1$ atom.

The structural nature of **6** implies that this compound cannot be considered as a 5-FU prodrug and we suspected that neither would the remaining compounds (**1**–**3**, **5**–**7**) be 5-FU prodrugs [10]. The effects of the uracil benzo-fused seven-membered *O*,*N*-acetal **4** were investigated in the MCF-7 human breast cancer cell line. The expression of cell-cycle-related proteins (cyclin D1, and p53) was also explored to investigate the potential mechanisms of the G_0/G_1 arrest activity of **4** [10]. In addition, the expression levels of CDKIs, such as p21Waf1/Cip1 and p27Kip1, were examined in MCF-7 cells [10].

We have reported that compounds **8** and **9**, with a thymine linked to a seven-membered ring (Chart 2) exhibited *in vitro* antiproliferative activities (12.74 ± 4.79 and 30.05 ± 0.71 μM, respectively) against the MCF-7 cell line [11].

Moreover, the uracil *O*,*N*-acetals **10**–**13** (Chart 3) derived from the tetrahydrobenzoxazepine moiety, whose syntheses were reported [12], show *in vitro* antiproliferative activities against the MCF-7 human breast cancer cell line in the micromolar range [13].

Taken together, the antiproliferative activities of the naturally occurring pyrimidine compounds **8**–**13** are an outstanding fact that has not been previously reported in bibliography. Therefore these compounds may serve as prototypes for the development of even more potent structures, endowed with a new mechanism of action. Once the alkylated pyrimidine derivatives had been studied, the shift was made to the more lipophilic purine ones [14]. Herein we will report the synthesis and antiproliferative activities of purine derivatives **14**–**24** (Chart 4) against the cancerous MCF-7 and MDA-MB-231 human breast cancer cell lines and the corresponding normal one (MCF-10A) to define the *in vitro* TI as a measure of the selectivity. From a structural point of view, the compounds studied herein differ from others previously reported [13] by the addition of an extra halogen or PhS- groups on the purine ring. Finally the most active racemic compound was resolved and the antiproliferative activity of its enantiomers was measured.

Modern drug discovery relies on high speed organic synthesis. Microwave-assisted organic synthesis [15–21] is proving to be instrumental for the rapid synthesis of compounds with new and improved biological activities [22,23]. We previously investigated the Vorbrüggen condensation in microwave-assisted organic synthesis [24]. Microwave advantage is chiefly the quick access to the target molecules as well as the better yield obtained in the only isomer formed making the purification processes much easier.

2. Results and discussion

2.1. Chemistry

2.1.1. Synthesis of derivatives

Preparation of the *O*,*N*-acetals **14**–**17** was achieved by the microwave-assisted Vorbrüggen one-pot condensation of the cyclic acetals **25** and **26** [25] and the commercially available purine bases 6-chloro-, 6-bromo- and 2,6-dichloro-purines, using chlorotrimethylsilane (TMSCl), 1,1,1,3,3,3-hexamethyldisilazane (HMDS) and tin(IV) chloride as the Lewis acid in anhydrous acetonitrile. The reaction mixture was microwave-irradiated at a temperature of 140 °C or 160 °C for 5 min (Scheme 1). Compounds **27** and **28** were isolated from the reactions and the acyclic *O*,*N*-acetal **23** was also obtained in the synthesis of **14**. Traces of the *N*-7′ regioisomer **24** were detected in the synthesis of **15**. The following modifications were carried out on **15**: a) selective nucleophilic substitution of the chorine atom at position 6 of the purine ring using NaI and trifluoroacetic acid (TFA) to yield **18**; b) reduction of the nitro group with $SnCl_2$ to give rise to **19** and **20**; and c) the treatment with the PhSH to produce **21** and **22** (see Experimental Part for details).

2.1.2. Other products in the reaction between acetals *25* and *26* and purines

Compounds **27** and **28** were obtained along with the cyclic and acyclic *O*,*N*-acetals in the reaction of purines with **25** and **26**, respectively. Their importance lies in the information that they provide on the mechanism of the reaction with purines as none of these olefins have

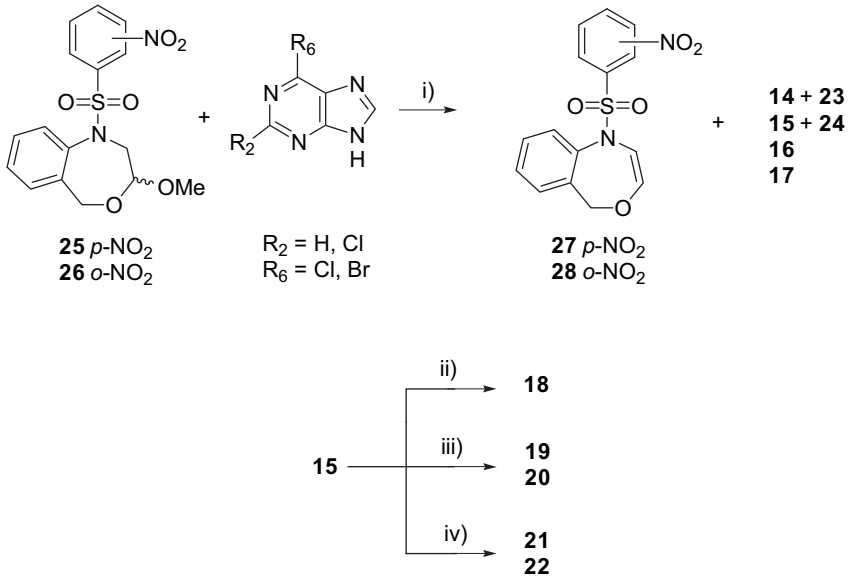

Scheme 1. Reagents and conditions: i) purine, TMSCl, HMDS, $SnCl_4$ (1 M solution in CH_2Cl_2), 140 or 160 °C, microwave, 5 min; ii) NaI, TFA, butanone, −15 °C, 6 h; iii) $SnCl_2 \cdot 2H_2O$, EtOH, reflux, 2 h; iv) PhSH, K_2CO_3, DMF, rt, 4 h.

been isolated in the corresponding reactions with uracil or 5-FU [12]. Although it could have been thought that the formation of the seven-membered sulfonenamides **27** and **28** was simply due to an elimination of methanol from the cyclic *O,O*-acetals **25** and **26**, our previous results reported on the acyclic *O,N*-acetals 6-chloro-7-{2-[*N*-(2-hydroxymethylphenyl)-2- or 4-nitrobenzenesulfonamide]-1-methoxyethyl}-7*H*-purines clearly support a more complicated reaction mechanism [26].

Compounds **27** and **28** could have been originated in a process which shared the reaction mechanism with the *N*-7″ → *N*-9″ transformation, *via* elimination of the purine ring after its activation as a leaving group by the coordination of the Lewis acid to one of its electron-rich positions. This elimination would be easier for the highest energy *N*-7″ regioisomers than for the more stable *N*-9″ ones. The formation of the cyclic olefin would be justified by the resonance of the final electronic system.

According to an elimination mechanism, loss of the purine ring would lead to the oxocarbenium ions **29** and **30**, which could either attack nucleophile positions of the purine giving rise to the formation of the *N*-9″ *O,N*-acetals (**14**–**17**), or eliminate one β proton in relation to the O^+ atom, with formation of a double bond to give **27** and **28** (Scheme 2). The progress of the cationic intermediate in one way or another would depend on the speed of each process.

2.1.3. Homochiral drugs

The issue of drug chirality is now a major theme in the design and development of new drugs, underpinned by a new understanding of the role of molecular recognition in many pharmacologically relevant events. In general, three methods are utilized for the production of a chiral drug: the chiral pool, separation of racemates, and asymmetric synthesis. Although the use of chiral drugs predates modern medicine, only since the 1980's has there been a significant increase in the development of chiral pharmaceutical drugs. An important commercial reason is that as patents on racemic drugs expire, pharmaceutical companies have the opportunity to extend patent coverage through development of the chiral switch enantiomers with desired bioactivity [27].

2.1.4. Resolution of (RS)-14 into its two enantiomers

(*RS*)-9-[1-(*p*-Nitrobenzenesulfonyl)-1,2,3,5-tetrahydro-4,1-benzoxazepin-3-yl]-2,6-dichloro-9*H*-purine (**14**) is resolved into its two enantiomers: [(*R*)-**14**: $[\alpha]^{25}_{D} = -43.6$ (c = 0.22, THF), and (*S*)-**14**: $[\alpha]^{25}_{D} = +41.0$ (c = 0.23, THF)] using a semipreparative column CHIRALPAK® and a mixture of hexane/*t*-BuOMe/*i*PrOH as eluant [28]. The details for the X-ray data for enantiomer (*S*)-**14** are shown in the Supporting Information Section.

2.2. Biological activities

Table 1 shows the antiproliferative activity (IC_{50} values) for **14**–**24** and **27**, **28**. All the compounds were first assayed as antiproliferative agents against the human breast adenocarcinoma cell line MCF-7 (p53 wild-type and ras mutated). The seven most active compounds (**14, 15, 18**–**20**, and **23**–**24**) were selected to be further assayed on the human breast cancer cell line MDA-MB-231, which has high levels of mutant p53, the most commonly mutated gene in human cancer. Additionally, we used a non-cancerous human mammary epithelial cell line (MCF-10A), in order to study the therapeutic index against breast cancer.

It must be pointed out that from the twenty IC_{50} values against the two cancerous cell lines, the majority of the IC_{50} values were below 1 μM. As shown in Table 1, all compounds were more active as antiproliferative agents against MDA-MB-231 than against the MCF-7 human breast cancer cell line, except for the acyclic derivative **23**, whose antiproliferative effect remains the same in both cancer cell lines. The $IC_{50} = 0.166$ μM for compound **14** against the

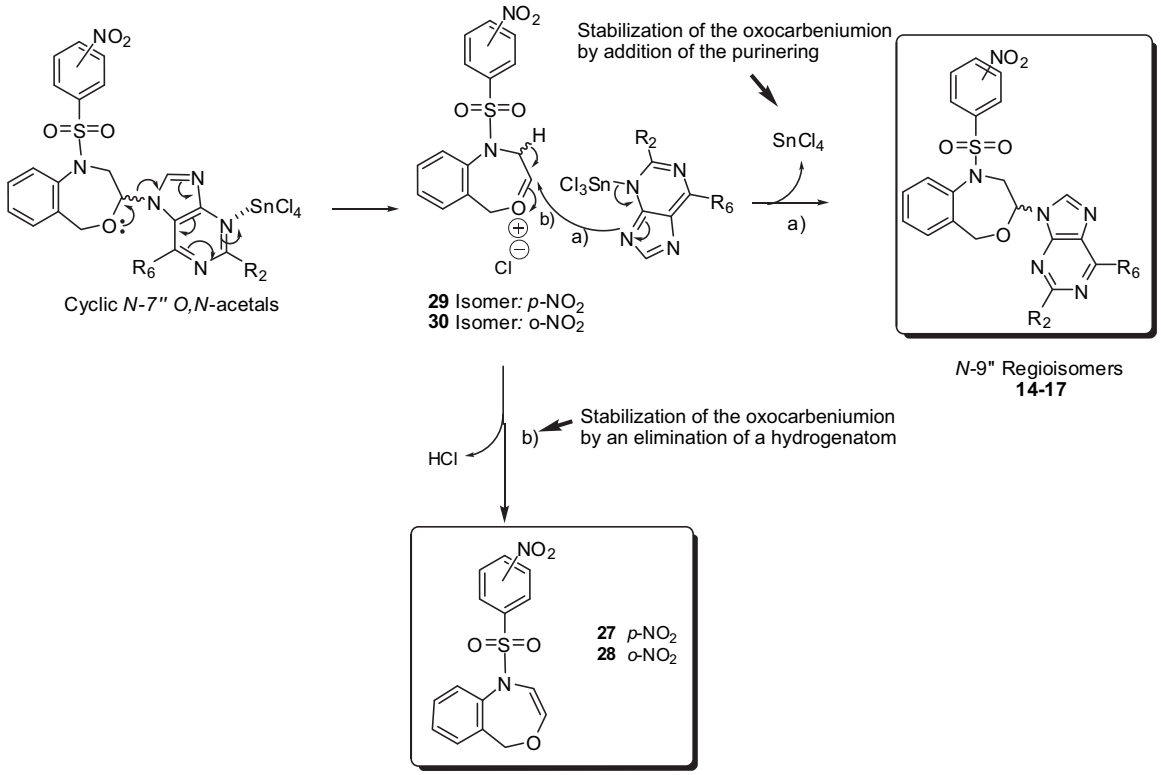

Scheme 2. Mechanism proposed for the formation of 1,5-dihydro-4,1-benzoxazepines **27** and **28** from cyclic *N*-7″ *O,N*-acetals.

Table 1
Antiproliferative activities[a] for compounds **14**–**24** against the cancerous cell lines MCF-7 and MDA-MB-231, and the non-cancerous cell line MCF-10A.

Compound	IC_{50} MCF-7 (μM)	IC_{50} MDA-MB-231 (μM)	IC_{50} MCF-10A (μM)
14	0.355 ± 0.011	0.166 ± 0.063	1.825 ± 0.503
15	0.383 ± 0.027	0.280 ± 0.006	1.530 ± 0.198
16	1.226 ± 0.348	N.D.[b]	N.D.[b]
17	3.618 ± 0.273	N.D.[b]	N.D.[b]
18	0.610 ± 0.043	0.256 ± 0.002	0.351 ± 0.020
19	0.820 ± 0.050	0.467 ± 0.017	1.520 ± 0.498
20	1.530 ± 0.040	0.487 ± 0.006	1.233 ± 0.217
21	9.710 ± 0.380	N.D.[b]	N.D.[b]
22	13.85 ± 1.790	N.D.[b]	N.D.[b]
23	0.355 ± 0.122	0.409 ± 0.074	1.863 ± 0.050
24	0.990 ± 0.090	0.318 ± 0.066	1.265 ± 0.163
5-FU[c]	4.32 ± 0.020	N.D.[b]	N.D.[b]

[a] All experiments were conducted in duplicate and gave similar results. The data are means ± SEM of three independent determinations. The treatment time was 48 h.
[b] N.D. = Not determined.
[c] Taken from Ref. [14].

human cancerous cell line MDA-MB-231 stands out over the rest of the values (Fig. 1).

A comparison between the cancerous cell lines (MCF-7 and MDA-MB-231) and the corresponding normal one (MCF-10A) was established in an intent to define the *in vitro* therapeutic index as a measure of the selectivity. The *in vitro* therapeutic index (TI) of a drug is defined as the ratio of the toxic dose to the therapeutic dose (*In vitro* TI = IC_{50} non-tumour cell line/IC_{50} tumour cell line) [29]. TI was better for compounds **14**, **15** and **23** against both cancer cell lines with values up to 11.0, 5.50 and 4.55, respectively against MDA-MB-231 cell line. 2,6-Dichloro derivatives **14** and **23** were the most selective compounds against the human breast adenocarcinoma MCF-7 cancer cell line (TIs = 5.1 and 5.2, respectively) in relation to the normal one. The iodine derivative **18** showed the most toxic effect against the non-tumour MCF-10A human mammary epithelial cell line (Table 2, Fig. 1).

2.2.1. *In vitro cytotoxic activities*

When the homochiral forms were analyzed we found differences in the IC_{50} values between (*S*)-**14** and (*R*)-**14** enantiomers, although no differences in activity were found between the two enantiomers against the MDA-MB-231 cell line. However both enantiomers present higher antiproliferative activity than the

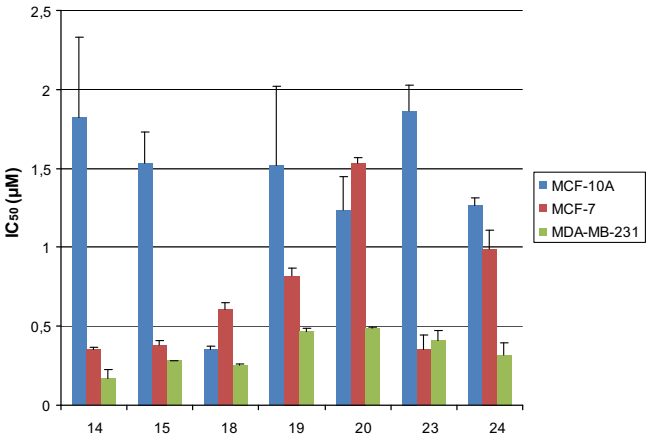

Fig. 1. Comparison between antiproliferative activities for the most representative compounds against the cancerous cell lines MCF-7 and MDA-MB-231, and the non-cancerous cell line MCF-10A.

Table 2
Therapeutic indexes for the most representative compounds.

Compound	Therapeutic index (TI)	
	MCF-7	MDA-MB-231
14	5.14	11.0
15	4.00	5.50
18	0.57	1.37
19	1.85	3.25
20	0.80	2.53
23	5.25	4.55
24	1.27	4.00

racemic compound showing the greatest differences against MCF-7 cells. (*S*)-**14** shows higher antitumour activity, up to twice that of (*R*)-**14** in the MCF-7 cell line. Studies with other compounds showed similar results with more potency in cytotoxicity in an enantiomer in comparison with the racemate. This enantioselective cytotoxicity indicates that the enantiomers of some chiral drugs may differ both quantitatively and qualitatively in their biological activity [30,31]. Moreover, enantiomers can posses minimal *in vitro* but a dramatic *in vivo* chiral dependency in their antitumour activities [32,33] (Table 3).

2.2.2. *Selection of compounds to study the cell cycle*

Once the antitumour activity of compounds was determined against the different breast cell lines, we carried out a selection between those that showed a great cytotoxic effect against MCF-7, including (*R*)-**14** and (*S*)-**14**, in order to determine their influence on the several cell-cycle phases. In this study we have included drugs used in clinic against breast cancer, such 5-FU and paclitaxel, with a known mechanism of action at the level of cell cycle.

2.2.3. *Cell-cycle analysis*

In order to analyze if the antitumour effects of the drugs involve changes in cell-cycle distribution, the non-tumour cell line MCF-10A and the breast cancer cell lines MCF-7 and MDA-MB-231 were treated with the compounds during 48 h and then analyzed by flow cytometry (Supporting Information Tables 1–3). The non-accumulation in a specific phase was detected during treatment with the drugs in most of the cell lines analyzed in comparison with control-DMSO-treated cells. Only the (*R*)-**14** enantiomer was able to induce in MDA-MB-231 cells an accumulation in both G_0/G_1 and G_2/M phases with the consequently significant decreased in the S phase. Also an accumulation in the phase G_2/M was detected in MCF-7-**18** treated cells. Treatment with 5-FU and paclitaxel, as have been described previously [34], induced accumulation in the S or G_2/M phases depending on the cell line analyzed. Similar data were obtained when cell lines were treated for 24 h with 0.5 mM mimosine to synchronize the cells in the G_1/S phase (data not shown). These results indicate that compounds inhibited all phases of the cell cycle, probably through the inhibition of protein synthesis as it has been proved with other antitumour drugs [35].

Table 3
Antiproliferative activities of (*RS*)-**14** and its enantiomers against the cancerous cell lines MCF-7 and MDA-MB-231.

Compound	MCF-7 (μM)	MDA-MB-231 (μM)
14	0.355 ± 0.011	0.166 ± 0.063
(*R*)-**14**	0.19 ± 0.001	0.11 ± 0.001
(*S*)-**14**	0.10 ± 0.001	0.11 ± 0.001

All experiments were conducted in duplicate and gave similar results. The data are means ± SEM of three independent determinations.

2.2.4. Apoptosis assay

Finally, to determine if the observed growth inhibition was due to apoptosis, both flow cytometry and confocal microscopy studies were carried out. The cells were treated with the IC_{50} values of compounds and stained using Annexin V and propidium iodide (PI) at 24 and 48 h post-drug treatment. Apoptosis assays were accomplished in the MCF-7 human breast cancer cell line, where the demonstration of programmed cell death by known apoptosis-inducing agents has proven difficult and only few cytotoxic agents act preferentially through an apoptotic mechanism in human breast cancer cells [36,37]. Paclitaxel (TAXOL®) induced programmed cell death of up to 43% of the cell population. Simultaneous staining with annexin V-FITC and the PI non-vital dye made it possible to distinguish between early apoptosis (stained positive for annexin V-FITC and negative for PI), and late apoptosis or cell death (stained positive for both annexin V-FITC and PI). In MCF-7 control-DMSO cultures neither early nor late apoptosis were detected after 24 h or 48 h. Similarly, compounds did not induce apoptosis after 24 h of treatment (Supporting Information, Table 4). In contrast, MCF-7 cells treated during 48 h with the novel compounds showed a significant increase of early apoptotic cells in relation to the control culture with percentages varying from 13.93% in cells treated with **24** to 43.30% and 41.99% after treatment with **23** and (*R*)-**14**, respectively. The percentage of late apoptotic cells also increased in MCF-7 cells treated with the drugs in comparison with control-DMSO-treated cells (Table 5 Supporting Information). It should be noted that levels of early apoptosis induced by (*R*)-**14** were almost double in comparison with the corresponding racemic compound **14,** which may explain the enantioselective antiproliferative activity shown by this enantiomer. These high apoptotic percentages shown by (*R*)-**14** are consistent with the G_1 and G_2/M arrest since cells exposed to specific agents typically enter apoptosis from a given phase of the cell cycle [10,36,38,39]. Differences in cytotoxicity, cell-cycle analysis or apoptotic levels between (*R*)-**14** and (*S*)-**14** suggest distinct signalling pathways as has been shown with other antitumour enantiomers [40]. Moreover, the amount of cells undergoing apoptosis in response to the compounds may likely have been higher than these values, due to the fact that only adherent cells were stained and counted. Representative results for the MCF-7 cells at 48 h of treatments are shown in Fig. 2A.

The effects of compounds on the pattern of cell death were also confirmed by confocal microscopy after staining with FITC-conjugated annexin V and the nuclear non-vital stain PI. MCF-7 cells treated with compounds showed several staining patterns (Fig. 2B). Some cells displayed an intense FITC staining located at the plasma membrane and a nucleus with intensely PI-labeled marginated chromatin, suggesting that they were in the course of apoptosis. Other cells showed a peculiar staining pattern, because they exhibited nuclei with the same features observed in true apoptotic cells and, at the same time, cytoplasms homogeneously stained for annexin V. In fact, the FITC staining was located not only at the cell surface, but also within the cytoplasm (Fig. 2B). Therefore, these cells were considered as aponecrotic cells as previously has been established [41]. In addition, patches of localised partially condensed chromatin were found in other cells abutted along the inner part of the nuclear membrane (Fig. 2B). In the control cultures, most of the cells turned out to be negative for both staining except for some dying cells with the staining features of apoptosis (data not shown). The present data support the effect of the compounds in some of the series of steps of the apoptotic process where a wide range of intermediate morphological and biochemical types of cell death occur [38,42].

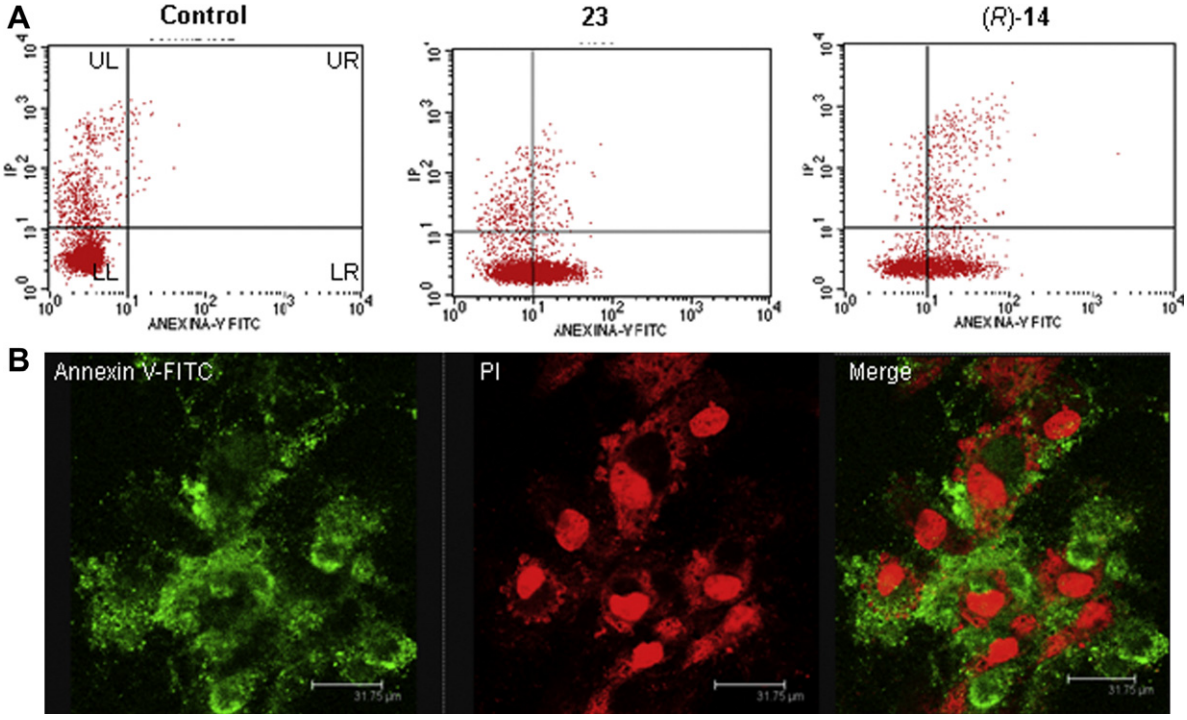

Fig. 2. Apoptosis induction in the MCF-7 human breast cancer cell line after treatment for 48 h with the compounds. (A) Representative panels of cytometry analysis for control cells treated with 0.5% DMSO alone, **23** and (*R*)-**14**. In each panel, lower left quadrant (LL) shows viable cells which are negative for both annexin V-FITC and PI, lower right (LR) shows annexin V positive cells which are in the early stage of apoptosis, upper left (UL) shows only PI positive cells which are dead, and upper right (UR) shows both annexin V and PI positive, which are in the stage of late apoptosis. (B) Confocal microscopy analysis using simultaneous staining with annexin V-FITC (green) and PI (red) in MCF-7 after treatment with **23**. (For interpretation of the references to colour in this figure legend, the reader is referred to the web version of this article).

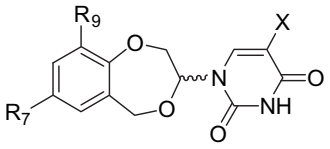

1 $R_7 = R_9 = H$, X = F
2 R_7 = OMe; R_9 = H; X = F
3 R_7 = H; R_9 = OMe; X = F
4 $R_7 = R_9 = H$; X = H

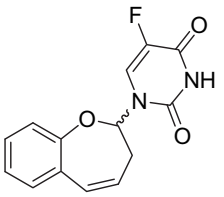

5

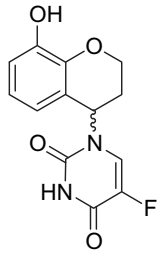

6

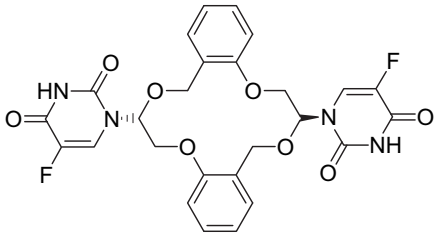

7

Chart 1.

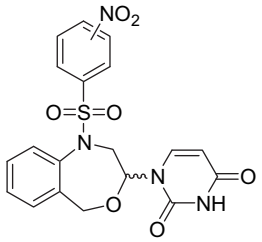

10 *ortho* isomer; IC_{50}: 45.17± 0.48 μM
12 *para* isomer; IC_{50}: 39.78±2.60 μM

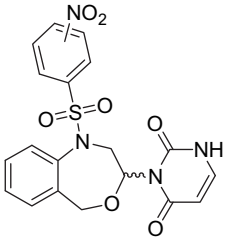

11 *ortho* isomer; IC_{50}: 50.90±3.87 μM
13 *para* isomer; IC_{50}: 44.28± 4.65 μM

Chart 3.

2.2.5. In vivo toxicity

Toxicity was determined selecting (*RS*)-**14,** which was the most *in vitro* cytotoxic compound against MCF-7 cells. We examined the acute-toxicity profile of (*RS*)-**14** in BALB/c mice when it was administered in a single i.p. bolus injection ($n = 25$) at dose levels of 50, 75, 100, 150 and 200 mg/kg or *via* gavage ($n = 25$) in a single p.o. bolus at dose levels of 0.05, 0.5, 5 and 50 mg/kg. (*RS*)-**14** was nontoxic to BALB/c mice even at the highest i.p. bolus dose of 200 mg/kg and p.o. bolus dose of 50 mg/kg after 2 weeks. Control mice ($n = 10$; 5 mice for the i.p. group and 5 mice for the p.o. group) were treated with vehicle alone. All 50 (*RS*)-**14**-treated mice remained healthy and gained weight throughout the 15-day observation period, with no evidence of morbidity.

3. Conclusion

The anticarcinogenic potency of the target molecules is reported against one non-tumour cell line and two cancerous ones. The most active compound (**14**) presents an IC_{50} of 166 nM, being the most potent structure so far reported. These results provide promising information for further development of potent antiproliferative agents. Compound **14** induces no acute toxicity in mice after 2 weeks of treatment. Compound **14** and its enantiomers associated with the inhibition of cancer cell proliferation caused in MCF-7 and MDA-MB-231 cells would make them very attractive agents, opening a new strategy in cancer chemotherapy using similar compounds endowed with potent antitumour activities with future clinical application in breast cancer. At present, studies are being carried out to determine the mechanism of action at the molecular level of the most active compounds.

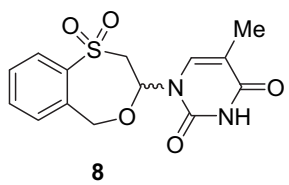

8

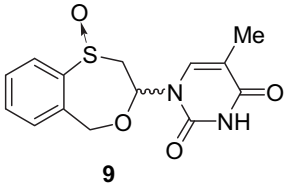

9

Chart 2.

4. Experimental protocols

4.1. Chemistry

Melting points were taken in open capillaries on an Electrothermal melting point apparatus and are uncorrected. Nuclear magnetic resonance spectra were recorded on a 400 MHz ^1H and 100 MHz ^{13}C NMR Varian NMR-System-TM 400 or 300 MHz ^1H and 75 MHz ^{13}C NMR Varian Inova-TM spectrometers at ambient temperature. Chemical shifts (δ) are quoted in parts per million (ppm) and are referenced to the residual solvent peak. Signals are designated as follows: s, singlet; d, doublet; dd, doublet of doublets; ddd, double doublet of doublets; dt, doublet of triplets; t, triplet; pt, pseudotriplet; m, multiplet. High-resolution liquid secondary ion mass spectra (HR LSIMS) were carried out on a VG AutoSpec Q high-resolution mass spectrometer (Fisons Instruments). Small scale microwave-assisted synthesis was carried out in an Initiator 2.0 single-mode microwave instrument producing controlled irradiation at 2.450 GHz (Biotage AB, Uppsala). Reaction time refers to hold time at 160 °C or 140 °C, not to total irradiation time. The temperature was measured with an IR sensor on the outside of the reaction vessel. Anhydrous acetonitrile was purchased from VWR International Eurolab. 6-Chloropurine, 6-bromopurine and 2,6-dichloropurine were purchased from Aldrich. Analyses indicated by the symbols of the elements or functions were within ±0.4% of the theoretical values.

4.1.1. General procedures for the preparation of the substituted purine O,N-acetals

A suspension of **25** or **26** and the corresponding purine base in anhydrous acetonitrile (5 mL/mmol) was prepared under argon atmosphere and cooled to 0 °C. At this temperature, TMSCl, HMDS and a 1.0 M solution of $SnCl_4$ in CH_2Cl_2 were added subsequently. The temperature was allowed to rise to 10 °C before microwave irradiating at 140 °C or 160 °C for 5 min. The reactions were quenched by cooling (ice/water bath) and by addition of distilled water. The pH was fixed to 7–8 with a saturated $NaHCO_3$ solution and the aqueous phase extracted with CH_2Cl_2 and EtOAc. The combined organic layers were dried (Na_2SO_4), filtered and evaporated. The residues were purified by flash chromatography under

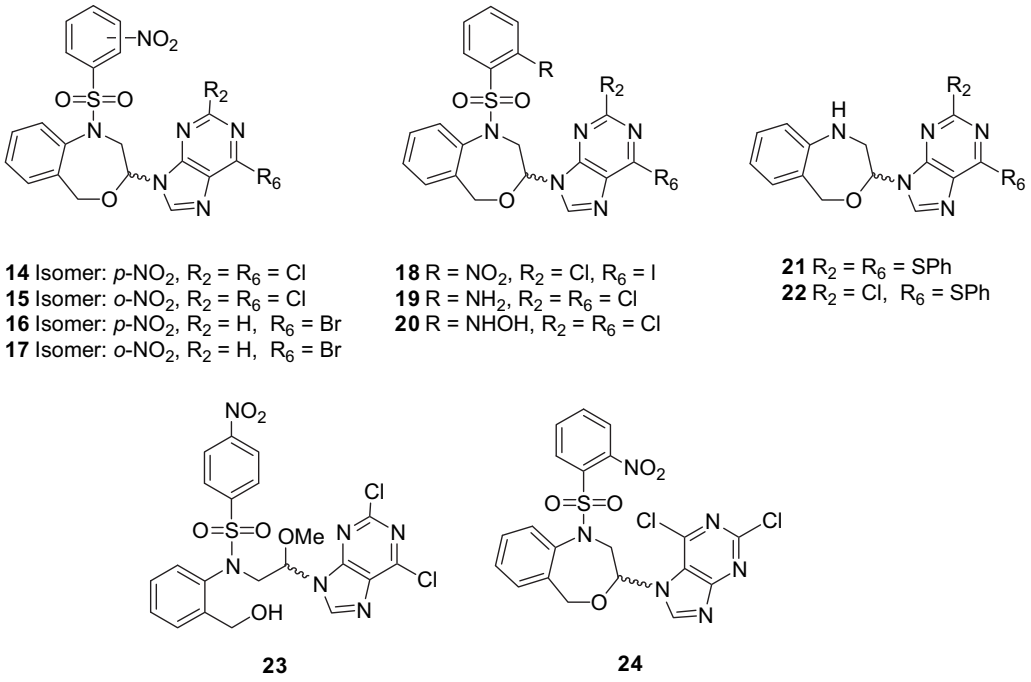

Chart 4.

gradient elution using mixtures of hexane/ethyl acetate (4/1 → 1/1) or CH_2Cl_2/MeOH (100/1 → 100/5) to afford **14**–**17**. Compounds **27** and **28** were also isolated in the reactions. Compound **23** was isolated in the synthesis of **14**. Traces of the *N*-7 regioisomer analogue was detected in the synthesis of **15**.

Three different conditions were investigated; method a): purine (2.5 equiv), TMSCl (4.0 equiv), HMDS (4.0 equiv), $SnCl_4$ (1 M solution in CH_2Cl_2, 4.0 equiv), 160 °C, microwave, 5 min; method b): purine (2.5 equiv), TMSCl (4.0 equiv), HMDS (4.0 equiv), $SnCl_4$ (1 M solution in CH_2Cl_2, 4.0 equiv), 140 °C, microwave, 5 min; method c): purine (1.5 equiv), TMSCl (1.5 equiv), HMDS (1.5 equiv), $SnCl_4$ (1 M solution in CH_2Cl_2, 1.5 equiv), 140 °C, microwave, 5 min.

*4.1.1.1. 1-[(p-Nitrophenyl)sulfonyl]-1,5-dihydro-4,1-benzoxazepin (**27**).* Yellow solid, [method b): 20%], mp: 178–180 °C. ^{1}H NMR ($CDCl_3$, 300 MHz): δ (ppm) 8.33 (d, J = 8.8 Hz, 2H, H-3,5$_{pnitro}$), 7.80 (d, J = 9.1 Hz, 2H, H-2,6$_{pnitro}$), 7.60 (dd, J = 0.9, 7.9 Hz, 1H, H-9), 7.44 (dt, J = 1.5, 7.7 × 2 Hz, 1H, H-8), 7.31 (dt, J = 1.5, 7.5 × 2 Hz, 1H, H-7), 7.14 (dd, J = 1.6, 7.5 Hz, 1H, H-6), 5.94 (d, J = 5.9 Hz, 1H, H-3), 5.78 (d, J = 5.9 Hz, 1H, H-2), 4.01 (s, 2H, H-5). ^{13}C NMR ($CDCl_3$, 75 MHz): δ (ppm) 150.49 (C-4$_{pnitro}$), 142.93 (C-1$_{pnitro}$), 141.37 (C-9a), 138.91 (C-3), 132.26 (C-5a), 130.16, 130.08, 130.00, 128.99 (C-6, 7, 8, 9), 128.90 (C-2$_{pnitro}$ and C-6$_{pnitro}$), 124.55 (C-3$_{pnitro}$ and C-5$_{pnitro}$), 104.27 (C-2), 70.24 (C-5). HR LSIMS (m/z) calcd. for $C_{15}H_{12}N_2O_5NaS$ $(M + Na)^+$ 355.0365, found 355.0364. Anal. $C_{15}H_{12}N_2O_5S$ (C, H, N, S).

*4.1.1.2. 1-[(o-Nitrophenyl)sulfonyl]-1,5-dihydro-4,1-benzoxazepin (**28**).* Brown sirup [method a): 36%; method b): 39%; method c): 29%], ^{1}H NMR ($CDCl_3$, 300 MHz): δ (ppm) 7.87 (dd, J = 1.8, 7.9 Hz, 1H, H-3$_{onitro}$), 7.75–7.63 (m, 2H, H-4$_{onitro}$ and H-5$_{onitro}$), 7.59 (dd, J = 1.3, 7.9 Hz, 1H, H-6$_{onitro}$), 7.47 (dd, J = 1.3, 7.9 Hz, 1H, H-6), 7.40 (ddd, J = 1.8, 7.70 × 2 Hz, 1H, H-7), 7.34 (ddd, J = 1.5, 7.4 × 2 Hz, 1H, H-8), 7.23 (dd, J = 1.5, 7.3 Hz, 1H, H-9), 5.96 (d, J = 5.7 Hz, 1H, H-3), 5.77 (d, J = 5.7 Hz, 1H, H-2), 4.49 (s, 2H, H-5). ^{13}C NMR ($CDCl_3$, 75 MHz): δ (ppm) 148.15, 141.88, 138.77, 134.12, 132.40, 131.57, 131.30, 130.74, 129.65 (×2), 128.97, 128.58, 123.83, 104.05, 70.06 (C-5). HR LSIMS (m/z) calcd. for $C_{15}H_{12}N_2O_5NaS$ $(M + Na)^+$ 355.0365, found 355.0365. Anal. $C_{15}H_{12}N_2O_5S$ (C, H, N, S).

*4.1.1.3. (RS)-2,6-Dichloro-9-[1-(p-nitrobenzenesulfonyl)-1,2,3,5-tetrahydro-4,1-benzoxazepin-3-yl]-9H-purine (**14**).* Yellowish solid [method b): 20%], mp: 173–175 °C. ^{1}H NMR ($CDCl_3$, 300 MHz): δ (ppm) 8.44 (d, J = 8.8 Hz, 2H), 8.17–8.11 (m, 3H), 7.43–7.31 (m, 4H), 6.00 (d, J = 8.8 Hz, 1H), 4.78 (d, J = 13.8 Hz, 1H), 4.74 (dd, J = 1.2, 14.7 Hz, 1H), 4.60 (d, J = 13.8 Hz, 1H), 3.65 (dd, J = 10.0, 14.7 Hz, 1H). ^{13}C NMR ($CDCl_3$, 75 MHz): δ (ppm) 153.72, 152.59, 152.16, 150.79, 146.29, 143.41, 138.78, 136.64, 131.01, 130.52, 130.40, 129.54, 129.10 (×2), 129.05, 125.18 (×2), 84.78, 72.05, 54.56. HR LSIMS (m/z) calcd. for $C_{20}H_{14}N_6O_5NaSCl_2$ $(M + Na)^+$ 543.0021, found 543.0024. Anal. $C_{20}H_{14}Cl_2N_6O_5S$ (C, H, N, S).

*4.1.1.4. (RS)-9-{2-[N-(2-Hydroxymethylphenyl)-p-nitrobenzenesulfonamide]-1-metoxyethyl}-2,6-dichloro-9H-purine (**23**).* White solid [method b): 12%]: mp: 172–174 °C. [conformer A (58%), conformer B (42%)] ^{1}H NMR ($CDCl_3$, 300 MHz): δ (ppm) 8.36–8.28 (m, 5H), 8.12 (s, 1H), 7.80 (d, J = 9.2 Hz, 2H), 7.72 (d, J = 8.8 Hz, 2H), 7.63 (d, J = 7.7 Hz, 1H), 7.61 (d, J = 7.7 Hz, 1H), 7.44–7.39 (m, 2H), 7.30–7.25 (m, 2H), 7.18–7.08 (m, 2H), 6.42 (dd, J = 0.9, 7.9 Hz, 1H), 6.38 (d, J = 0.9, 7.9 Hz, 1H), 5.86 (pt, J = 6.1 Hz, 1H), 5.69 (dd, J = 4.8, 7.5 Hz, 1H), 4.58–4.53 (m, 3H), 4.44–4.36 (m, 2H), 4.27 (d, J = 12.7 Hz, 1H), 4.19 (dd, J = 7.5, 14.5 Hz, 1H), 3.96 (dd, J = 5.7, 14.5 Hz, 1H), 3.30 (s, 6H). ^{13}C NMR ($CDCl_3$, 75 MHz): δ (ppm) 152.9, 150.1, 143.5, 143.3, 141.8, 141.7, 141.1, 136.5, 135.2, 131.3, 130.8, 129.7, 129.4, 129.1, 128.8, 128.6, 128.2, 126.6, 126.4, 123.9, 85.5, 85.2, 60.2, 60.0, 57.0, 56.7, 54.7, 53.6. HR LSIMS (m/z) calcd. for $C_{21}H_{18}N_6O_6NaSCl_2$ $(M + Na)^+$ 575.0283, found 575.0287. Anal. $C_{21}H_{18}Cl_2N_6O_6S$ (C, H, N, S).

*4.1.1.5. (RS)-2,6-Dichloro-9-[1-(o-nitrobenzenesulfonyl)-1,2,3,5-tetrahydro-4,1-benzoxazepin-3-yl]-9H-purine (**15**).* White solid [method a): 32%, b): 37%, c): 47%], mp: 154–155 °C. ^{1}H NMR ($CDCl_3$, 300 MHz): δ (ppm) 8.18 (s, 1H), 8.07 (dd, J = 1.8, 7.9 Hz, 1H), 7.80 (m, 3H), 7.40 (m, 2H), 7.31 (m, 1H), 7.08 (d, J = 7.5 Hz, 1H), 6.09 (dd,

J = 1.8, 10.1 Hz, 1H), 5.05 (d, J = 13.6 Hz, 1H), 4.82 (d, J = 13.6 Hz, 1H), 4.72 (dd, J = 1.8, 13.2 Hz, 1H), 3.84 (dd, J = 10.1, 13.2 Hz, 1H). ^{13}C NMR ($CDCl_3$, 75 MHz): δ (ppm) 153.68, 152.48, 152.38, 148.03, 143.70, 138.89, 137.75, 134.95, 133.71, 132.60, 132.55, 131.03, 130.56, 130.04, 129.58, 128.82, 125.02, 85.22, 72.12, 54.80. HR LSIMS (m/z) calcd. for $C_{20}H_{14}N_6O_5NaSCl_2$ $(M + Na)^+$ 543.0021, found 543.0020. Anal. $C_{20}H_{14}Cl_2N_6O_5S$ (C, H, N, S).

*4.1.1.6. (RS)-2,6-Dichloro-7-[1-(o-nitrobenzenesulfonyl)-1,2,3,5-tetrahydro-4,1-benzoxazepin-3-yl]-7H-purine (**24**).* White solid, [method a): 2%; method b): 1%; method c): 2%], mp: 172–174 °C. ^{1}H NMR (acetone-d_6, 400 MHz): δ (ppm) 8.93 (s, 1H), 8.10–8.07 (m, 3H), 7.94 (m, 1H), 7.57 (d, J = 7.5 Hz, 1H), 7.42–7.44 (m, 2H), 7.21 (d, J = 7.8 Hz, 1H), 6.56 (dd, J = 2.0, 10.2 Hz, 1H), 5.01–4.98 (m, 3H), 4.16 (dd, J = 10.0, 13.7 Hz, 1H). ^{13}C NMR (DMSO-d_6, 100 MHz): δ (ppm) 163.88, 160.85, 152.18, 144.00, 139.25, 137.93, 136.29, 133.91, 132.67, 131.00, 130.89, 130.32, 129.96, 129.54, 128.63, 125.86, 121.01, 85.38, 70.40, 53.85. HR LSIMS (m/z) calcd. for $C_{20}H_{14}Cl_2N_6NaO_5S$ $(M + Na)^+$ 543.0021, found 543.0018. Anal. $C_{20}H_{14}Cl_2N_6O_5S$ (C, H, N, S).

*4.1.1.7. (RS)-6-Bromo-9-[1-(p-nitrobenzenesulfonyl)-1,2,3,5-tetrahydro-4,1-benzoxazepin-3-yl]-9H-purine (**16**).* Viscous oil [method d): 4%]. ^{1}H NMR ($CDCl_3$, 300 MHz): δ (ppm) 8.79 (s, 1H), 8.41 (d, J = 8.8 Hz, 2H), 8.21 (s, 1H), 8.07 (d, J = 8.8 Hz, 2H), 7.42–7.35 (m, 3H), 7.29–7.27 (m, 1H), 6.14(dd, J = 1.8, 10.0 Hz, 1H), 4.80–4.76 (m, 2H), 4.60 (d, J = 13.8 Hz, 1H), 3.75 (dd, J = 10.0, 14.7 Hz, 1H). ^{13}C NMR ($CDCl_3$, 75 MHz): δ (ppm) 152.74, 151.92, 150.73, 146.47, 142.94, 142.80, 138.76, 137.05, 131.91, 130.53, 130.36, 129.58, 128.93 (×2), 128.72, 125.06 (×2), 84.98, 71.84, 54.76. HR LSIMS (m/z) calcd. for $C_{20}H_{15}N_6O_5NaSBr$ $(M + Na)^+$ 552.9906, found 552.9906. Anal. $C_{20}H_{15}BrN_6O_5S$ (C, H, N, S).

*4.1.1.8. (RS)-6-Bromo-9-[1-(o-nitrobenzenesulfonyl)-1,2,3,5-tetrahydro-4,1-benzoxazepin-3-yl]-9H-purine (**17**).* Viscous oil, [method d): 4%], ^{1}H NMR (CD_3OD, 400 MHz): δ (ppm) 8.71 (s, 1H), 8.67 (s, 1H), 8.02 (d, J = 8.0 Hz, 1H), 7.91 (m, 2H), 7.81 (m, 1H), 7.47 (d, J = 8.0 Hz, 1H), 7.40 (t, 1H), 7.33 (m, 1H), 7.09 (d, J = 8.0 Hz, 1H), 6.25 (dd, J = 2.0, 10.2 Hz, 1H), 5.02 (d, J = 13.3 Hz, 1H), 4.84 (d, J = 13.3 Hz, 1H), 4.72 (dd, J = 2.0, 14.9 Hz, 1H), 4.12 (dd, J = 10.2, 14.9 Hz, 1H). ^{13}C NMR (CD_3OD, 75 MHz): δ (ppm) 153.33, 151.27, 149.32, 146.06, 143.62, 140.32, 139.60, 136.30, 135.08, 134.26, 133.64, 132.67, 131.25, 130.69, 130.27, 129.60, 126.72, 86.41, 72.41, 55.14. HR LSIMS (m/z) calcd. for $C_{20}H_{15}N_6O_5NaSBr$ $(M + Na)^+$ 552.9906, found 552.9899. Anal. $C_{20}H_{15}BrN_6O_5S$ (C, H, N, S).

*4.1.2. Substitutions on **15**: formation of 6-iodo derivative **18***

To a solution of **15** (1.0 equiv) in butanone (20 mL/mmol), NaI (20.0 equiv) and TFA (5.0 equiv) were added subsequently at −15 °C and the reaction mixture was stirred at this temperature for 6 h. The solvent was evaporated and water was added to the residue. The aqueous layer was extracted (CH_2Cl_2) and the combined organic layers were washed ($NaHSO_4$ and brine), dried (Na_2SO_4) and evaporated. Purification of **18** was carried out by flash chromatography using EtOAc/hexane 1/2 as eluent.

*4.1.2.1. (RS)-2-Chloro-6-iodo-9-[1-(o-nitrobenzenesulfonyl)-1,2,3,5-tetrahydro-4,1-benzoxazepin-3-yl]-9H-purine (**18**).* Yellow solid (66%), mp: 129–132 °C ^{1}H NMR ($CDCl_3$, 300 MHz): δ (ppm) 8.18 (s, 1H), 8.08 (d, J = 8.0 Hz, 1H), 7.81–7.79 (m, 3H), 7.42–7.40 (m, 2H), 7.31–7.32 (m, 1H), 7.10 (d, J = 8.0 Hz, 1H), 6.06 (dd, J = 8.0, 16.0 Hz, 1H), 5.04 (dd, J = 8.0, 12.0 Hz, 1H), 4.82 (d, J = 12.0 Hz, 1H), 4.73 (dd, J = 4.0, 16.0 Hz, 1H), 3.82–3.80 (m, 1H). ^{13}C NMR ($CDCl_3$, 75 MHz): δ (ppm) 153.10, 152.46, 152.34, 148.81, 147.86, 143.64, 138.85, 137.72, 137.68, 134.90, 133.68, 132.57, 132.52, 130.53, 130.00, 128.82, 124.99, 85.18, 72.12, 54.76. HR LSIMS (m/z) calcd. for $C_{20}H_{14}N_6O_5NaSClI$ $(M + Na)^+$ 634.9377, found 634.9381. Anal. $C_{20}H_{14}ClIN_6O_5S$ (C, H, N, S).

*4.1.3. Reduction of **15**: formation of amino **19** and hydroxylamino **20** derivatives*

$SnCl_2 \cdot 2H_2O$ (5.0 equiv) was added at room temperature to a suspension of **15** in EtOH (2.5 mL/mmol) and heated at the reflux temperature for 2 h. The reaction mixture was then cooled at 0 °C and the pH was fixed to 7–8 with saturated $NaHCO_3$ solution. The aqueous layer was extracted with CH_2Cl_2 and the combined organic layers were washed with brine, dried (Na_2SO_4) and evaporated. Purification of **19** and **20** was carried out by flash chromatography using CH_2Cl_2/acetone (9.9/0.1) as eluent.

*4.1.3.1. (RS)-9-[1-(o-Aminobenzenesulfonyl)-1,2,3,5-tetrahydro-4,1-benzoxazepin-3-yl]-2,6-dichloro- 9H-purine (**19**).* White solid (35%); mp: 225–227 °C. ^{1}H NMR ($CDCl_3$, 400 MHz): δ (ppm) 8.14 (s, 1H), 7.83–7.81 (m, 2H), 7.63 (dd, J = 1.6, 8.2 Hz, 1H), 7.55 (dd, J = 1.2, 7.8 Hz, 1H), 7.44–7.25 (m, 4H), 6.02 (dd, J = 2.0, 10.2 Hz, 1H), 4.70–4.67 (m, 3H), 3.53 (dd, J = 10.2, 14.9 Hz, 1H). ^{13}C NMR ($CDCl_3$, 75 MHz): δ (ppm) 153.52, 152.34, 152.15, 145.42, 143.81, 143.49, 139.57, 136.83, 135.45, 130.70, 130.07, 129.99, 129.96, 128.76, 121.59, 118.31, 118.25, 84.37, 71.90, 54.23. HR LSIMS (m/z) calcd. for $C_{20}H_{16}N_6O_3NaSCl_2$ $(M + Na)^+$ 513.0279, found 513.0284. Anal. $C_{20}H_{16}Cl_2N_6O_3S$ (C, H, N, S).

*4.1.3.2. (RS)-2,6-Dichloro-9-[1-(o-hydroxylaminobenzene-sulfonyl)-1,2,3,5-tetrahydro-4,1-benzoxazepin-3-yl]-9H-purine (**20**).* Viscous oil (35%). ^{1}H NMR ($CDCl_3$, 400 MHz): δ (ppm) 8.13 (s, 1H), 7.42 (ddd, J = 1.2, 8.2, 16.6 Hz, 1H), 7.60 (ddd, J = 1.6, 7.4 × 2 Hz, 1H), 7.47 (ddd, J = 1.6, 7.8 Hz, 1H), 7.36 (ddd, J = 1.2, 7.4 Hz, 1H), 7.29 (dd, J = 1.4, 8.0 Hz, 1H), 7.26 (m, 1H), 7.20 (dd, J = 1.6, 7.4 Hz, 1H), 6.84 (ddd, J = 1.2, 7.8 Hz, 1H), 6.66 (dd, J = 2.1, 10.0 Hz, 1H), 4.77 (dd, J = 2.0, 14.9 Hz, 1H), 4.38 (d, J = 13.7 Hz, 1H), 3.67 (d, J = 13.3 Hz, 1H), 3.53 (dd, J = 10.3, 15.1 Hz, 1H). ^{13}C NMR ($CDCl_3$, 75 MHz): δ (ppm) 153.64, 153.24, 151.86, 147.03, 143.82, 138.29, 136.97, 135.41, 131.70, 131.12, 130.15, 129.75, 129.71, 129.20, 123.84, 120.71, 115.20, 83.23, 71.35, 54.70. HR LSIMS (m/z) calcd. for $C_{20}H_{17}Cl_2N_6O_4S$ $(M + H)^+$ 507.0404, found 507.0441. Anal. $C_{20}H_{16}Cl_2N_6O_4S$ (C, H, N, S).

*4.1.4. Substitutions on **15**: formation of 2,6-dithiophenyl **21** and 6-thiophenyl **22** derivatives*

*4.1.4.1. (RS)-2,6-Dithiophenyl-9-[1,2,3,5-tetrahydro-4,1-benzoxazepin-3-yl]-9H-purine (**21**).* K_2CO_3 (3.0 equiv) and PhSH (1.1 equiv) were added at room temperature to a solution of **15** (1.0 equiv) in DMF (5 mL/mmol). The mixture was stirred at room temperature for 4 h. The solvent was evaporated and water was added to the residue. The aqueous layer was extracted with CH_2Cl_2 and the combined organic layers were washed with brine, dried (Na_2SO_4) and evaporated. Purification of **21** was carried out by flash chromatography using EtOAc/hexane 1/4 as eluent. White solid, (42%), mp: 82–86 °C. ^{1}H NMR ($CDCl_3$, 300 MHz): δ (ppm) 8.17 (s, 1H), 7.6 (ddd, J = 0.9, 7.5 × 2 Hz, 1H), 7.53–718 (m, 13H), 6.92 (d, J = 7.9 Hz, 1H), 6.03 (dd, J = 2.4, 7.7 Hz, 1H), 4.95 (d, J = 14.1 Hz, 1H), 4.80 (d, J = 14.1 Hz, 1H), 3.73 (dd, J = 2.6, 13.6 Hz, 1H), 3.59 (dd, J = 7.5, 13.6 Hz, 1H). ^{13}C NMR ($CDCl_3$, 75 MHz): δ (ppm) 177.21, 165.50, 161.25, 149.10, 141.13, 135.39 (×2), 135.26 (×2), 130.25, 129.72 (×2), 129.42, 129.39, 129.26 (×2), 129.06 (×2), 129.00, 128.55, 127.02, 122.21, 119.29, 85.22, 70.48, 51.79, one carbon missing. HR LSIMS (m/z) calcd. for $C_{26}H_{21}N_5ONaS_2$ $(M + Na)^+$ 506.1085, found 506.1084. Anal. $C_{26}H_{21}N_5OS_2$ (C, H, N, S).

*4.1.4.2. (RS)-2-Chloro-6-phenylthio-9-[1,2,3,5-tetrahydro-4,1-benzoxazepin-3-yl]-9H-purine (**22**).* K_2CO_3 (1.6 equiv) and PhSH (0.8 equiv) were added at room temperature to a solution of **15**

(1.0 equiv) in DMF (5 mL/mmol). The mixture was stirred at room temperature for 4 h. The solvent was evaporated and water was added to the residue. The aqueous layer was extracted with CH_2Cl_2 and the combined organic layers were washed with brine, dried (Na_2SO_4) and evaporated. Purification of **22** was carried out by flash chromatography using EtOAc/hexane 1/2 as eluent. White solid, (40%), mp: 161–163 °C. ^{1}H NMR ($CDCl_3$, 300 MHz): δ (ppm) 8.27 (s, 1H), 7.95 (ddd, $J = 0.4$, 7.5 Hz, 1H), 7.64 (m, 2H), 7.46 (m, 3H) 7.19 (m, 2H), 6.87 (d, $J = 7.9$ Hz, 1H), 6.11 (dd, $J = 2.2$, 7.4 Hz, 1H), 4.88 (s, 2H), 3.83 (dd, $J = 2.2$, 13.6 Hz, 1H), 3.40 (dd, $J = 7.4$, 13.6 Hz, 1H). ^{13}C NMR ($CDCl_3$, 75 MHz): δ (ppm) 163.13, 154.06, 149.70, 147.99, 142.22, 135.59 (×2), 129.97, 129.75, 129.73, 129.56, 129.50 (×2), 128.46, 126.71, 122.03, 119.19, 85.02, 71.02, 52.85. HR LSIMS (m/z) calcd. for $C_{20}H_{16}N_5ONaSCl$ $(M + Na)^+$ 432.0662, found 432.0660. Anal. $C_{20}H_{16}ClN_5O_5S$ (C, H, N, S).

*4.1.4.3. Resolution of (RS)-**14**.* (*RS*)-9-[1-(*p*-Nitrobenzenesulfonyl)-1,2,3,5-tetrahydro-4,1-benzoxazepin-3-yl]-2,6-dichloro-9*H*-purine (**14**) is resolved into its enantiomers: the one that elutes first is (*R*)-**14** (retention time = 8.5 min), and the one which comes second is (*S*)-**14** (retention time = 19.8 min), using a column CHIRALPAK® IA (DAICEL CHEMICAL INDUSTRIES, LTD.) semipreparative, and as eluent a mixture of hexane/*t*-BuOMe/*i*PrOH (26/65/9).

4.2. Biology

4.2.1. Cell culture

MCF-7 and MDA-MB-231 cells were grown at 37 °C in an atmosphere containing 5% CO_2, with Dubelcco's modified Eagle Medium (DMEM) (Gibco, Grand Island, NY) supplemented with 10% heat-inactivated fetal bovine serum (FBS) (Gibco), 2% L-glutamine, 2.7% sodium bicarbonate, 1% Hepes buffer, 40 mg/L gentamicin and 500 mg/L ampicillin.

4.2.2. Drugs and drug treatments

The drugs were dissolved in DMSO or water and stored at −20 °C. For each experiment, the stock solutions were further diluted in medium to obtain the desired concentrations. The final solvent concentration in cell culture was ≤0.1% v/v of DMSO, a concentration without effect on cell replication. Parallel cultures of cells in medium with DMSO were used as controls.

4.2.3. Cytotoxicity assays in vitro

The effect of anticancer drugs on cell viability was assessed using the sulforhodamine-B colorimetric assay [38]. Aliquots of MCF-7 cells suspension (1×10^3 cells/well) were seeded onto 24-well plates and incubated for 24 h. The cells were then treated with different concentrations of drugs in the culture medium. Three days later, the wells were aspirated, fresh medium and treatment were added, and cells were maintained for 3 additional days. Thereafter, cells were processed as described previously [38], using a Titertek Multiscan apparatus (Flow, Irvine, California) at 492 nm. We evaluated linearity of the SRB assay with cell number for each cell line before each cell growth experiment. The IC_{50} values were calculated from semilogarithmic dose–response curves by linear interpolation. All of the experiments were plated in triplicate wells and were carried out at least twice.

4.2.4. Cell-cycle distribution analysis

The cells at 70% confluence were treated with either DMSO alone or with concentrations of the compounds determined by their IC_{50} values. FACS analysis was performed after 48 h of treatment as described [38]. All experiments were performed in triplicate and yielded similar results.

4.2.5. Apoptosis detection by staining with annexin V-FITC and propidium iodide

The annexin V-FITC apoptosis detection kit I (Pharmingen, San Diego, CA, USA) was used to detect apoptosis by flow cytometry according to Marchal et al. [38]. All experiments were performed in triplicate and yielded similar results.

4.2.6. Apoptosis detection by confocal microscopy

Cells (5×10^3 cells/well) were seeded onto Labtek chamber-slide 8-well plates. Cells were allowed to adhere for 24 h before dosing with required concentrations of compounds. Culture medium was removed and cells were washed with cold 1X PBS. After that, cells were incubated with both Annexin V-FITC and propidium iodide for 15 min at room temperature in the dark. Cells were then washed with binding buffer, prepared with mounting medium and cover slips before confocal microscopic imaging [42]. Cells were imaged by confocal microscopy using a Leica SP2 Confocal Microscope.

4.2.7. Toxicity assays in vivo

Acute toxicity was determined in six-week old BALB/c female mice (average, 20 g weight) during 2 weeks. (*RS*)-**14** dissolved in 0.25 mL of a mixture of 0.9% sodium chloride and DMSO was administered in BALB/c in a single i.p. bolus injection ($n = 25$) at dose levels of 50, 75, 100, 150 and 200 mg/kg or *via* gavage ($n = 25$) in a single p.o. bolus at dose levels of 0.05, 0.5, 5 and 50 mg/kg. Control mice were inoculated with the same volume of sodium chloride (control group) and DMSO alone (DMSO group). Mice were maintained under standard conditions and for each treatment schedule, were weighed and assessed twice weekly for systemic toxicity (listlessness, weight loss) and local toxicity (alopecia, skin reaction, and leg motility).

Acknowledgments

This study was supported by the European Commission (A.C-G. Marie Curie Programme MERG-CT-2005-030616) and the Instituto de Salud Carlos III (Fondo de Investigación Sanitaria) through projects no. PI070227 and PI070527. The project "Factoría de Cristalización, CONSOLIDER INGENIO-2010" (CSD2006-00015) provided X-ray structural facilities for this work. We gratefully acknowledge the BM16 Spanish beamline at ESRF (Grenoble, France) for access to synchrotron radiation and for helpful assistance during data collection. D Ch-L thanks CSD2006-00015 for his research contract.

Appendix. Supplementary data

Supplementary data associated with this article can be found, in the online version, at doi:10.1016/j.ejmech.2010.11.011.

References

[1] B.W. Stewart, P. Kleihues (Eds.), World Cancer Report, International Agency for Research on Cancer, World Health Organization, 2003.
[2] P. Fresco, F. Borges, M.P.M. Marques, C. Diniz, The anticancer properties of dietary polyphenols and its relation with apoptosis, Curr. Pharm. Des. 16 (2010) 114–134.
[3] M. Hajduch, L. Havlieek, J. Vesely, R. Novotny, V. Mihal, M. Strnad, Synthetic cyclin-dependent kinase inhibitors: new generation of potent anti-cancer drugs, Adv. Exp. Med. Biol. 457 (1999) 341–353.
[4] C.J. Sherr, Cancer cell cycles, Science 274 (1996) 1672–1677.
[5] S. Nagata, Apoptosis by death factor, Cell 88 (1997) 355–365.
[6] U. Testa, Apoptotic mechanisms in the control of erythropoiesis, Leukemia 18 (2004) 1176–1199.
[7] J. Zivny, P. Klener Jr., R. Pytlik, L. Andera, The role of apoptosis in cancer development and treatment: focusing on the development and treatment of hematologic malignancies, Curr. Pharm. Des. 16 (2010) 11–33.
[8] E. Saniger, J.M. Campos, A. Entrena, J.A. Marchal, I. Suárez, A. Aránega, D. Choquesillo, J. Niclós, M.A. Gallo, A. Espinosa, Medium benzene-fused oxacycles

with the 5-fluorouracil moiety: synthesis. Antiproliferative activities and apoptosis induction in breast cancer cells, Tetrahedron 59 (2003) 5457–5467.
[9] E. Saniger, J.M. Campos, A. Entrena, J.A. Marchal, H. Boulaiz, A. Aránega, M.A. Gallo, A. Espinosa, Neighbouring-group participation as the key step in the reactivity of acyclic and cyclic salicyl-derived *O,O*-acetals with 5-fluorouracil. Antiproliferative activity, cell cycle dysregulation and apoptotic induction of new *O,N*-acetals against breast cancer cells, Tetrahedron 59 (2003) 8017–8026.
[10] J.A. Marchal, M.C. Núñez, I. Suárez, M. Díaz-Gavilán, J.A. Gómez-Vidal, H. Boulaiz, F. Rodríguez-Serrano, A. Aránega, M.A. Gallo, A. Espinosa, J.M. Campos, A synthetic uracil derivative with antitumor activity through decreasing cyclin D1 and Cdk1, and increasing p21 and p27 in MCF-7 cells, Breast Cancer Res. Tr. 105 (2007) 237–246.
[11] M.C. Núñez, A. Entrena, F. Rodríguez-Serrano, J.A. Marchal, A. Aránega, M.A. Gallo, A. Espinosa, J.M. Campos, Synthesis of novel 1-(2.3-dihydro-5*H*-4.1-benzoxathiepin-3-yl)-uracil and -thymine, and their corresponding *S*-oxidized derivatives, Tetrahedron 61 (2005) 10363–10369.
[12] M. Díaz-Gavilán, J.A. Gómez-Vidal, A. Entrena, M.A. Gallo, A. Espinosa, J.M. Campos, Study of the factors that control the ratio of the products between 5-fluorouracil, uracil, and tetrahydrobenzoxazepine *O,O*-acetals bearing electron-withdrawing groups on the nitrogen atom, J. Org. Chem. 71 (2006) 1043–1054.
[13] M. Díaz-Gavilán, J.A. Gómez-Vidal, F. Rodríguez-Serrano, J.A. Marchal, O. Caba, A. Aránega, M.A. Gallo, A. Espinosa, J.M. Campos, Anticancer activity of (1.2.3.5-tetrahydro-4.1-benzoxazepine-3-yl)-pyrimidines and -purines against the MCF-7 cell line: preliminary cDNA microarray studies, Bioorg. Med. Chem. Lett. 18 (2008) 1457–1460.
[14] M.C. Núñez, M. Díaz-Gavilán, A. Conejo-García, O. Cruz-López, M.A. Gallo, A. Espinosa, J.M. Campos, Design, synthesis and anticancer activity against the MCF-7 cell line of benzo-fused 1.4-dihetero seven- and six-membered tethered pyrimidines and purines, Curr. Med. Chem. 15 (2008) 2614–2631.
[15] C.O. Kappe, Synthetic methods. Controlled microwave heating in modern organic synthesis, Angew. Chem. Int. Ed. 43 (2004) 6250–6284.
[16] B.L. Hayes, Recent advances in microwave-assisted synthesis, Aldrichim. Acta 37 (2004) 66–77.
[17] A. De la Hoz, A. Díaz-Ortiz, A. Moreno, Microwaves in organic synthesis. Thermal and non-thermal microwave effects, Chem. Soc. Rev. 34 (2005) 164–178.
[18] C.O. Kappe, A. Stadler, Microwaves in Organic and Medicinal Chemistry. Wiley-VCH, Weinheim, 2005.
[19] P. Lidström, J.P. Tierney (Eds.), Microwave-assisted Organic Synthesis, Blackwell, Oxford, 2005.
[20] A. Loupy, Microwaves in Organic Synthesis. Wiley-VCH, Weinheim, 2002.
[21] B.L. Hayes, Microwave Synthesis: Chemistry at the Speed of Light. CEM, Matthews, NC, 2002.
[22] F. Al-Obeidi, R.E. Austin, J.F. Okonya, D.R.S. Bond, Microwave-assisted solid-phase synthesis (MASS): parallel and combinatorial chemical library synthesis, Mini-Rev. Med. Chem. 3 (2003) 449–460.
[23] C. Kappe, O.D. Dallinger, The impact of microwave synthesis on drug discovery, Nat. Rev. Drug Discov. 5 (2006) 51–63.
[24] A. Conejo-García, M.C. Núñez, J.A. Marchal, F. Rodríguez-Serrano, A. Aránega, M.A. Gallo, A. Espinosa, J.M. Campos, Regioespecific microwave-assisted synthesis and cytotoxic activity against human breast cancer cells of (RS)-6-substituted-7- or 9-(2.3-dihydro-5H-1.4-benzodioxepin-3-yl)-7H- or -9H-purines, Eur. J. Med. Chem. 43 (2008) 1742–1748.
[25] M. Díaz-Gavilán, F. Rodríguez-Serrano, J.A. Gómez-Vidal, J.A. Marchal, A. Aránega, M.A. Gallo, A. Espinosa, J.M. Campos, Synthesis of tetrahydrobenzoxazepine acetals with electron-withdrawing groups on the nitrogen atom. Novel scaffolds endowed with anticancer activity against breast cancer cells, Tetrahedron 60 (2004) 11547–11557.
[26] M. Díaz-Gavilán, D. Choquesillo-Lazarte, J.M. González-Pérez, M.A. Gallo, A. Espinosa, J.M. Campos, Synthesis and reactivity of (*RS*)-6-chloro-7- or 9-(1,2,3,5-tetrahydro-4,1-benzoxazepin-3-yl)-7*H*- or 9*H*-purines bearing a nitrobenzenesulfonyl group on the nitrogen atom, Tetrahedron 63 (2007) 5274–5286.
[27] M.C. Núñez, M.E. García-Rubiño, A. Conejo-García, O. Cruz-López, M. Kimatrai, M.A. Gallo, A. Espinosa, J.M. Campos, Homochiral drugs: a demanding tendency of the pharmaceutical industry, Curr. Med. Chem. 16 (2009) 2064–2074.
[28] J.A. Marchal, A. Aránega, A. Conejo García, M.A. García Chaves, O. Cruz-López, H. Boulaiz, F. Rodríguez-Serrano, C. Cativiela, M. Perán, A.I. Jiménez, J.M. García-Ruiz, D. Choquesillo-Lasarte, J.M. Campos, Enantiómeros de derivados benzoheteroepínicos y su uso como agentes anticancerígenos. Universidad de Granada, 2010, P201030415.
[29] M.C. Núñez, F. Rodríguez-Serrano, J.A. Marchal, O. Caba, A. Aránega, M.A. Gallo, A. Espinosa, J.M. Campos, 6′-Chloro-7- or 9-(2,3-dihydro-5*H*-4,1-benzoxathiepin-3-yl)-7*H*- or 9*H*-purines and their corresponding sulfones as a new family of cytotoxic drugs, Tetrahedron 63 (2007) 183–190.
[30] H. Liu, L. Xu, M. Zhao, W. Liu, C. Zhang, S. Zhou, Enantiomer-specific, bifenthrin-induced apoptosis mediated by MAPK signalling pathway in Hep G2 cells, Toxicology 261 (2009) 119–125.
[31] M.D. Shelley, L. Hartley, R.G. Fish, P. Groundwater, J.J.G. Morgan, D. Mort, M. Mason, A. Evans, Stereo-specific cytotoxic effects of gossypol enantiomers and gossypolone in tumour cell lines, Cancer Lett. 135 (1999) 171–180.
[32] J.C. Lai, B.D. Brown, A.M. Voskresenskiy, S. Vonhoff, S. Klussman, W. Tan, M. Colombini, R. Weeratna, P. Miller, L. Benimetskaya, C.A. Stein, Comparison of D-G3139 and its enantiomer L-G3139 in melanoma cells demonstrates minimal in vitro but dramatic in vivo chiral dependency, Mol. Ther. 15 (2007) 270–278.
[33] N.M. Brown, C.A. Belles, S.L. Lindley, L.D. Zimmer-Nechemias, X. Zhao, D.P. Witte, M.O. Kim, K.D.R. Setchell, The chemopreventive action of equol enantiomers in a chemically induced animal model of breast cancer, Carcinogenesis 31 (2010) 886–893.
[34] J.L. Grem, D. Nguyen, B.P. Monahan, V. Kao, F.J. Geoffroy, Sequence-dependent antagonism between fluorouracil and paclitaxel in human breast cancer cells, Biochem. Pharmacol. 58 (1999) 477–486.
[35] K.J. Duncan, K.A. Eckert, G.A. Clawson, Mechanisms of growth inhibition in human papillomavirus positive and negative cervical cancer cells by the chloromethyl ketone protease inhibitor, succinyl-alanine-alanine-proline-phenylalanine chloromethyl ketone, J. Pharmacol. Exp. Ther. 330 (2009) 359–366.
[36] D.E. Saunders, W.D. Lawrence, C. Christensen, N.L. Wappler, H. Ruan, G. Deppe, Paclitaxel-induced apoptosis in MCF-7 breast cancer cells, Int. J. Cancer 70 (1997) 214–220.
[37] A. Chadderton, D.J. Villeneuve, S. Gluck, A.F. Kirwan-Rhude, B.R. Gannon, D.E. Blais, A.M. Parissenti, Role of specific apoptotic pathways in the restoration of paclitaxel-induced apoptosis by valspodar in doxorubicin-resistant MCF-7 breast cancer cells, Breast Cancer Res. Tr. 59 (2000) 231–244.
[38] J.A. Marchal, H. Boulaiz, I. Suárez, E. Saniger, J. Campos, E. Carrillo, J. Prados, M.A. Gallo, A. Espinosa, A. Aránega, Growth inhibition, G_1-arrest, and apoptosis in MCF-7 human breast cancer cells by novel highly lipophilic 5-fluorouracil derivatives, Invest. New Drugs 22 (2004) 379–389.
[39] A.S. Lundberg, R.A. Weinberg, Control of the cell cycle and apoptosis, Eur. J. Cancer 35 (1999) 531–539.
[40] A. De Fátima, W.F. Zambuzzi, L.V. Modolo, C.A.B. Tarsitano, F.R. Gadelha, S. Hyslop, J.E. de Carvalho, I. Salgado, C.V. Ferreira, R.A. Pilli, Cytotoxicity of goniothalamin enantiomers in renal cancer cells: involvement of nitric oxide, apoptosis and autophagy, Chem. Biol. Interact. 176 (2008) 143–150.
[41] L. Formigli, S. Zecchi Orlandini, S. Capaccioli, M.F. Poupon, D. Bani, Energy-dependent types of cell death in MCF-7 breast cancer cell tumors implanted into nude mice, Cells Tissues Organs 170 (2002) 99–110.
[42] J.L. Gooch, D. Yee, Strain-specific differences in formation of apoptotic DNA ladders in MCF-7 breast cancer cells, Cancer Lett. 144 (1999) 31–37.

Drug Design, Development and Therapy

Dovepress
open access to scientific and medical research

Open Access Full Text Article

ORIGINAL RESEARCH

Bozepinib, a novel small antitumor agent, induces PKR-mediated apoptosis and synergizes with IFNα triggering apoptosis, autophagy and senescence

Juan Antonio Marchal[1,2]
Esther Carrasco[1]
Alberto Ramirez[1,3]
Gema Jiménez[1,2]
Carmen Olmedo[4]
Macarena Peran[1,3]
Ahmad Agil[5]
Ana Conejo-García[6]
Olga Cruz-López[6]
Joaquin María Campos[6]
María Ángel García[4,7]

[1]Biopathology and Regenerative Medicine Institute, Centre for Biomedical Research, [2]Department of Human Anatomy and Embryology, Faculty of Medicine, University of Granada, Granada, [3]Department of Health Sciences, University of Jaén, Jaén, [4]Experimental Surgery Research Unit, Virgen de las Nieves University Hospital, Granada, [5]Department of Pharmacology and Neurosciences Institute, Faculty of Medicine, [6]Department of Pharmaceutical and Organic Chemistry, Faculty of Pharmacy, University of Granada, Granada, [7]Department of Oncology, Virgen de las Nieves University Hospital, Granada, Spain

Correspondence: María Ángel García
Hospital Universitario Virgen de las Nieves, E-18012 Granada, Spain
Tel +34 958 249 321
Fax +34 958 246 296
Email mangelgarcia@ugr.es

Juan Antonio Marchal
Universidad de Granada, E-18100 Granada, Spain
Tel +34 958 249 321
Fax +34 958 246 296
Email jmarchal@ugr.es

Abstract: Bozepinib [(*RS*)-2,6-dichloro-9-[1-(*p*-nitrobenzenesulfonyl)-1,2,3,5-tetrahydro-4,1-benzoxazepin-3-yl]-9*H*-purine] is a potent antitumor compound that is able to induce apoptosis in breast cancer cells. In the present study, we show that bozepinib also has antitumor activity in colon cancer cells, showing 50% inhibitory concentration (IC_{50}) values lower than those described for breast cancer cells and suggesting great potential of this synthetic drug in the treatment of cancer. We identified that the double-stranded RNA-dependent protein kinase (PKR) is a target of bozepinib, being upregulated and activated by the drug. However, p53 was not affected by bozepinib, and was not necessary for induction of apoptosis in either breast or colon cancer cells. In addition, the efficacy of bozepinib was improved when combined with the interferon-alpha (IFNα) cytokine, which enhanced bozepinib-induced apoptosis with involvement of protein kinase PKR. Moreover, we report here, for the first time, that in combined therapy, IFNα induces a clear process of autophagosome formation, and prior treatment with chloroquine, an autophagy inhibitor, is able to significantly reduce IFNα/bozepinib-induced cell death. Finally, we observed that a minor population of caspase 3-deficient MCF-7 cells persisted during long-term treatment with lower doses of bozepinib and the bozepinib/IFNα combination. Curiously, this population showed β-galactosidase activity and a percentage of cells arrested in S phase, that was more evident in cells treated with the bozepinib/IFNα combination than in cells treated with bozepinib or IFNα alone. Considering the resistance of some cancer cells to conventional chemotherapy, combinations enhancing the diversity of the cell death outcome might succeed in delivering more effective and less toxic chemotherapy.

Keywords: seven-member heterocycles, purines, IC_{50}, interferon cytokine, cell death, breast and colon cancer cells

Introduction

The mortality to incidence ratio in cancer patients is extremely high, positioning cancer as a major cause of death worldwide.[1] Chemotherapy has a role as either strategic treatment for locally advanced disease or palliative treatment for metastatic tumors. However, clinical use of chemotherapy is still unsatisfactory due to limited response rates, a small survival benefit, and a poor prognosis. Therefore, more effective and safer anticancer drugs are urgently needed. In this sense, combination therapies that enhance efficacy or permit administration of reduced doses have been successfully used in a broad variety of therapeutic applications.

Previous studies have demonstrated the potent antiproliferative activity of pyrimidine and purine benzo-fused seven-membered *O*,*N*-acetals in human breast and colon cancer

submit your manuscript | www.dovepress.com
Dovepress
http://dx.doi.org/10.2147/DDDT.S51354

cell lines in the micromolar range.[2–4] Bozepinib shows a 50% inhibitory concentration (IC_{50}) of 0.166 μM against the MDA-MB-231 human breast adenocarcinoma cell line. Moreover, this compound is able to selectively induce high levels of apoptosis in tumor cells and shows no acute toxicity in mice.[5]

Many chemotherapeutic drugs eradicate cancer cells by inducing apoptosis, and regardless of their primary targets, many are similar in terms of the cellular response to the apoptosis induced.[6] However, many tumors have a seriously compromised apoptosis pathway, and new drugs inducing other cytotoxic effects must be explored in order to evade chemoresistance. Therefore, although apoptosis has been considered as the typical mechanism for cell death, accumulating evidence suggests that alternative cell death pathways play a role in the tumor response to chemotherapy.[7,8] A potential mechanism of caspase-independent cell death is autophagy, which is defined as controlled lysosomal degradation of macromolecules and organelles. Autophagy was initially identified as a cell survival mechanism to protect against nutrient deprivation;[9] however, in certain conditions, it results in a form of cell death now described as type II programmed cell death, which is being targeted for novel therapeutic strategies in cancer.[10]

Senescence was first described as a state of irreversible growth arrest that normal human fibroblasts enter into at the end of their replicative lifespan.[11] By restricting cell proliferation and thereby impeding the accumulation of mutations, senescence acts as an important tumor suppression mechanism. Further, senescence induced by aberrant activation of oncogenes, oxidative stress, or DNA damage prevents proliferation of cells at risk of malignant transformation. Therefore, senescence offers an attractive therapeutic option if it can be induced in tumor cells.[12]

Interferons (IFNs) are agents with antiviral, antiproliferative, and immunomodulatory properties. Interferon-alpha (IFNα), a pleiotropic cytokine that regulates more than 100 genes, is used in the treatment of hematologic malignancies and solid tumors.[13,14] Although IFNs are effective as single agents in certain clinical pathologic entities, increasing experience with these cytokines suggests that their greatest therapeutic potential may be realized when they are used in combination with other biological response modifiers and cytotoxic or antiviral agents.[15] The apoptosis event has been well characterized for several combinations with IFNα; however, other mechanisms involved in the antitumor effectiveness of such combinations have not been explored. In fact, numerous studies in vitro and in vivo, including clinical trials, have used different IFN combinations with favorable outcomes.[16–19] The double-stranded RNA-dependent protein kinase (PKR), induced by IFN type I, was initially identified as an innate immune antiviral protein.[20,21] Since then, PKR has been linked to normal cell growth and differentiation, inflammation, cytokine signaling, and apoptosis, and is involved in the antiviral and antitumor activity of IFNs cytokines.[21] It has been recently suggested the major role of PKR in the induction of apoptosis by several chemotherapeutic drugs such as etoposide, doxorubicin and 5-fluorouracil,[22–24] with a potential clinical use in the future.

The aims of this work were to investigate the mechanisms by which bozepinib induces apoptosis in breast and colon cancer cells and to explore the activation of the proapoptotic proteins, tumor suppressor p53 and IFN-induced kinase PKR. In order to improve the antitumor efficacy of bozepinib, we analyzed the synergistic effect of a bozepinib/IFNα combination in breast and colon cancer cells and explored the mechanisms involved in the effectiveness of this combination. Our results show that PKR, but not p53, is involved in the apoptosis induced by bozepinib used alone and in combination with IFNα. In addition, we determined that bozepinib is able to induce other antitumor effects, including senescence and autophagy, which are strongly improved by using the IFNα combination.

Materials and methods

Cells and reagents

A human breast MCF-7 cell line (ECACC: 86012803) and human colon cancer RKO (ATCC: CRL-2577) and HCT-116 (ECACC: 91091005) cell lines were provided by the Cell Bank of the University of Granada (Granada, Spain). $PKR^{+/+}$ and $PKR^{-/-}$ mouse embryonic fibroblasts[25] and human colon HCT-116 $p53^{+/+}$ and $p53^{-/-}$ cells[26] were kindly provided by M Esteban (National Center of Biotechnology, Madrid, Spain) and B Vogelstein (Johns Hopkins Oncology Center, Baltimore, MD, USA), respectively. PKR was knocked down by RNA interference using shRNA-PKR as described previously.[24] The cells were maintained in Dulbecco's Modified Eagle's Medium supplemented with 10% fetal bovine serum, 1% penicillin-streptomycin, and 1% nonessential amino acid solution. Exponentially growing cells were used for all experiments. Bozepinib (Figure 1A) was synthesized as previously described,[4] dissolved in dimethyl sulfoxide, and stored at –20°C. For each experiment, the stock solutions were further diluted in medium to obtain the desired concentrations. Human IFNα2b (Intron A®) was obtained from Schering-Plough (Union, NJ, USA) and mouse IFNα was sourced from Peprotech (Rocky Hill, NJ, USA).

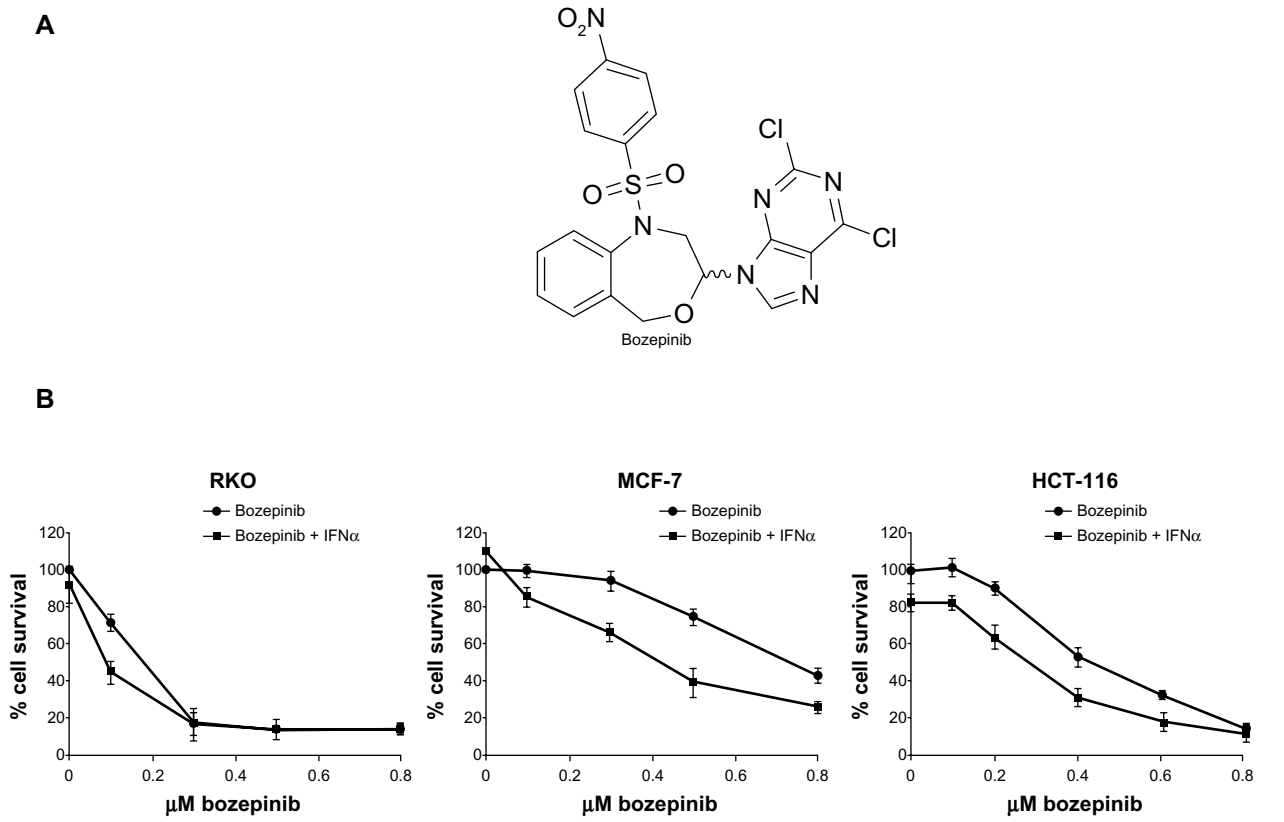

Figure 1 Cytotoxic effect of bozepinib and combined bozepinib/IFNα therapy. (**A**) Chemical structure of bozepinib. (**B**) MCF-7, HCT-116, and RKO cell lines treated with increasing amounts of bozepinib alone (circle) or in combination with 50 IU/mL IFNα (square) for 6 days as described in the Materials and methods section. Cell lines have been defined in material and methods section. The curve for cell survival is represented as a percentage compared to mock-treated cells. Values shown represent the mean of triplicate determinations calculated from a single experiment. Experiments were repeated at least three times.
Abbreviation: IFNα, interferon-alpha.

Z-VAD-FMK, a pan-caspase inhibitor, was provided by Santa Cruz Biotechnology (Santa Cruz, CA, USA) and chloroquine was obtained from Sigma-Aldrich (St Louis, MO, USA).

Cell survival assay

The effect of bozepinib on cell viability was assessed using the sulforhodamine-B colorimetric assay. Aliquots of cell suspension (5×10^3 cells/well) were seeded onto 12-well plates and incubated for 24 hours. The cells were then treated with different concentrations of bozepinib in culture medium. Three days later, the wells were aspirated, fresh medium and treatment was added, and the cells were maintained for a further 3 days. Thereafter, the cells were processed as previously described,[27] using a Titertek Multiscan apparatus (Flow Laboratories, Irvine, UK) at 492 nm. We evaluated the linearity of the sulforhodamine-B assay with the cell number for each cell stock before each cell growth experiment. The IC_{50} values were calculated by linear interpolation from semilogarithmic dose-response curves. To analyze the synergistic effect of addition of IFNα, cell viability was assayed as described above, treating cells with different concentrations of bozepinib in combination with IFNα (50 IU/mL). All experiments were plated in triplicate wells and carried out at least twice.

Apoptosis analysis

Cells were plated in six-well plates and maintained in an incubator overnight. The cells were then treated for 48 hours with bozepinib alone or in combination with IFNα (500 IU/mL). IFNα was added 8 hours before treatment with bozepinib. After 48 hours, the cells were trypsinized and analyzed using an Annexin V-fluorescein isothiocyanate detection kit (eBioscience Inc., San Diego, CA, USA). The samples were immediately processed using a FACSAria III flow cytometer (Becton Dickinson, BD Biosciences, Franklin Lakes, NJ, USA) from the service of the Scientific Instrumental Center (University of Granada).

Cell viability assay based on the metabolic cell activity

Cells in the exponential growth phase were plated on 96-well plates (5×10^3 cells/well) and maintained in the incubator overnight. On the following day, the cells were

treated with dimethyl sulfoxide (control), 5 μM bozepinib, 500 IU/mL IFNα, or both concentrations of the bozepinib/IFNα combination. The cells were treated, or not, 2 hours before with 25 μM of the pan-caspase inhibitor Z-VAD-FMK or 20 μM chloroquine. After 48 hours, cell viability was measured using a sensitive colorimetric assay, ie, the Cell Counting Kit-8 (Dojindo Laboratories, Kumamoto, Japan), following the manufacturer's instructions. The Cell Counting Kit-8 is based on use of tetrazolium salt that is reduced to formazan dye in the presence of living cells. The microplate was read using a 450 nm filter.

Cell cycle analysis

Cells in the exponential growth phase were plated on six-well plates (5×10^4 cells/well) and maintained in the incubator overnight. On the following day, the cells were treated with dimethyl sulfoxide (control), 5 μM bozepinib, 500 IU/mL IFNα, or with both concentrations of the bozepinib/IFNα combination for 7 days. The cells were harvested, washed twice with phosphate-buffered saline, and fixed in 70% (vol/vol) cold ethanol for up to 1 week. Next, the cells were centrifuged, and the pellet was washed once with phosphate-buffered saline and resuspended in 250 μL of propidium iodide solution (100 μL/mL RNAse, 40 μL/mL propidium iodide in phosphate-buffered saline) for 30 minutes in the dark at 37°C. The samples were immediately analyzed using a FACScan flow cytometer from the Scientific Instrumental Centre (University of Granada).

Western blot analysis

The cells were plated on six-well plates in their respective medium. After treatment, the medium was removed and the cells were lysed in Laemmli buffer. The protein sample was subjected to electrophoresis, transferred onto nitrocellulose membranes (Bio-Rad, Hercules, CA, USA), and blocked in phosphate-buffered saline containing 5% nonfat dry milk for 1 hour at room temperature. Primary antibodies used included a polyclonal antibody to total human PKR (Santa Cruz Biotechnology), a polyclonal antibody to phospho-PKR (Thr 451, Sigma-Aldrich), a polyclonal antibody to phospho-eIF2α (Ser 51, Invitrogen, Carlsbad, CA, USA), a polyclonal antibody to phospho-p53 (Ser 15, 92845, Cell Signaling Technology, Beverly, MA, USA), and a monoclonal antibody to β-actin (Sigma-Aldrich, A2228). Secondary antibodies used included anti-rabbit immunoglobulin (Ig)G peroxidase conjugate (Sigma-Aldrich, A0545) and anti-mouse IgG peroxidase conjugate (Sigma-Aldrich, A9044). Bands were visualized using an enhanced chemiluminescent system (Amersham Pharmacia Biotech, Little Chalfont, UK) and a Kodak detector image.

Autophagy-related assay

The cells were plated on cover slips and transfected with pCMV-GFP-LC3 plasmid and pCMV-GFP control plasmid using Lipofectamine™ 2000 (Invitrogen). At 24 hours post-transfection, the cells were mock-treated (using a similar volume of dimethyl sulfoxide) or treated with 5 μM bozepinib, 500 IU/mL IFNα, or both concentrations of the bozepinib/IFNα combination over 48 hours. After treatment, the cells were washed with phosphate-buffered saline and fixed with 4% paraformaldehyde. Images were obtained using a Radiance 2100 confocal laser microscope (Bio-Rad).

Transmission electron microscopy

The cells were mock-treated (using a similar volume of dimethyl sulfoxide) or treated with 5 μM bozepinib, 500 IU/mL IFNα, or both concentrations of the bozepinib/IFNα combination over 48 hours. After treatment, the cells were washed three times with phosphate-buffered saline and then fixed with 0.5 mL of ice-cold glutaraldehyde (2.5% in 0.1 mol/L cacodylate buffer, pH 7.4) at 4ºC overnight. After washing, the cells were fixed in 1% OsO_4 and embedded in Poly/Bed® resin (Polysciences Inc., Warrington, PA, USA). The ultrathin sections were doubly stained with uranyl acetate and lead citrate and analyzed by high resolution transmission electron microscopy (CM20; Philips, Eindhoven, the Netherlands).

Beta-galactosidase staining

Cells were plated on six-well plates in their respective medium. After 7 days of treatment, the medium was removed and the cells were fixed and stained using the Senescence β-Galactosidase Staining Kit (Cell Signaling Technology) according to the manufacturer's protocol following overnight incubation at 37°C in pH 6.0 buffer. Senescent cells were observed by positive staining of a blue color and were photographed under a 10 × objective.

Statistical analysis

All data are presented as the mean ± standard deviation. Differences between groups were analyzed for statistical significance using the two-tailed Student's *t*-test. $P<0.05$ was accepted as the statistical significance level.

Results

Interferon enhances cytotoxicity of bozepinib in colon and breast cancer cells by increasing apoptotic cell death

We have previously described the antitumor effect of bozepinib in an MCF-7 breast cancer cell line,[4,5] and the antitumor and

antiproliferative effects of IFNα are well characterized in cancer cells.[21,24] In order to analyze if bozepinib also has a cytotoxic effect on colon cancer cells, we determined the IC50 values in several cancer cell lines. HCT-116 and RKO colon cancer cell lines were more sensitive to the cytotoxic effect of bozepinib, showing lower IC_{50} values than the MCF-7 breast cancer cell line (Table 1). Moreover, we investigated whether addition of a low dose (50 IU/mL) of IFNα was able to improve the cytotoxic effect of bozepinib. This low dose by itself was not able to induce a significant antiproliferative effect in the RKO and MCF-7 cancer cell lines, but slightly affected the viability of HCT-116 cells (Figure 1B). However, both compounds synergistically induced death of the cancer cell lines analyzed (Figure 1B), and consequently, the IC_{50} for bozepinib was reduced when combined with IFNα (Table 1).

In order to determine if the effectiveness of the bozepinib/IFNα combination is due in part to an improvement in the apoptosis phenomenon, we treated MCF-7, HCT-116, and RKO cell lines with bozepinib alone or in combination with 500 IU/mL IFNα. As shown in Figure 2, the apoptosis induced by bozepinib at 48 hours was significantly increased when IFNα was added in all the cell lines analyzed (Figure 2).

PKR but not p53 is involved in bozepinib-induced apoptosis and effectiveness of bozepinib/IFNα

We first analyzed PKR phosphorylation and its natural substrate, eIF2α, in the MCF-7 and HCT-116 cell lines. Treatment with bozepinib induced PKR and eIF2α phosphorylation in both tumor cell lines. Importantly, it was also observed that there was an increase in PKR levels after treatment with bozepinib that was more evident in the HCT-116 cell line, in which the basal PKR level (total and phosphorylated) was lower than that in MCF-7 cells. In contrast, levels of p53 and phospho-p53 were not affected during treatment with bozepinib in either cell line (Figure 3A).

Table 1 Antiproliferative effects of bozepinib and bozepinip + IFNα on several cell lines

Cell line	IC_{50} (μM)[a]	
	Bozepinib	Bozepinib + IFNα
RKO	0.13 ± 0.01	0.09 ± 0.01
MCF-7	0.78 ± 0.06	0.44 ± 0.03
HCT-116	0.48 ± 0.08	0.31 ± 0.02
MEFsPKR$^{+/+}$	1.12 ± 0.18	0.89 ± 0.08
MEFsPKR$^{-/-}$	1.74 ± 0.28	1.77 ± 0.18

Notes: [a]All experiments were conducted in triplicate and gave similar results. The data are the mean ± standard error of the mean of three independent determinations. IC_{50} was determined after 6 days of treatment.
Abbreviations: IFNα, interferon-alpha; IC_{50}, 50% inhibitory concentration.

Next, we analyzed the contribution of PKR and p53 to the apoptosis induced by bozepinib. Further, because PKR is an IFN-induced protein that is involved in most of the antiviral and antitumor effects of this cytokine,[21] we also analyzed the effect of absence of PKR on the effectiveness of the bozepinib/IFNα combination. Bozepinib and IFNα were independently able to induce important levels of apoptosis in PKR$^{+/+}$ mouse embryonic fibroblasts that was enhanced when the two compounds were combined. However, low levels of apoptosis were induced in the absence of the PKR protein in PKR$^{-/-}$ mouse embryonic fibroblasts, even when bozepinib and IFNα were combined (Figure 3B, upper panel).

To demonstrate the role of PKR in the cytotoxic effect of bozepinib and the bozepinib/IFNα combination, we also analyzed cell survival in PKR$^{+/+}$ and PKR$^{-/-}$ mouse embryonic fibroblasts treated with increasing amounts of bozepinib, and the cytotoxic effect of bozepinib was found to be higher in PKR$^{+/+}$ mouse embryonic fibroblasts in comparison with PKR$^{-/-}$ mouse embryonic fibroblasts (Figure 3B, lower panel, and Table 1). Further, our results showed that whereas viability was significantly reduced in PKR$^{+/+}$ mouse embryonic fibroblasts when IFNα was added to bozepinib, cell viability was not affected by the bozepinib/IFNα combination in PKR$^{-/-}$ mouse embryonic fibroblasts.

Although p53 modification after treatment with bozepinib was not detected by Western blotting (Figure 3A), we went on to analyze the effect of bozepinib, IFNα, and the bozepinib/IFNα combination in the presence or absence of p53 protein in wild-type HCT-116 and HCT-116-p53 knockout cells (Figure 3C). Levels of apoptosis after the treatments were similar in both cell lines; however, when PKR was knocked down by RNA interference using shRNA-PKR, apoptosis was significantly reduced (Figure 3C). Taken together, these results suggest that, in part, PKR but not p53 contributes to the response of cancer cells to the bozepinib and bozepinib/IFNα combination.

Autophagy is involved in the synergistic effect of bozepinib/IFNα

We analyzed the ability of bozepinib to induce autophagy as well as regulation of this process by IFNα in the MCF-7 cell line, which is deficient in caspase 3 activation.[28] Despite the low level of endogenous LC3 protein, LC3-II levels were weakly detected 48 hours after treatment with bozepinib and were more evident when IFNα was added (Figure 4A). Confocal microscopy was used to analyze the redistribution

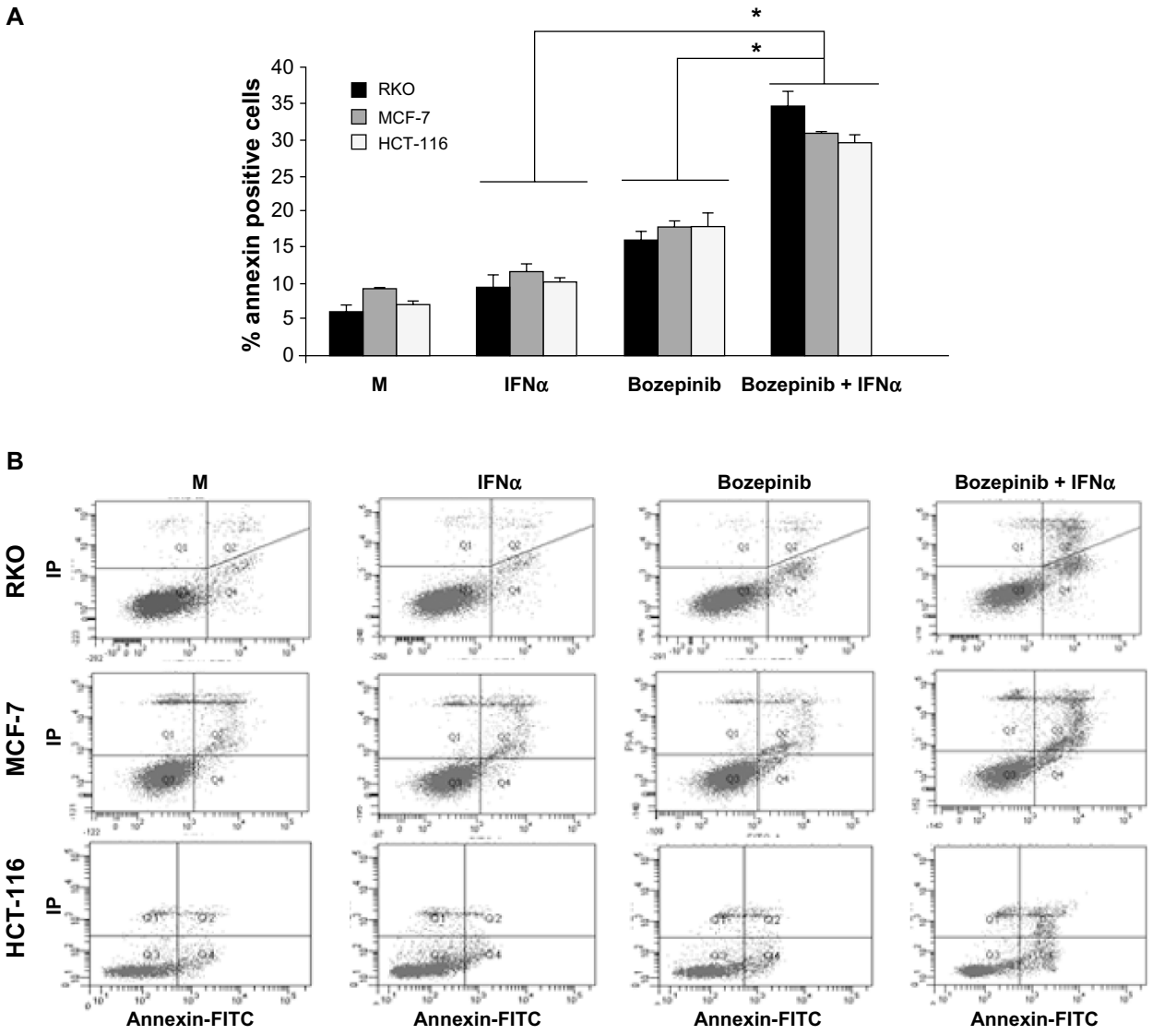

Figure 2 Apoptosis is enhanced by combination of bozepinib and IFNα. MCF-7, HCT-116, and RKO cell lines were mock-treated or treated with 5 μM bozepinib, 500 IU/mL IFNα, or the bozepinib/IFNα combination for 48 hours. Treated cells were then trypsinized and analyzed by flow cytometry using an Annexin V-fluorescein isothiocyanate detection kit. (**A**) Data are expressed as the mean ± standard error of the mean of three independent experiments. *$P<0.05$ (*t*-test). (**B**) Representative images from flow cytometry analysis.

Abbreviations: FITC, fluorescein isothiocyanate; IFNα, interferon-alpha; M, mock treated cells.

of LC3 protein into the autophagosomes of MCF-7 cells transfected with the pCMV-GFP-LC3 vector and the pCMV-GFP control vector, and the cells were then mock-treated or treated with bozepinib, IFNα, or the bozepinib/IFNα combination. As shown in Figure 4B, 48 hours post-treatment, the mock-treated cells displayed diffuse staining. However, a speckled fluorescent staining pattern was detected in almost all cells analyzed after treatment with bozepinib/IFNα, indicating redistribution of LC3 to autophagosomes. The speckled fluorescent stain was less pronounced after treatment with bozepinib alone or IFNα alone, and was detected in less than half of the cells analyzed (Figure 4B). Cells expressing the control vector pCMV-GFP displayed diffuse staining, even in the presence of treatment with bozepinib/IFNα (Figure 4B).

Moreover, we analyzed cell morphology using transmission electron microscopy 48 hours post-treatment. The most spectacular morphologic effects were observed when IFNα was combined with bozepinib. As shown in Figure 4C, autophagic vacuoles surrounded by a double-layered membrane and containing cytoplasmic constituents were observed after treatment with bozepinib/IFNα. Similar to the MCF-7 cell line, colon cancer HCT-116 cells showed autophagic vacuoles after the treatments, and this was also observed in the transmission electron microscopy images (Figure 4C).

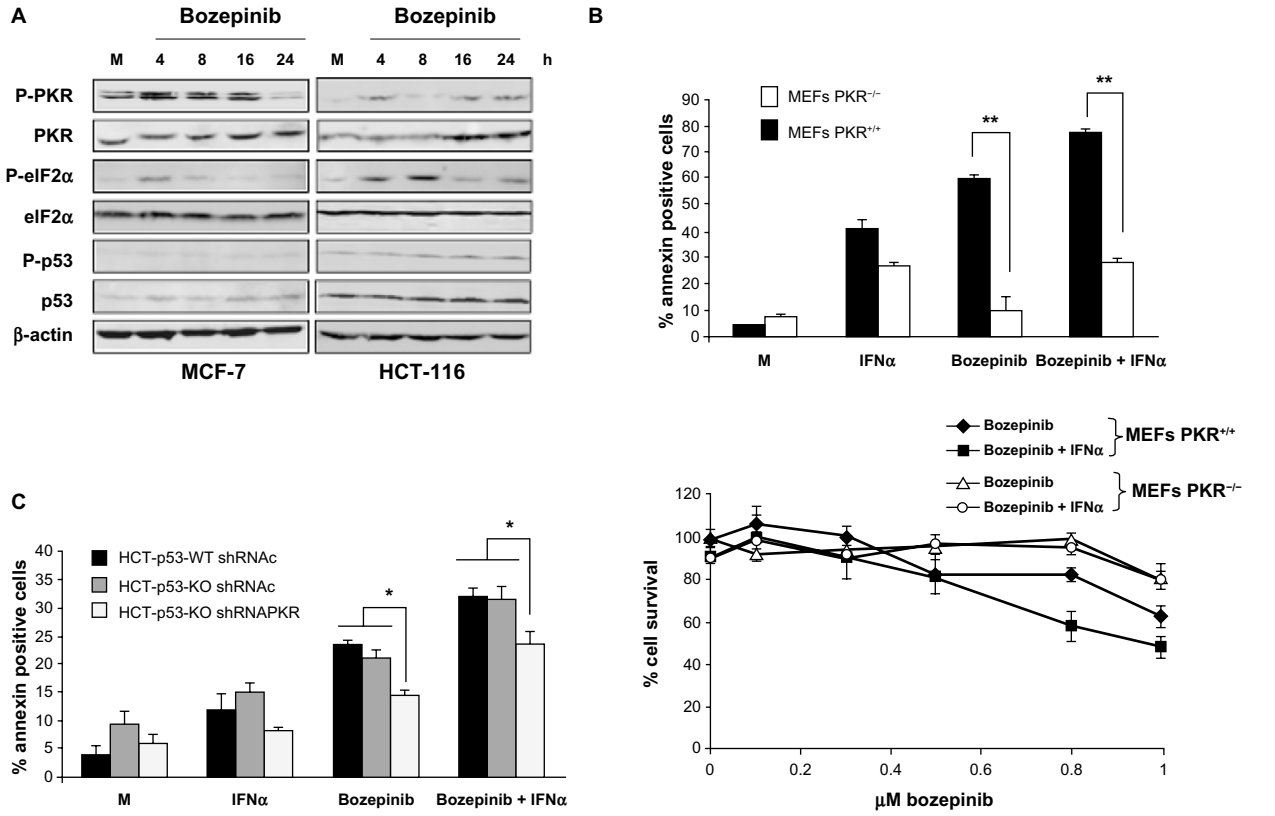

Figure 3 PKR and p53 activation during bozepinib treatment and its involvement in apoptosis and cell viability on bozepinib, IFNα, and the bozepinib/IFNα combination. (**A**) MCF-7 and HCT-116 cell lines were mock-treated or treated with 5 μM bozepinib for 4, 8, 16, and 24 hours. Total proteins were extracted for immunoblot analysis using anti-phospho PKR, anti-whole PKR, anti-phospho eIF2α, anti-whole eIF2α, anti-phospho p53, anti-whole p53, and anti-β-actin antibodies. (**B**) $PKR^{+/+}$ and $PKR^{-/-}$ mouse embryonic fibroblasts were mock-treated or treated with 2.5 μM bozepinib, 500 IU/mL IFNα, or the bozepinib/IFNα combination over 48 hours. $^{**}P<0.01$, by *t*-test (upper panel). Subsequently, the cells were trypsinized and analyzed by flow cytometry for Annexin V positive determination. Cells were treated with increasing amounts of bozepinib alone or in combination with 50 IU/mL of mouse IFNα over 6 days as described in the Materials and methods section. The curve for cell survival was represented as the percentage compared to mock-treated cells. Values shown represent the mean of triplicate determinations calculated from a single experiment. Experiments were repeated at least three times (lower panel). (**C**) A wild-type HCT-116 p53 cell line and an HCT-116 p53 knockout cell line expressing short hairpin RNAs targeting PKR or expressing a control short hairpin RNA were mock-treated or treated with 5 μM bozepinib, 500 IU/mL human IFNα, or a combination of bozepinib/IFNα for 48 hours. $^{*}P<0.05$ (*t*-test).

Abbreviations: IFNα, interferon-alpha; MEFs, mouse embryonic fibroblasts; shRNAc, control short hairpin RNA; PKR, RNA-dependent protein kinase; h, hours; M, mock treated cells; shRNAPKR, PKR short hairpin RNA.

In order to analyze involvement of the autophagy process induced by the bozepinib/IFNα combination in cell viability, MCF-7 cells were treated with the autophagy inhibitor chloroquine and the caspase-3 inhibitor Z-VAD 2 hours before treatment with bozepinib, IFNα, or bozepinib/IFNα (Figure 4D). Whereas Z-VAD did not affect cell death induced by either bozepinib alone or the bozepinib/IFNα combination, viability after bozepinib/IFNα treatment was significantly higher in cells pretreated with chloroquine. Treatment with chloroquine caused accumulation of LC3-II, that has been suggested to be the result of chloroquine-induced inhibition of fusion between autophagosome and lysosomes,[29,30] and was more evident after treatment with bozepinib/IFNα (Figure 4D).

These results indicate that bozepinib is able to induce the autophagy process in cancer cells that is clearly evidenced when it is combined with the IFNα cytokine, and suggest the contribution of autophagy to the cell death induced by the combination of bozepinib/IFNα.

IFNα enhances ability of bozepinib to induce lysosomal senescence-associated ß-galactosidase activity

During long-term treatment with bozepinib and the bozepinib/IFNα combination at low doses, we observed that a minority population remained in all the cell lines analyzed, but was more evident in the MCF-7 cell line. In order to characterize this population, we investigated ß-galactosidase activity and the cell cycle in MCF-7 cells. ß-galactosidase activity was detected in the residual surviving population after 7 days of treatment with bozepinib, as shown in Figure 5A. However, although this population

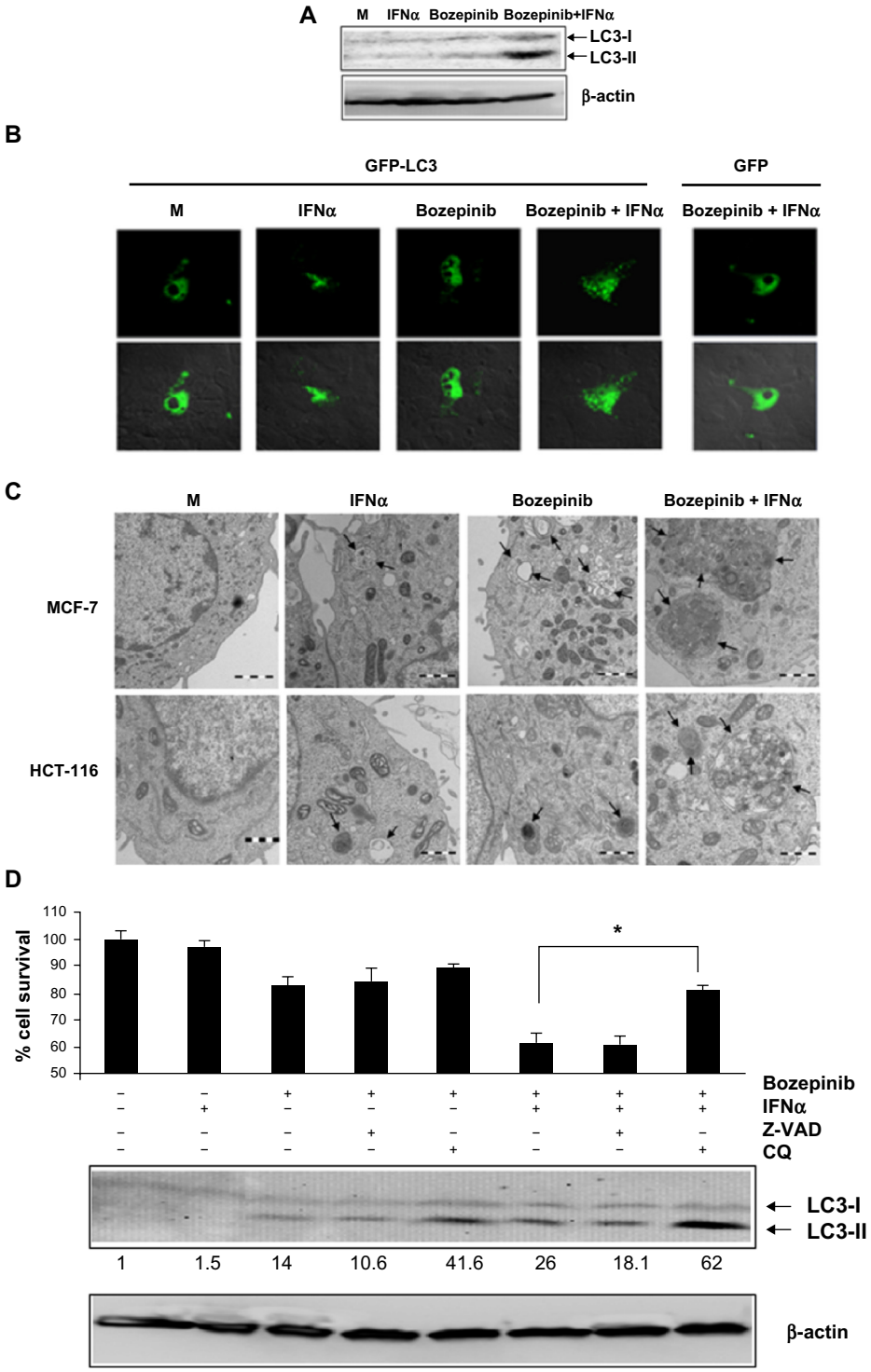

Figure 4 Bozepinib induced LC3-autophagosome formation that was strongly enhanced when combined with IFNα. (**A**) MCF-7 cells were mock-treated or treated with 5 μM bozepinib, 500 IU/mL human IFNα, or a combination of bozepinib/IFNα for 48 hours. Total proteins were extracted for immunoblot analysis using anti-LC3 and anti-β-actin antibodies. (**B**) MCF-7 cells were plated on cover slips supported in six-well plates and transfected with 5 μg of GFP-LC3 or GFP-control plasmids as described in the Materials and methods section. After 24 hours, the cells were treated with 5 μM bozepinib, 500 IU/mL human IFNα, or a combination of bozepinib/IFNα for 48 hours. Cells were fixed and visualized using a Radiance 2000 confocal microscope. (**C**) MCF-7 and HCT-116 cells were mock-treated or treated with 5 μM bozepinib, 500 IU/mL human IFNα, or a combination of bozepinib/IFNα for 48 hours. Cells were fixed and prepared for visualization by transmission electron microscopy as described in the Materials and methods section. Transmission electron microscopy images show that the treated cells included typical autophagolysosomes (arrows) containing organelles and lamellar structures. (**D**) MCF-7 cells were treated with 20 μM of chloroquine or 25 μM of Z-VAD inhibitors 2 hours before 5 μM bozepinib, 500 IU/mL IFNα, or a combination of bozepinib/IFNα. After 48 hours, the cells were treated with a Cell Counting Kit-8, measured at 450 nm optical density and represented as described in the Materials and methods section. Total proteins were extracted for immunoblot analysis using anti-LC3 and anti-β-actin antibodies. *$P<0.05$ (*t*-test). Western blot signals were quantified using Image J software, and relative β-actin-normalized values were assigned in reference to nontreated cells (value 1).

Abbreviations: CQ, chloroquine; IFNα, interferon-alpha; M, mock treated cells.

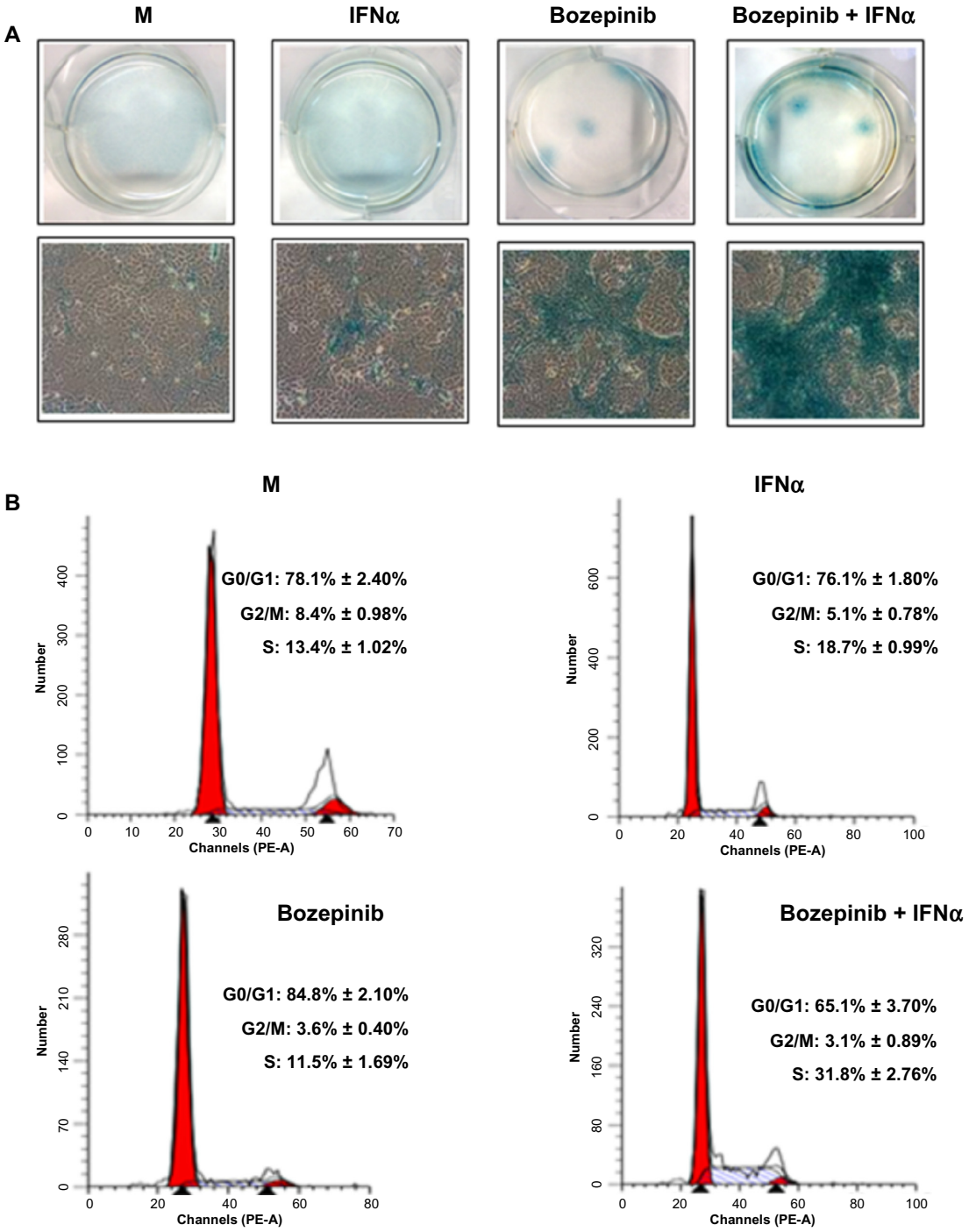

Figure 5 IFNα enhanced the ability of bozepinib to induce ß-galactosidase activity. MCF-7 cells were mock-treated or treated with 2.5 μM of bozepinib, 500 IU/mL human IFNα, or a combination of bozepinib/IFNα over 7 days. (**A**) Cells were fixed and stained using the Senescence β-Galactosidase Staining Kit as described in the Materials and methods section and photographed under a 10 × objective with a microscope (Leica) using visible light (lower panel) and the corresponding six wells were photographed under a 1 × objective using a standard camera (upper panel). (**B**) Cells were fixed and analyzed by flow cytometry after staining with propidium iodide. Values represent the mean of triplicate determinations calculated from a single experiment. Experiments were repeated at least three times.
Abbreviations: IFNα, interferon-alpha; M, mock treated cells.

was minor after 7 days of treatment with bozepinib/IFNα, ß-galactosidase activity was more evident. Moreover, the percentage of cells arrested in S phase after treatment with bozepinib/IFNα was around 30%, whereas the mock-treated cells and those treated with bozepinib alone showed 11%–13% in S phase (Figure 5B) after 7 days of treatment. Therefore, both bozepinib and IFNα were able to induce senescence in the residual surviving population, and this was more evident when bozepinib and IFNα were used in combination.

Discussion

Purine derivatives have shown potent antitumor activity and represent a new generation of anticancer drugs.[4] We have previously reported that bozepinib has an IC_{50} value ten times smaller than that of 5-fluorouracil in MCF-7 breast cancer cells. Moreover, bozepinib induces a considerable level of cell death by apoptosis via a mechanism that is still unknown. Bozepinib does not trigger acute toxicity in mice after 2 weeks of treatment.[5] In the present study, we demonstrated that bozepinib also has antitumor activity in colon cancer cells, with IC_{50} values lower than those described for breast cancer cells (Figure 1 and Table 1), suggesting great potential of this synthetic drug in the treatment of cancer. In order to identify the molecular targets involved in bozepinib-mediated apoptosis, we analyzed the induction and activation of the proapoptotic proteins, PKR and tumor suppressor p53. PKR but not p53 was markedly induced and activated in breast and colon cancer cell lines during treatment with bozepinib, thereby triggering phosphorylation of eIF2α. It is well established that eIF2α phosphorylation is correlated with translational block and consequently leads to inhibition of protein synthesis, providing the cell with an opportunity to make adaptive responses to stress that could finally trigger cell death by apoptosis.[31] Analysis of the level of PKR messenger (m)RNA during treatment with bozepinib suggested that upregulation of the PKR protein was not due to a transcriptional phenomenon (data not shown), similar to what we have described for 5-fluorouracil.[24] It is widely known that p53 is critical for the apoptotic response to agents that damage DNA and cause cytotoxicity, such as 5-fluorouracil, etoposide, paclitaxel, and cisplatin.[32] However, loss of p53 function is frequently involved in the resistance of tumors to chemotherapeutic agents. Moreover, apoptosis can also occur in mutant p53 cell lines in response to some of these chemotherapeutic drugs, suggesting that more targets are involved in induction of apoptosis in response to chemotherapy.[24,33,34] Recently, it has been shown that the PKR protein plays an important role in induction of apoptosis by doxorubicin, etoposide, and 5-fluorouracil, with both p53 and PKR being necessary for cancer cell death by apoptosis in response to chemotherapy.[22–24] Curiously, this study provides the first evidence that PKR but not p53 is involved in induction of apoptosis by an antitumor purine derivative (Figure 3). In fact, the levels of apoptosis induced by bozepinib are similar in HCT-116 colon cancer cells regardless of the presence or absence of p53 protein (Figure 3C). However, the absence or downregulation of PKR expression in mouse embryonic fibroblast knockout cells or in human colon cancer cells expressing PKR interference significantly decreased the apoptosis induced by bozepinib (Figure 3). Since p53 is mutated in more than 50% of tumors, drugs inducing apoptosis through molecular targets different from p53 are of great clinical interest.

Drug combinations in cancer therapy that enhance efficacy have had great success in a variety of therapeutic applications.[16] Our results show that bozepinib and IFNα act synergistically to suppress the viability of breast and colon cancer cells to a greater extent than when either agent is used alone, reducing cell viability by more than 20% in all cell lines analyzed (Figure 1B). Several studies have demonstrated that IFNα enhances the chemosensitivity of cancer cells to a number of drugs, mainly via improvement of apoptosis. It has recently been reported that a combination of 9-*cis*-retinoic acid and IFNα induces marked antiproliferative and proapoptotic effects in cancer cells by modulation of critical targets, such as p27 Kip1 and p21 WAF1/Cip1 proteins.[16] Moreover, several *in vitro* and *in vivo* studies have demonstrated the effectiveness of a combination of IFNα and 5-fluorouracil,[35] where p27 Kip1, Fas/FasL, and TNF-related apoptosis-inducing ligand (TRAIL) have been found to be involved in enhancement of apoptosis. In addition, we have identified PKR protein as an interesting molecular target that is key to the effectiveness of the 5-fluorouracil/IFNα combination.[24] The present study shows that one of the mechanisms by which IFNα improves the cytotoxic effect of bozepinib involves enhancement of apoptosis, and that the synergistic apoptotic effect induced by the bozepinib/IFNα combination is affected by the absence or downregulation of PKR protein (Figure 3). In fact, the cytotoxic effect of bozepinib was higher in $PKR^{+/+}$ mouse embryonic fibroblasts in comparison with $PKR^{-/-}$ mouse embryonic fibroblasts, and cell viability was significantly reduced when IFNα was combined with bozepinib in $PKR^{+/+}$ mouse embryonic fibroblasts. In contrast, cell viability was not affected by the bozepinib/IFNα combination in $PKR^{-/-}$ mouse embryonic fibroblasts. These data suggest that PKR, in part, contributes to the effectiveness of the bozepinib/IFNα combination, and therefore we hypothesize that its deregulation in tumors could affect the response of patients to combined therapies.

Given that most cancer cells show low levels of active caspases or mutations that inactivate the effectors of apoptosis,[36] antitumor drugs inducing additional or alternative mechanisms of cell death are of great interest. It has been suggested that autophagy could constitute an alternative cell death pathway in cells with a disrupted apoptotic path-

way.[10] In this sense, MCF-7 cells are a good model system to study drug-induced cell death by autophagy due to their defective caspase activation.[37,38] Moreover, effects other than apoptosis induced by combined IFNα antitumor therapies have not yet been explored. In our study, bozepinib was able to induce autophagosomes, as shown by the conversion of LC3-I to LC 3-II (Figure 4A), relocalization of the GFP-LC3 protein (Figure 4B), and electron microscopic images (Figure 4C). Surprisingly, addition of IFNα clearly increased autophagosome levels in MCF-7 cells (Figure 4). Moreover, previous treatment with a low dose of chloroquine was able to significantly reduce the cell death induced by bozepinib/IFNα (Figure 4D). Similar as described for rottlerin and etoposide,[38,39] autophagy leads to cell death in response to bozepinib/IFNα treatment. Consistent with the inability of MCF-7 cells to induce activation of caspase-3,[28] pretreatment with the pan-caspase inhibitor Z-VAD did not affect the cell viability seen after the treatments (Figure 4D). Although it is known that autophagy is required for the production of IFNα by plasmacytoid dendritic cells during viral infection,[40] and it has been recently shown that type I IFN induces autophagic trafficking of viral proteins of hepatitis C virus,[41] the role of IFNα in the autophagy process is still unclear and knowledge is restricted to its antiviral function. Our results show, for the first time, evidence that IFNα is involved in the autophagy process in combination with an antitumor agent. The mechanism of action involved in this process needs to be investigated further, and might have important therapeutic implications.

Finally, we observed that during long-term treatment with even low doses of bozepinib and the bozepinib/IFNα combination, a minority population showing β-galactosidase activity persisted in MCF-7 cells, being once again more evident in surviving cells treated with the bozepinib/IFNα combination (Figure 5A). Moreover, this population showed a high percentage of cells arrested in S phase in comparison with cells treated or not with bozepinib or IFNα separately (Figure 5B). Because tumors often develop resistance to apoptosis induced by anticancer treatment, induction of senescence in tumor cells could be an alternative approach to cancer therapy, and be especially effective in the treatment of cancer cells in which apoptotic pathways are disabled.[12] Although the exact mechanism by which IFNα regulates senescence is still under investigation, it has been suggested that IFNα downregulates telomerase activity along with inhibition of growth in Daudi lymphoma cells.[42] It has also been suggested that overexpression of two IFN regulatory transcription factors (IRF5 and IRF7) is able to induce a senescence-related phenotype in immortal cells.[43] More recently, early evidence has been reported showing that a combination of IFNα and a chemotherapeutic agent, vinblastine, triggers senescence; however, the authors showed this effect in endothelial cells in the context of angiogenesis within the tumor.[44] Our results show that IFNα enhances the senescence provoked in tumor cells by bozepinib, suggesting that this cytokine could act directly in this process when combined with other antitumor drugs.

Conclusion

The development of novel anticancer drugs that are more effective and have fewer side effects in patients is an important research topic in cancer, and understanding the mechanisms involved in the antitumor effects of new compounds is necessary for their clinical application. Bozepinib is a potent antitumor agent that is able to induce apoptosis in breast and colon cancer cells. In this study, we have demonstrated that PKR but not p53 is involved in the apoptosis induced by bozepinib, which has encouraged us to explore targets for new compounds with high antitumor activity and enabling effectiveness at low doses. Given that p53 is mutated in more than 50% of tumors, drugs inducing apoptosis through molecular targets different to p53 are of great clinical interest. Moreover, our results highlight the benefit of combination chemotherapy using natural cytokines, such as IFNα, which can potentiate the apoptosis induced by chemotherapy. IFNα also enhances autophagy and senescence, which are processes suggested to be of great importance, especially in tumor cells that show resistance to conventional chemotherapy. Our study increases our knowledge about the synergistic effect induced by IFN, and supports the need to explore new combinations with potent antitumor agents such as bozepinib, which can enhance the diversity of cell death outcomes, leading to more effective and less toxic chemotherapy.

Acknowledgments

We gratefully acknowledge Jaime Lazuen for providing excellent technical assistance with the cytometry studies and Manuela Expósito for statistical assistance. We also thank staff from the Experimental Surgery Research Unit, and Pablo Bueno for support with equipment. This work was supported in part by grants from the Instituto de Salud Carlos III (Fondo de Investigación Sanitaria FEDER funds, CP08/0063, PI10/02295, and PI10/00592).

Disclosure

The authors report no conflicts of interest in this work.

References

1. Ferlay J, Shin HR, Bray F, Forman D, Mathers C, Parkin DM. Estimates of worldwide burden of cancer in 2008: GLOBOCAN 2008. *Int J Cancer*. 2010;127(12):2893–2917.
2. Díaz-Gavilán M, Conejo-García A, Cruz-López O, et al. Synthesis and anticancer activity of (*R,S*)-9-(2,3-dihydro-1,4-benzoxathiin-3-ylmethyl)-9*H*-purines. *ChemMedChem*. 2008;3(1):127–135.
3. Díaz-Gavilán M, Gómez-Vidal JA, Entrena A, Gallo MA, Espinosa A, Campos JM. Study of the factors that control the ratio of the products between 5-fluorouracil, uracil, and tetrahydrobenzoxazepine *O,O*-acetals bearing electron-withdrawing groups on the nitrogen atom. *J Org Chem*. 2006;71(3):1043–1054.
4. Núñez MC, Díaz-Gavilán M, Conejo-García A, et al. Design, synthesis and anticancer activity against the MCF-7 cell line of benzo-fused 1,4-dihetero seven- and six-membered tethered pyrimidines and purines. *Curr Med Chem*. 2008;15(25):2614–2631.
5. López-Cara LC, Conejo-García A, Marchal JA, et al. New (*RS*)-benzoxazepin-purines with antitumour activity: the chiral switch from (*RS*)-2,6-dichloro-9-[1-(*p*-nitrobenzenesulfonyl)-1,2,3,5-tetrahydro-4,1-benzoxazepin-3-yl]-9*H*-purine. *Eur J Med Chem*. 2011;46(1):249–258.
6. Ferri KF, Kroemer G. Organelle-specific initiation of cell death pathways. *Nat Cell Biol*. 2001;3(11):E255–E263.
7. de Bruin EC, Medema JP. Apoptosis and non-apoptotic deaths in cancer development and treatment response. *Cancer Treat Rev*. 2008;34(8):737–749.
8. Mansilla S, Llovera L, Portugal J. Chemotherapeutic targeting of cell death pathways. *Anticancer Agents Med Chem*. 2012;12(3):226–238.
9. White E, Karp C, Strohecker AM, Guo Y, Mathew R. Role of autophagy in suppression of inflammation and cancer. *Curr Opin Cell Biol*. 2010;22(2):212–217.
10. Dalby KN, Tekedereli I, Lopez-Berestein G, Ozpolat B. Targeting the prodeath and prosurvival functions of autophagy as novel therapeutic strategies in cancer. *Autophagy*. 2010;6(3):322–329.
11. Hayflick L, Moorhead PS. The serial cultivation of human diploid cell strains. *Exp Cell Res*. 1961;25(3):585–621.
12. Kong Y, Cui H, Ramkumar C, Zhang H. Regulation of senescence in cancer and aging. *J Aging Res*. 2011;2011:963172.
13. Hasselbalch HC. Interferon alpha2 in the treatment of hematological malignancies. Status and perspectives. *Curr Drug Targets*. 2011;12(3):387–391.
14. Tarhini AA, Gogas H, Kirkwood JM. IFN-alpha in the treatment of melanoma. *J Immunol*. 2012;189(8):3789–3793.
15. Kirkwood J. Cancer immunotherapy: the interferon-alpha experience. *Semin Oncol*. 2002;29(3 Suppl 7):18–26.
16. Dal Col J, Mastorci K, Fae DA, et al. Retinoic acid/alpha-interferon combination inhibits growth and promotes apoptosis in mantle cell lymphoma through Akt-dependent modulation of critical targets. *Cancer Res*. 2012;72(7):1825–1835.
17. Tarhini AA, Cherian J, Moschos SJ, et al. Safety and efficacy of combination immunotherapy with interferon alfa-2b and tremelimumab in patients with stage IV melanoma. *J Clin Oncol*. 2012;30(3):322–328.
18. Simonsson B, Hjorth-Hansen H, Bjerrum OW, Porkka K. Interferon alpha for treatment of chronic myeloid leukemia. *Curr Drug Targets*. 2011;12(3):420–428.
19. Negrier S, Gravis G, Perol D, et al. Temsirolimus and bevacizumab, or sunitinib, or interferon alfa and bevacizumab for patients with advanced renal cell carcinoma (TORAVA): a randomised phase 2 trial. *Lancet Oncol*. 2011;12(7):673–680.
20. Esteban M, Kerr IM. The synthesis of encephalomyocarditis virus polypeptides in infected L-cells and cell-free systems. *Eur J Biochem*. 1974;45(2):567–576.
21. García MA, Gil J, Ventoso I, et al. Impact of protein kinase PKR in cell biology: from antiviral to antiproliferative action. *Microbiol Mol Biol Rev*. 2006;70(4):1032–1060.
22. Yoon CH, Lee ES, Lim DS, Bae YS. PKR, a p53 target gene, plays a crucial role in the tumor-suppressor function of p53. *Proc Natl Acad Sci U S A*. 2009;106(19):7852–7857.
23. Peidis P, Papadakis AI, Muaddi H, Richard S, Koromilas AE. Doxorubicin bypasses the cytoprotective effects of eIF2alpha phosphorylation and promotes PKR-mediated cell death. *Cell Death Differ*. 2011;18(1):145–154.
24. García MA, Carrasco E, Aguilera M, et al. The chemotherapeutic drug 5-fluorouracil promotes PKR-mediated apoptosis in a p53-independent manner in colon and breast cancer cells. *PLoS One*. 2011;6(8):e23887.
25. Yang YL, Reis LF, Pavlovic J, et al. Deficient signaling in mice devoid of double-stranded RNA-dependent protein kinase. *EMBO J*. 1995;14(24):6095–6106.
26. Bunz F, Hwang PM, Torrance C, et al. Disruption of p53 in human cancer cells alters the responses to therapeutic agents. *J Clin Invest*. 1999;104(3):263–269.
27. Villalobos C, García-Sancho J. Capacitative Ca2+ entry contributes to the Ca2+ influx induced by thyrotropin-releasing hormone (TRH) in GH3 pituitary cells. *Pflugers Arch*. 1995;430(6):923–935.
28. Yang XH, Sladek TL, Liu X, Butler BR, Froelich CJ, Thor AD. Reconstitution of caspase 3 sensitizes MCF-7 breast cancer cells to doxorubicin- and etoposide-induced apoptosis. *Cancer Res*. 2001;61(1):348–354.
29. Yoon YH, Cho KS, Hwang JJ, Lee SJ, Choi JA, Koh JY. Induction of lysosomal dilatation, arrested autophagy, and cell death by chloroquine in cultured ARPE-19 cells. *Invest Ophthalmol Vis Sci*. 2010;51(11):6030–6037.
30. Geng Y, Kohli L, Klocke BJ, Roth KA. Chloroquine-induced autophagic vacuole accumulation and cell death in glioma cells is p53 independent. *Neuro Oncol*. 2010;12(5):473–481.
31. Holcik M, Sonenberg N. Translational control in stress and apoptosis. *Nat Rev Mol Cell Biol*. 2005;6(4):318–327.
32. Martínez-Rivera M, Siddik ZH. Resistance and gain-of-resistance phenotypes in cancers harboring wild-type p53. *Biochem Pharmacol*. 2012;83(8):1049–1062.
33. Konstantakou EG, Voutsinas GE, Karkoulis PK, Aravantinos G, Margaritis LH, Stravopodis DJ. Human bladder cancer cells undergo cisplatin-induced apoptosis that is associated with p53-dependent and p53-independent responses. *Int J Oncol*. 2009;35(2):401–416.
34. Backus HH, Wouters D, Ferreira CG, et al. Thymidylate synthase inhibition triggers apoptosis via caspases-8 and -9 in both wild-type and mutant p53 colon cancer cell lines. *Eur J Cancer*. 2003;39(9):1310–1317.
35. Nakamura M, Nagano H, Sakon M, et al. Role of the Fas/FasL pathway in combination therapy with interferon-alpha and fluorouracil against hepatocellular carcinoma *in vitro*. *J Hepatol*. 2007;46(1):77–88.
36. Philchenkov A, Zavelevich M, Kroczak TJ, Los M. Caspases and cancer: mechanisms of inactivation and new treatment modalities. *Exp Oncol*. 2004;26(2):82–97.
37. Janicke RU, Ng P, Sprengart ML, Porter AG. Caspase-3 is required for alpha-fodrin cleavage but dispensable for cleavage of other death substrates in apoptosis. *J Biol Chem*. 1998;273(25):15540–15545.
38. Akar U, Chaves-Reyez A, Barria M, et al. Silencing of Bcl-2 expression by small interfering RNA induces autophagic cell death in MCF-7 breast cancer cells. *Autophagy*. 2008;4(5):669–679.
39. Xue L, Fletcher GC, Tolkovsky AM. Autophagy is activated by apoptotic signalling in sympathetic neurons: an alternative mechanism of death execution. *Mol Cell Neurosci*. 1999;14(3):180–198.
40. Lee HK, Lund JM, Ramanathan B, Mizushima N, Iwasaki A. Autophagy-dependent viral recognition by plasmacytoid dendritic cells. *Science*. 2007;315(5817):1398–1401.
41. Desai MM, Gong B, Chan T, et al. Differential, type I interferon-mediated autophagic trafficking of hepatitis C virus proteins in mouse liver. *Gastroenterology*. 2011;141(2):674–685.

42. Akiyama M, Iwase S, Horiguchi-Yamada J, et al. Interferon-alpha repressed telomerase along with G1-accumulation of Daudi cells. *Cancer Lett*. 1999;142(1):23–30.
43. Li Q, Tang L, Roberts PC, et al. Interferon regulatory factors IRF5 and IRF7 inhibit growth and induce senescence in immortal Li-Fraumeni fibroblasts. *Mol Cancer Res*. 2008;6(5):770–784.
44. Upreti M, Koonce NA, Hennings L, Chambers TC, Griffin RJ. Pegylated IFN-alpha sensitizes melanoma cells to chemotherapy and causes premature senescence in endothelial cells by IRF-1 mediated signaling. *Cell Death Dis*. 2010;1:e67.

MINISTERIO
DE INDUSTRIA, TURISMO
Y COMERCIO

Oficina Española
de Patentes y Marcas

Justificante de presentación electrónica de solicitud de patente

Este documento es un justificante de que se ha recibido una solicitud española de patente por vía electrónica, utilizando la conexión segura de la O.E.P.M. Asimismo, se le ha asignado de forma automática un número de solicitud y una fecha de recepción, conforme al artículo 14.3 del Reglamento para la ejecución de la Ley 11/1986, de 20 de marzo, de Patentes. La fecha de presentación de la solicitud de acuerdo con el art. 22 de la Ley de Patentes, le será comunicada posteriormente.

Número de solicitud:	P201430048	
Fecha de recepción:	20 enero 2014, 10:30 (CET)	
Oficina receptora:	OEPM Madrid	
Su referencia:	IPR-524	
Solicitante:	UNIVERSIDAD DE GRANADA	
Número de solicitantes:	1	
País:	ES	
Título:	SULFONAMIDAS DERIVADAS DE AMINAS SECUNDARIAS CON GRUPOS 1,3-DIOXOLANILALQUÍLICOS Y FENILMETILPURÍNICOS, Y SU UTILIZACIÓN COMO AGENTES ANTICANCERÍGENOS	
Documentos enviados:	Descripcion.pdf (42 p.) Reivindicaciones.pdf (7 p.) Resumen.pdf (1 p.) OLF-ARCHIVE.zip	package-data.xml es-request.xml application-body.xml es-fee-sheet.xml feesheet.pdf request.pdf
Enviados por:	CN=NOMBRE CHAMORRO MARTINEZ JESUS - NIF 24274994N,OU=501079135,OU=FNMT Clase 2 CA,O=FNMT,C=ES	
Fecha y hora de recepción:	20 enero 2014, 10:30 (CET)	
Codificación del envío:	75:DC:85:91:54:BC:B3:59:DB:29:F3:90:D6:E0:D9:1D:E0:72:78:07	

/Madrid, Oficina Receptora/